



Digitized by the Internet Archive
in 2019 with funding from
University of Alberta Libraries

<https://archive.org/details/Alexander1965>



Thesis
1965
81

THE UNIVERSITY OF ALBERTA

MODEL STUDY OF HYPERBOLIC PARABOLOID SHELL

by

BRUCE ALEXANDER

A THESIS

SUBMITTED TO THE FACULTY OF GRADUATE STUDIES
IN PARTIAL FULFILMENT OF THE REQUIREMENTS FOR THE DEGREE
OF MASTER OF SCIENCE

DEPARTMENT OF CIVIL ENGINEERING

EDMONTON, ALBERTA

MAY, 1965

THE UNIVERSITY OF ALBERTA
FACULTY OF GRADUATE STUDIES

The undersigned certify that they have read, and recommend to the Faculty of Graduate Studies for acceptance, a thesis entitled MODEL STUDY OF HYPERBOLIC PARABOLOID SHELL, submitted by Bruce Alexander in partial fulfilment of the requirements for the degree of Master of Science.

ABSTRACT

A mortar model of a gable type hyperbolic paraboloid shell was built and instrumented. Uniform loads were applied (a) symmetrically over the entire shell and (b) over one half of the shell only. Without the application of external load, the shell was subjected to differential foundation movement. Finally, the shell was tested to destruction under uniform, symmetrical loading.

The purpose of the study was threefold. As a pilot project, the aim was to examine the practicability of testing model shells and to recommend improvements in technique for future shell research, presently contemplated at the University of Alberta. Secondly, it was the purpose of this investigation to study the behaviour of one type of shell at working loads under the various loading patterns discussed above, and to compare the results with simple membrane theory. Thirdly, the behaviour of the shell at ultimate load was to be examined and the results compared with membrane theory.

Load was applied by a hydraulic jack, through a load distributing apparatus consisting of pin ended members which applied the load equally to sixty four rubber pads bearing on the model.

THE CONSTITUTION

THE CONSTITUTION OF THE UNITED STATES OF AMERICA

WE THE PEOPLE, in Order to form a more perfect Union, establish Justice, insure domestic Tranquility, provide for the common defence, promote the general Welfare, and secure the Blessings of Liberty to ourselves and our Posterity, do hereby adopt this Constitution for the United States of America.

ARTICLE I

SECTION 1. All legislative Powers herein granted shall be vested in a Congress of the United States, which shall consist of a Senate and House of Representatives.

SECTION 2. The House of Representatives shall be composed of Members chosen every second Year by the People of the several States, and the Electors in each State shall have the Qualifications requisite for Electors of the most numerous Branch of the State Legislature. No Person shall be a Representative who shall not, when elected, have seven Years since attained to the Age of twenty five Years, and seven Years since been seven Years a Citizen of the United States, and when elected shall have been seven Years a Citizen of that State in which he shall be chosen. Representatives and Electors may be removed by the People of the State in which they shall have been chosen.

SECTION 3. The Senate shall be composed of two Senators from each State, chosen by the Legislature thereof, for a Term of six Years; and each Senator shall have the Qualifications requisite for Representatives.

SECTION 4. The Senators and Representatives before Congress, and the Members of the several State Legislatures, and the Electors in each State, shall have the Qualifications requisite for Electors of the most numerous Branch of the State Legislature.

SECTION 5. The Senate shall have the sole Power to try all Cases of Impeachment.

SECTION 6. The Senators and Representatives before Congress, and the Members of the several State Legislatures, and the Electors in each State, shall have the Qualifications requisite for Electors of the most numerous Branch of the State Legislature.

Strains were recorded by a 100 channel digital data processor. Deflections were measured by Ames dials mounted on the ridge and gable beams.

Bending moments and axial thrusts in the ridge and gable beams were lower than predicted by membrane theory under uniform, symmetrical loading due to the "flange action" of the shell. Shell stresses were approximately equal to those derived from membrane theory, with a small biaxial compression superimposed. Bending moments were present in the shell elements but they were small and not considered particularly significant.

Under asymmetrical loading, the loaded shell quadrants behaved almost identically to typical shell quadrants under uniform, symmetrical loading. For this model, the asymmetrical loading produced effects on the ridge and gable beams which were no more critical than those produced by symmetrical loading, but the location of the maximum moments was shifted.

Under foundation settlement, the shell was not seriously affected by a total settlement of 1/96th of the span. Gable beams were affected most, while ridge beams appeared to be almost unstressed by the settlement.

Ultimate failure occurred as a result of a premature ridge beam failure attributed to faulty welding. Membrane theory appeared to be valid well beyond the elastic limit of the material.

ACKNOWLEDGEMENTS

This investigation was carried out using the facilities of the Department of Civil Engineering of the University of Alberta, Edmonton, Alberta. Funds for the purchase of materials and equipment were provided by National Research Council of Canada Operating Grant A-1691.

Labour and materials for the placing of pneumatic mortar were donated by Dominion Gunitite Ltd. Special acknowledgement goes to Mr. R. R. Blackwood for his time and effort in supervising the placing of the "Gunitite".

The author wishes to express his grateful appreciation to Dr. S. H. Simmonds for his assistance during the investigation and preparation of the manuscript, and takes this opportunity to thank Dr. D. G. Bellow for the use of the digital data processor and his many helpful suggestions concerning instrumentation. The author is grateful to his father-in-law, Mr. H. D. Stewart for his many hours of help in constructing the formwork and placing the reinforcing for the shell. He is also indebted to Mr. H. Winklemeier for the preparation of drawings, to Mrs. D. Hooper for the typing of the manuscript, and to Associated Engineering Services Ltd. for their assistance in printing the thesis.

ACKNOWLEDGMENTS

This investigation was carried out under the auspices of the Department of Civil Engineering of the University of Alberta, Edmonton, and financial support for the purchase of materials and equipment was provided by the Natural Research Council of Canada (Grant A-1087).

Liberal and thoughtful criticism in the placing of problems, results, and conclusions by Dr. J. H. D. Burrows, and the assistance in preparing the placing of the manuscript by Dr. J. H. D. Burrows, are gratefully acknowledged.

The author wishes to express his grateful appreciation to Dr. J. H. D. Burrows for his assistance during the investigation and preparation of the manuscript, and also the opportunity to thank Dr. J. H. D. Burrows for his help in the design of the apparatus and his many helpful suggestions concerning the design of the apparatus. The author is grateful to the Department of Civil Engineering for the use of the laboratory and for the facilities provided for the investigation. He is also indebted to Mr. H. W. H. Burrows for his help in the design of the apparatus, and to Mr. H. W. H. Burrows for his help in the design of the apparatus, and to Mr. H. W. H. Burrows for his help in the design of the apparatus.

TABLE OF CONTENTS

	Page
Title Page	i
Approval Sheet	ii
Abstract	iii
Acknowledgements	v
Table of Contents	vi
List of Figures	xi
 CHAPTER I INTRODUCTION	 1
1.1 Shell Construction	1
1.2 Model Studies	1
1.3 Object of Testing Program	2
 CHAPTER II THEORY	 4
2.1 Assumptions in Membrane Theory	4
2.2 Notation	4
2.3 Geometric Equations	5
2.4 Equilibrium Equations	6
2.5 The Hyperbolic Paraboloid	8
2.6 Gable Type Hyperbolic Paraboloid	9
 CHAPTER III FABRICATION OF MODEL AND TESTING APPARATUS	 11
3.1 Formwork	11
3.2 Details of the Model	11

THE HISTORY OF THE

Page

3.3	Design of the Model	17
3.4	Reinforcement	18
3.5	Placing Reinforcement	18
3.6	Placing Concrete	21
3.7	Mix Properties	22
3.8	Curing the Model	22
3.9	Corner Supports	23
3.10	Test Setup	29
3.11	Load Distributing System	30
CHAPTER IV TESTING PROGRAM		35
4.1	Description of Tests	35
4.2	Symmetrical Load Tests	35
4.3	Asymmetrical Load Tests	37
4.4	Foundation Settlement	37
4.5	Test to Destruction	37
4.6	Test Procedure	38
CHAPTER V INSTRUMENTATION		40
5.1	Introduction	40
5.2	Load Cells	40
5.3	Tie Rods	42
5.4	Measurement of Surface Strains	42

5.5	The Data Processor	42
5.6	Location of Strain Gauges	44
5.7	Application of Strain Gauges	44
5.8	Deflection Measurements	47

CHAPTER VI PRESENTATION AND DISCUSSION OF SYMMETRICAL

	LOAD TESTS	50
6.1	Introduction	50
6.2	External Reactions	52
6.3	Gable Beams	52
6.4	Ridge Beams	64
6.5	Compression diagonal of Shell	73
6.6	Tension Diagonal of the Shell	76
6.7	Generator K L	76
6.8	Discussion of Uniform Load Series	81

CHAPTER VII PRESENTATION AND DISCUSSION OF ASYMMETRICAL

	LOAD TESTS	85
7.1	Introduction	85
7.2	External Reactions	85
7.3	Gables Parallel to Axis of Symmetry	87
7.4	Gables Perpendicular to Axis of Symmetry	93
7.5	Ridge Beam Perpendicular to Axis of Symmetry	100
7.6	Ridge Beam Parallel to Axis of Symmetry	104

100	101	102	103	104	105	106	107	108	109	110	111	112	113	114	115	116	117	118	119	120	121	122	123	124	125	126	127	128	129	130	131	132	133	134	135	136	137	138	139	140	141	142	143	144	145	146	147	148	149	150	151	152	153	154	155	156	157	158	159	160	161	162	163	164	165	166	167	168	169	170	171	172	173	174	175	176	177	178	179	180	181	182	183	184	185	186	187	188	189	190	191	192	193	194	195	196	197	198	199	200	201	202	203	204	205	206	207	208	209	210	211	212	213	214	215	216	217	218	219	220	221	222	223	224	225	226	227	228	229	230	231	232	233	234	235	236	237	238	239	240	241	242	243	244	245	246	247	248	249	250	251	252	253	254	255	256	257	258	259	260	261	262	263	264	265	266	267	268	269	270	271	272	273	274	275	276	277	278	279	280	281	282	283	284	285	286	287	288	289	290	291	292	293	294	295	296	297	298	299	300	301	302	303	304	305	306	307	308	309	310	311	312	313	314	315	316	317	318	319	320	321	322	323	324	325	326	327	328	329	330	331	332	333	334	335	336	337	338	339	340	341	342	343	344	345	346	347	348	349	350	351	352	353	354	355	356	357	358	359	360	361	362	363	364	365	366	367	368	369	370	371	372	373	374	375	376	377	378	379	380	381	382	383	384	385	386	387	388	389	390	391	392	393	394	395	396	397	398	399	400	401	402	403	404	405	406	407	408	409	410	411	412	413	414	415	416	417	418	419	420	421	422	423	424	425	426	427	428	429	430	431	432	433	434	435	436	437	438	439	440	441	442	443	444	445	446	447	448	449	450	451	452	453	454	455	456	457	458	459	460	461	462	463	464	465	466	467	468	469	470	471	472	473	474	475	476	477	478	479	480	481	482	483	484	485	486	487	488	489	490	491	492	493	494	495	496	497	498	499	500	501	502	503	504	505	506	507	508	509	510	511	512	513	514	515	516	517	518	519	520	521	522	523	524	525	526	527	528	529	530	531	532	533	534	535	536	537	538	539	540	541	542	543	544	545	546	547	548	549	550	551	552	553	554	555	556	557	558	559	560	561	562	563	564	565	566	567	568	569	570	571	572	573	574	575	576	577	578	579	580	581	582	583	584	585	586	587	588	589	590	591	592	593	594	595	596	597	598	599	600	601	602	603	604	605	606	607	608	609	610	611	612	613	614	615	616	617	618	619	620	621	622	623	624	625	626	627	628	629	630	631	632	633	634	635	636	637	638	639	640	641	642	643	644	645	646	647	648	649	650	651	652	653	654	655	656	657	658	659	660	661	662	663	664	665	666	667	668	669	670	671	672	673	674	675	676	677	678	679	680	681	682	683	684	685	686	687	688	689	690	691	692	693	694	695	696	697	698	699	700	701	702	703	704	705	706	707	708	709	710	711	712	713	714	715	716	717	718	719	720	721	722	723	724	725	726	727	728	729	730	731	732	733	734	735	736	737	738	739	740	741	742	743	744	745	746	747	748	749	750	751	752	753	754	755	756	757	758	759	760	761	762	763	764	765	766	767	768	769	770	771	772	773	774	775	776	777	778	779	780	781	782	783	784	785	786	787	788	789	790	791	792	793	794	795	796	797	798	799	800	801	802	803	804	805	806	807	808	809	810	811	812	813	814	815	816	817	818	819	820	821	822	823	824	825	826	827	828	829	830	831	832	833	834	835	836	837	838	839	840	841	842	843	844	845	846	847	848	849	850	851	852	853	854	855	856	857	858	859	860	861	862	863	864	865	866	867	868	869	870	871	872	873	874	875	876	877	878	879	880	881	882	883	884	885	886	887	888	889	890	891	892	893	894	895	896	897	898	899	900	901	902	903	904	905	906	907	908	909	910	911	912	913	914	915	916	917	918	919	920	921	922	923	924	925	926	927	928	929	930	931	932	933	934	935	936	937	938	939	940	941	942	943	944	945	946	947	948	949	950	951	952	953	954	955	956	957	958	959	960	961	962	963	964	965	966	967	968	969	970	971	972	973	974	975	976	977	978	979	980	981	982	983	984	985	986	987	988	989	990	991	992	993	994	995	996	997	998	999	1000
-----	-----	-----	-----	-----	-----	-----	-----	-----	-----	-----	-----	-----	-----	-----	-----	-----	-----	-----	-----	-----	-----	-----	-----	-----	-----	-----	-----	-----	-----	-----	-----	-----	-----	-----	-----	-----	-----	-----	-----	-----	-----	-----	-----	-----	-----	-----	-----	-----	-----	-----	-----	-----	-----	-----	-----	-----	-----	-----	-----	-----	-----	-----	-----	-----	-----	-----	-----	-----	-----	-----	-----	-----	-----	-----	-----	-----	-----	-----	-----	-----	-----	-----	-----	-----	-----	-----	-----	-----	-----	-----	-----	-----	-----	-----	-----	-----	-----	-----	-----	-----	-----	-----	-----	-----	-----	-----	-----	-----	-----	-----	-----	-----	-----	-----	-----	-----	-----	-----	-----	-----	-----	-----	-----	-----	-----	-----	-----	-----	-----	-----	-----	-----	-----	-----	-----	-----	-----	-----	-----	-----	-----	-----	-----	-----	-----	-----	-----	-----	-----	-----	-----	-----	-----	-----	-----	-----	-----	-----	-----	-----	-----	-----	-----	-----	-----	-----	-----	-----	-----	-----	-----	-----	-----	-----	-----	-----	-----	-----	-----	-----	-----	-----	-----	-----	-----	-----	-----	-----	-----	-----	-----	-----	-----	-----	-----	-----	-----	-----	-----	-----	-----	-----	-----	-----	-----	-----	-----	-----	-----	-----	-----	-----	-----	-----	-----	-----	-----	-----	-----	-----	-----	-----	-----	-----	-----	-----	-----	-----	-----	-----	-----	-----	-----	-----	-----	-----	-----	-----	-----	-----	-----	-----	-----	-----	-----	-----	-----	-----	-----	-----	-----	-----	-----	-----	-----	-----	-----	-----	-----	-----	-----	-----	-----	-----	-----	-----	-----	-----	-----	-----	-----	-----	-----	-----	-----	-----	-----	-----	-----	-----	-----	-----	-----	-----	-----	-----	-----	-----	-----	-----	-----	-----	-----	-----	-----	-----	-----	-----	-----	-----	-----	-----	-----	-----	-----	-----	-----	-----	-----	-----	-----	-----	-----	-----	-----	-----	-----	-----	-----	-----	-----	-----	-----	-----	-----	-----	-----	-----	-----	-----	-----	-----	-----	-----	-----	-----	-----	-----	-----	-----	-----	-----	-----	-----	-----	-----	-----	-----	-----	-----	-----	-----	-----	-----	-----	-----	-----	-----	-----	-----	-----	-----	-----	-----	-----	-----	-----	-----	-----	-----	-----	-----	-----	-----	-----	-----	-----	-----	-----	-----	-----	-----	-----	-----	-----	-----	-----	-----	-----	-----	-----	-----	-----	-----	-----	-----	-----	-----	-----	-----	-----	-----	-----	-----	-----	-----	-----	-----	-----	-----	-----	-----	-----	-----	-----	-----	-----	-----	-----	-----	-----	-----	-----	-----	-----	-----	-----	-----	-----	-----	-----	-----	-----	-----	-----	-----	-----	-----	-----	-----	-----	-----	-----	-----	-----	-----	-----	-----	-----	-----	-----	-----	-----	-----	-----	-----	-----	-----	-----	-----	-----	-----	-----	-----	-----	-----	-----	-----	-----	-----	-----	-----	-----	-----	-----	-----	-----	-----	-----	-----	-----	-----	-----	-----	-----	-----	-----	-----	-----	-----	-----	-----	-----	-----	-----	-----	-----	-----	-----	-----	-----	-----	-----	-----	-----	-----	-----	-----	-----	-----	-----	-----	-----	-----	-----	-----	-----	-----	-----	-----	-----	-----	-----	-----	-----	-----	-----	-----	-----	-----	-----	-----	-----	-----	-----	-----	-----	-----	-----	-----	-----	-----	-----	-----	-----	-----	-----	-----	-----	-----	-----	-----	-----	-----	-----	-----	-----	-----	-----	-----	-----	-----	-----	-----	-----	-----	-----	-----	-----	-----	-----	-----	-----	-----	-----	-----	-----	-----	-----	-----	-----	-----	-----	-----	-----	-----	-----	-----	-----	-----	-----	-----	-----	-----	-----	-----	-----	-----	-----	-----	-----	-----	-----	-----	-----	-----	-----	-----	-----	-----	-----	-----	-----	-----	-----	-----	-----	-----	-----	-----	-----	-----	-----	-----	-----	-----	-----	-----	-----	-----	-----	-----	-----	-----	-----	-----	-----	-----	-----	-----	-----	-----	-----	-----	-----	-----	-----	-----	-----	-----	-----	-----	-----	-----	-----	-----	-----	-----	-----	-----	-----	-----	-----	-----	-----	-----	-----	-----	-----	-----	-----	-----	-----	-----	-----	-----	-----	-----	-----	-----	-----	-----	-----	-----	-----	-----	-----	-----	-----	-----	-----	-----	-----	-----	-----	-----	-----	-----	-----	-----	-----	-----	-----	-----	-----	-----	-----	-----	-----	-----	-----	-----	-----	-----	-----	-----	-----	-----	-----	-----	-----	-----	-----	-----	-----	-----	-----	-----	-----	-----	-----	-----	-----	-----	-----	-----	-----	-----	-----	-----	-----	-----	-----	-----	-----	-----	-----	-----	-----	-----	-----	-----	-----	-----	-----	-----	-----	-----	-----	-----	-----	-----	-----	-----	-----	-----	-----	-----	-----	-----	-----	-----	-----	-----	-----	-----	-----	-----	-----	-----	-----	-----	-----	-----	-----	-----	-----	-----	-----	-----	-----	-----	-----	-----	-----	-----	-----	-----	-----	-----	-----	-----	-----	-----	-----	-----	-----	-----	-----	-----	-----	-----	-----	-----	-----	-----	-----	-----	-----	-----	-----	-----	-----	-----	-----	-----	-----	-----	-----	-----	-----	-----	-----	-----	-----	-----	-----	-----	-----	-----	-----	-----	-----	-----	-----	-----	-----	-----	-----	-----	-----	-----	-----	-----	-----	-----	-----	-----	-----	-----	-----	-----	-----	-----	-----	-----	-----	-----	-----	-----	-----	-----	-----	-----	-----	-----	-----	-----	-----	-----	-----	-----	-----	-----	-----	-----	-----	-----	-----	-----	-----	-----	-----	-----	-----	-----	-----	-----	-----	------

APPENDIX A: SUMMARY OF THE DATA COLLECTION PROCESS

100	101	102	103	104	105	106	107	108	109	110	111	112	113	114	115	116	117	118	119	120	121	122	123	124	125	126	127	128	129	130	131	132	133	134	135	136	137	138	139	140	141	142	143	144	145	146	147	148	149	150	151	152	153	154	155	156	157	158	159	160	161	162	163	164	165	166	167	168	169	170	171	172	173	174	175	176	177	178	179	180	181	182	183	184	185	186	187	188	189	190	191	192	193	194	195	196	197	198	199	200	201	202	203	204	205	206	207	208	209	210	211	212	213	214	215	216	217	218	219	220	221	222	223	224	225	226	227	228	229	230	231	232	233	234	235	236	237	238	239	240	241	242	243	244	245	246	247	248	249	250	251	252	253	254	255	256	257	258	259	260	261	262	263	264	265	266	267	268	269	270	271	272	273	274	275	276	277	278	279	280	281	282	283	284	285	286	287	288	289	290	291	292	293	294	295	296	297	298	299	300	301	302	303	304	305	306	307	308	309	310	311	312	313	314	315	316	317	318	319	320	321	322	323	324	325	326	327	328	329	330	331	332	333	334	335	336	337	338	339	340	341	342	343	344	345	346	347	348	349	350	351	352	353	354	355	356	357	358	359	360	361	362	363	364	365	366	367	368	369	370	371	372	373	374	375	376	377	378	379	380	381	382	383	384	385	386	387	388	389	390	391	392	393	394	395	396	397	398	399	400	401	402	403	404	405	406	407	408	409	410	411	412	413	414	415	416	417	418	419	420	421	422	423	424	425	426	427	428	429	430	431	432	433	434	435	436	437	438	439	440	441	442	443	444	445	446	447	448	449	450	451	452	453	454	455	456	457	458	459	460	461	462	463	464	465	466	467	468	469	470	471	472	473	474	475	476	477	478	479	480	481	482	483	484	485	486	487	488	489	490	491	492	493	494	495	496	497	498	499	500	501	502	503	504	505	506	507	508	509	510	511	512	513	514	515	516	517	518	519	520	521	522	523	524	525	526	527	528	529	530	531	532	533	534	535	536	537	538	539	540	541	542	543	544	545	546	547	548	549	550	551	552	553	554	555	556	557	558	559
-----	-----	-----	-----	-----	-----	-----	-----	-----	-----	-----	-----	-----	-----	-----	-----	-----	-----	-----	-----	-----	-----	-----	-----	-----	-----	-----	-----	-----	-----	-----	-----	-----	-----	-----	-----	-----	-----	-----	-----	-----	-----	-----	-----	-----	-----	-----	-----	-----	-----	-----	-----	-----	-----	-----	-----	-----	-----	-----	-----	-----	-----	-----	-----	-----	-----	-----	-----	-----	-----	-----	-----	-----	-----	-----	-----	-----	-----	-----	-----	-----	-----	-----	-----	-----	-----	-----	-----	-----	-----	-----	-----	-----	-----	-----	-----	-----	-----	-----	-----	-----	-----	-----	-----	-----	-----	-----	-----	-----	-----	-----	-----	-----	-----	-----	-----	-----	-----	-----	-----	-----	-----	-----	-----	-----	-----	-----	-----	-----	-----	-----	-----	-----	-----	-----	-----	-----	-----	-----	-----	-----	-----	-----	-----	-----	-----	-----	-----	-----	-----	-----	-----	-----	-----	-----	-----	-----	-----	-----	-----	-----	-----	-----	-----	-----	-----	-----	-----	-----	-----	-----	-----	-----	-----	-----	-----	-----	-----	-----	-----	-----	-----	-----	-----	-----	-----	-----	-----	-----	-----	-----	-----	-----	-----	-----	-----	-----	-----	-----	-----	-----	-----	-----	-----	-----	-----	-----	-----	-----	-----	-----	-----	-----	-----	-----	-----	-----	-----	-----	-----	-----	-----	-----	-----	-----	-----	-----	-----	-----	-----	-----	-----	-----	-----	-----	-----	-----	-----	-----	-----	-----	-----	-----	-----	-----	-----	-----	-----	-----	-----	-----	-----	-----	-----	-----	-----	-----	-----	-----	-----	-----	-----	-----	-----	-----	-----	-----	-----	-----	-----	-----	-----	-----	-----	-----	-----	-----	-----	-----	-----	-----	-----	-----	-----	-----	-----	-----	-----	-----	-----	-----	-----	-----	-----	-----	-----	-----	-----	-----	-----	-----	-----	-----	-----	-----	-----	-----	-----	-----	-----	-----	-----	-----	-----	-----	-----	-----	-----	-----	-----	-----	-----	-----	-----	-----	-----	-----	-----	-----	-----	-----	-----	-----	-----	-----	-----	-----	-----	-----	-----	-----	-----	-----	-----	-----	-----	-----	-----	-----	-----	-----	-----	-----	-----	-----	-----	-----	-----	-----	-----	-----	-----	-----	-----	-----	-----	-----	-----	-----	-----	-----	-----	-----	-----	-----	-----	-----	-----	-----	-----	-----	-----	-----	-----	-----	-----	-----	-----	-----	-----	-----	-----	-----	-----	-----	-----	-----	-----	-----	-----	-----	-----	-----	-----	-----	-----	-----	-----	-----	-----	-----	-----	-----	-----	-----	-----	-----	-----	-----	-----	-----	-----	-----	-----	-----	-----	-----	-----	-----	-----	-----	-----	-----	-----	-----	-----	-----	-----	-----	-----	-----	-----	-----	-----	-----	-----	-----	-----	-----	-----	-----	-----	-----	-----	-----	-----	-----	-----	-----	-----

7.7	Compression Diagonal EJ	110
7.8	Tension Diagonal HF	113
7.9	Generator KL	113
7.10	Discussion of Asymmetrical Load Tests	118

CHAPTER VIII PRESENTATION AND DISCUSSION OF TEST RESULTS

	FOUNDATION SETTLEMENT	125
8.1	Introduction	125
8.2	Measured Reactions	125
8.3	Gable Beams	126
8.4	Ridge Beams	126
8.5	Compression Diagonal EJ	132
8.6	Tension Diagonal HF	132
8.7	Discussion of Test 5	132

CHAPTER IX PRESENTATION AND DISCUSSION OF TEST

	TO DESTRUCTION	136
9.1	Introduction	136
9.2	Mode of Failure	136
9.3	Linearity of Strains	140
9.4	Deflection Readings	140
9.5	Bending Moments	140
9.6	Primary Cause of Failure	142
9.7	Discussion	147

CHAPTER X	SUMMARY, RECOMMENDATIONS AND CONCLUSIONS	149
10.1	Summary	149
10.2	Recommendations for Future Work	152
10.3	Conclusions	153

BIBLIOGRAPHY	156
--------------	-----

APPENDIX A	Cements for the Application of Strain Gauges to a Concrete Surface	A-1
------------	--	-----

APPENDIX B	Concrete Properties	B-1
------------	---------------------	-----

192. *Chlorophyll a* and *Chlorophyll b* in *Chlorella* sp.

193. *Chlorophyll a* and *Chlorophyll b* in *Chlorella* sp.

194. *Chlorophyll a* and *Chlorophyll b* in *Chlorella* sp.

195. *Chlorophyll a* and *Chlorophyll b* in *Chlorella* sp.

196. *Chlorophyll a* and *Chlorophyll b* in *Chlorella* sp.

197. *Chlorophyll a* and *Chlorophyll b* in *Chlorella* sp.

198. *Chlorophyll a* and *Chlorophyll b* in *Chlorella* sp.

199. *Chlorophyll a* and *Chlorophyll b* in *Chlorella* sp.

LIST OF FIGURES

FIGURE		Page
2.1	Element of a Shell of Double Curvature	10
2.2	Isometric View of Hyperbolic Paraboloid Surface	10
2.3	Beam Thrusts in Gable Type H. P. Shell as Found by Membrane Theory	10
3.1	Details of Formwork	12
3.2	Details of Formwork	13
3.3	View of Completed Formwork	14
3.4	Finished Model After Curing Period	14
3.5	Plan, Elevation and Sections of Model	15
3.6	Beam Cross Sections	16
3.7	Reinforcing Details	20
3.8	Corner Support Assembly Drawing	24
3.9	Corner Support Details	25
3.10	Shoe Plate Detail	26
3.11	Settling Support Details	27
3.12	Load Cell and Roller Details	28
3.13	General Arrangement of Loading System	31
3.14	Load Distribution System Details	32

FIGURE		Page
3.15	Load Distribution System Details	33
3.16	View of Typical Support	34
3.17	View of Test Setup	34
4.1	Summary of Loading Patterns Used	36
5.1	Location and Numbering of Strain Gauges	45
5.2	Location and Numbering of Ames Dials	48
5.3	View of Completed Instrumentation	49
5.4	View of Data Processor	49
	SYMMETRICAL LOAD TESTS	
6.1	Strain vs Load Curves for Symmetrical Loading	51
6.2	Measured Strains in Gable Beams - Test #1 - 6,000# Load	53
6.3	Measured Strains in Gable Beams - Test #4 - 6,000# Load	54
6.4	Measured Strains in Gable Beams - Test #6 - 6,000# Load	56
6.5	Measured Strains in Gable Beams - Test #7	57
6.6	Gable Beam Deflections - Tests No. 1 and 4	59
6.7	Gable Beam Deflections - Tests No. 6 and 7	60
6.8	Gable Beam Bending Moments Derived From Measured Strains and Deflections - 6,000# Load	62
6.9	Gable Beam Axial Thrusts Derived From Strain Readings - 6,000# Uniform Load	62A

100		
101		1000000
102	1000000	1000000
103	1000000	1000000
104	1000000	1000000
105	1000000	1000000
106	1000000	1000000
107	1000000	1000000
108	1000000	1000000
109	1000000	1000000
110	1000000	1000000
111	1000000	1000000
112	1000000	1000000
113	1000000	1000000
114	1000000	1000000
115	1000000	1000000
116	1000000	1000000
117	1000000	1000000
118	1000000	1000000
119	1000000	1000000
120	1000000	1000000
121	1000000	1000000
122	1000000	1000000
123	1000000	1000000
124	1000000	1000000
125	1000000	1000000
126	1000000	1000000
127	1000000	1000000
128	1000000	1000000
129	1000000	1000000
130	1000000	1000000
131	1000000	1000000
132	1000000	1000000
133	1000000	1000000
134	1000000	1000000
135	1000000	1000000
136	1000000	1000000
137	1000000	1000000
138	1000000	1000000
139	1000000	1000000
140	1000000	1000000
141	1000000	1000000
142	1000000	1000000
143	1000000	1000000
144	1000000	1000000
145	1000000	1000000
146	1000000	1000000
147	1000000	1000000
148	1000000	1000000
149	1000000	1000000
150	1000000	1000000

FIGURE

Page

6.10	Measured Strains in Ridge Beams - Test No. 1 - 6,000# Load	67
6.11	Measured Strains in Ridge Beams - Test No. 4 - 6,000# Load	68
6.12	Measured Strains in Ridge Beams - Test No. 6 - 6,000# Load	69
6.13	Ridge Beam Deflections Relative to Gable Beam Junction	70
6.14	Ridge Beam Bending Moments Derived From Strain Readings	71
6.15	Ridge Beam Axial Thrusts Derived From Strain Readings	72
6.16	Surface Strains, Bending Moments and Axial Stresses for Diagonal E-J - Tests No. 1 and 4	74
6.17	Surface Strains, Bending Moments and Axial Stresses for Diagonal E-J - Tests No. 6 and 7	75
6.18	Surface Strains, Bending Moments and Axial Stresses for Diagonal H-F - Tests No. 1 and 4	77
6.19	Surface Strains, Bending Moments and Axial Stresses for Diagonal H-F - Tests No. 6 and 7	78
6.20	Surface Strains, Bending Moments and Axial Stresses for Section K-L - Test No. 4	79
6.21	Surface Strains, Bending Moments and Axial Stresses for Section K-L - Test No. 6	80
ASYMMETRICAL LOAD TESTS		
7.1	Horizontal and Vertical Reactions at the Corners	86
7.2	Measured Strains in Gable Beams Without Loading Symmetry Top Fibres - Tests No. 2 and 3	88

Page	Description	Amount
101	Jan 1 1880 Balance forward	100 00
102	Jan 2 1880 To Cash	50 00
103	Jan 3 1880 By Cash	25 00
104	Jan 4 1880 To Cash	75 00
105	Jan 5 1880 By Cash	30 00
106	Jan 6 1880 To Cash	100 00
107	Jan 7 1880 By Cash	40 00
108	Jan 8 1880 To Cash	60 00
109	Jan 9 1880 By Cash	20 00
110	Jan 10 1880 To Cash	80 00
111	Jan 11 1880 By Cash	10 00
112	Jan 12 1880 To Cash	90 00
113	Jan 13 1880 By Cash	5 00
114	Jan 14 1880 To Cash	70 00
115	Jan 15 1880 By Cash	15 00
116	Jan 16 1880 To Cash	110 00
117	Jan 17 1880 By Cash	35 00
118	Jan 18 1880 To Cash	65 00
119	Jan 19 1880 By Cash	25 00
120	Jan 20 1880 To Cash	85 00
121	Jan 21 1880 By Cash	10 00
122	Jan 22 1880 To Cash	95 00
123	Jan 23 1880 By Cash	5 00
124	Jan 24 1880 To Cash	75 00
125	Jan 25 1880 By Cash	15 00
126	Jan 26 1880 To Cash	105 00
127	Jan 27 1880 By Cash	35 00
128	Jan 28 1880 To Cash	65 00
129	Jan 29 1880 By Cash	25 00
130	Jan 30 1880 To Cash	85 00
131	Jan 31 1880 By Cash	10 00
132	Feb 1 1880 To Cash	95 00
133	Feb 2 1880 By Cash	5 00
134	Feb 3 1880 To Cash	75 00
135	Feb 4 1880 By Cash	15 00
136	Feb 5 1880 To Cash	105 00
137	Feb 6 1880 By Cash	35 00
138	Feb 7 1880 To Cash	65 00
139	Feb 8 1880 By Cash	25 00
140	Feb 9 1880 To Cash	85 00
141	Feb 10 1880 By Cash	10 00
142	Feb 11 1880 To Cash	95 00
143	Feb 12 1880 By Cash	5 00
144	Feb 13 1880 To Cash	75 00
145	Feb 14 1880 By Cash	15 00
146	Feb 15 1880 To Cash	105 00
147	Feb 16 1880 By Cash	35 00
148	Feb 17 1880 To Cash	65 00
149	Feb 18 1880 By Cash	25 00
150	Feb 19 1880 To Cash	85 00
151	Feb 20 1880 By Cash	10 00
152	Feb 21 1880 To Cash	95 00
153	Feb 22 1880 By Cash	5 00
154	Feb 23 1880 To Cash	75 00
155	Feb 24 1880 By Cash	15 00
156	Feb 25 1880 To Cash	105 00
157	Feb 26 1880 By Cash	35 00
158	Feb 27 1880 To Cash	65 00
159	Feb 28 1880 By Cash	25 00
160	Feb 29 1880 To Cash	85 00
161	Feb 30 1880 By Cash	10 00
162	Mar 1 1880 To Cash	95 00
163	Mar 2 1880 By Cash	5 00
164	Mar 3 1880 To Cash	75 00
165	Mar 4 1880 By Cash	15 00
166	Mar 5 1880 To Cash	105 00
167	Mar 6 1880 By Cash	35 00
168	Mar 7 1880 To Cash	65 00
169	Mar 8 1880 By Cash	25 00
170	Mar 9 1880 To Cash	85 00
171	Mar 10 1880 By Cash	10 00
172	Mar 11 1880 To Cash	95 00
173	Mar 12 1880 By Cash	5 00
174	Mar 13 1880 To Cash	75 00
175	Mar 14 1880 By Cash	15 00
176	Mar 15 1880 To Cash	105 00
177	Mar 16 1880 By Cash	35 00
178	Mar 17 1880 To Cash	65 00
179	Mar 18 1880 By Cash	25 00
180	Mar 19 1880 To Cash	85 00
181	Mar 20 1880 By Cash	10 00
182	Mar 21 1880 To Cash	95 00
183	Mar 22 1880 By Cash	5 00
184	Mar 23 1880 To Cash	75 00
185	Mar 24 1880 By Cash	15 00
186	Mar 25 1880 To Cash	105 00
187	Mar 26 1880 By Cash	35 00
188	Mar 27 1880 To Cash	65 00
189	Mar 28 1880 By Cash	25 00
190	Mar 29 1880 To Cash	85 00
191	Mar 30 1880 By Cash	10 00
192	Mar 31 1880 To Cash	95 00
193	Apr 1 1880 By Cash	5 00
194	Apr 2 1880 To Cash	75 00
195	Apr 3 1880 By Cash	15 00
196	Apr 4 1880 To Cash	105 00
197	Apr 5 1880 By Cash	35 00
198	Apr 6 1880 To Cash	65 00
199	Apr 7 1880 By Cash	25 00
200	Apr 8 1880 To Cash	85 00
201	Apr 9 1880 By Cash	10 00
202	Apr 10 1880 To Cash	95 00
203	Apr 11 1880 By Cash	5 00
204	Apr 12 1880 To Cash	75 00
205	Apr 13 1880 By Cash	15 00
206	Apr 14 1880 To Cash	105 00
207	Apr 15 1880 By Cash	35 00
208	Apr 16 1880 To Cash	65 00
209	Apr 17 1880 By Cash	25 00
210	Apr 18 1880 To Cash	85 00
211	Apr 19 1880 By Cash	10 00
212	Apr 20 1880 To Cash	95 00
213	Apr 21 1880 By Cash	5 00
214	Apr 22 1880 To Cash	75 00
215	Apr 23 1880 By Cash	15 00
216	Apr 24 1880 To Cash	105 00
217	Apr 25 1880 By Cash	35 00
218	Apr 26 1880 To Cash	65 00
219	Apr 27 1880 By Cash	25 00
220	Apr 28 1880 To Cash	85 00
221	Apr 29 1880 By Cash	10 00
222	Apr 30 1880 To Cash	95 00
223	May 1 1880 By Cash	5 00
224	May 2 1880 To Cash	75 00
225	May 3 1880 By Cash	15 00
226	May 4 1880 To Cash	105 00
227	May 5 1880 By Cash	35 00
228	May 6 1880 To Cash	65 00
229	May 7 1880 By Cash	25 00
230	May 8 1880 To Cash	85 00
231	May 9 1880 By Cash	10 00
232	May 10 1880 To Cash	95 00
233	May 11 1880 By Cash	5 00
234	May 12 1880 To Cash	75 00
235	May 13 1880 By Cash	15 00
236	May 14 1880 To Cash	105 00
237	May 15 1880 By Cash	35 00
238	May 16 1880 To Cash	65 00
239	May 17 1880 By Cash	25 00
240	May 18 1880 To Cash	85 00
241	May 19 1880 By Cash	10 00
242	May 20 1880 To Cash	95 00
243	May 21 1880 By Cash	5 00
244	May 22 1880 To Cash	75 00
245	May 23 1880 By Cash	15 00
246	May 24 1880 To Cash	105 00
247	May 25 1880 By Cash	35 00
248	May 26 1880 To Cash	65 00
249	May 27 1880 By Cash	25 00
250	May 28 1880 To Cash	85 00
251	May 29 1880 By Cash	10 00
252	May 30 1880 To Cash	95 00
253	May 31 1880 By Cash	5 00
254	May 31 1880 Balance forward	100 00

FIGURE

Page

7.3	Measured Strains in Gable Beams Without Loading Symmetry Bottom Fibres - Tests No. 2 and 3	89
7.4	Deflections of Gable Beams Without Loading Symmetry - Tests No. 2 and 3	90
7.5	Bending Moments in Gable Beams Without Loading Symmetry - Tests No. 2 and 3	91
7.6	Axial Thrusts in Gable Beams Without Loading Symmetry - Tests No. 2 and 3	92
7.7	Measured Strains in Gable Beams Having Loading Symmetry (Loaded Side) - Tests No. 2 and 3	95
7.8	Measured Strains in Gable Beams Having Loading Symmetry (Unloaded Side) - Tests No. 2 and 3	96
7.9	Deflection of Gable Beams Having Loading Symmetry - Tests No. 2 and 3	97
7.10	Bending Moments of Gable Beams Having Loading Symmetry - Tests No. 2 and 3	98
7.11	Axial Thrusts in Gable Beams Having Loading Symmetry - Tests No. 2 and 3	99
7.12	Measured Strains in Ridge Beam Having Loading Symmetry - Tests No. 2 and 3	101
7.13	Deflection of Ridge Beam Having Loading Symmetry - Tests No. 2 and 3	102

FIGURE

Page

7.14	Moments and Thrusts for Ridge Beam Having Loading Symmetry - Tests No. 2 and 3	103
7.15	Measured Strains in Ridge Beam Without Loading Symmetry - Top Fibres - Tests No. 2 and 3	105
7.16	Measured Strain in Ridge Beam Without Loading Symmetry - Bottom Fibres - Tests No. 2 and 3	106
7.17	Deflection of Ridge Beam Without Loading Symmetry - Tests No. 2 and 3	107
7.18	Bending Moments for Ridge Beam Without Loading Symmetry - Tests No. 2 and 3	108
7.19	Axial Thrust for Ridge Beam Without Loading Symmetry - Tests No. 2 and 3	109
7.20	Surface Strains, Bending Moments and Axial Stresses for Diagonal E-J - Test No. 3	111
7.21	Surface Strains, Bending Moments & Axial Stresses for Diagonal E-J - Test No. 2	112
7.22	Surface Strains, Bending Moments & Axial Stresses for Diagonal E-J - Test No. 3	114
7.23	Surface Strains, Bending Moments & Axial Stresses for Diagonal H-F - Test No. 2	115
7.24	Surface Strains, Bending Moments & Axial Stresses for Section K-L - Test No. 3	116

FIGURE		Page
7.25	Surface Strains, Bending Moments & Axial Stresses for Section K-L - Test No. 2	117
7.26	Equilibrium under Asymmetrical Loading	123
FOUNDATION SETTLEMENT		
8.1	Measured Strains in Gable Beams - Top Fibres - Test No. 5	127
8.2	" " " " " - Bottom " - " "	128
8.3	Bending Moments for Gable Beams - Test No. 5	129
8.4	Axial Thrusts for Gable Beams - Test No. 5	130
8.5	Measured Strains in Ridge Beams - Test No. 5	131
8.6	Surface Strains, Bending Moments & Axial Stresses for Diagonal E-J - Test No. 5	133
8.7	Surface Strains, Bending Moments & Axial Stresses for Diagonal H-F - Test No. 5	134
TEST TO DESTRUCTION		
9.1	Top View of Model after failure	138
9.2	Ridge Beam Junction Viewed from Underside after Failure	138
9.3	Crack Pattern on Underside of Model (Support "C")	139
9.4	Crack Pattern on Underside of Model (Support "A")	139
9.5	Strain vs Load for Gauges on Top of Gable G-H - Test No. 7	141
9.6	Strain vs Load for Gauges on Bottom of Gable GH - Test No. 7	141

FIGURE		Page
9.7	Bending Moments for Ridge Beam DEF at Various Load Increments - Test No. 7	143
9.8	Bending Moments for Gable JFC at Various Load Increments - Test No. 7	144
9.9	Interaction Diagram for Ridge Beam at Centerline	146

CHAPTER I

INTRODUCTION

1.1 Shell Construction

In recent years, there has been a trend towards thin shell construction. Because of the complex mathematics involved in their analysis, many structural engineers have been reluctant to enter into this field in the past. Due to the growing popularity of these shells, however, steps have been taken to advance theories and design methods for various forms of thin shells. To date, very little information has been published about the actual behaviour of concrete shells at working loads or at collapse.

1.2 Model Studies

In arriving at a theoretical solution to a three dimensional problem such as a shell, certain idealizations must be made to simplify the resulting mathematical expressions. These idealizations tend to distort the problem to some extent and for this reason, models are built to see if the assumptions are justified. In Portugal, the design of a structure can be made from model studies without the need to confirm it theoretically. German code DIN 1050 states: "Model studies and photoelastic studies may in certain cases, fully or partially replace the analytical approach".

In England, a number of model studies have been carried out by the Building Research Station (Mitchell, 1957). The Portland Cement Association carried out extensive tests on an umbrella type hyperbolic paraboloid shell in recent years. (PCA - ST 85).

The results of these studies have been helpful in establishing behaviour patterns for particular shells. Due to the time involved in casting such models, however, the data is not nearly so plentiful as, for example, test data on beams or columns. Conclusions must be limited to the parameters used in the model. Extrapolation of results to include a variety of parameters beyond the scope of the tests could be dangerous.

1.3 Object of Testing Program

The scope of this study is limited to one type of shell, the gable type hyperbolic paraboloid having a rise to span ratio of 1:8. The objectives are as follows:

- (a) To build and instrument a model, taking note of difficulties encountered and to make recommendations for a future program of shell research now being contemplated at the University of Alberta.
- (b) To observe the behaviour of the model under various loading patterns and foundation settlements.
- (c) To calculate axial thrusts and bending moments and to compare the results with membrane theory.

- (d) To test the shell to destruction and to observe the mode of failure and study the crack patterns.

CHAPTER II

THEORY

2.1 Assumptions in Membrane Theory

In deriving the membrane theory, it is assumed that bending moments and torsional shears and moments are negligible quantities. It is assumed that deformations are small and the radius of curvature remains unchanged from the unloaded to the loaded state. With this simplification, the problem of solving the stresses in the shell becomes statically determinate. The shell is not required to satisfy conditions of compatibility, but only to satisfy equilibrium requirements. The load is assumed to be carried by direct stresses and shearing stresses acting in the plane of the shell.

2.2 Notation

x, y, z	direction of co-ordinate axes
a	panel length in x direction, or side dimension of square shell
b	panel length in y direction, unless panels are square
h	rise of shell
T_x, T_y	direct stresses tangential to surface
T_{xp}, T_{yp}	stresses projected on the xy plane
S	shearing stresses in the plane of the shell

CHAPTER 1

1.1

1.1.1 Introduction to the Chapter

The first chapter of the book is devoted to the study of the properties of the function $f(x)$ defined on the interval $[a, b]$. The function $f(x)$ is assumed to be continuous on $[a, b]$ and to have a finite limit at the endpoints a and b . The first section of the chapter is devoted to the study of the properties of the function $f(x)$ on the interval $[a, b]$. The second section of the chapter is devoted to the study of the properties of the function $f(x)$ on the interval $[a, b]$. The third section of the chapter is devoted to the study of the properties of the function $f(x)$ on the interval $[a, b]$. The fourth section of the chapter is devoted to the study of the properties of the function $f(x)$ on the interval $[a, b]$. The fifth section of the chapter is devoted to the study of the properties of the function $f(x)$ on the interval $[a, b]$. The sixth section of the chapter is devoted to the study of the properties of the function $f(x)$ on the interval $[a, b]$. The seventh section of the chapter is devoted to the study of the properties of the function $f(x)$ on the interval $[a, b]$. The eighth section of the chapter is devoted to the study of the properties of the function $f(x)$ on the interval $[a, b]$. The ninth section of the chapter is devoted to the study of the properties of the function $f(x)$ on the interval $[a, b]$. The tenth section of the chapter is devoted to the study of the properties of the function $f(x)$ on the interval $[a, b]$.

1.1.2

1.1.2.1 The function $f(x)$ on the interval $[a, b]$

The first section of the chapter is devoted to the study of the properties of the function $f(x)$ on the interval $[a, b]$. The second section of the chapter is devoted to the study of the properties of the function $f(x)$ on the interval $[a, b]$. The third section of the chapter is devoted to the study of the properties of the function $f(x)$ on the interval $[a, b]$. The fourth section of the chapter is devoted to the study of the properties of the function $f(x)$ on the interval $[a, b]$. The fifth section of the chapter is devoted to the study of the properties of the function $f(x)$ on the interval $[a, b]$. The sixth section of the chapter is devoted to the study of the properties of the function $f(x)$ on the interval $[a, b]$. The seventh section of the chapter is devoted to the study of the properties of the function $f(x)$ on the interval $[a, b]$. The eighth section of the chapter is devoted to the study of the properties of the function $f(x)$ on the interval $[a, b]$. The ninth section of the chapter is devoted to the study of the properties of the function $f(x)$ on the interval $[a, b]$. The tenth section of the chapter is devoted to the study of the properties of the function $f(x)$ on the interval $[a, b]$.

1.1.2.2 The function $f(x)$ on the interval $[a, b]$

1.1.2.3 The function $f(x)$ on the interval $[a, b]$

1.1.2.4 The function $f(x)$ on the interval $[a, b]$

1.1.2.5 The function $f(x)$ on the interval $[a, b]$

1.1.2.6 The function $f(x)$ on the interval $[a, b]$

S_p	shearing stresses projected on the xy plane
ϕ	slope from x axis
ψ	slope from y axis
w	uniform vertical load on shell element per unit of area

2.3 Geometric Equations

In shells of translation, the Cartesian system of co-ordinates is usually adopted and will be used herein. FIGURE 2.1 shows an element of a doubly curved shell with its vertical projection on the xy plane. Direct stresses T_x and T_y , measured in pounds per unit of length, are considered positive when they produce tension. Shearing stresses, S also in pounds per unit length are considered positive in the direction shown. That is, a positive shear acting on a positive face acts in the direction of increasing x or y . The surface load, w in pounds per square foot is considered positive when acting downward.

All membrane forces are resolved into components parallel to the co-ordinate system but act tangential to the surface. Thus the force T_x is parallel to the (xz) plane but makes an angle ϕ with the (xy) plane. To simplify the equilibrium equations, the actual forces are transformed into fictitious forces acting on a fictitious element whose dimensions are found by projecting the actual element onto the (xy) plane. These forces are given the subscript p , indicating a projected force.

From geometry, $dp \cos \psi = dy$ 2.1 (a)

$dq \cos \phi = dx$ 2.1 (b)

THE UNIVERSITY OF CHICAGO

1962

THE UNIVERSITY OF CHICAGO

1962

THE UNIVERSITY OF CHICAGO

1962

THE UNIVERSITY OF CHICAGO

1962

THE UNIVERSITY OF CHICAGO

THE UNIVERSITY OF CHICAGO

THE UNIVERSITY OF CHICAGO

THE UNIVERSITY OF CHICAGO

THE UNIVERSITY OF CHICAGO

THE UNIVERSITY OF CHICAGO

THE UNIVERSITY OF CHICAGO

THE UNIVERSITY OF CHICAGO

THE UNIVERSITY OF CHICAGO

THE UNIVERSITY OF CHICAGO

THE UNIVERSITY OF CHICAGO

THE UNIVERSITY OF CHICAGO

THE UNIVERSITY OF CHICAGO

THE UNIVERSITY OF CHICAGO

THE UNIVERSITY OF CHICAGO

THE UNIVERSITY OF CHICAGO

THE UNIVERSITY OF CHICAGO

THE UNIVERSITY OF CHICAGO

The normal force on face "ad" of the element is $T_x dp$ and the horizontal component of this force is $T_x dp \cos \theta$ or $T_x \frac{\cos \theta}{\cos \psi} dy$.

Since the normal force on the projected element must be equal to the force on the actual element,

$$T_{xp} dy = T_x \frac{\cos \theta}{\cos \psi} dy$$

$$\text{or } T_{xp} = T_x \frac{\cos \theta}{\cos \psi} \dots \dots \dots 2.2$$

$$\text{Similarly, } T_{yp} = T_y \frac{\cos \psi}{\cos \theta} \dots \dots \dots 2.3$$

Equating the horizontal component of the shear on face ad to the shear on the projected element,

$$S dp \cos \psi = S_p dy \dots \dots \dots 2.4 (a)$$

From equation 2.1 (a),

$$S = S_p \dots \dots \dots 2.4 (b)$$

2.4 Equilibrium Equations

Only vertical forces will be considered since this is the only type of loading in the scope of this study. Considering the equilibrium in the x direction,

$$(T_{xp} + \frac{\partial T_{xp}}{\partial x} dx) dy - T_{xp} dy + (S_p + \frac{\partial S_p}{\partial y} dy) dx - S_p dx = 0$$

$$\frac{\partial T_{xp}}{\partial x} + \frac{\partial S_p}{\partial y} = 0 \dots \dots \dots 2.5$$

Similarly, in the y direction,

$$\frac{\partial T_{yp}}{\partial y} + \frac{\partial S_p}{\partial x} = 0 \quad . \quad . \quad . \quad 2.6$$

In order to write the equilibrium equations for forces in the z direction, the vertical components of the forces must be found. The vertical component of the force on face ad is $T_x dp \sin \theta$

$$\begin{aligned} \text{But } T_x dp \sin \theta &= T_{xp} \frac{\cos \psi}{\cos \theta} \frac{dy}{\cos \psi} \sin \theta = T_{xp} \tan \theta dy \\ &= T_{xp} \frac{\partial z}{\partial x} dy. \quad 2.7 \end{aligned}$$

The vertical component acting per unit length along the y axis is, therefore, $T_{xp} \frac{\partial z}{\partial x}$ and along the x axis is $T_{yp} \frac{\partial z}{\partial y}$.

The vertical component of shear force on face ad is

$$S dp \sin \psi = S_p \tan \psi dy = S_p \frac{\partial z}{\partial y} dy$$

or, per unit length, is $S_p \frac{\partial z}{\partial y}$

Now, considering equilibrium in the z direction,

$$\frac{\partial}{\partial x} (T_{xp} \frac{\partial z}{\partial x}) + \frac{\partial}{\partial y} (T_{yp} \frac{\partial z}{\partial y}) + \frac{\partial}{\partial x} (S_p \frac{\partial z}{\partial y}) + \frac{\partial}{\partial y} (S_p \frac{\partial z}{\partial x}) + w = 0 \quad . \quad 2.8$$

where w is the load per unit of projected area.

This reduces to

$$\begin{aligned} T_{xp} \frac{\partial^2 z}{\partial x^2} + T_{yp} \frac{\partial^2 z}{\partial y^2} + 2 S_p \frac{\partial^2 z}{\partial x \partial y} \\ + \frac{\partial z}{\partial x} \left(\frac{\partial T_{xp}}{\partial x} + \frac{\partial S_p}{\partial y} \right) + \frac{\partial z}{\partial y} \left(\frac{\partial T_{yp}}{\partial y} + \frac{\partial S_p}{\partial x} \right) = -w \quad . \quad 2.8 (b) \end{aligned}$$

which may be reduced by means of equation 2.9 (c) to

$$- S_p = \frac{ab}{2h} w \dots \dots \dots 2.13$$

By equations 2.5 and 2.6,

$$T_{xp} = C_1 \text{ and } T_{yp} = C_2$$

where C_1 and C_2 are constants of integration.

If we assume the gable beams are unable to carry lateral load, the boundary conditions require that $C_1 = C_2 = 0$

$$\text{Therefore, } T_{xp} = T_{yp} = 0 \dots \dots \dots 2.14$$

Equation 2.14 indicates that the shell is in a state of pure shear of constant intensity when uniformly loaded. Around the periphery the shear must be resisted by the edge members.

2.6 Gable Type Hyperbolic Paraboloid

Applying the foregoing theory to a gable type of H.P. shell, the thrusts in the ridge and gable beams may be readily found. The thrust configurations are plotted in FIGURE 2.3 for the beams.

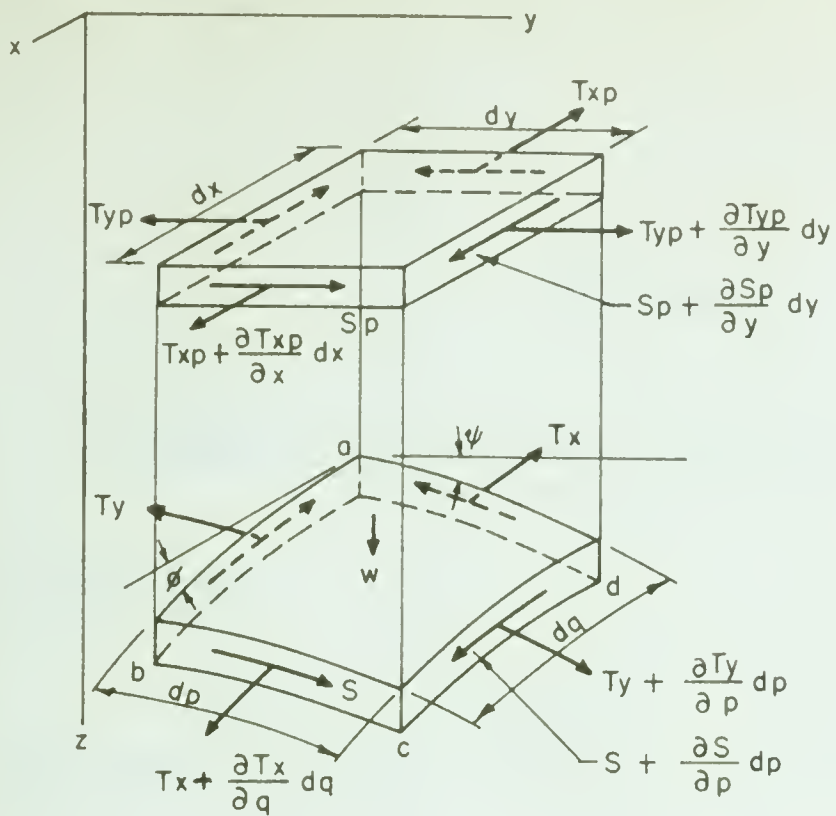


FIGURE 2.1 ELEMENT OF A SHELL OF DOUBLE CURVATURE

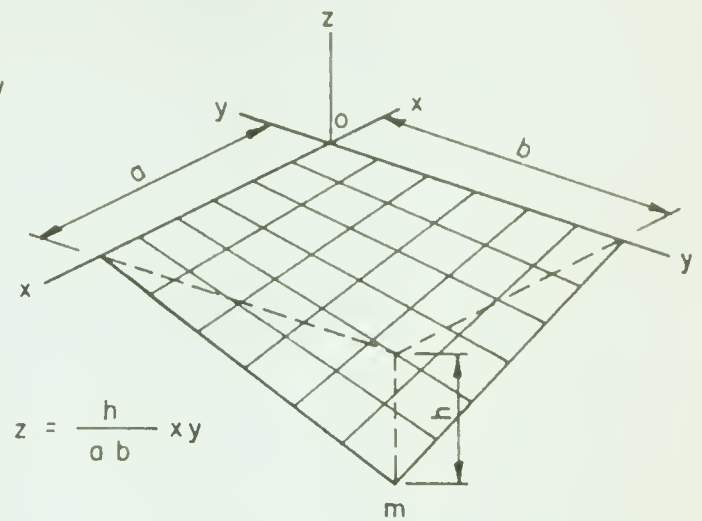


FIGURE 2.2 ISOMETRIC VIEW OF H.P. SURFACE

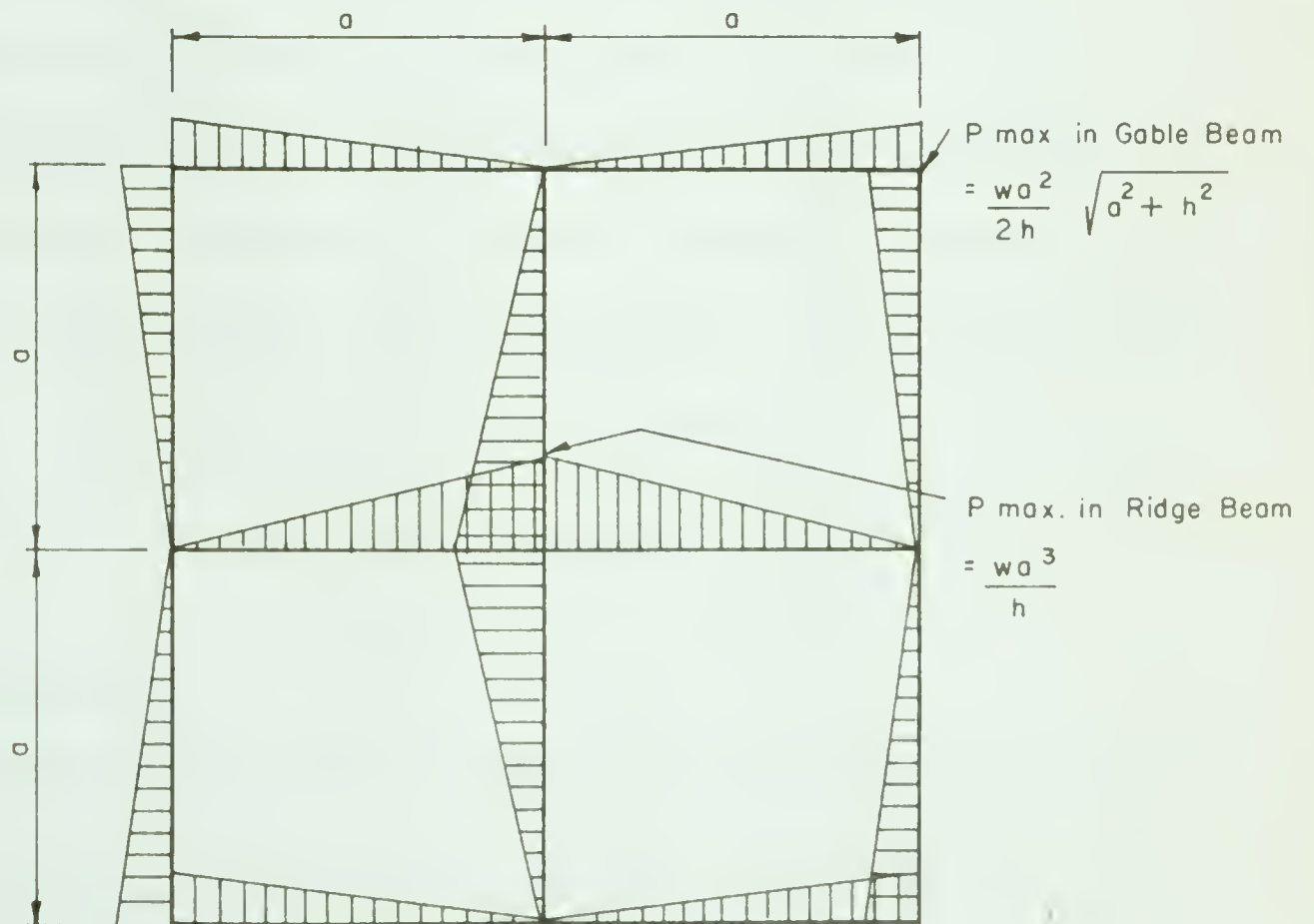


FIGURE 2.3 BEAM THRUSTS IN GABLE TYPE H.P. SHELL AS FOUND BY MEMBRANE THEORY

CHAPTER III

FABRICATION OF MODEL AND TESTING APPARATUS

3.1 Formwork

The formwork for the model shell was built in sections and later assembled by bolting the individual sections together. A plan view of the formwork is shown in FIGURE 3.1, together with cross sections showing the typical details used. FIGURE 3.2 shows details of the ridge and gable frames, and a pictorial view of the completed formwork is given in FIGURE 3.3.

Adjustable foot bolts in the lower plate of the ridge and gable frames permitted easy removal of formwork after the concrete had been cured. Tongue and groove hardwood flooring formed the underside of the shell surface and was easily warped to fit the doubly curved surface. The boards were sanded until no light could be seen under a steel straightedge held at various positions in each direction along the straight line generators of the shell.

3.2 Details of the Model

A pictorial view of the model after casting is given in FIGURE 3.4 while details of the general arrangement and cross sections through the ridge and gable beams are shown in FIGURE 3.5 and 3.6.

The model had a square planform, measuring eight feet between

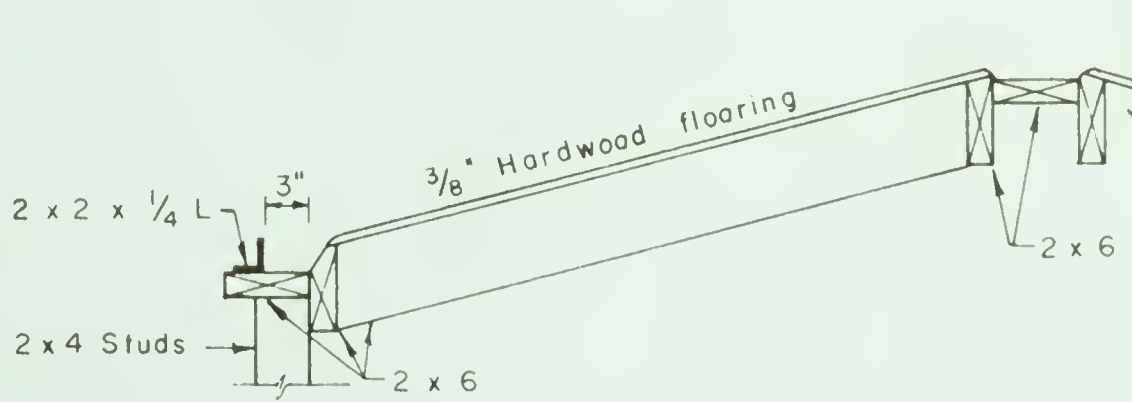
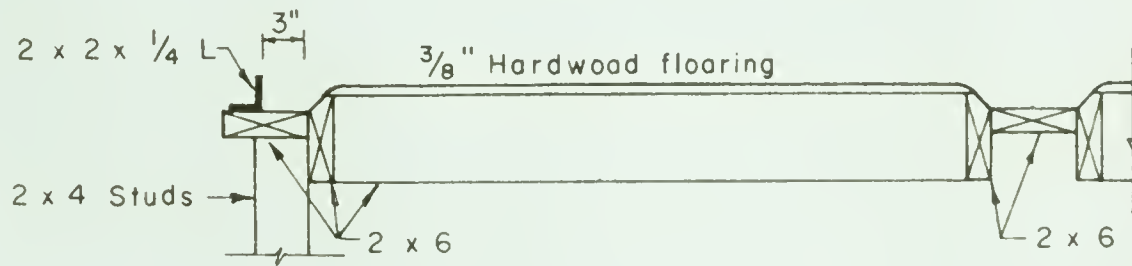
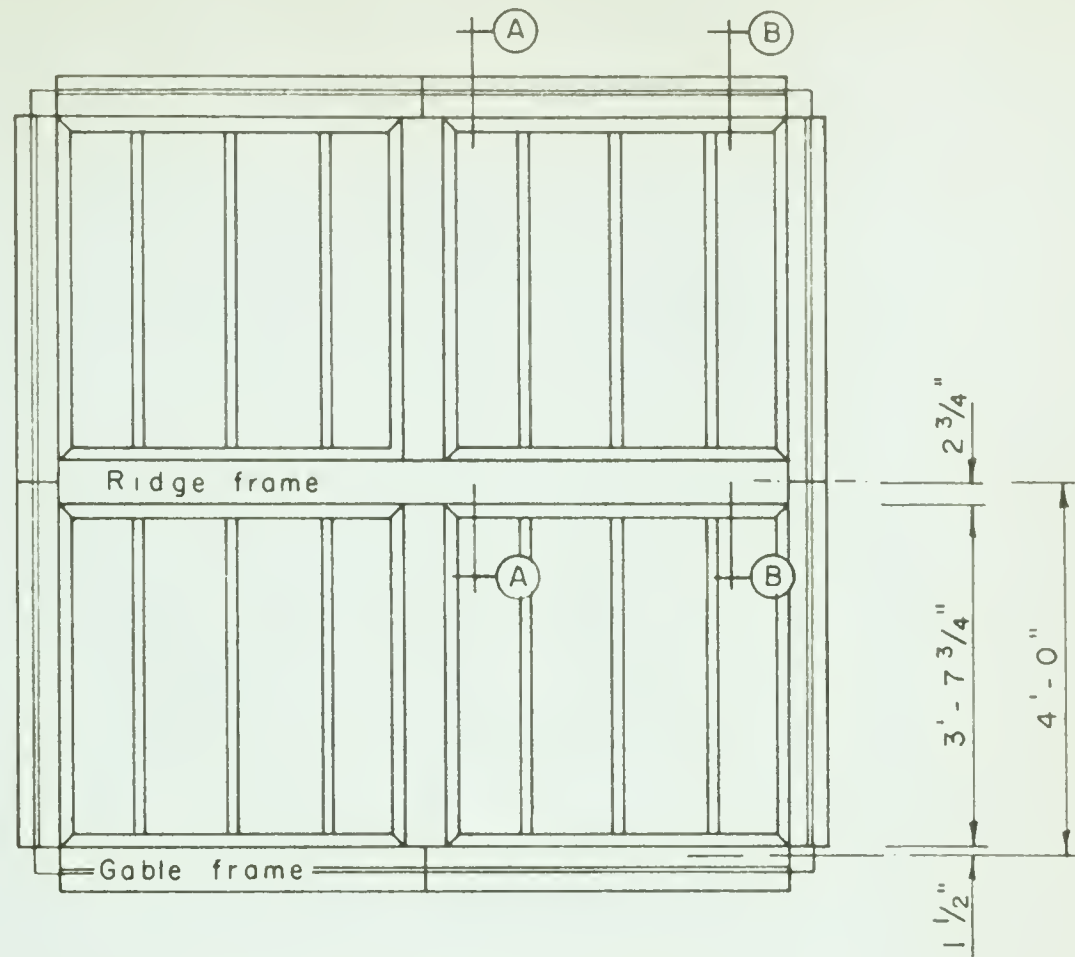
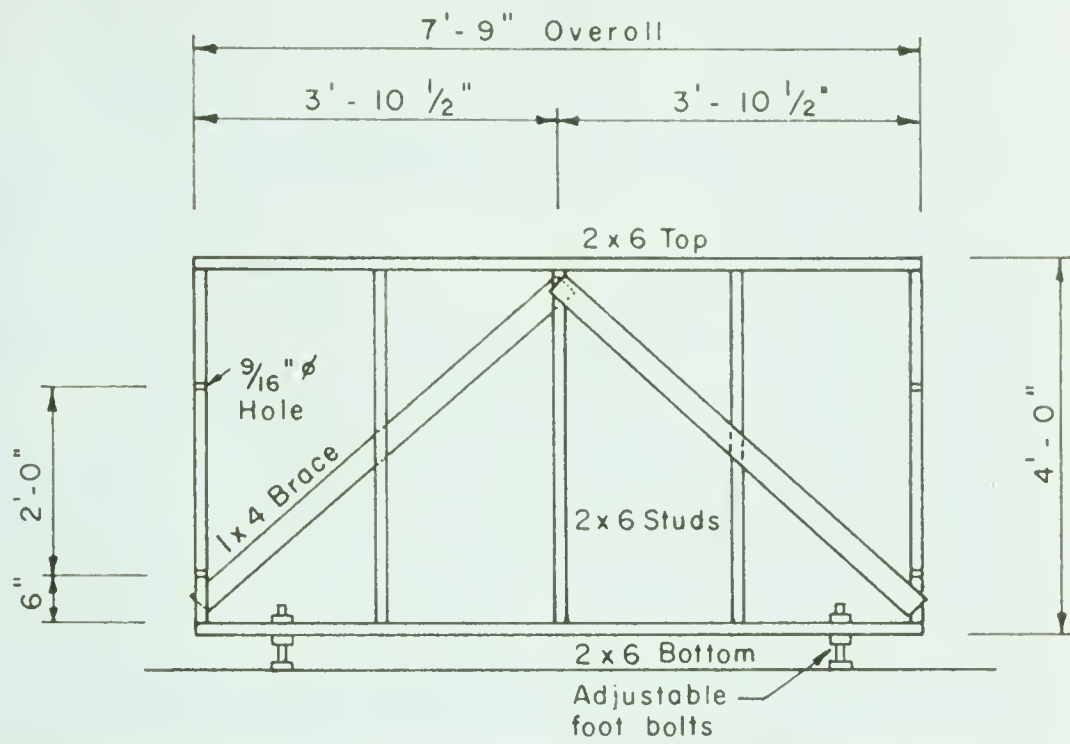


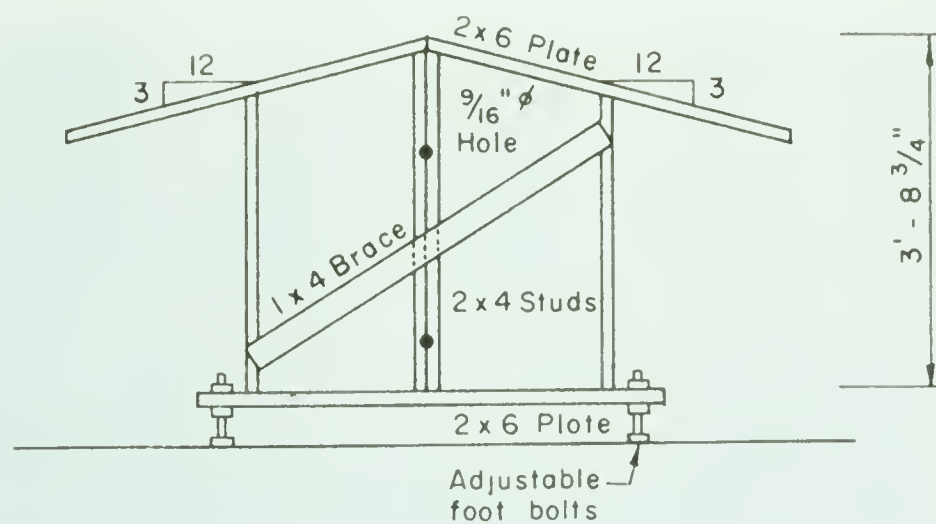
FIGURE 3.1 DETAILS OF FORMWORK





RIDGE FRAME (1 - req'd.)

SCALE: $\frac{3}{8}" = 1' - 0"$



TYPICAL GABLE FRAME (4 - req'd.)

SCALE: $\frac{3}{8}" = 1' - 0"$

FIGURE 3.2 DETAILS OF FORMWORK



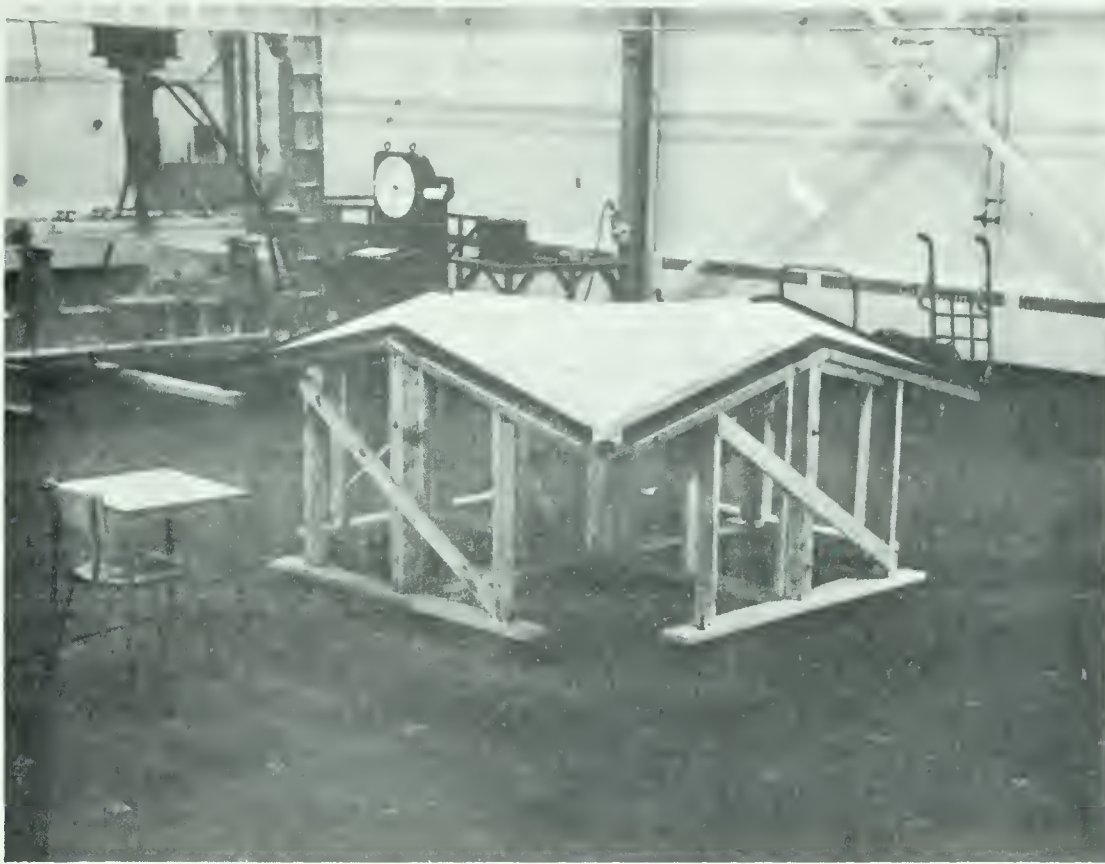


FIGURE 3.3 VIEW OF COMPLETED FORMWORK



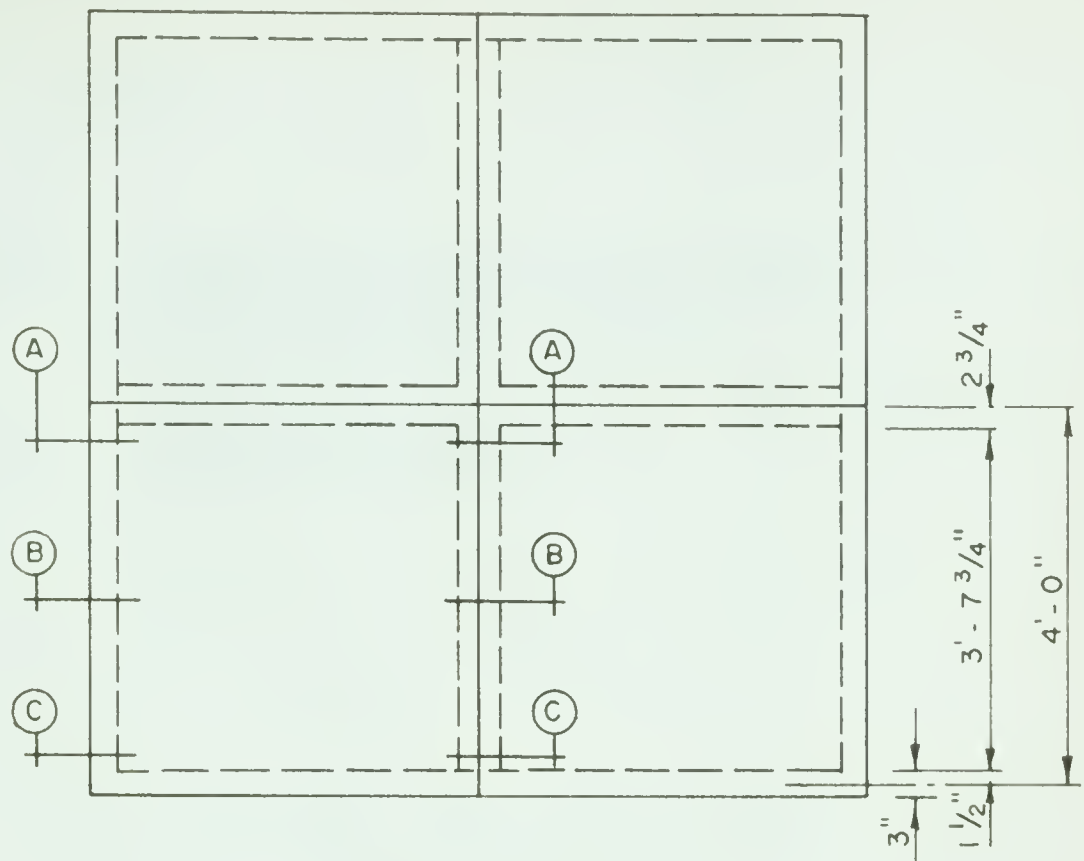
FIGURE 3.4 FINISHED MODEL AFTER CURING PERIOD



THE GREAT HILL, N. B. 1880



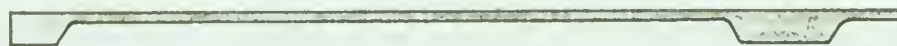
THE GREAT HILL, N. B. 1880



PLAN VIEW
SCALE: $\frac{3}{8}" = 1'-0"$



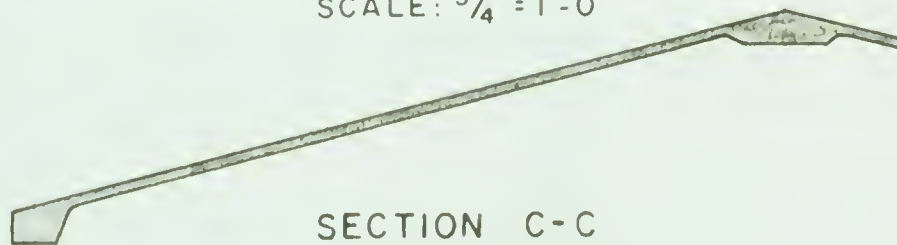
TYPICAL ELEVATION
SCALE: $\frac{3}{4}" = 1'-0"$



SECTION A-A
SCALE: $\frac{3}{4}" = 1'-0"$



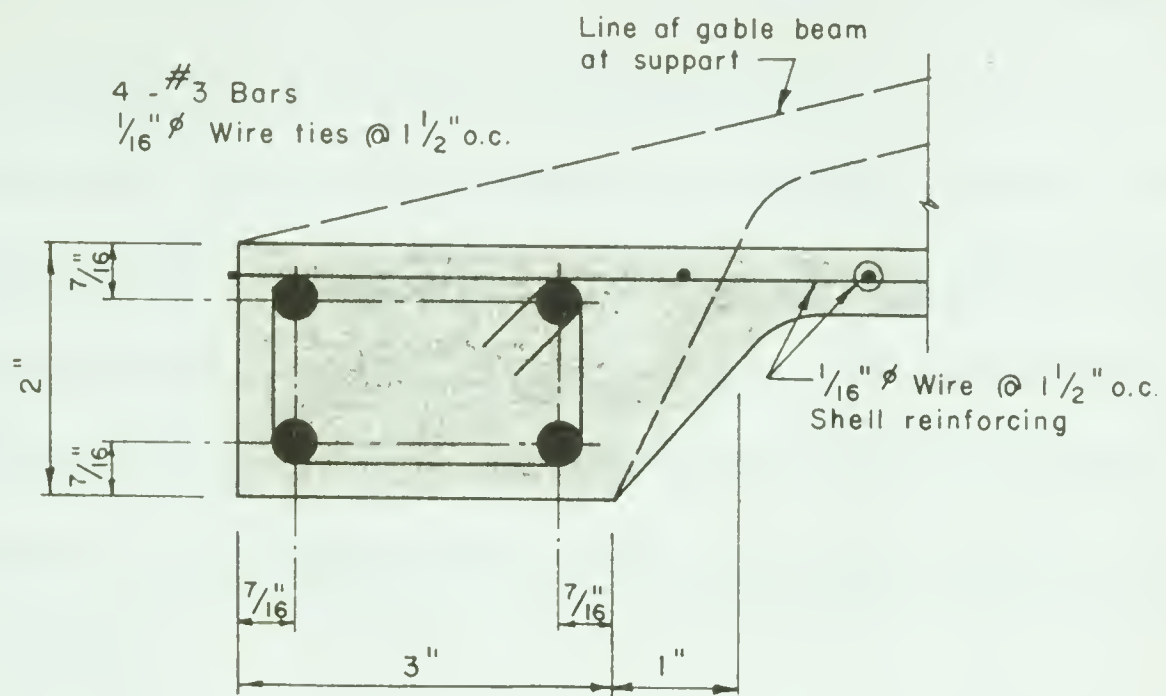
SECTION B-B
SCALE: $\frac{3}{4}" = 1'-0"$



SECTION C-C
SCALE: $\frac{3}{4}" = 1'-0"$

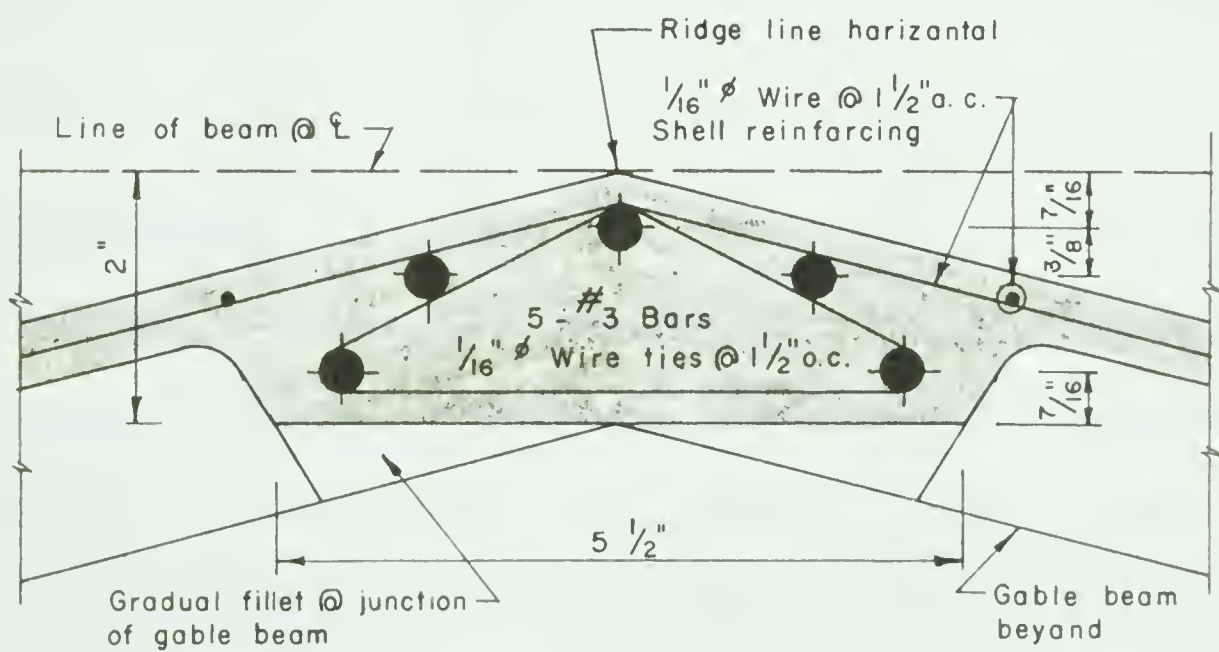
FIGURE 3.5 PLAN, ELEVATION AND SECTIONS OF MODEL





SECTION THRU GABLE BEAM

SCALE: HALF SIZE



SECTION THRU RIDGE BEAM

SCALE: HALF SIZE

FIGURE 3.6 BEAM CROSS SECTIONS

support centres. Both ridge beams were horizontal, and one foot higher than the supports, thus giving a 1:4 slope to the gable beams.

The shell thickness was one half inch. Half inch diameter holes one foot on centre each way were originally intended to accept a system of yolks suspended from the shell, with loads applied by means of four hydraulic jacks located below the floor of the laboratory. Due to the arrival of the loading frames, however, it was later decided to abandon the original scheme in favor of overhead loading.

It may be seen that the centroid of the ridge and gable beams are not coincident with the middle surface of the shell, as assumed in simplified membrane theory, (Timoshenko, 1959; Flugge, 1962). While this feature complicates the analysis, it nevertheless represents a more typical situation in prototype structures, resulting from aesthetic and practical formwork considerations.

3.3 Design of the Model

The model was designed in accordance with simplified membrane theory, except that, in designing the ridge and gable beams, the eccentricity of the applied shear from the shell was taken into account. The Portland Cement Association (1960) advises "the steel should be detailed so that its centroid coincides with the line of application of the shear forces, otherwise, due account should be taken of the eccentricity".

Although the model was considered as a structure in its own right,

to arrive at a reasonable value for dead load as a basis of design, it was assumed to be a model of a hypothetical prototype ten times the size of the model. Thus the model may be considered as representative of a shell having a five inch thickness and a span of eighty feet. Using an assumed snow load of thirty pounds per square foot and a dead load of sixty pounds per square foot, the model was designed to carry a total load of ninety pounds per square foot, uniformly distributed over the projected plan surface.

3.4 Reinforcement

Reinforcing steel used in the ridge and gable beams was taken from stock and was assumed in the design to be intermediate grade, deformed steel conforming to ASTM Specification A 15 - 54T. Subsequent tests showed that the steel had a yield point of 54.6 kips per square inch and an ultimate strength of 82 kips per square inch, which indicates a hard grade steel.

Shell reinforcing steel was 16 gauge (one sixteenth inch diameter) Cold - Drawn Steel Wire conforming to ASTM Specification A 82 - 58T, having a minimum yield point of 64 ksi and an ultimate tensile strength of 80 ksi.

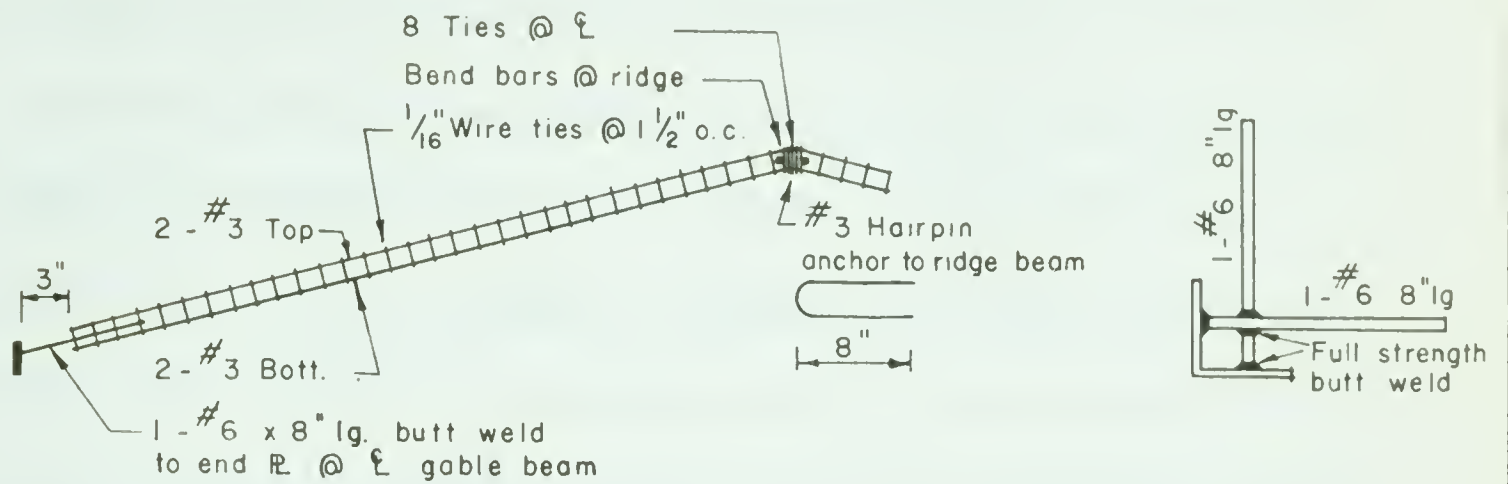
3.5 Placing Reinforcement

The reinforcing steel for the ridge beams and gable beams was prefabricated in cages and later placed on plastic "chairs" on the forms. To insure the accurate placing of steel, plywood templates were built, one for the ridge beam and one for the gable beam, in which holes were drilled at the

theoretical centre of reinforcing steel as shown in FIGURE 3.6. Three eighths inch diameter bolts were inserted in the holes and the stirrups were bent to the correct size around the bolt projection. Stirrups consisted of 16 gauge wire as used for the shell reinforcement.

In order to provide equal effective depth in each ridge beam, it was necessary to butt weld the reinforcing bars at the junction of the two ridge beams. The location of these welds is shown in FIGURE 3.7. To avoid interference at the corners, the gable reinforcing was terminated at the inside face of the corner shoe plate and an equivalent area of steel was added in one bar, crossed and welded as shown in the corner detail of FIGURE 3.7. At the gable and ridge beam junction, a hairpin bar was added to provide a nominal tie between these beams.

The 16 gauge shell reinforcing was anchored at the ends by means of a steel angle which was bolted to the gable frames as shown in FIGURE 3.1. These angles were drilled at one and one half inches on center to permit the wire to pass through at the middle surface of the shell. Wires were stretched across the model in one direction and anchored at each end temporarily by bending the wire through ninety degrees at the outside face of the steel angle. The upper bar in the ridge beam cage served as a chair for the wires and held them firmly in position. Wires in the opposite direction were then threaded through in similar fashion, this time weaving them over and under alternate wires placed previously.

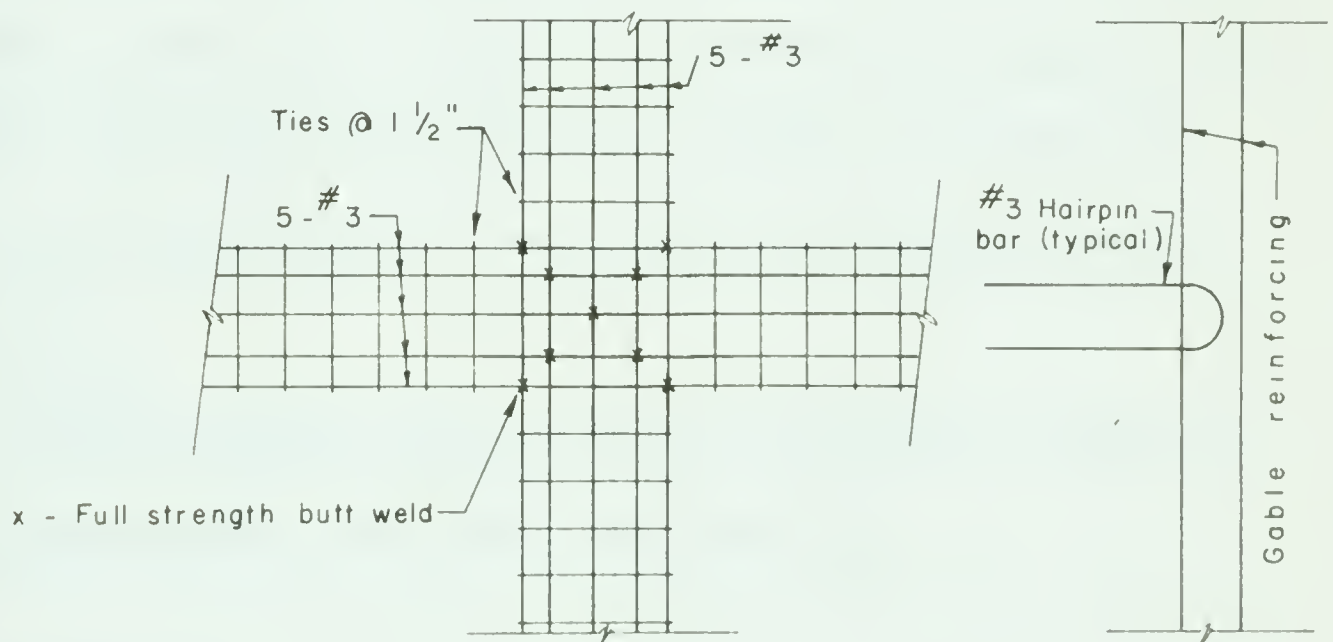


ELEVATION OF REINFORCING CAGE
FOR GABLE BEAM

SCALE $\frac{3}{4}" = 1' - 0"$

CORNER DETAIL

SCALE $1\frac{1}{2}" = 1' - 0"$



REINFORCING DETAIL
@ JUNCTION OF TWO RIDGE BEAMS

SCALE $1\frac{1}{2}" = 1' - 0"$

FIGURE 3.7 REINFORCING DETAILS

Some difficulties were encountered in the weaving operation. Prior to placing any wire, the forms were generously coated with form oil to permit easy removal of the forms from the concrete. During the wire weaving operation, there was a tendency for the wires to come in contact with the form oil which could reduce its bond strength or, perhaps, destroy bond completely in local areas. To prevent such an occurrence, the wires were carefully cleaned after they were finally in position, but this proved to be a particularly arduous task and it is felt that a better method might have been to place a sheet of polythene over the oiled surface until after the wires were in position, then to remove it through the gaps between wires.

A further difficulty was that, as one wire was tightened, the adjacent wires were loosened, and as a result, the wires had to be retightened several times. Due to the brittle nature of the wire, a number of strands broke at the ends through repeated bending. A more ductile wire would have proved more satisfactory .

When the operation was complete, the wires formed a rather stiff mesh which held its position well, without sags and humps.

3.6 Placing Concrete

In order to obtain a strong, well compacted concrete without permitting vibration, a pneumatically placed mortar under the trade name of "Gunit" was used to cast the shell. In this process, the aggregate and cement is first mixed in a dry state. The mixture is forced by compressed

air through the nozzle of a cement "gun" where it comes in contact with water and is projected against the forms with considerable velocity.

During the guniting operation, the heavier sand particles "rebound" from the forms and tend to cause a richer mixture in contact with the forms than is found further away. Once the concrete starts to adhere, however, the rebound is greatly reduced.

The concrete was first placed in the gable and ridge beams, removing the plastic chairs from under the reinforcing cages as the work progressed. Following this, the concrete shell was placed between beams. Frequent pauses were made, at the discretion of the operator, to clean away excess rebound before commencing work in a new area. Final finishing was done by scraping with the edge of a steel trowel using screed plugs on a one foot square grid as a guide to the correct elevations. The entire operation was completed in six hours.

3.7 Mix Properties

The mix consisted of one part cement to two parts sand, mixed dry. Three gallons of water per bag were introduced at the nozzle of the cement gun. The aggregate was well graded and 100% passed the No. 4 screen.

3.8 Curing the Model

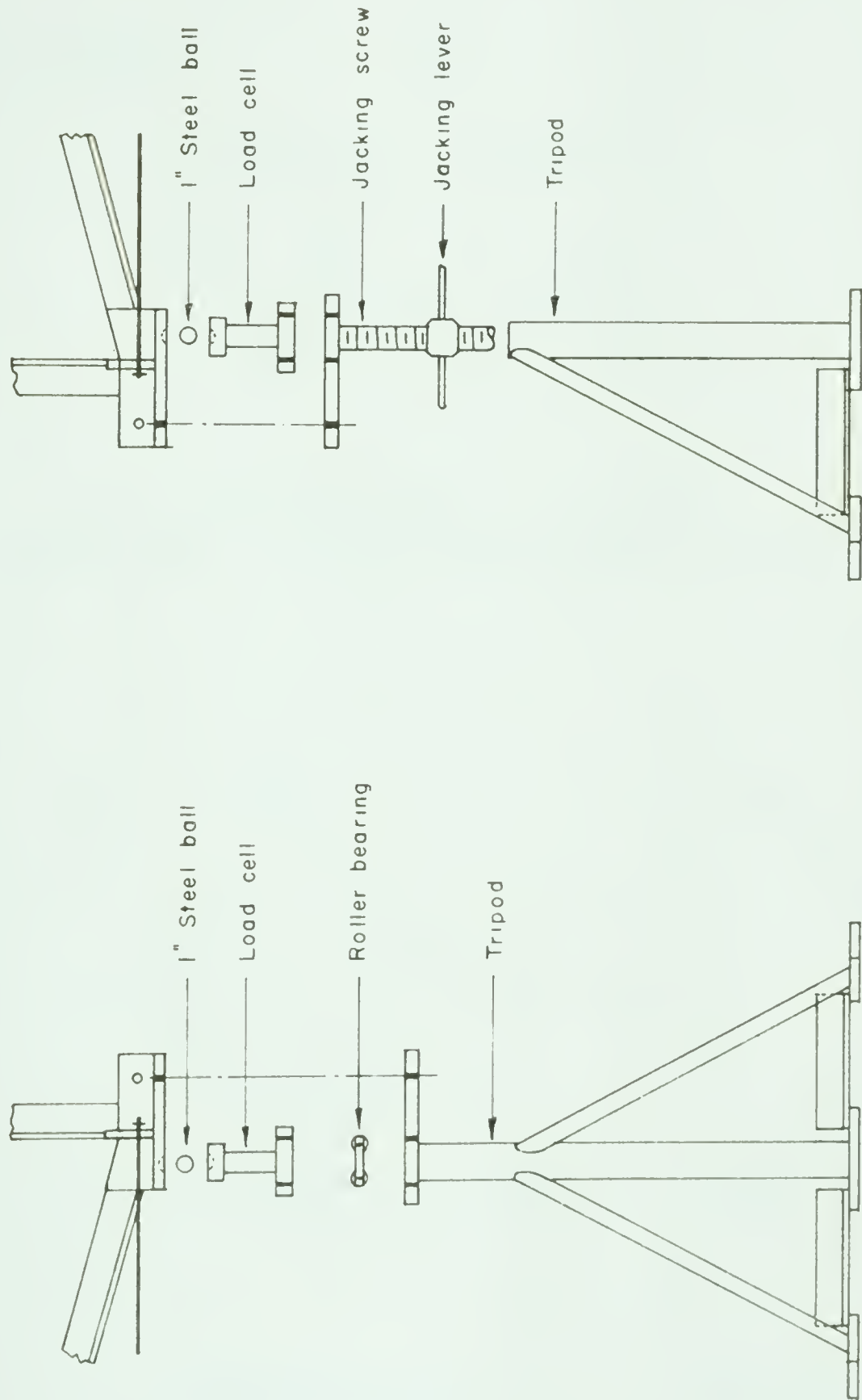
Immediately upon completion of concreting, the model was covered with a large sheet of polythene to prevent drying. After twelve hours, the

polythene was removed and the model was soaked with a hose. Burlap was laid over the wet surface and was itself soaked with a hose. The burlap was again covered with polythene. Twice a day, for fourteen days, the polythene was removed and the burlap soaked. The formwork was removed before finally removing the burlap to prevent any drying shrinkage from taking place while the shell was restrained by the forms.

3.9 Corner Supports

The model was supported on four tripods, one at each corner. The height above the laboratory floor was sufficient to allow access to the underside of the shell to apply instrumentation and to examine the crack patterns during and after the tests. Three of the supports were fixed in elevation while one was vertically adjustable. A corner shoe which was rigidly connected to the concrete shell rested on a one inch diameter steel ball, which rested in a spherical recess in the top of a load cell which, in turn rested on a roller bearing which rolled on a flat plate rigidly fixed to the tripod. Details of the supports are shown in FIGURE 3.8 to 3.12 inclusive.

The vertically adjustable support was not fitted with a roller bearing, so that it became the "pinned" support. The remaining three supports had roller bearings which were oriented in such a way as to confine the movement of the point in question to a line joining the pinned support and the respective roller. Thus the roller in the corner diagonally across from the pinned support was placed at forty five degrees to each gable beam meeting at the

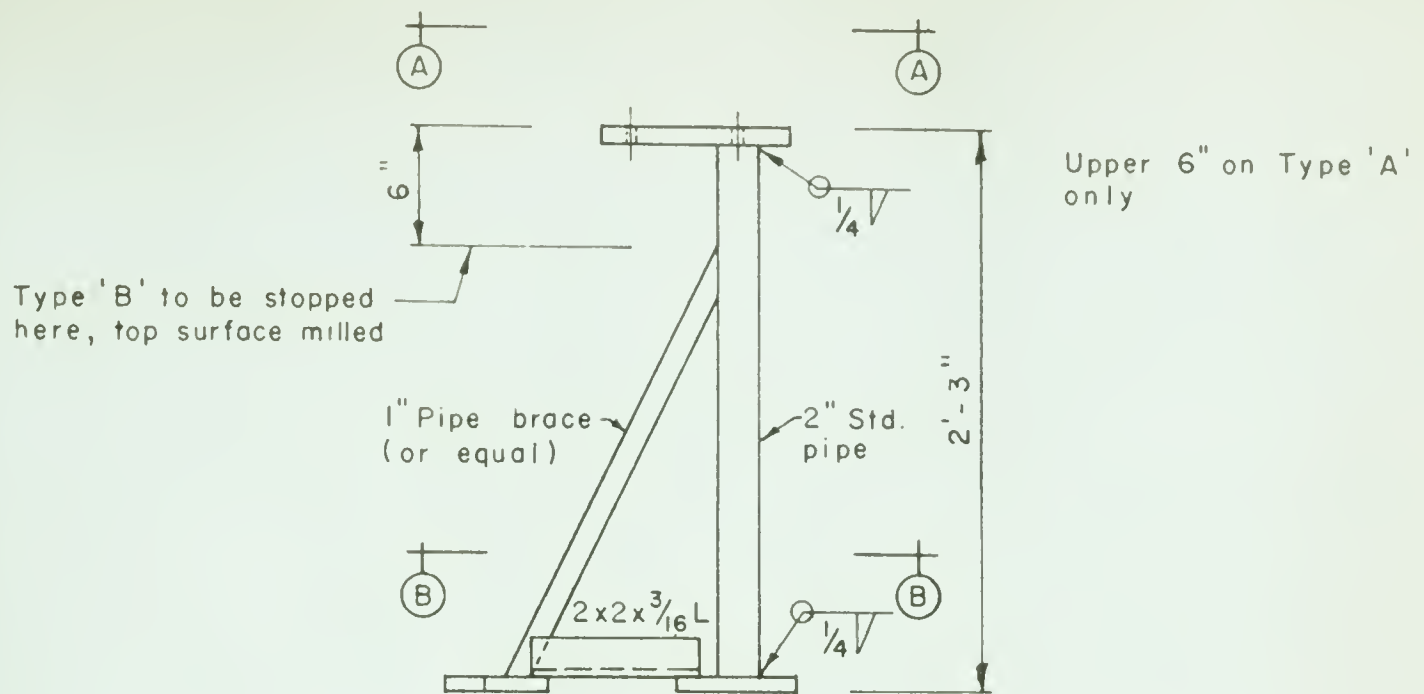


SUPPORT TYPE 'A' (3 - req'd.)
 WITH HORIZONTAL MOVEMENT PERMITTED
 SCALE 1" = 1'-0"

SUPPORT TYPE 'B' (1 - req'd.)
 WITH ADJUSTABLE VERTICAL MOVEMENT
 SCALE 1" = 1'-0"

FIGURE 3.8 CORNER SUPPORT ASSEMBLY

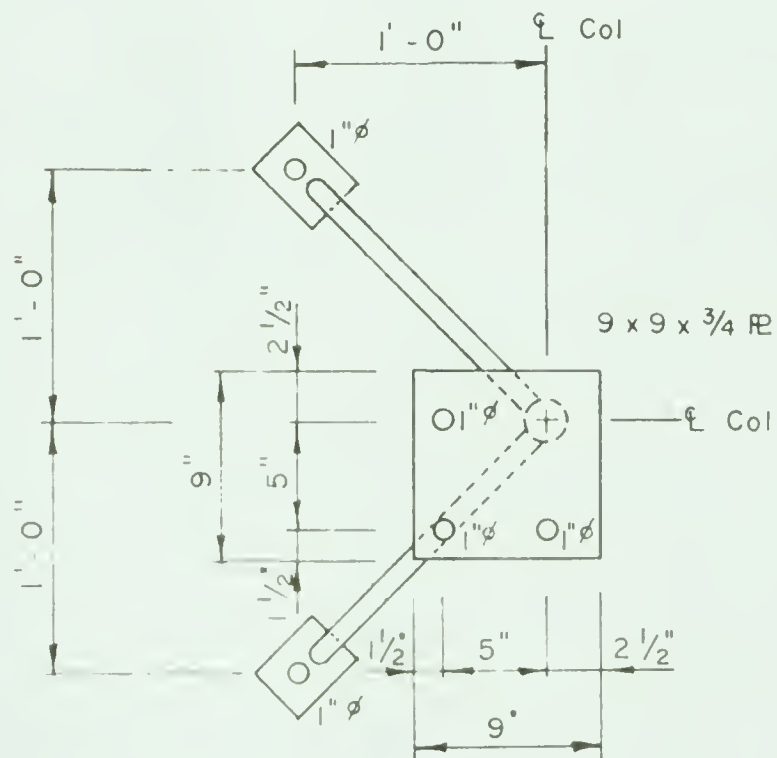




SUPPORT TYPE 'A' (3 - req'd.)

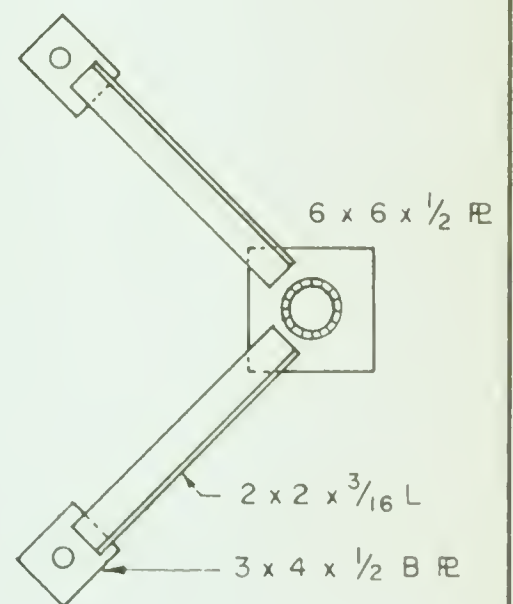
Support Type 'B' - similar except as noted (1 - req'd.)

SCALE 1" = 1'-0"



SECTION A-A

SCALE 1" = 1'-0"



SECTION B-B

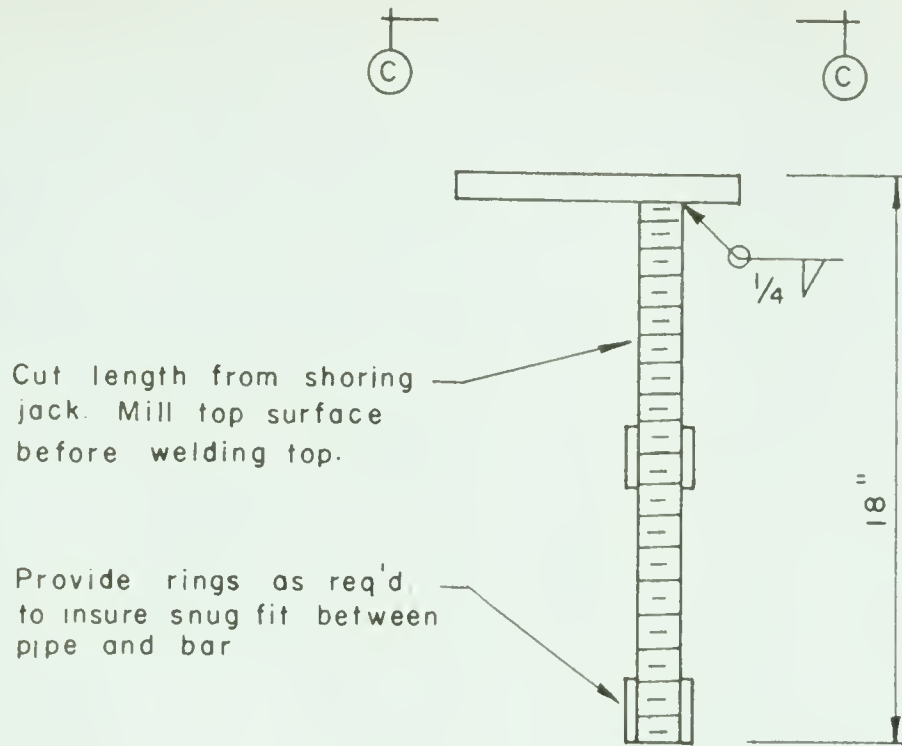
SCALE : 1" = 1'-0"

FIGURE 3.9 CORNER SUPPORT DETAILS

Technical drawing showing a cross-section of a bearing assembly. The drawing includes the following dimensions and labels:

- Two vertical bars, each labeled $\frac{1}{4}"$ Reinforcing bar welded to R_E .
- A central bearing surface labeled $\frac{3}{4}"$ Bearing surface.
- A dimension of $1\frac{1}{4}"$ for the distance from the centerline to the center of each bar.
- A dimension of $1\frac{1}{2}" R.$ for the radius of the bearing surface.
- A label $1" \text{ Ball bearing to fit in this depression}$ pointing to the central area.

FIGURE 3.10 SHOE PLATE DETAIL

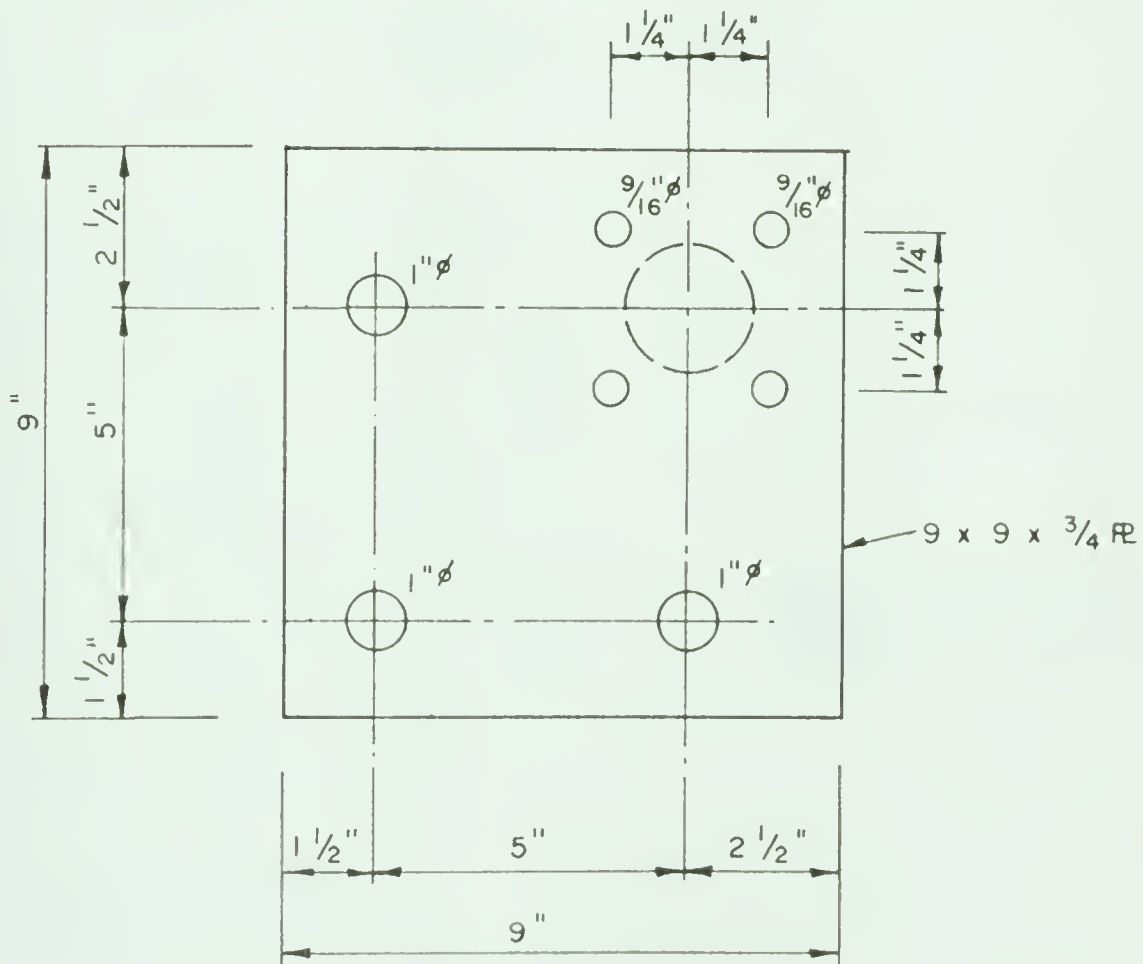


NOTE:

Bearing surface of jacking lever to be milled

VERTICAL ADJUSTING SCREW

SCALE: 1 1/2" = 1' - 0"

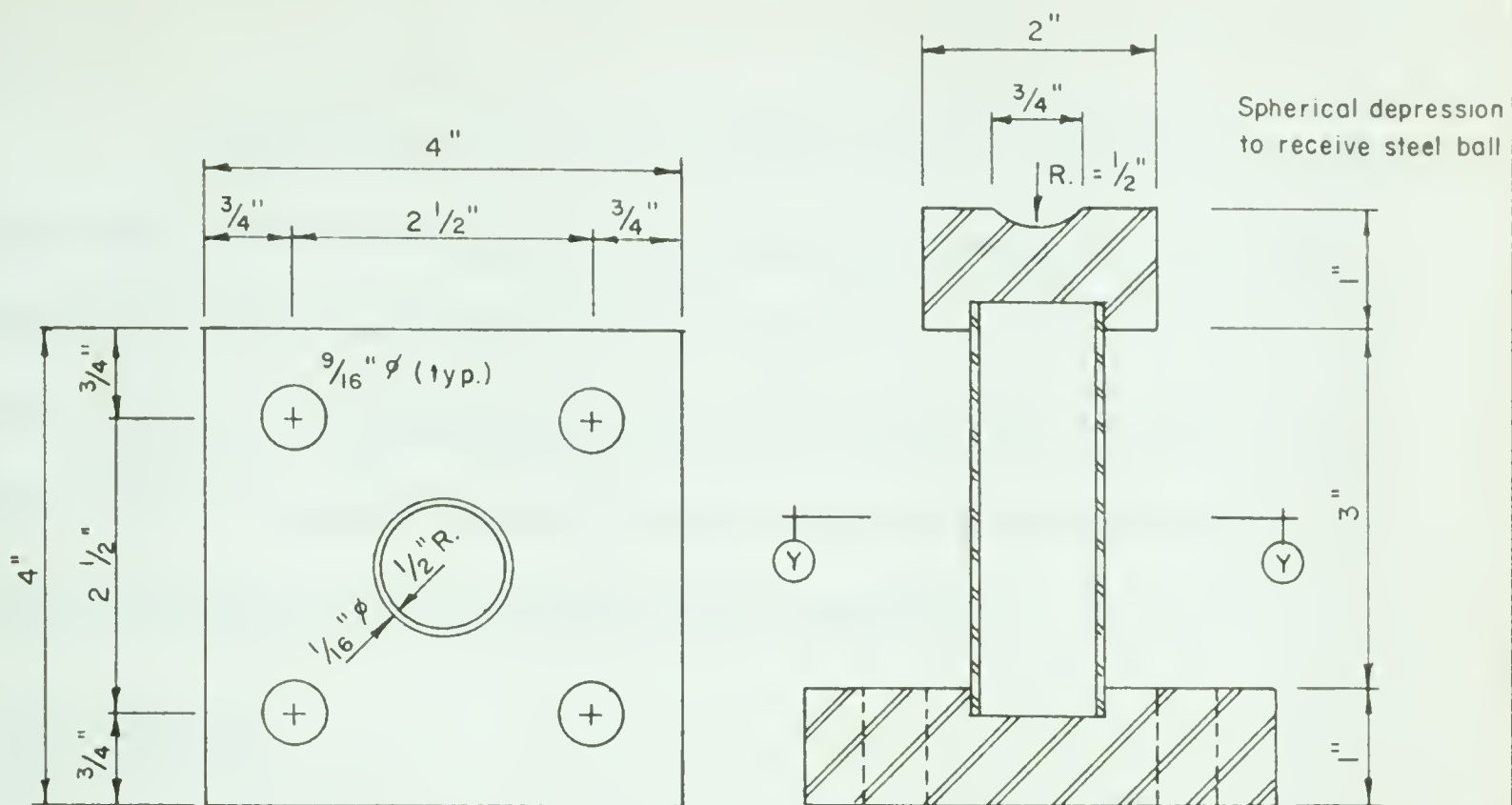


SECTION C-C

SCALE: 3" = 1' - 0"

FIGURE 3.II SETTLING SUPPORT DETAIL



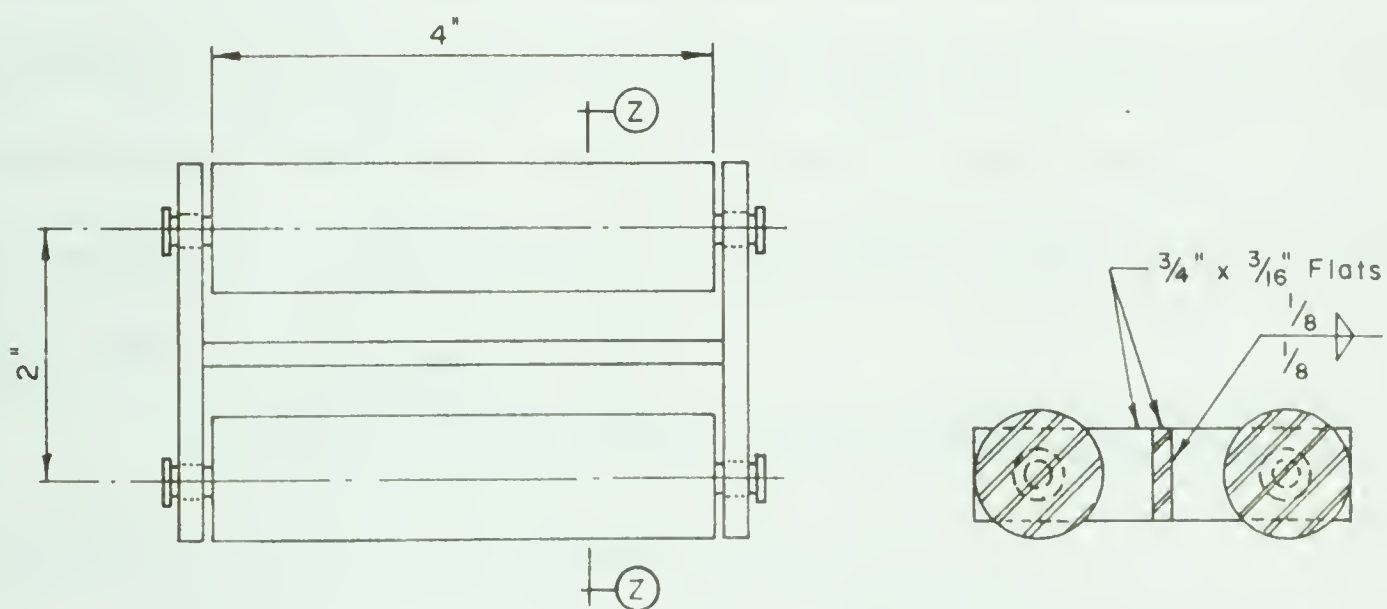


SECTION Y-Y

CROSS SECTION THRU C

LOAD CELL DETAIL

SCALE : 1/2 FULL SIZE



PLAN VIEW

SECTION Z-Z

ROLLER DETAIL

SCALE : 1/2 FULL SIZE

FIGURE 3.12 LOAD CELL AND ROLLER DETAILS

corner.

A closeup view of the corner support is given in FIGURE 3.16. The three bolts which held the corner shoe in position while concrete was placed were left in position during all testing, but the nuts were loosened and the bolts were not permitted to bind during the test. It was felt that in the event of a roller slipping out, the bolts would prevent excessive damage to the shell. As it was later discovered, such precaution was unnecessary.

3.10 Test Setup

FIGURE 3.17 shows an overall view of the testing equipment used. The load was applied at a single point by an Amsler hydraulic jack of forty four kips capacity. This load was distributed through a series of pin jointed members to rubber bearing pads on the surface of the shell on a one foot square grid. The jack was bolted to the main beam of the loading frame and was adjustable along the length of that beam. As a safety feature, a load catching device was suspended from the loading frame to a saddle about two inches below the main beam of the load distributing system.

The load was measured by the Amsler Pendulum Dynamometer, Type PM 103, seen in the foreground of FIGURE 3.17.

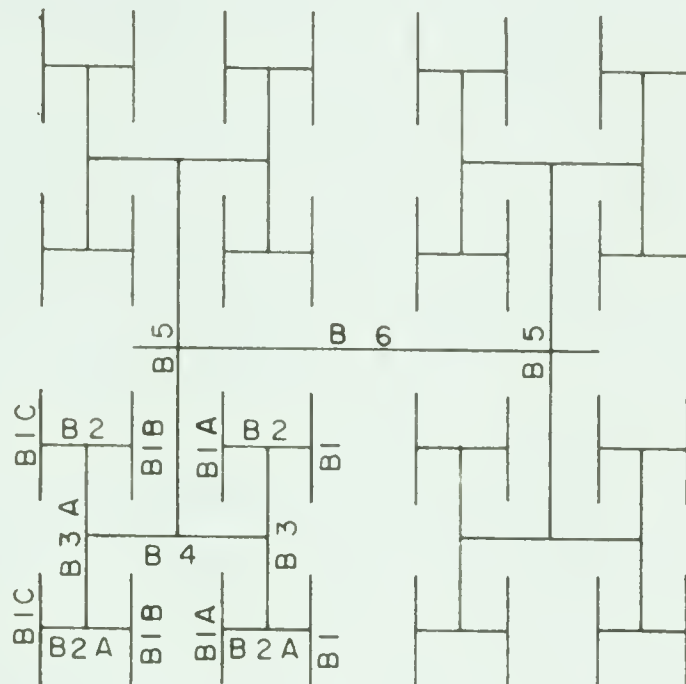
The apparatus on the left is an automatic data processor which was used to record surface strains on the model and will be described in more detail in Chapter IV.

3.11 Load Distributing System

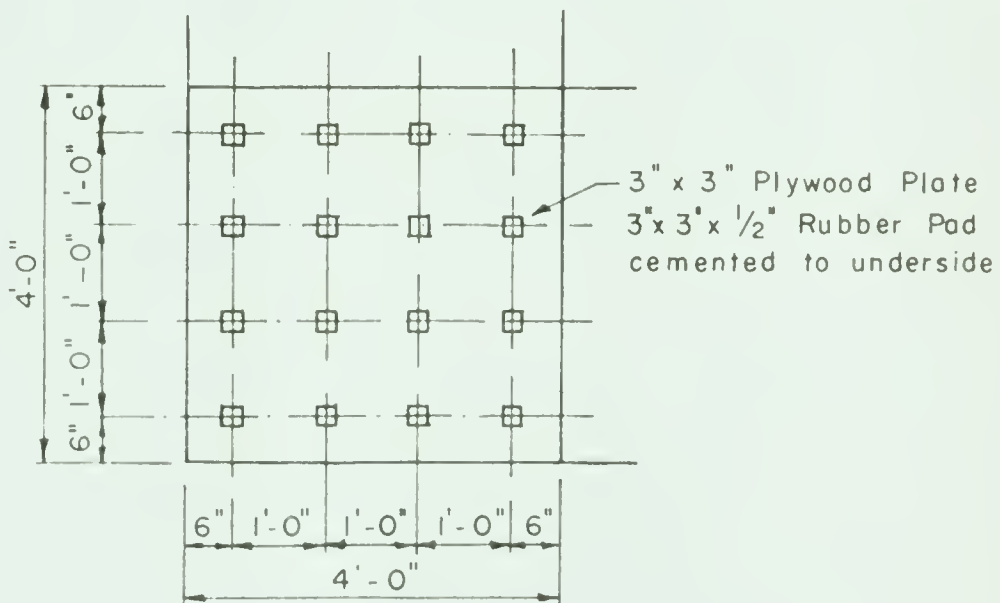
The load, as mentioned previously, was applied at the midspan of beam B6 as shown in FIGURE 3.13. This beam was pinned at each end so that half the load was distributed to each beam B5. In a similar way, the load was further subdivided by pin ended beams until finally, it was applied as sixty four point loads at each end of each Beam B1. These point loads were applied to 3" x 3" plywood plates with 3" x 3" x 1/2" rubber bearing pads glued to the underside of the plywood. In this way, it was thought that, as nearly as practicable, the applied load could be considered as uniformly distributed over the surface of the shell.

Furthermore, by simply shifting the position of the jack along beam B6, the amount of uniform load on one half of the shell could be varied with respect to the load on the other half. By applying the load at the junction of beam B5 and B6, theoretically all the load is applied to one half of the shell only. In actual practice, a small portion of the load may be transmitted to the opposite side due to frictional resistance to rotation on the head of the jack.

Details of the individual beams in the load distributing system are given in FIGURES 3.14 and 3.15.



DIAGRAMATIC REPRESENTATION
OF LOAD DISTRIBUTION SYSTEM
SCALE: $\frac{3}{8}" = 1'-0"$



PLAN VIEW - TYPICAL QUADRANT
SHOWING LOAD BEARING PADS
SCALE $\frac{3}{8}" = 1'-0"$

FIGURE 3.13 GENERAL ARRANGEMENT OF LOADING SYSTEM

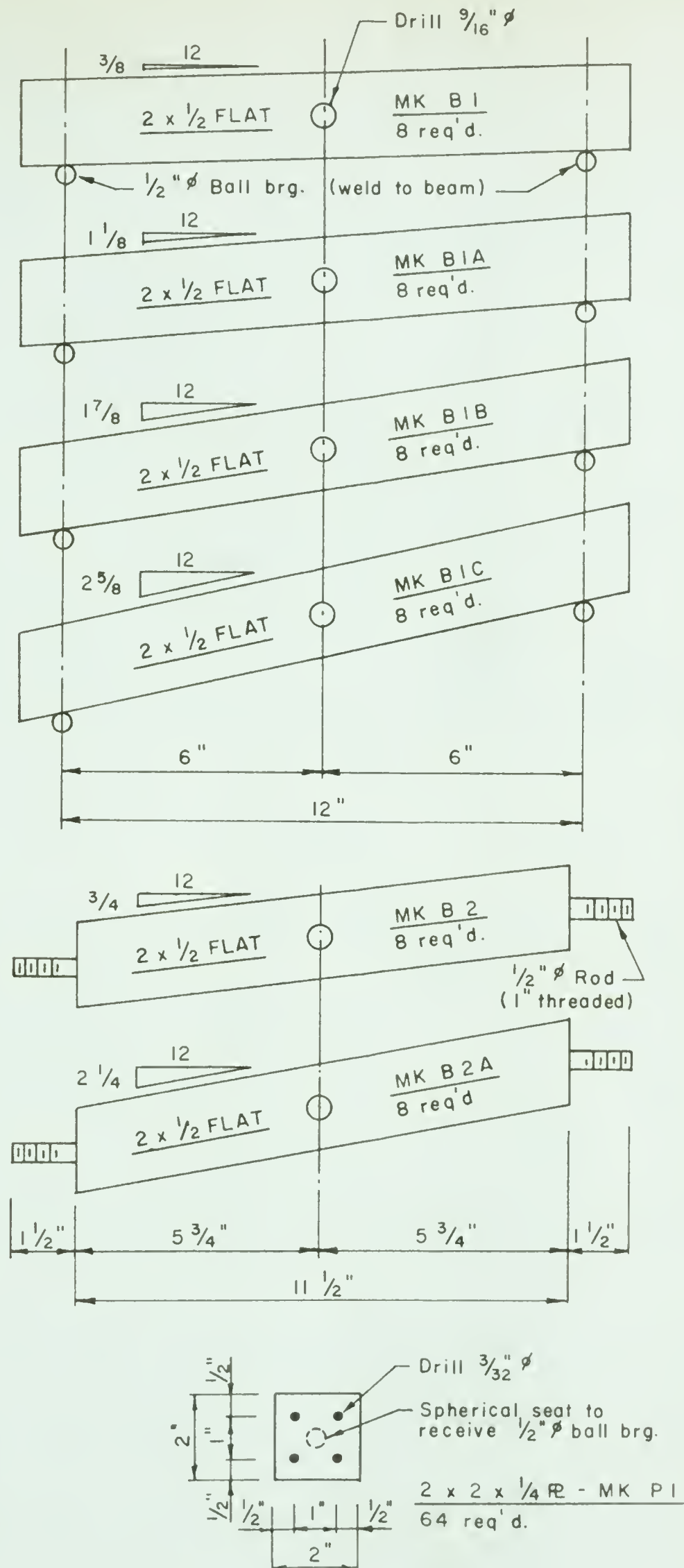


FIGURE 3.14 LOAD DISTRIBUTION SYSTEM DETAILS

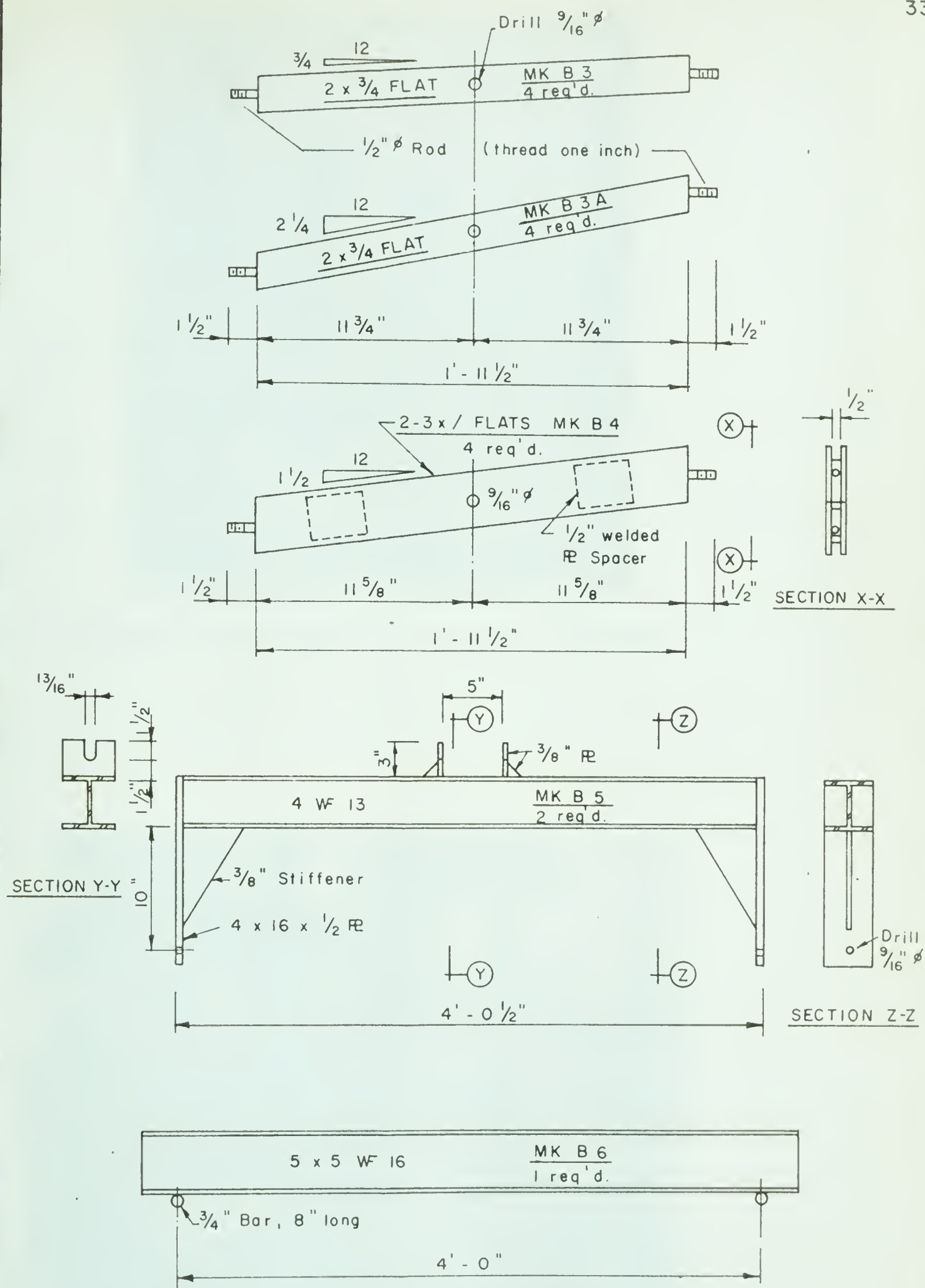


FIGURE 3.15 LOAD DISTRIBUTION SYSTEM DETAILS

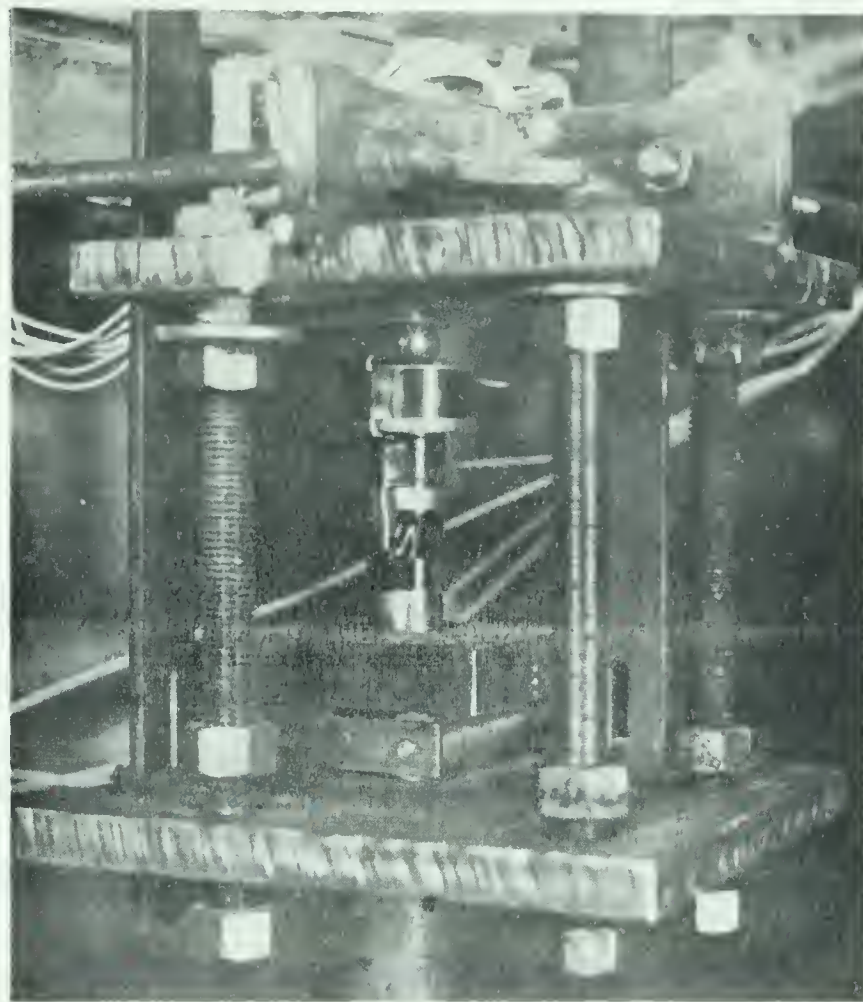


FIGURE 3.16 VIEW OF TYPICAL SUPPORT

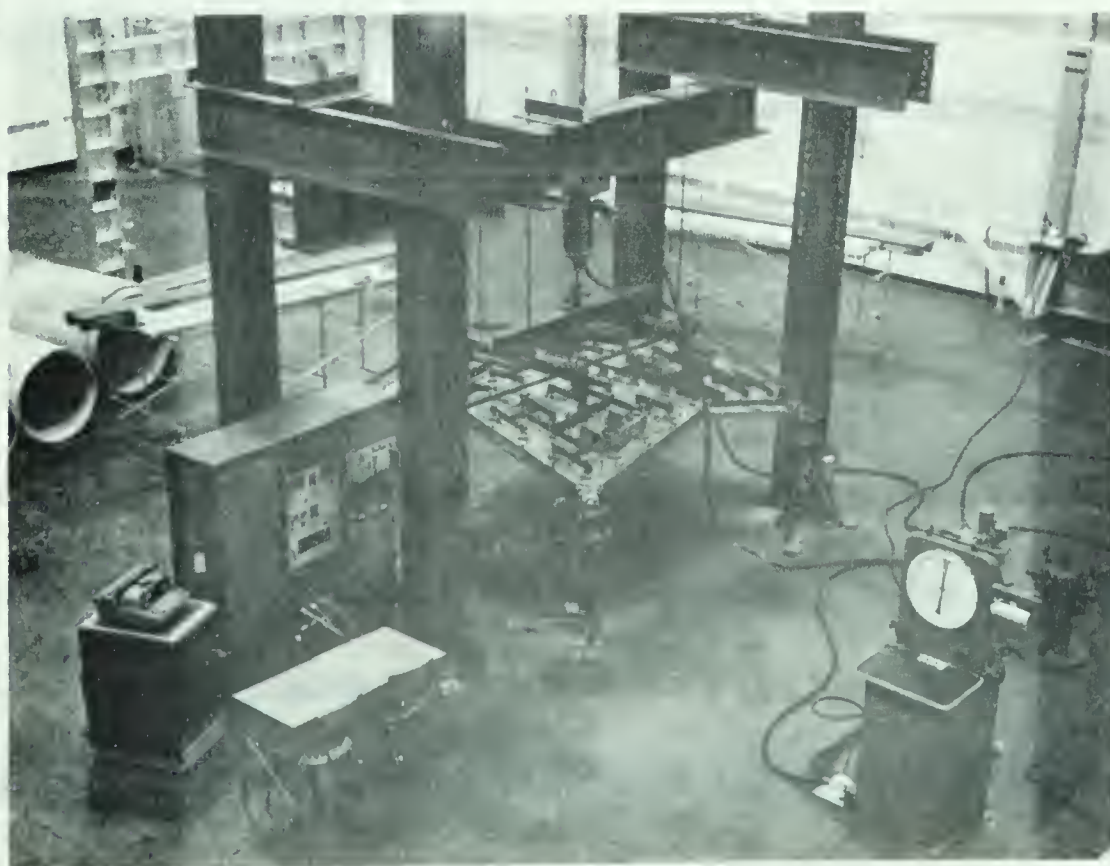


FIGURE 3.17 VIEW OF TEST SETUP



Figure 1. A rectangular object, possibly a book cover or a piece of paper, with a dark, textured surface.



Figure 2. A rectangular object, possibly a book cover or a piece of paper, with a dark, textured surface.

CHAPTER IV

TESTING PROGRAM

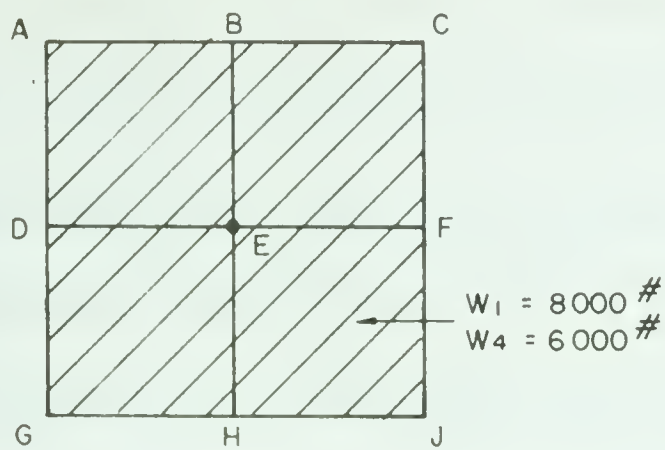
4.1 Description of Tests

In total, seven tests were carried out on the shell, each test unique in at least one respect, however, the testing may be broken down into three main categories. The first was a uniform load over the entire shell surface, the second a uniform load over only two adjacent quadrants and the third a test on the effect of a foundation settlement at one corner without the application of any superimposed load other than the weight of the load distributing device. FIGURE 4.1 shows the various load patterns used in Tests 1 through 7.

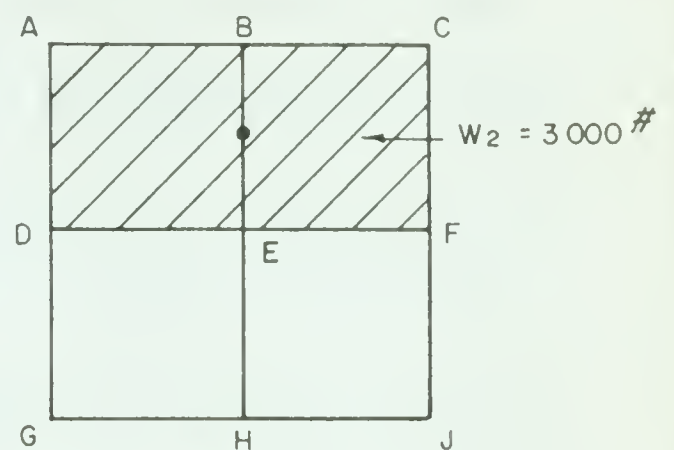
4.2 Symmetrical Load Tests

Tests 1, 4, 6 and 7 were each carried out with uniform load over the entire shell surface. In Test 1, a one half inch tie rod was used, which was sized on the basis of conventional membrane analysis as mentioned previously and is considered representative of a typical prototype designed economically. Test 4 is almost identical to Test 1 and serves as a check on the latter. The only difference was the method of reading the strain gauges which will be mentioned later. In Tests 1 and 4 the load was increased in increments of one thousand pounds to a maximum of 8,000# and 6,000# respectively.

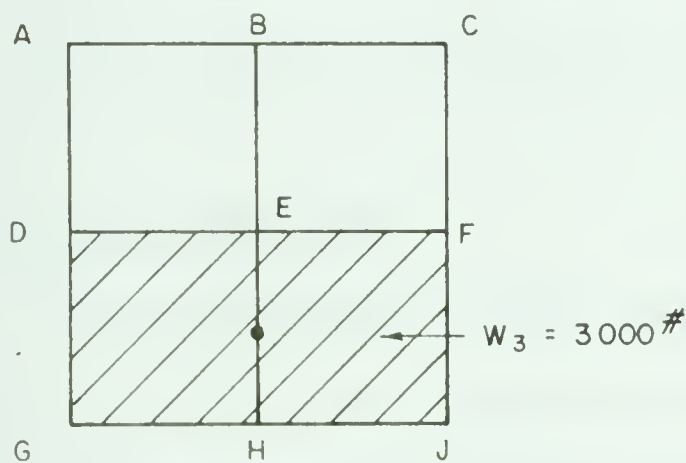
ALL VALUES "W" ARE TOTAL LOADS



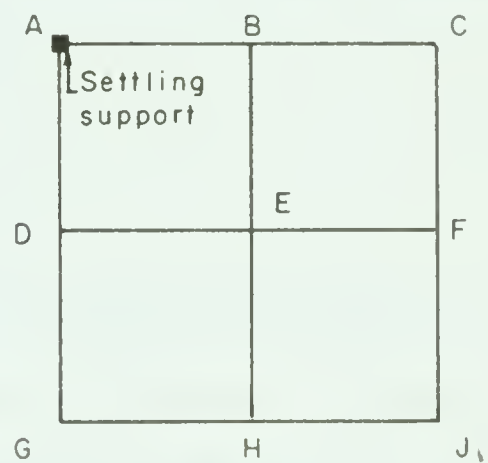
TEST #1 & #4
SYMMETRIC LOAD
SINGLE $1/2" \phi$ TIE RODS



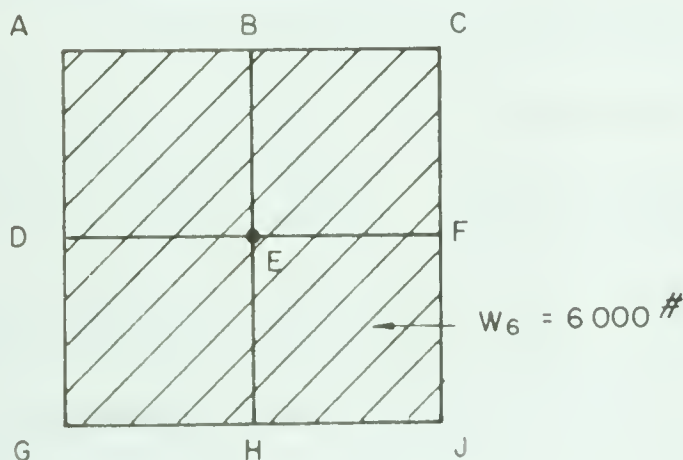
TEST #2
ASYMMETRIC LOAD
SINGLE $1/2" \phi$ TIE RODS



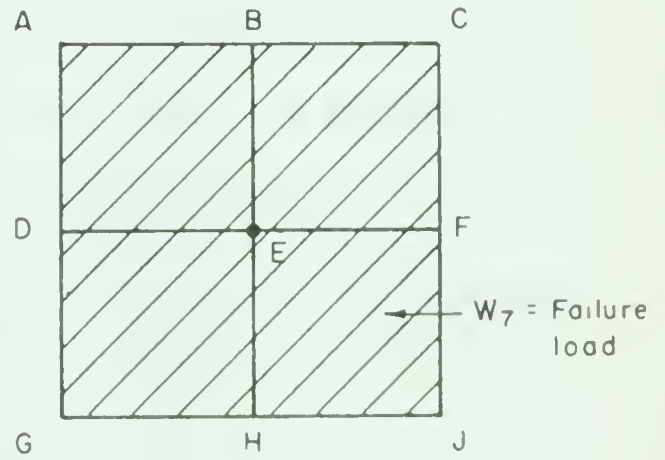
TEST #3
ASYMMETRIC LOAD
SINGLE $1/2" \phi$ TIE RODS



TEST #5
FOUNDATION SETTLEMENT
SINGLE $1/2" \phi$ TIE RODS



TEST #6
SYMMETRIC LOAD
DOUBLE TIE RODS - $1-1/2" \phi$
 $1-3/4" \phi$



TEST #7
SYMMETRIC LOAD
(TO FAILURE)
DOUBLE TIE RODS - $1-1/2" \phi$
 $1-3/4" \phi$

FIGURE 4.1 SUMMARY OF LOADING PATTERNS USED

In Tests 6 and 7, the half inch diameter tie rods between corners were left in position, but in addition, three quarter inch diameter tie rods were added, thus considerably reducing the lateral extension of the shell under load. This represents a condition which would not be likely to occur in a prototype structure unless the ties were grossly oversized or the abutments received firm support from the ground (such as abutments founded in bedrock). However, the tie rods were required in Test 7 to preclude a trivial failure by yielding of the steel tie rods. The loads were increased in increments of one thousand pounds to 6,000# in Test 6 and to failure in Test 7.

4.3 Asymmetrical Load Tests

Test 2 was carried out using a uniformly distributed load over one half of the structure only, the opposite half under load in Test 3. Loads were incremented in 500# steps in each test, to a maximum of 3,000#.

4.4 Foundation Settlement

To simulate differential settlement in the foundations, one of the supports, by means of the vertical adjustment in the tripod, was gradually lowered from its original position. Each increment of settlement was 0.1" to a maximum of one inch. In the latter part of the test, the support was returned, again in increments, to its original position.

4.5 Test to Destruction

Had it been possible to fail the model in more than one way, the re-

sults may have proved very interesting. Unfortunately, once failure has taken place, the model is no longer useful for further testing. Much consideration was given to which mode of failure should be chosen to provide the most useful information and it was decided that the uniform load should be used since only under uniform load could the membrane theory be employed as a basis for predicting ultimate capacity.

4.6 Test Procedure

At the beginning of each test zero readings were taken and recorded for deflections and strains. Strains and deflections at various points on the shell, as will be discussed in Chapter V, were measured at each load (or settlement) increment. Strains in the tie rods and load cells were also measured.

In order to measure all the strain gauges, due to the limited capacity of the recorder, it was necessary to change eight cables in the rear of the console. In Test 1, this change was made after each loading increment and it was thought that erroneous readings were resulting from variable contact resistance of the connections.

To eliminate this problem, it was decided to run through the loading sequence twice, once for each set of a hundred gauges, thereby eliminating the necessity for changing connections after the zero readings had been recorded. This technique was used in Test 2 and all subsequent tests, and this is the only difference between Test 1 and Test 4.

In the test to failure, Test 7, in order to obtain readings for all gauges, the earlier method of changing cables at each load increment was attempted once again. Unfortunately, the results proved erratic so that, finally, the method was abandoned. As a result, only half the strains were recorded in Test 7. This meant that most of the gable and ridge beam strains were recorded, but none of the shell strains were included.

CHAPTER V

INSTRUMENTATION

5.1 Introduction

To gain as much information about the behaviour of the shell as possible, a large number of measurements were required. These included the measurement of (a) corner reactions, (b) tie rod strains and forces, (c) surface strains on the shell and beams, and (d) deflections of the ridge and gable beams. It was the function of the instrumentation to accurately measure these values for each load increment in a relatively short time so that each test could be conducted in a continuous operation without having to compensate for the effects of varying temperature and humidity or random drift of the gauges with time.

5.2 Load Cells

Although the corner vertical reactions for most of the tests could be calculated from symmetry and statics, it was thought that an actual measurement of the reactions would serve as a check on how well the load distributing apparatus was functioning.

The basic requirements of a load cell are (a) to carry the maximum expected load without excessive strain and (b) to measure loads much smaller

APPENDIX I

1990/01/01-1990/01/01

3.1.1.1.1.1

The first part of the document is devoted to the study of the
theoretical aspects of the problem. It is divided into two parts:
the first part is devoted to the study of the theoretical aspects
of the problem, and the second part is devoted to the study
of the experimental aspects of the problem. The first part
is devoted to the study of the theoretical aspects of the
problem, and the second part is devoted to the study of
the experimental aspects of the problem. The first part
is devoted to the study of the theoretical aspects of the
problem, and the second part is devoted to the study of
the experimental aspects of the problem.

and the

3.1.1.1.1.2

The second part of the document is devoted to the study of the
experimental aspects of the problem. It is divided into two parts:
the first part is devoted to the study of the experimental aspects
of the problem, and the second part is devoted to the study
of the theoretical aspects of the problem. The first part
is devoted to the study of the experimental aspects of the
problem, and the second part is devoted to the study of
the theoretical aspects of the problem. The first part
is devoted to the study of the experimental aspects of the
problem, and the second part is devoted to the study of
the theoretical aspects of the problem.

and the

The third part of the document is devoted to the study of the
theoretical aspects of the problem. It is divided into two parts:
the first part is devoted to the study of the theoretical aspects
of the problem, and the second part is devoted to the study
of the experimental aspects of the problem. The first part
is devoted to the study of the theoretical aspects of the
problem, and the second part is devoted to the study of
the experimental aspects of the problem. The first part
is devoted to the study of the theoretical aspects of the
problem, and the second part is devoted to the study of
the experimental aspects of the problem.

than the maximum with sufficient sensitivity to make the results meaningful. The principle of the load cell is that loads are calculated from a measured strain on a known cross sectional area. The material which best satisfies requirements (a) and (b) above is one which has a high ratio of proportional limit to Young's modulus. The material selected for these tests was a high strength steel, having an ultimate strength of 100 ksi which enabled the loads to be measured to within a tolerance of about fifty pounds.

A three inch length of one inch diameter high strength steel tube with a wall thickness of one sixteenth of an inch was pressed into undersize holes in the cap plate and base plate. Details of the construction of the load cell were shown earlier (FIGURE 3.12). The load was introduced by means of a one inch diameter steel ball, seated in a spherical recess machined in the cap plate concentrically over the axis of the tube. Each load cell had two strain gauges connected in series. These were mounted parallel to the axis of the tube and diametrically opposite. The average of the two gauges was read, which automatically compensated for the effect of accidental eccentricities which may have been present due to errors in machining. The temperature compensating gauge was built in a similar way, using a scrap length of tubing.

The load cells were calibrated by applying a known load using the Amsler hydraulic jack and recording the resulting strain by means of a Baldwin Strain Indicator. After the load cells were installed in the model, they were hooked up permanently to the same indicator and the results were read

manually for each load increment in each test.

5.3 Tie Rods

To determine the force in the tie rods, a single strain gauge was mounted on each of the tie rods at the mid-length of the rod. The temperature compensating gauge consisted of a short length of similar rod with a single strain gauge mounted thereon.

5.4 Measurement of Surface Strains

In order to read the large number of strain gauge outputs required, a 100 channel digital data processor, recently constructed by the Mechanical Engineering Department at the University of Alberta, was used. The task of manually balancing, reading and recording the large number of strains required in these tests would be very time consuming with resulting errors due to creep of concrete, changes in temperature and humidity and difficulty in maintaining constant load over an extended period. An automatic means of measuring strains in such a project was considered mandatory.

A complete description of the data processor is given by Bellow and Kennedy (1963) and the following is a very brief summary of its salient features.

5.5 The Data Processor

The data processor consists of two balancing modules, each with one hundred channels, a one hundred channel scanning unit, an analog digital

voltmeter, a program unit and a combination typewriter and tape perforator output which may be used singly or collectively.

Each balancing module is made up of two groups of fifty channels each. Initial balancing of each channel is accomplished by adjusting finely machined screws on the front of the machine which in turn deflect a small cantilever beam, thereby changing the resistance of strain gauges mounted on the upper and lower surfaces of the beam. These gauges serve as two arms on the Wheatstone bridge.

The scanning unit sequentially samples, manually or automatically up to one hundred channels of information. When used in conjunction with the typewriter output, one hundred channels are processed in four minutes, although a much faster rate is possible when the tape perforator output is used alone. Gold plated contacts in the scanning unit minimize variations in contact resistance. The channel number is visually displayed in neon lights on the front panel of the unit.

After the channel is selected, the unknown voltage is fed to the analog digital voltmeter. This unit automatically balances the unknown signal against a standard voltage. When balance is attained, a null indicator on the front panel is extinguished and the digital value with its algebraic sign is displayed in neon lights.

The program unit controls the operation of the scanner and digital voltmeter and will sequentially arrange the data and control the format of the

data in the output devices. It controls the method in which the data is sampled and the final output form.

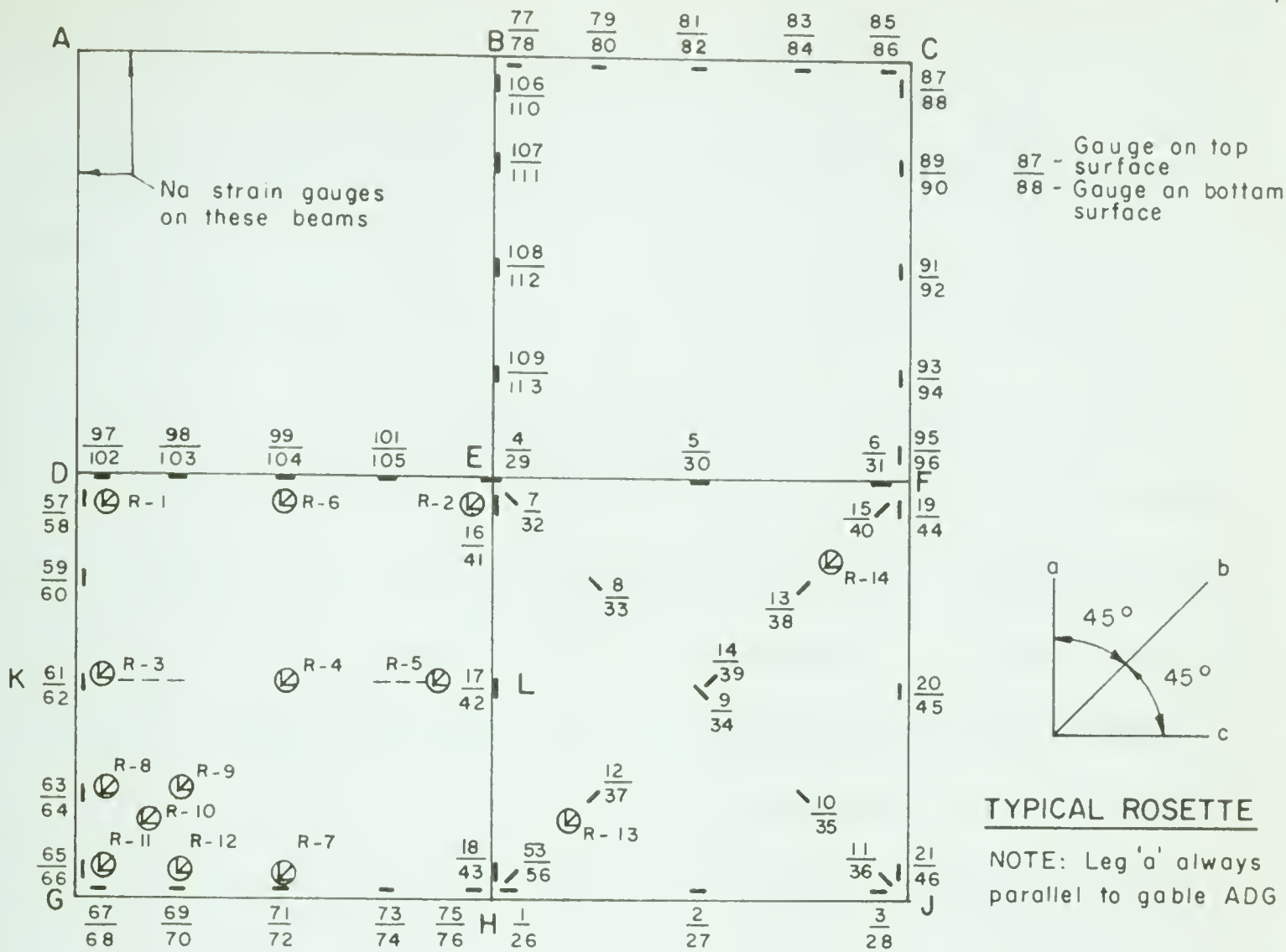
The data may be recorded in either or both of two ways, (1) it may be recorded on an electric typewriter and (2) it may be punched out on a perforated tape which in turn may be introduced as data to a Royal McBee LGP-30 computer. In these tests, all information was recorded on the typewriter output only.

5.6 Location of Strain Gauges

A total of one hundred and fourteen SR-4 strain gauges and twenty eight strain rosettes were mounted on the surface of the model giving a total of one hundred and ninety eight individual readings, requiring the full capacity of the data processor. The strain gauges were type A-5-1-S6 paperbacks with a resistance of 120 ohms and a gauge factor of 2.00 plus or minus one percent. All gauges had a gauge length of one half inch. Eighty gauges were mounted on the upper and lower surfaces of the ridge and gable beams, while the remaining thirty four gauges and all the rosettes were mounted on the shell surface between beams. The positioning of strain gauges on the model is shown in **FIGURE 5.1** where it may be seen that primary attention was focused on the beams, the shell diagonals and generator KL.

5.7 Application of Strain Gauges

Strain gauge applications on metal surfaces presented no real pro-



NUMBERING OF ROSETTE GAUGES							
ROSETTE NUMBER	LEG			ROSETTE NUMBER	LEG		
	a	b	c		a	b	c
R 1	$\frac{114}{117}$	$\frac{115}{118}$	$\frac{116}{119}$	R 8	$\frac{162}{183}$	$\frac{163}{184}$	$\frac{164}{185}$
R 2	$\frac{120}{123}$	$\frac{121}{124}$	$\frac{122}{125}$	R 9	$\frac{165}{186}$	$\frac{166}{187}$	$\frac{167}{188}$
R 3	$\frac{126}{141}$	$\frac{127}{142}$	$\frac{128}{143}$	R 10	$\frac{168}{189}$	$\frac{169}{190}$	$\frac{170}{191}$
R 4	$\frac{132}{147}$	$\frac{133}{148}$	$\frac{134}{149}$	R 11	$\frac{171}{192}$	$\frac{172}{193}$	$\frac{173}{194}$
R 5	$\frac{138}{153}$	$\frac{139}{154}$	$\frac{140}{155}$	R 12	$\frac{174}{195}$	$\frac{175}{196}$	$\frac{176}{197}$
R 6	$\frac{156}{177}$	$\frac{157}{178}$	$\frac{158}{179}$	R 13	$\frac{25}{50}$	$\frac{51}{54}$	$\frac{52}{55}$
R 7	$\frac{159}{180}$	$\frac{160}{181}$	$\frac{161}{182}$	R 14	$\frac{22}{47}$	$\frac{23}{48}$	$\frac{24}{49}$

FIGURE 5.1 LOCATION & NUMBERING OF STRAIN GAUGES

blems. The metal surface was first roughened with emery cloth and thoroughly cleaned with trichloroethylene until no trace of dirt was visible on a white paper tissue after wiping the surface of the metal with the tissue. Budd GA-1 contact cement was used to bond the strain gauge to the metal surface. The cement comes in a kit, complete with neutralizer and activator. After cleaning the surface, the neutralizer was applied and later wiped dry. The strain gauge was positioned with a small piece of cellulose tape adhering to the felt protective cover of the gauge and to the metal surface on one side of the gauge location. The tape was folded back so that the contact surface of the gauge was turned up. Activator was spread over the gauge and allowed to dry completely before spreading cement on the metal surface. The gauge was then pressed against the metal surface, guided to the correct position by the tape, and was held firmly with a uniform finger pressure until the cement had set.

Application of strain gauges to concrete surfaces presented a more difficult problem. Several types of adhesive were tried and the results are summarized in Appendix A. As a result of these trials, the cement which was finally selected to size the concrete surface was Budd GA-5 with activator. This material was spread over the area to receive the strain gauge and allowed to set for two days. All the small surface depressions were filled by the cement, and excess thickness of cement was removed by grinding. The strain gauges were then cemented to the sized surface with CIL household cement.

Wires were tied in bundles on a bench, each wire banded with the

appropriate gauge number at each end. These bundles were attached to the shell surface by taping. On the underside of the shell, it was found that the tape did not continue to adhere to the concrete, and a very effective method of keeping the wires in position was found by using contact cement, spreading a small quantity on both the wire bundle and the concrete surface. The wires were then soldered to the strain gauges and the opposite ends were connected to a junction box which was clamped to one of the columns of the loading frame.

5.8 Deflection Measurements

To measure deflections of the ridge and gable beams, Ames dials were mounted at one foot centres along all beams. A total of forty one Ames dials were positioned as shown in FIGURE 5.2. Under the stem of each dial, a small metal platen was cemented to the surface of the model to provide a smooth bearing surface for the dial. The steel angles, which had served as the outer forms for the gable beams at an earlier stage, now became the supports for the Ames dials. A view of the dials mounted over the model is given in FIGURE 5.3. Deflection measurements were taken for each load (or settlement) increment in each test.

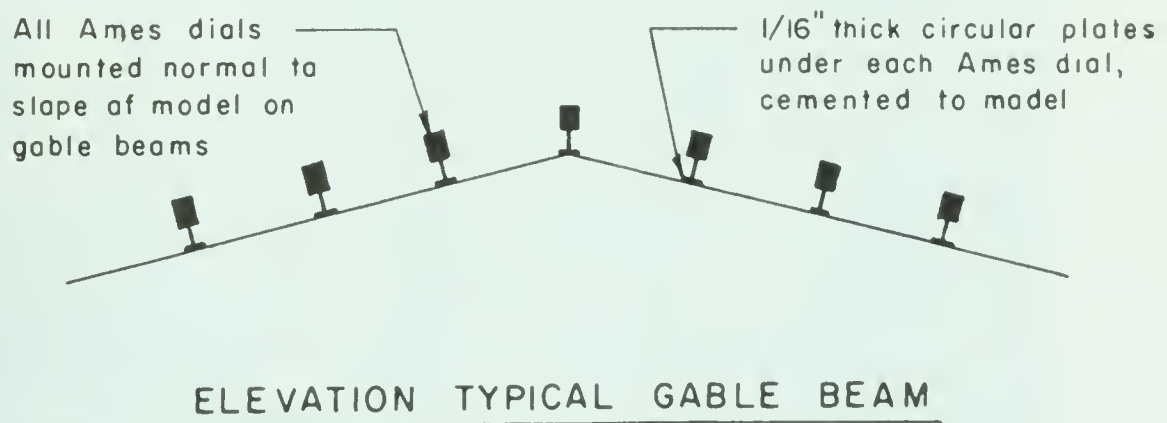
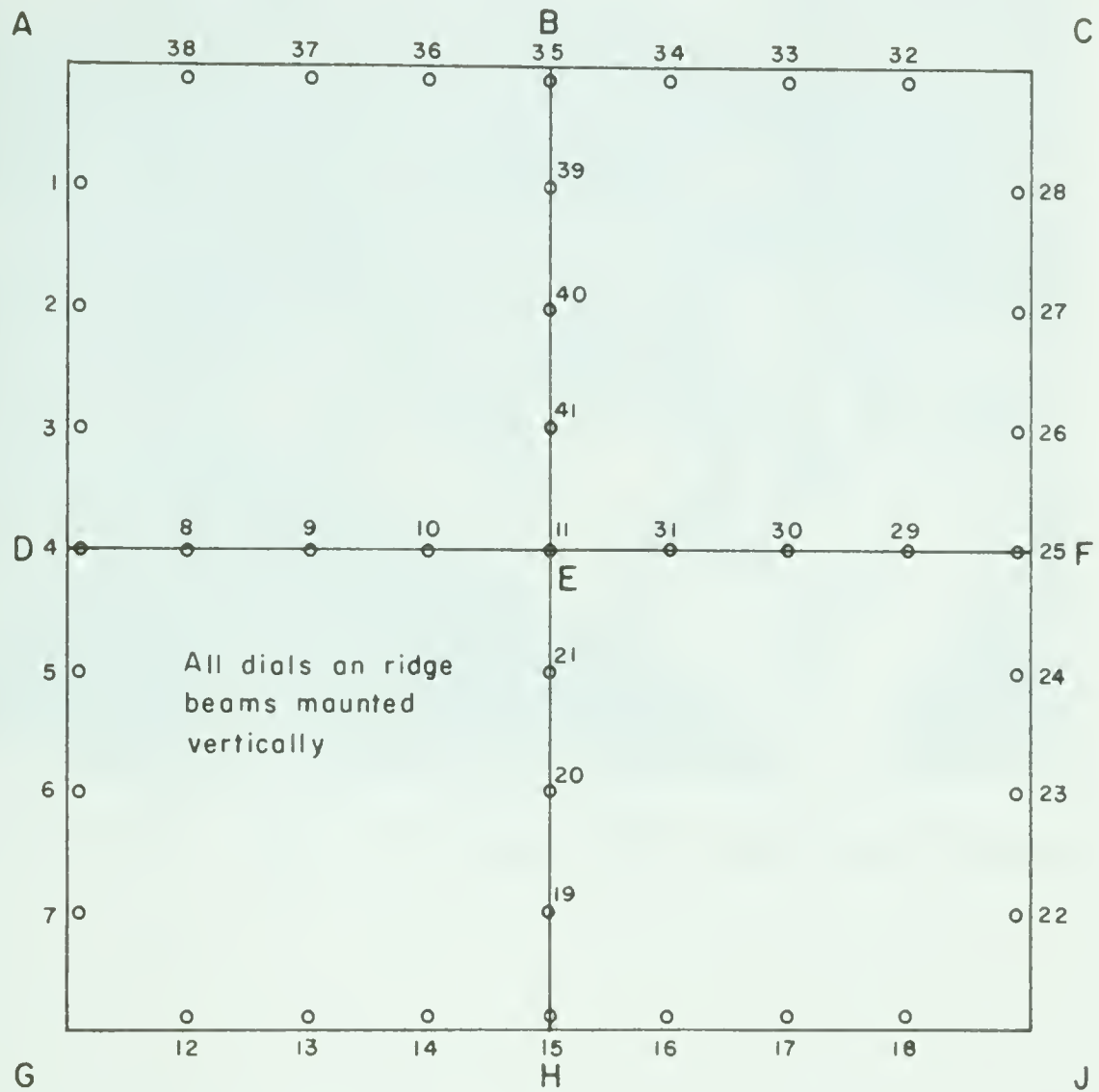


FIGURE 5.2 LOCATION & NUMBERING OF AMES DIALS

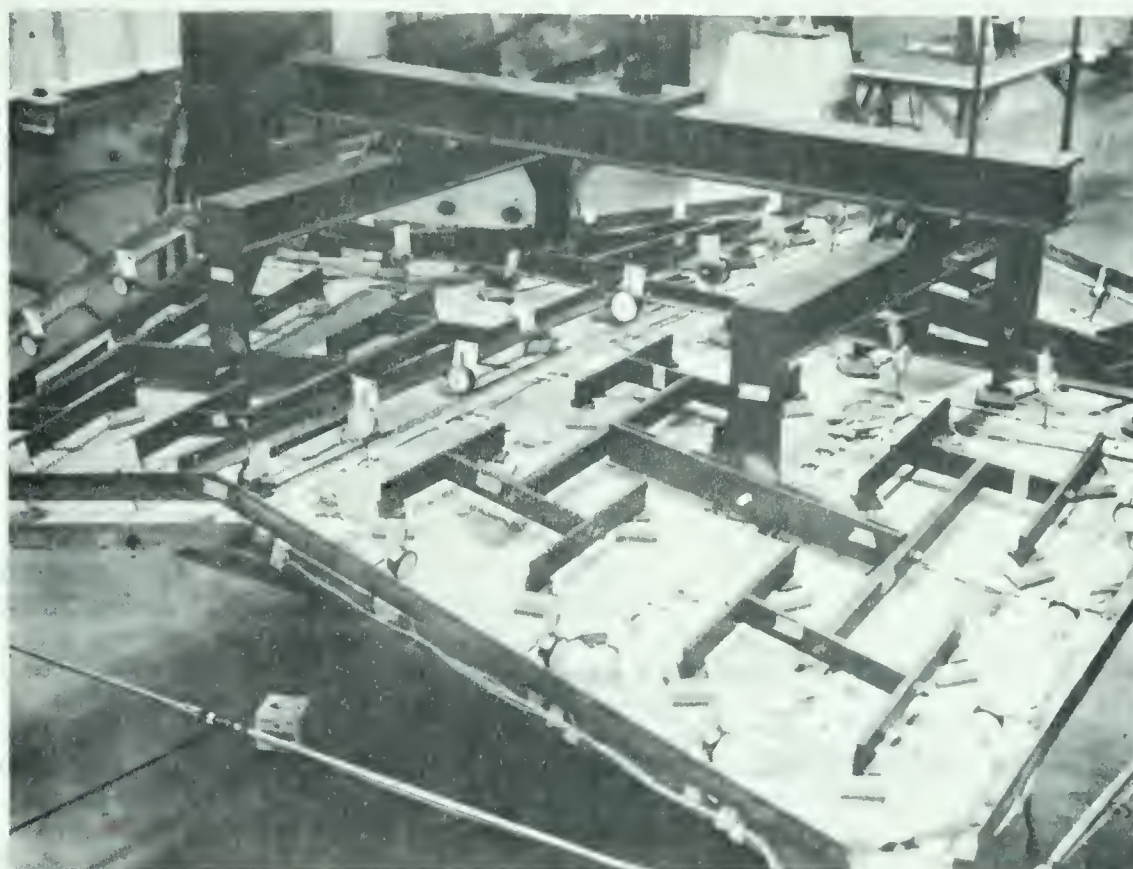


FIGURE 5.3 VIEW OF COMPLETED INSTRUMENTATION

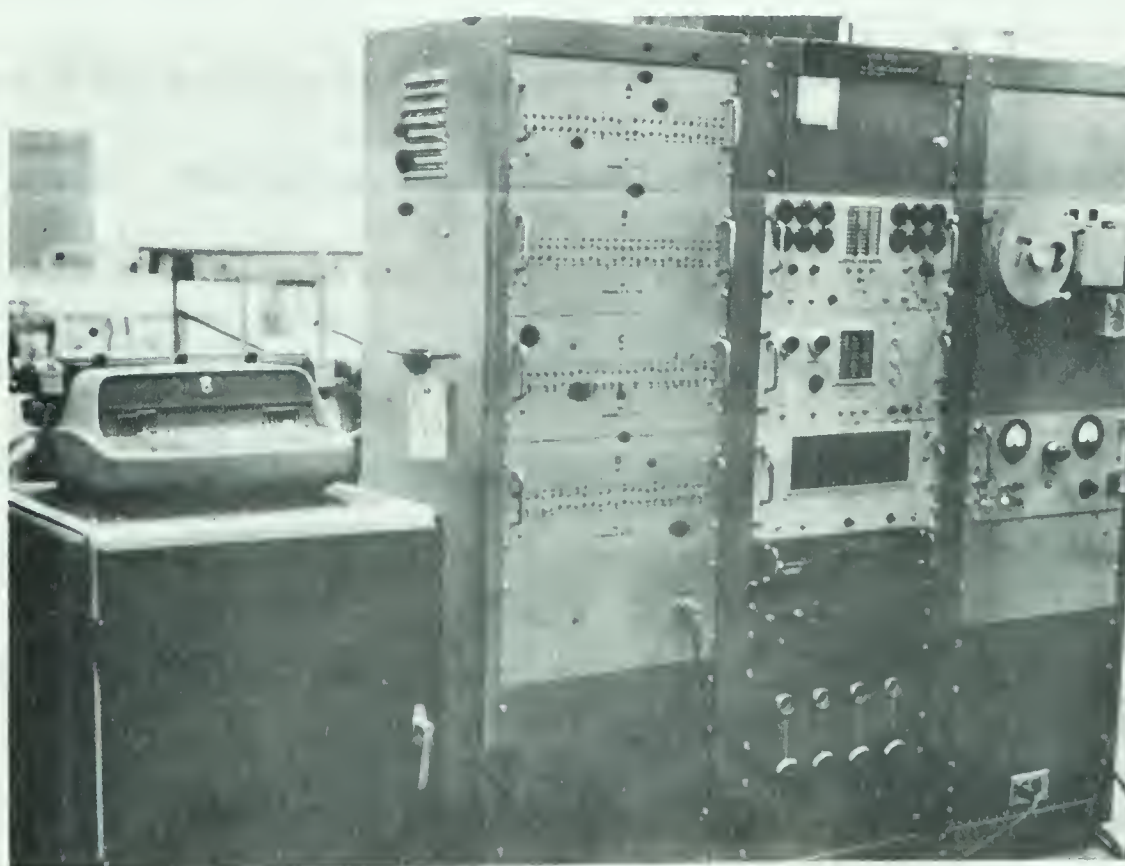


FIGURE 5.4 VIEW OF DIGITAL DATA PROCESSOR

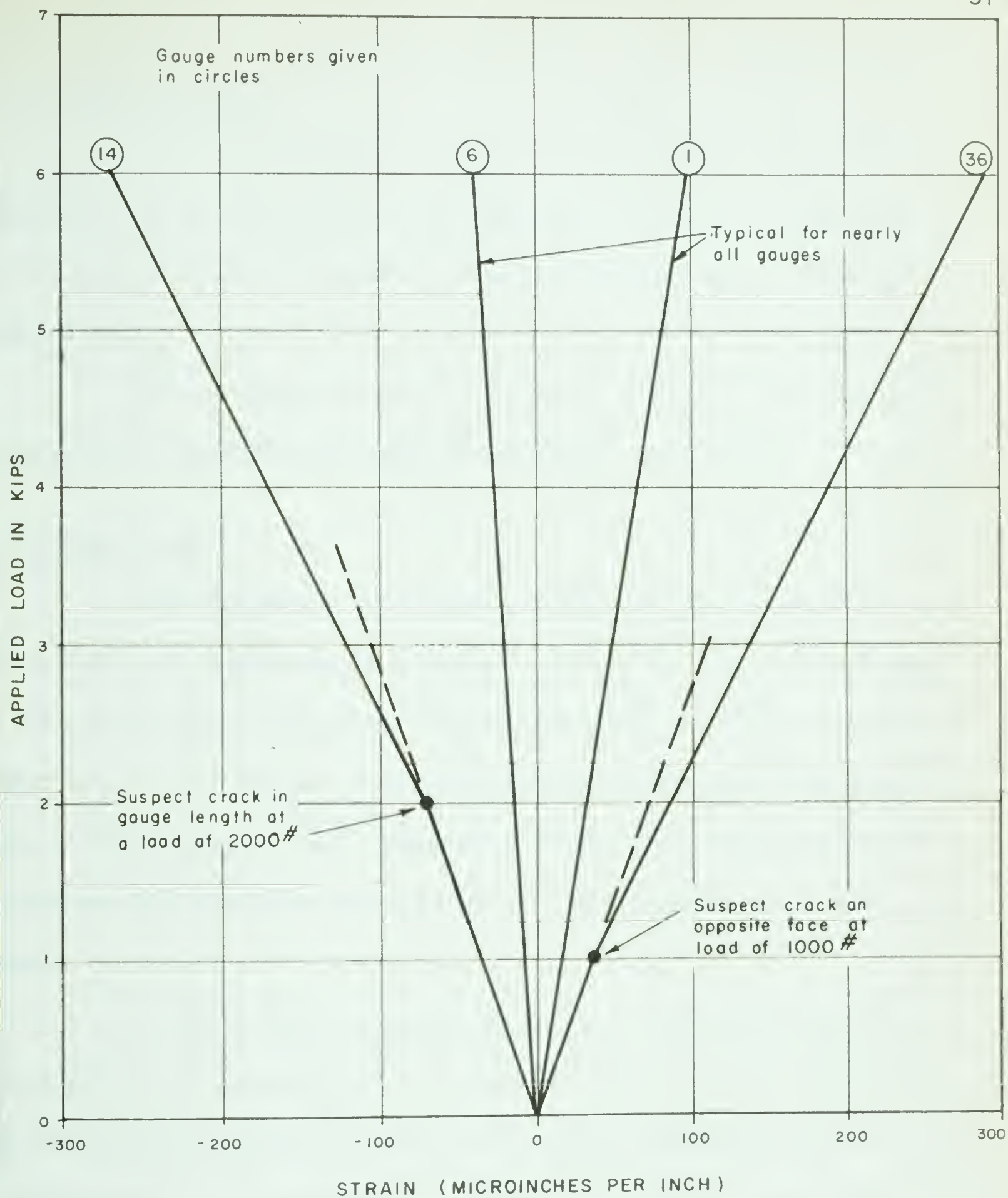
CHAPTER VI

PRESENTATION AND DISCUSSION OF SYMMETRICAL LOAD TESTS

6.1 Introduction

Included in the symmetrical load series are Test 1, 4, 6 and 7. With the exception of Test 7, which was carried to destruction, the maximum load applied to the shell was eight thousand pounds in Test 1. The maximum load in Tests 4 and 6 was six thousand pounds.

Strain versus load diagrams were plotted for each gauge for every load increment in Tests 1 and 4. With only two exceptions, the variation in strain was linear with respect to load. It may be concluded from this that each component of the model behaved elastically for loads not in excess of eight thousand pounds. Six thousand pounds has been used as a basis for comparison of the various relationships discussed herein. For loads less than six thousand pounds, the strains, deflections, bending moments and axial thrusts should be proportionately reduced. A few typical strain versus load curves are plotted in FIGURE 6.1 which illustrate the linearity of measured strains through the various loading stages.



Negative sign indicates tensile strain
 Positive sign indicates compressive strain

FIGURE 6.1 LINEARITY OF STRAIN READINGS

6.2 External Reactions

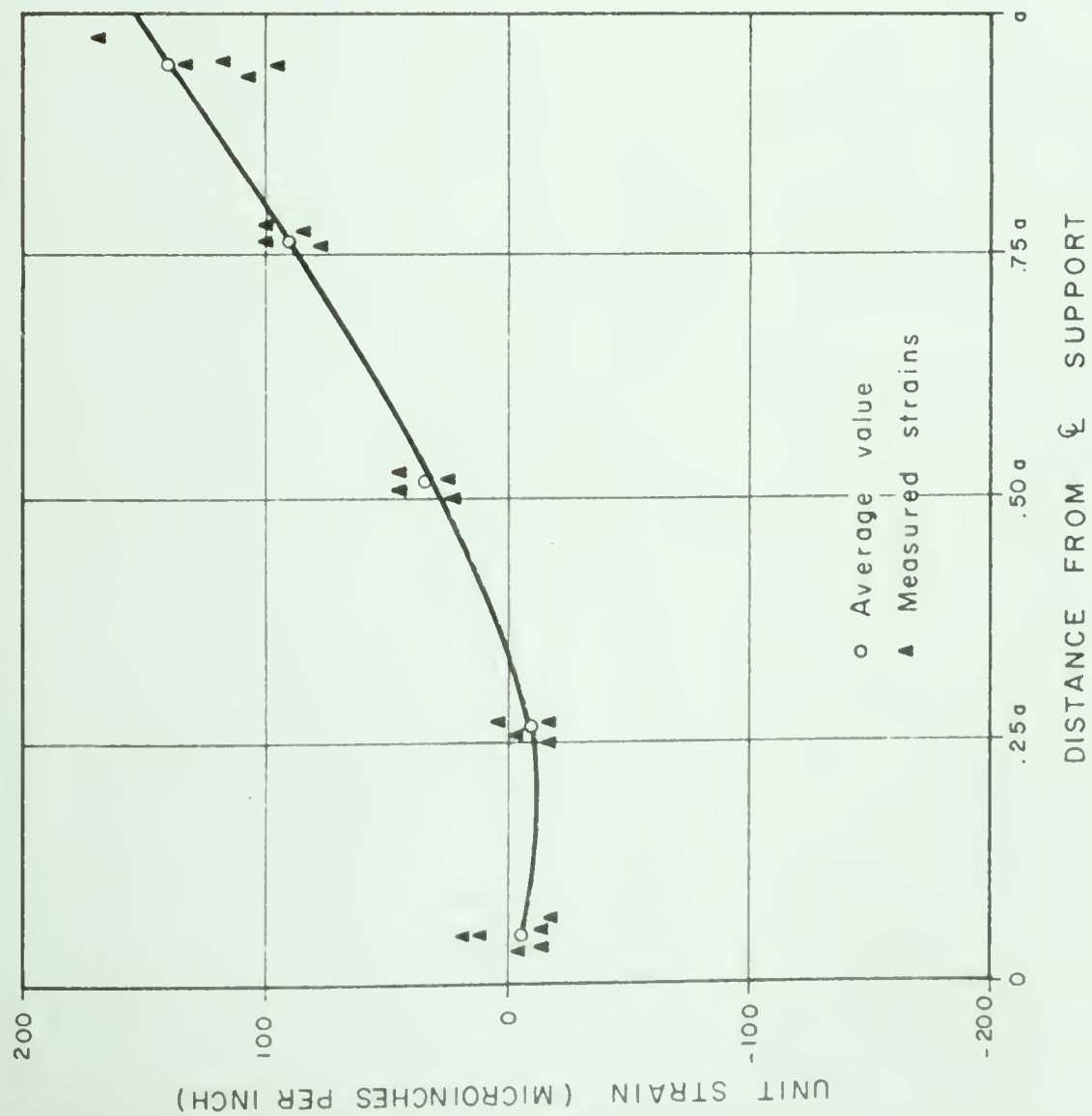
The measured vertical reactions at the four corners of the shell checked well with statics. The average value was found to be 1,540 pounds, or a total of 6,160 pounds over the entire shell, just 160 pounds greater than the applied load.

The average tie rod strain was found to be 457 microinches per inch which corresponds to an average tie rod force of 2,600 pounds.

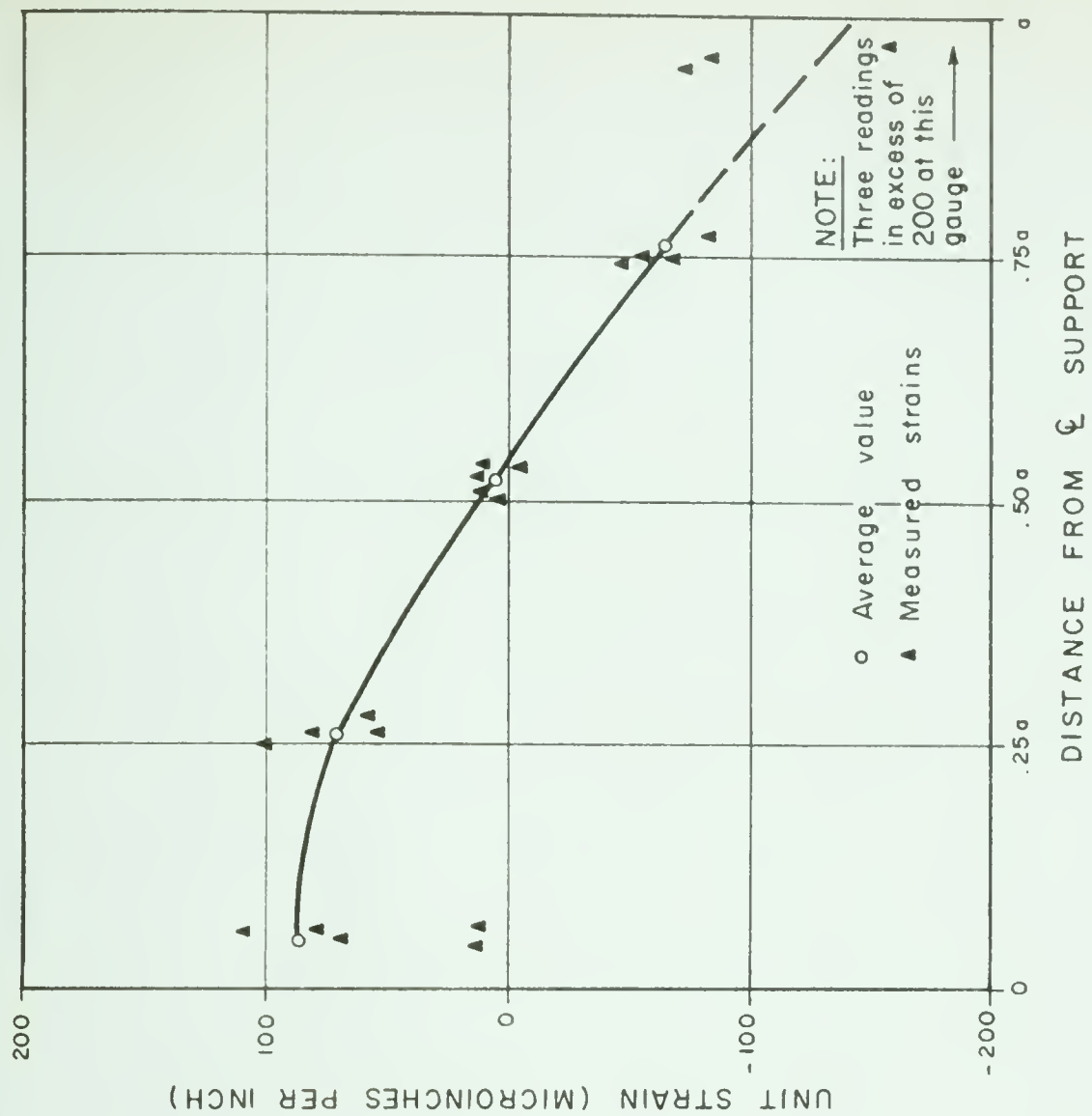
6.3 Gable Beams

Measured strains versus distance from support for the top and bottom fibres of the gable beams are plotted in FIGURES 6.2 and 6.3 for Tests 1 and 4 respectively. The distance from support is given in terms of the distance "a", which is the span of each shell quadrant, half the span of the structure, or in this case, four feet. These are composite plots, so that the plotted values are taken from more than one member. This is justified due to symmetry.

A study of the points reveals that they are quite closely grouped in the central portion of the beams. A considerable scatter of values is found at the extremities of the beams. Three of the measured strains in the bottom fibres in the vicinity of the ridge fall completely off the graph. It should be noted, however, that the cracking strain for the concrete is probably in the order of one hundred microinches per inch (negative values on the graph indicate tensile strain). It is felt that the high values in this region are caused

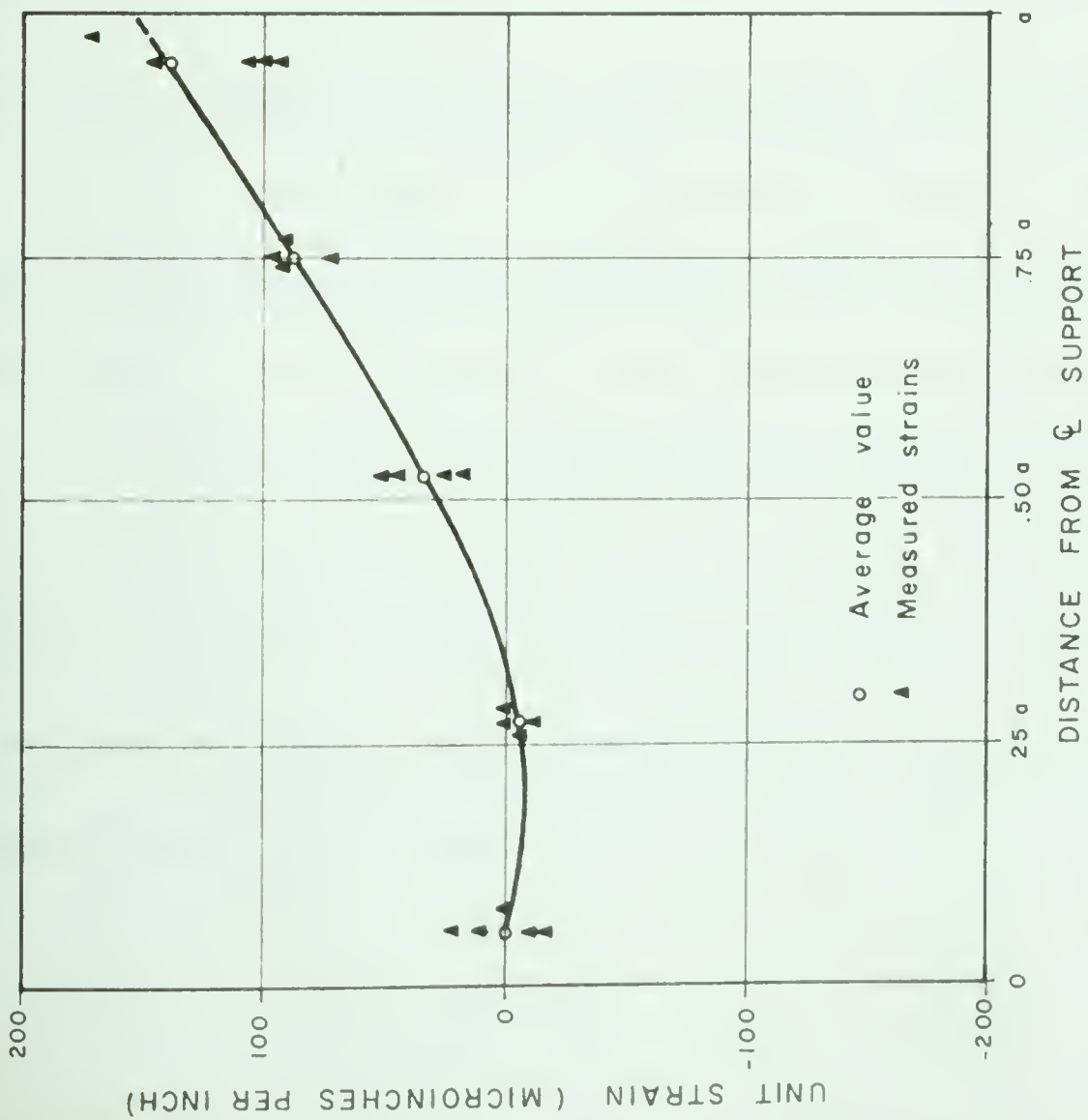


(a) STRAIN IN TOP FIBRE

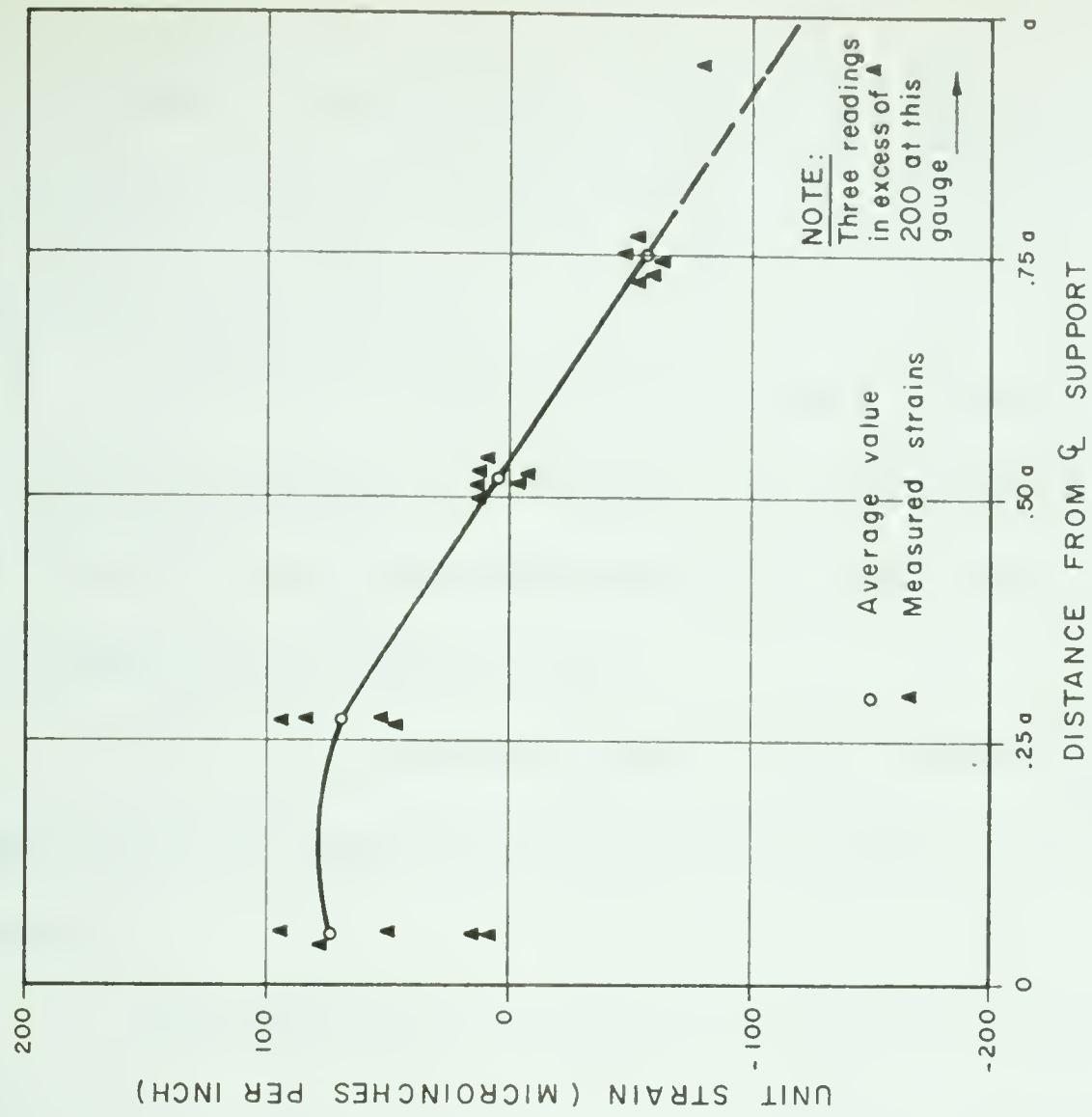


(b) STRAIN IN BOTTOM FIBRE

FIGURE 6.2 MEASURED STRAINS IN GABLE BEAMS - TEST # 1 - 6000 # LOAD



(a) STRAIN IN TOP FIBRE



(b) STRAIN IN BOTTOM FIBRE

FIGURE 6.3 MEASURED STRAINS IN GABLE BEAMS - TEST #4 - 6000 # LOAD

by the presence of cracks in the gauge length. For this reason, all readings considerably in excess of one hundred microinches per inch tension have been discarded as meaningless.

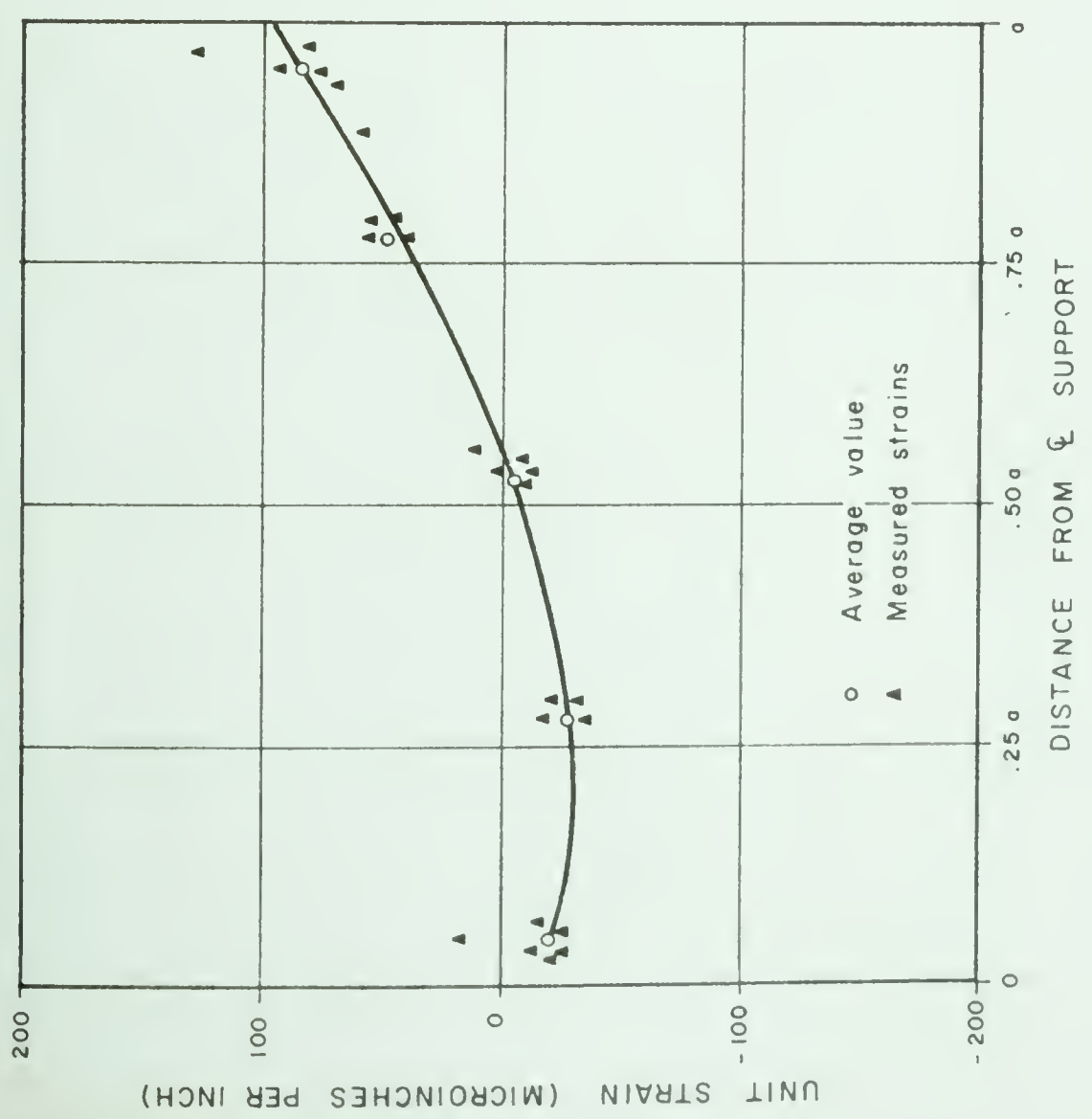
The solid line represents the joining of the numerical averages of the individual readings. A portion of the curve showing the strains in the bottom fibres has been shown dotted since it is not based on the average value, but an extrapolation of the curve beyond.

The curves plotted for Tests 1 and 4 are almost identical, as is the pattern of scatter, indicating that the individual gauges behaved in a consistent manner.

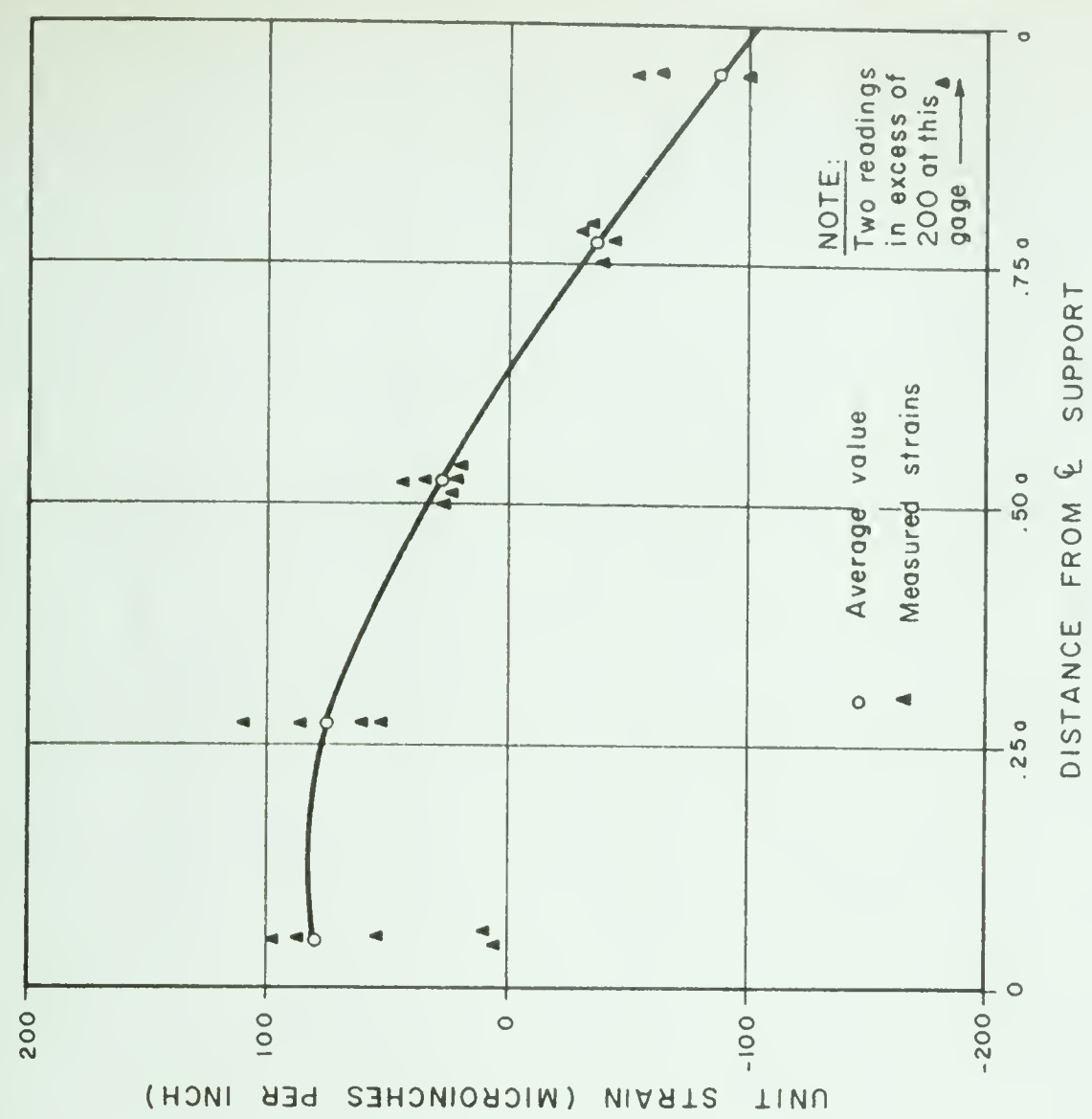
FIGURE 6.4 is a similar plot for Test 6, where the tie rods were stiffened by the addition of larger tie rods. It may be seen that the shapes of the curves are similar to those plotted for Test 1 and 4, but the compressive strains are reduced in the top fibres and increased in the bottom fibres.

A similar plot for Test 7 is nearly coincident with Test 6. In addition, corresponding strains are plotted for a load of twelve thousand pounds and it may be seen that the strain - load relationship is not far from linear.

Before plotting absolute deflections of the gable beams, the measured values were corrected for lateral strain in the model under load. Since the deflection gauges were bearing on sloping metal platens, a horizontal movement of the platen produced an indicated deflection in the dial. The magnitude of horizontal movement for each platen was calculated from its distance from the

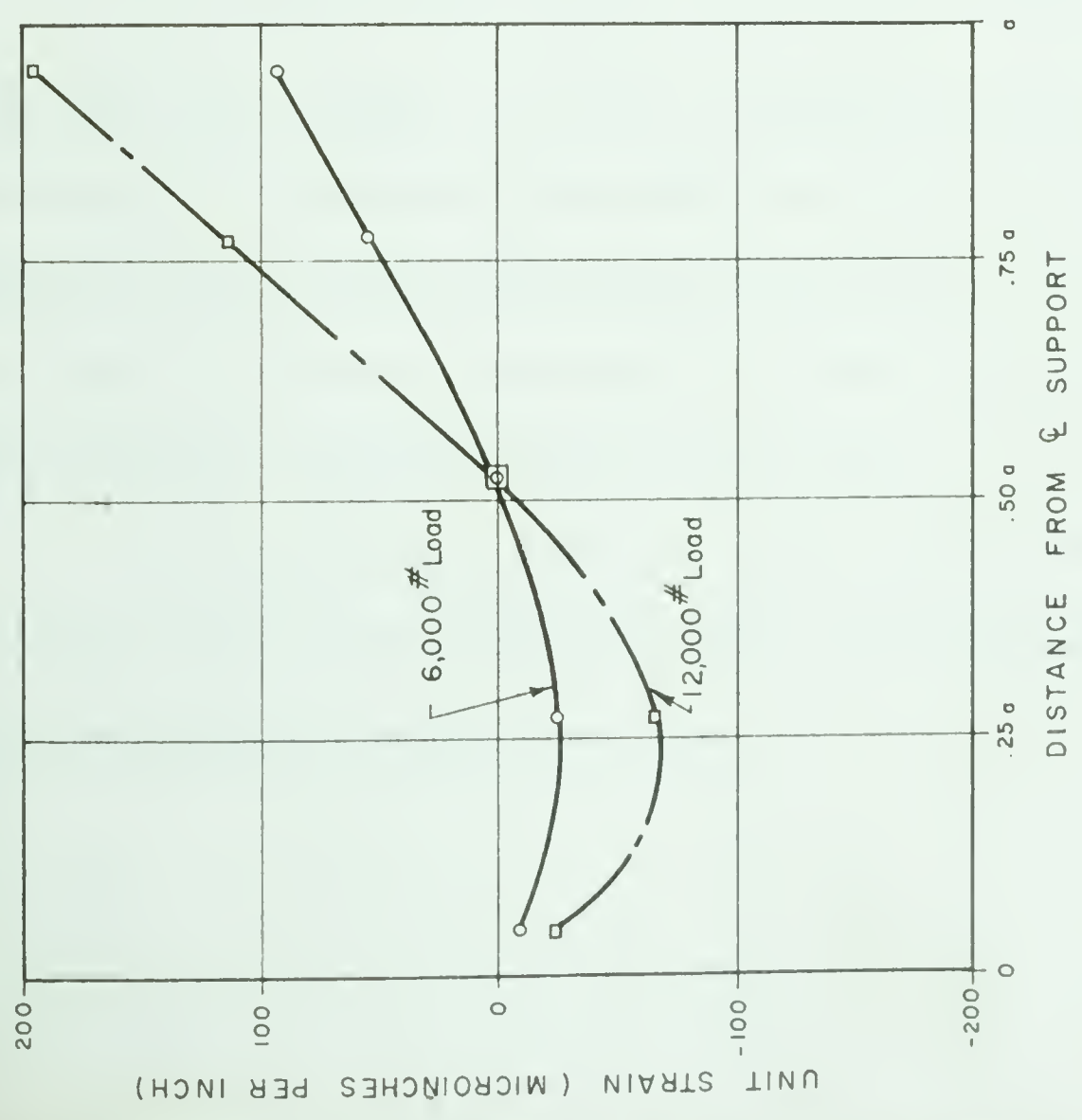


(a) STRAIN IN TOP FIBRE

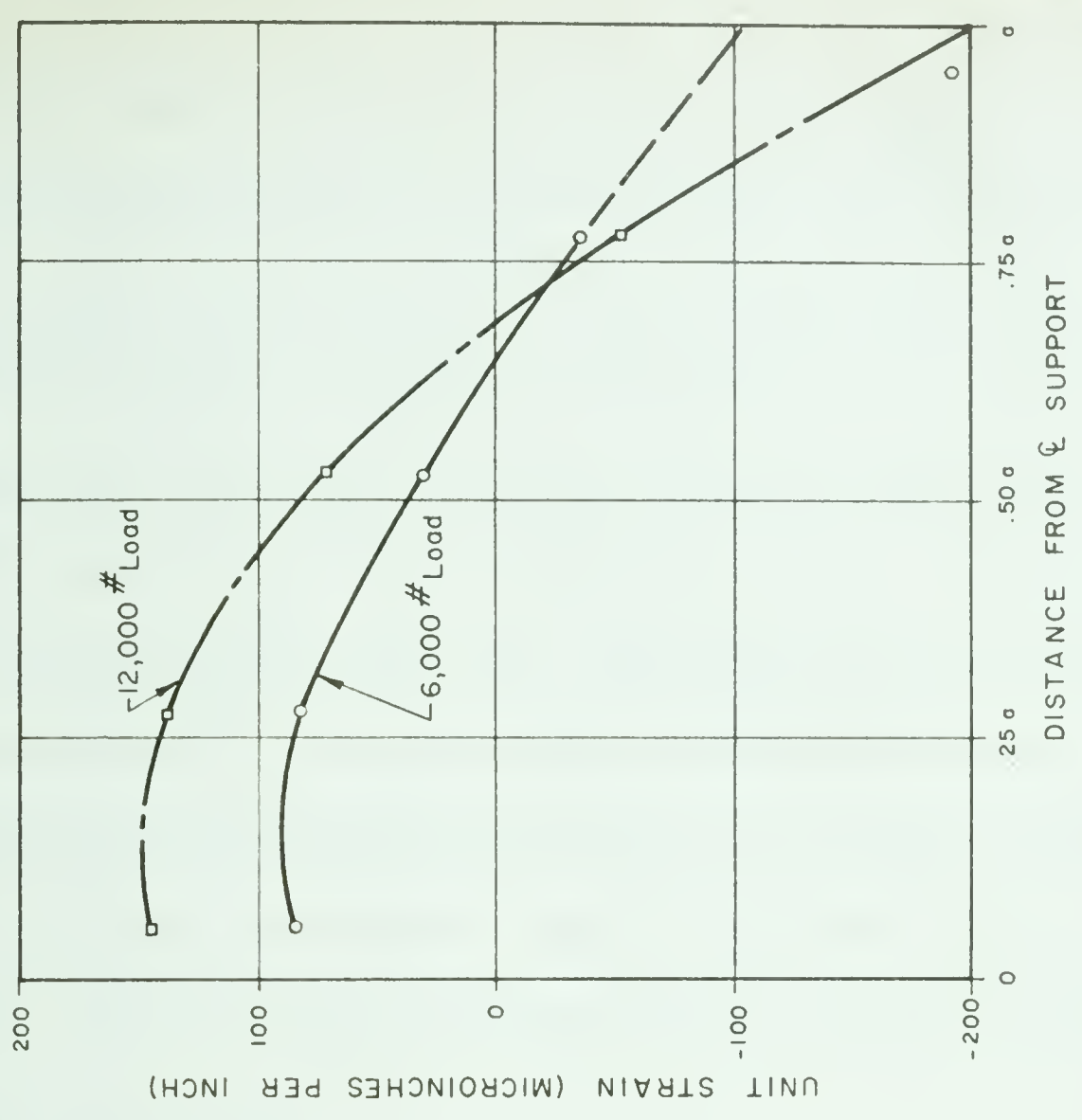


(b) STRAIN IN BOTTOM FIBRE

FIGURE 6.4 MEASURED STRAINS IN GABLE BEAMS - TEST #6 - 6000 # LOAD



(a) STRAIN IN TOP FIBRE



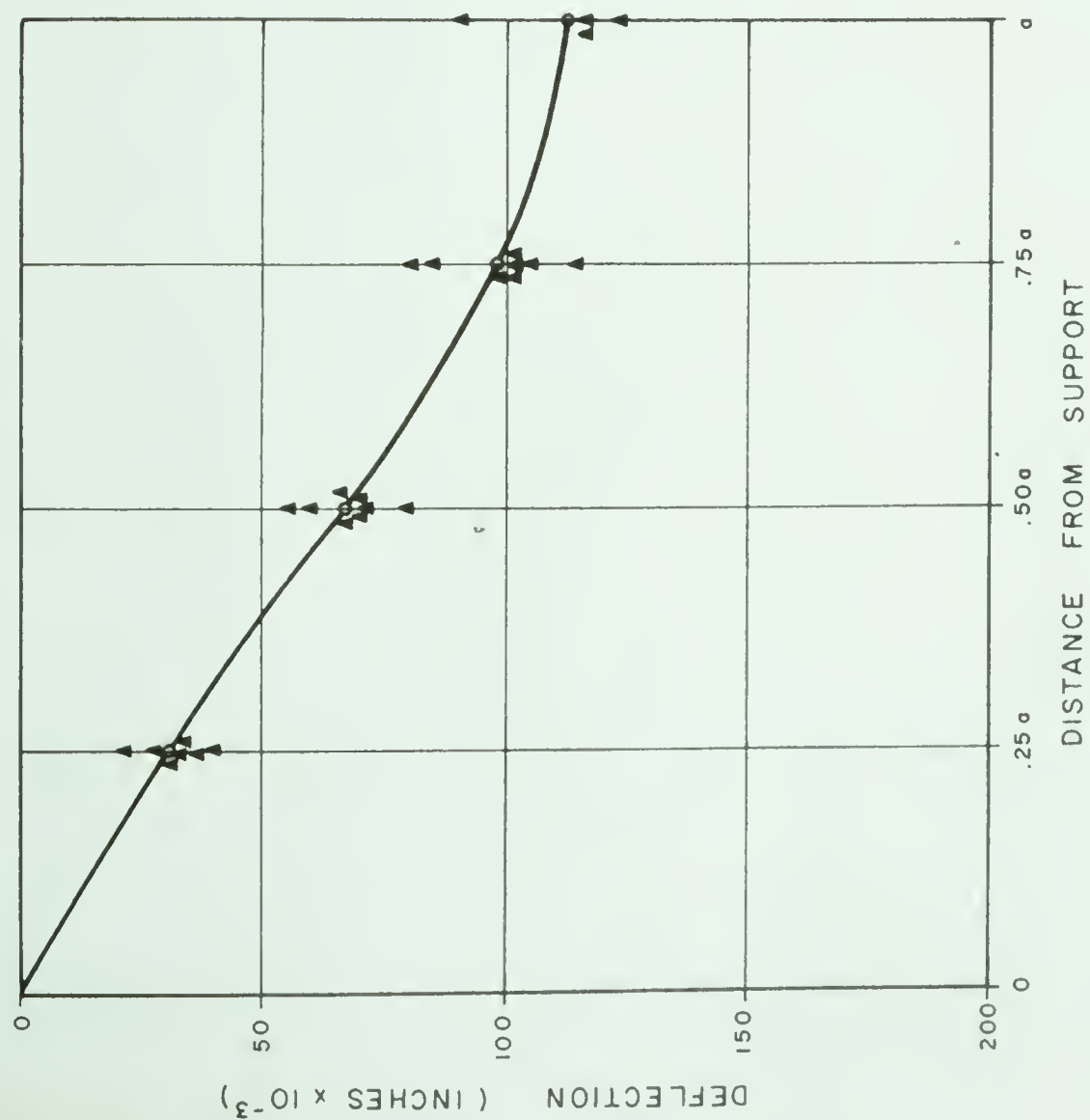
(b) STRAIN IN BOTTOM FIBRE

FIGURE 6.5 MEASURED STRAINS IN GABLE BEAMS - TEST # 7

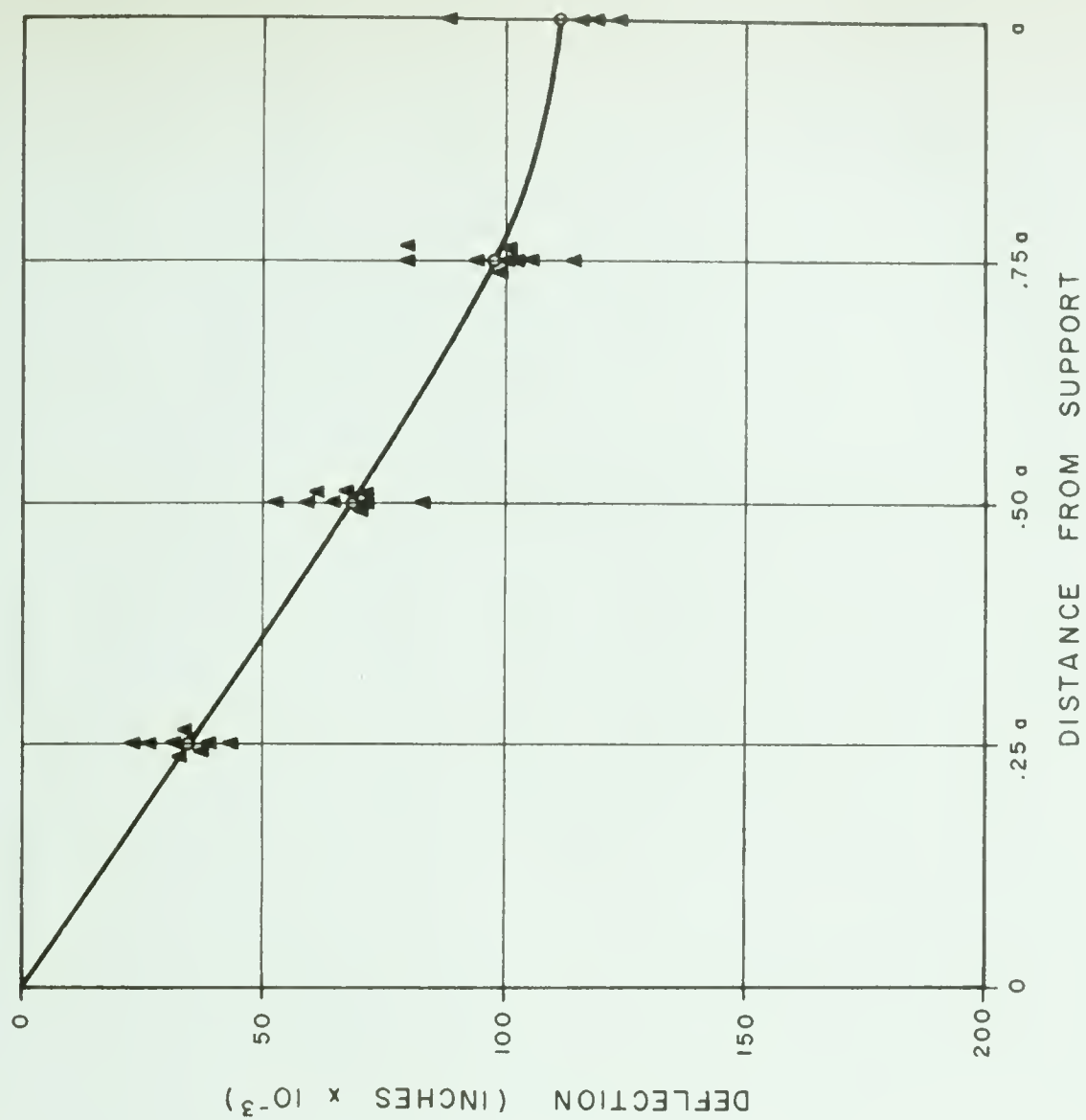
"pinned" support and from the total strain from one support to another, which could be found from the tie rod strains. Thus if the tie rod strain were 100 microinches per inch, the overall strain over the length of the tie rod would be 9,600 microinches. A gauge point twenty four inches from the pinned support would have moved 2,400 microinches horizontally towards the moveable support, resulting in an indicated deflection of $2,400 \sin \alpha$ microinches, where α is the slope of the gable beam. The measured deflection would be reduced by $2,400 \sin \alpha$. For a point five feet from the pinned support, the measured deflection would be increased by $6,000 \sin \alpha$ as the indicated deflection beyond the ridge beam was of opposite sign due to the downhill slope of the far gable beam. No correction was required in the case of ridge beam deflections since they were horizontal.

FIGURES 6.6 and 6.7 show a composite plot of the deflected shape of the gable beam for Tests 1, 4, 6 and 7. Considerable scatter is found in the plotted points which indicates that the conditions of symmetry were not entirely fulfilled by either the model or the load distributor, or both. It is evident, however, that the deflections in Tests 6 and 7 are considerably less than in Tests 1 and 4 which fact is attributed to the heavier tie rods.

Bending moments for the beams were calculated in two ways. From the strain readings on the top and bottom fibres, the bending moment may be found from elementary bending theory to be:

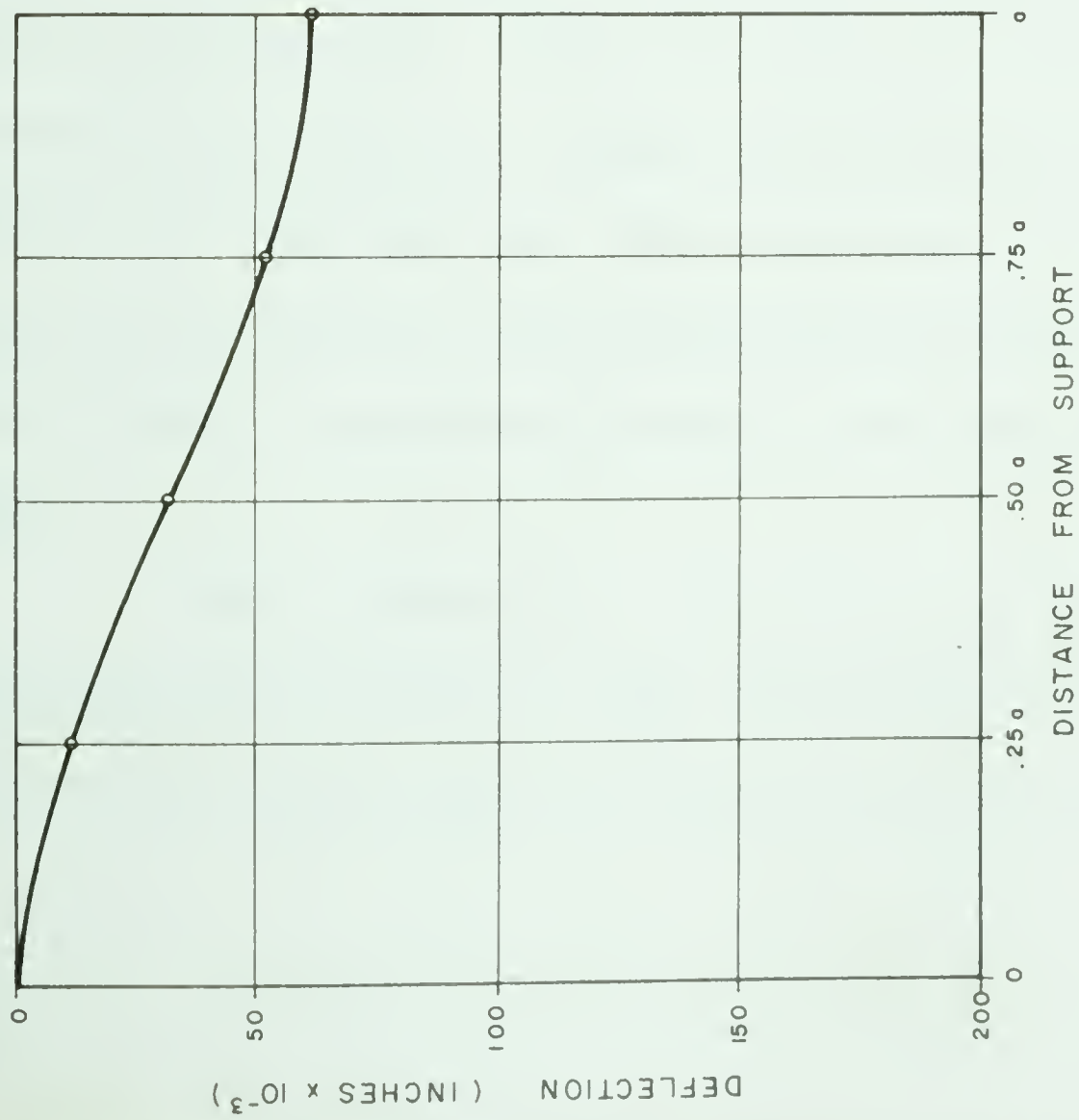


(a) TEST No. 1 - 6000 # LOAD

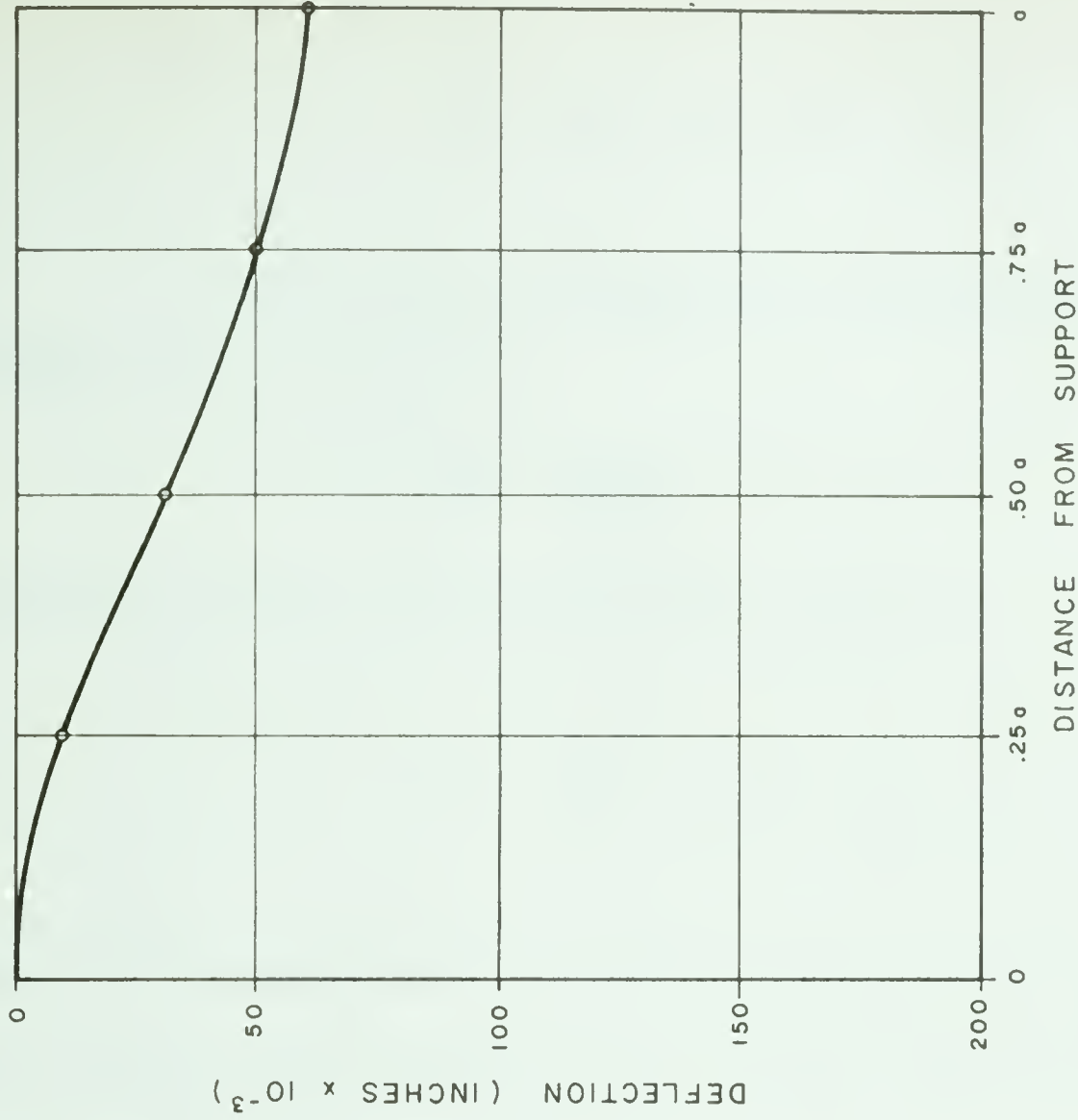


(b) TEST No. 4 - 6000 # LOAD

FIGURE 6.6 GABLE BEAM DEFLECTIONS (CORRECTED FOR LATERAL STRAIN)



(a) TEST No. 6



(b) TEST No. 7

FIGURE 6.7 GABLE BEAM DEFLECTIONS (CORRECTED FOR LATERAL STRAIN)

$$M = \frac{EI}{d} (\epsilon_T - \epsilon_B)$$

Secondly, bending moments may be calculated from the deflection readings using the relationship:

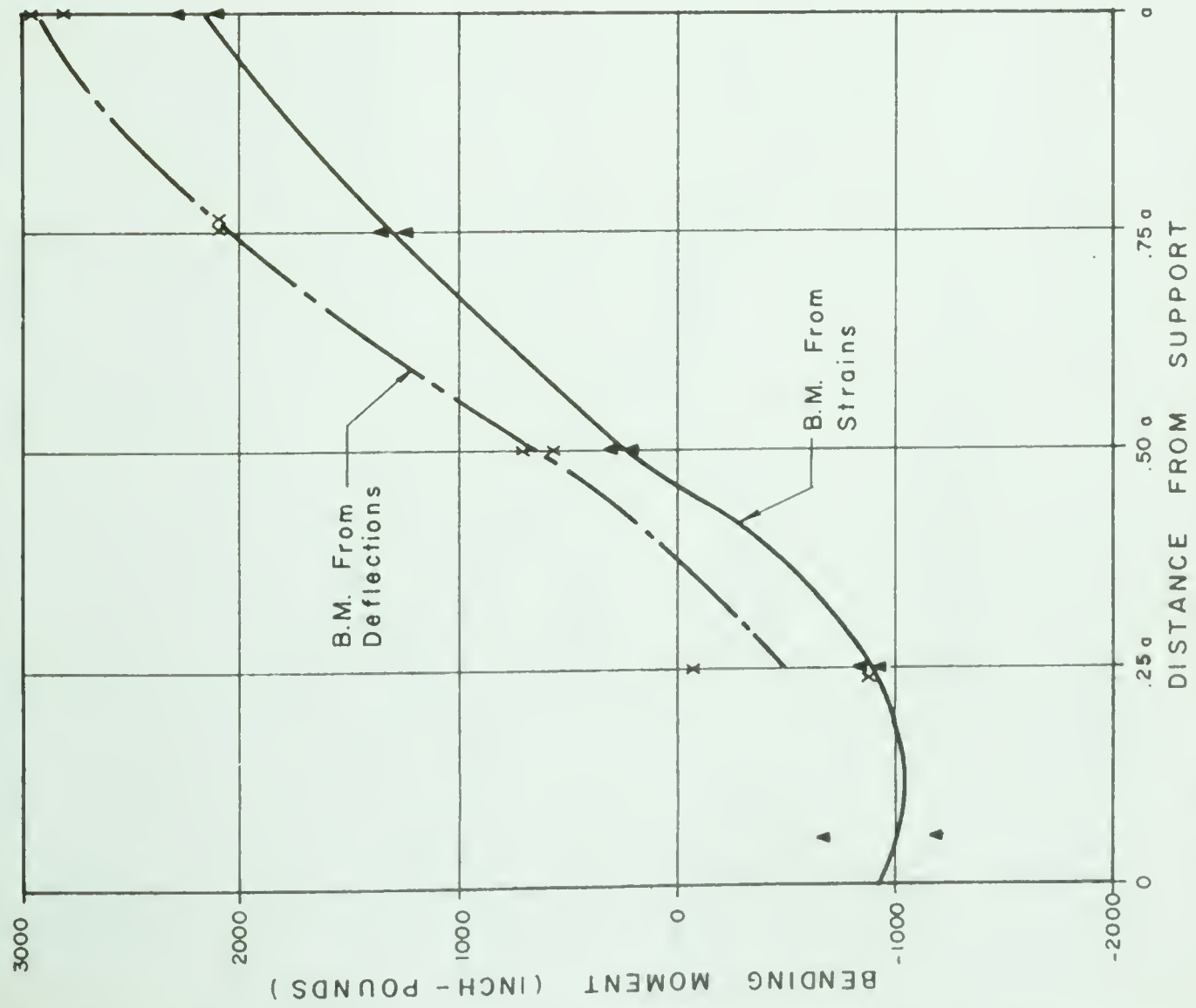
$$\frac{M}{EI} = \frac{d^2 y}{dx^2}$$

An attempt was made to write a polynomial of the form

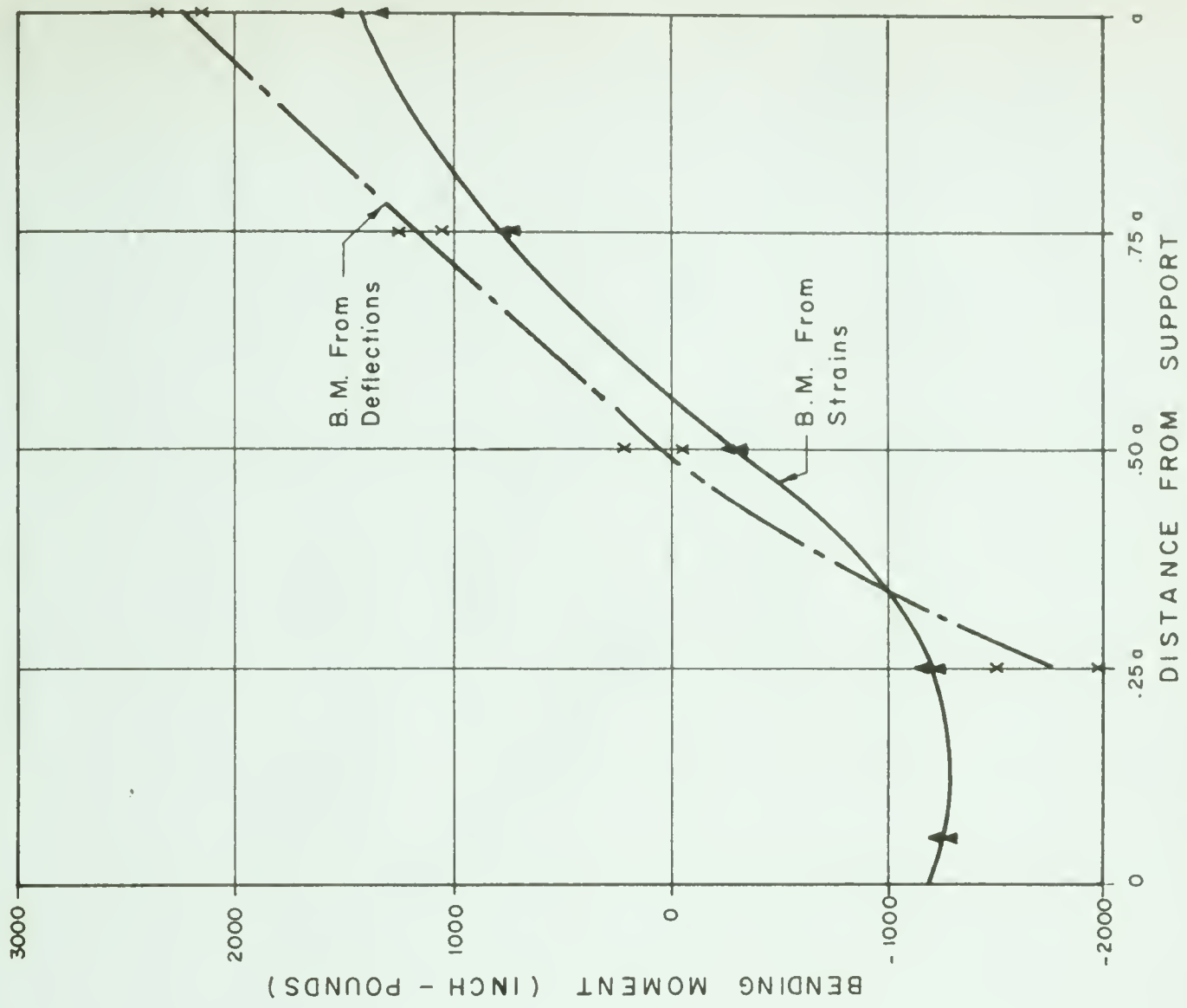
$$y = Ax^4 + Bx^3 + Cx^2 + Dx + E$$

and by inserting the measured values of deflection at the corresponding value of x , to solve for the constants A , B , C , D and E . This resulted in a smooth curve, but the second differential was of necessity a second order curve which was not necessarily correct. Finally, the bending moment was calculated using the method of finite differences, taking the second difference in the measured deflections as a concentrated angle change and assuming that the average angle change over a given interval was the concentrated angle change divided by the length of interval. This permitted the bending moment diagram to assume any shape.

A study of FIGURE 6.8 (a) and (b) indicates that the bending moments as found from the deflection readings were considerably greater than those found from the strain readings, but the same general trend is found by each



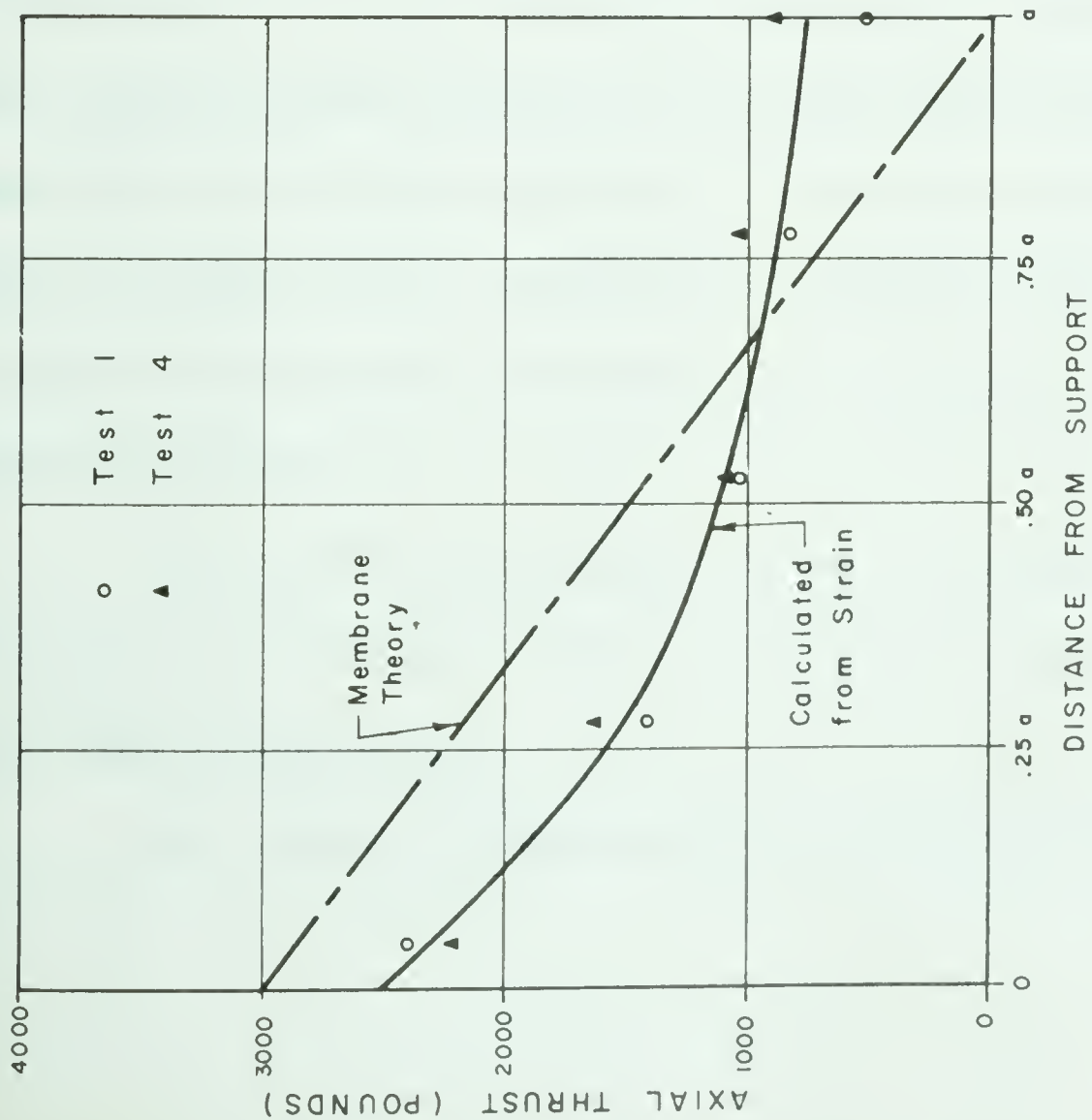
(a) TESTS 1 & 4 - (1/2" TIE ROD ONLY)



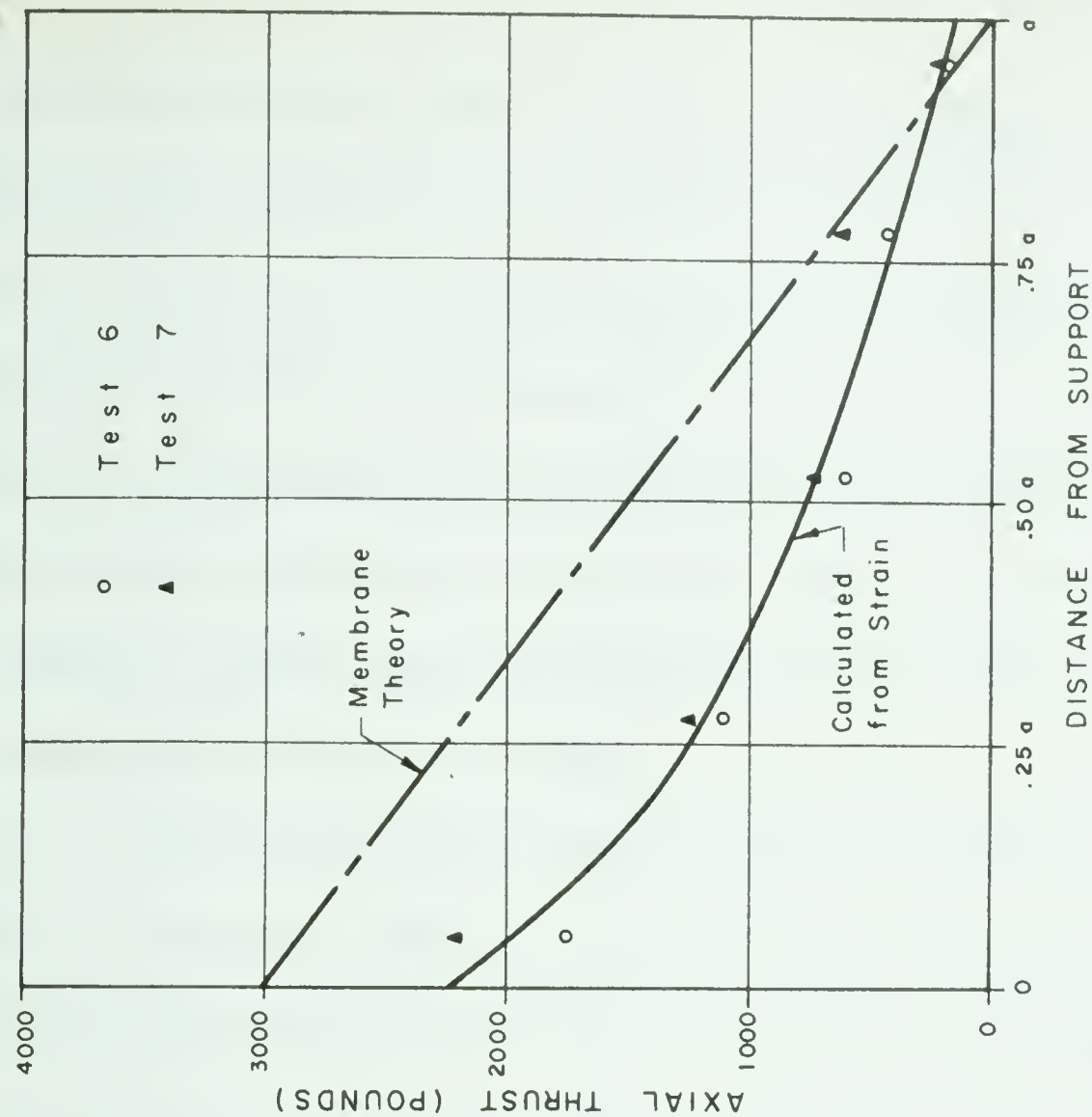
(b) TESTS 6 & 7 - (3/4" TIE RODS ADDED)

FIGURE 6.8 GABLE BEAM BENDING MOMENTS DERIVED FROM MEASURED

STRAINS & DEFLECTIONS - 6000# UNIFORM LOAD



(a) SINGLE 1/2" TIE ROD ONLY



(b) 3/4" TIE RODS ADDED

FIGURE 6.9 GABLE BEAM AXIAL THRUSTS DERIVED FROM STRAIN READINGS
6000 # UNIFORM LOAD

method. This deviation is attributed to cracks in the beams, which were noticed in the higher loads in Test 1 and remained throughout all other tests. Since the uncracked moment of inertia was used in the calculation of bending moments, and since the section was in fact cracked in the areas of high moment, the indicated bending moments based on deflections could be expected to be high. Indicated bending moments, as computed from deflection readings, are extremely sensitive to slight errors in measurements and serve only as a rough check on the accuracy of the strain readings.

The effect of cracks on the strain gauge readings is not so simple. Where a crack occurs within the gauge length, the reading is excessive. When this excess was apparent, the reading was discarded in determining both bending moments and axial thrusts. Where a strain gauge occurs between cracks, the indicated strain is lower than would be expected if the cracks were not present. In processing data, however, it is not known whether cracks were present or not, so that the indicated strains are taken as the actual strain of an elastic, uncracked section. The gauges on the compressive face of a beam having cracks on the opposite side would tend to read higher than would be expected without cracks.

The net effect of the presence of cracks on bending moments derived from strain readings is probably to produce apparent moments which are lower than the actual moments.

The conclusion drawn from the above discussion is that the solid

and dotted curves in FIGURE 6.8 represent a lower and upper bound respectively to the actual bending moments in the gable beams, but it is thought that the strain readings are a more reliable measure of actual B.M. than the deflection readings.

It may be seen that the positive moment in Test 6 and 7, where the additional tie rods were used, is reduced from the value found in Tests 1 and 4, although the negative moments at the support are nearly the same.

Axial thrusts computed from strain measurements for the gable beams are plotted for the uniform loading series in FIGURE 6.9 (a) and (b). FIGURE 6.9 (a) shows that in Test 1 and 4 the maximum thrust occurs at the support, gradually diminishing towards the centre as predicted by membrane theory. The rate of transfer of stress to the shell in the central half of the gable beam is considerably lower than would be expected, leaving a residual compression in the gable beam at the ridge. Tests 6 and 7 follow the same general pattern, but the magnitude of the residual compression in the gable at the ridge is notably reduced due to the additional tie rods. In both cases, the thrust in the vicinity of the support is lower than predicted by membrane theory. This is attributed to the flange action of the shell which effectively increases the area of the beam.

6.4 Ridge Beams

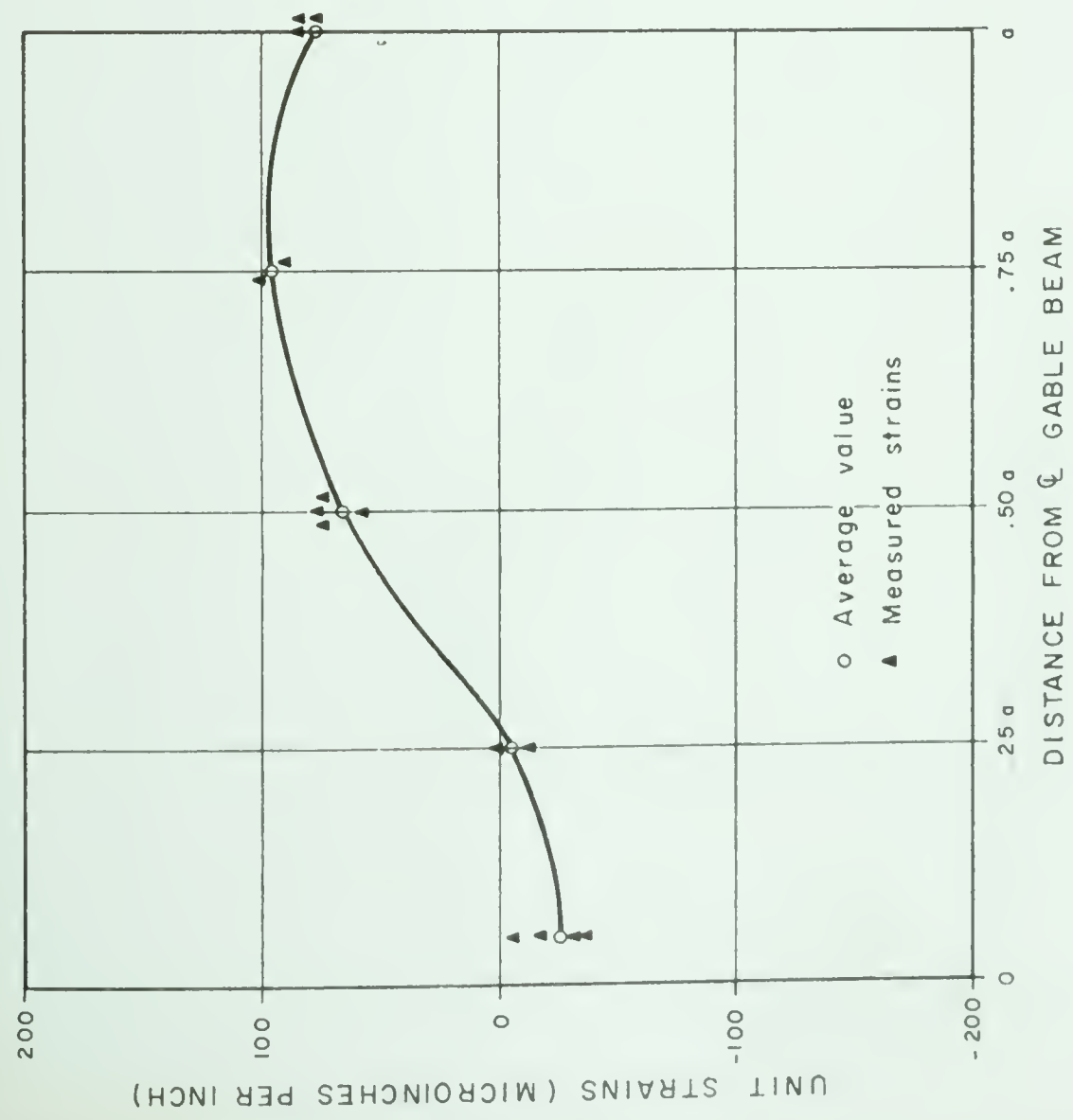
FIGURES 6.10 and 6.11 indicate the magnitude of measured strains in the ridge beams for Tests 1 and 4. Again, as for the gables, the curves

are similar, each showing a peculiar change in continuity in the bottom strains near the support. FIGURE 6.12 is a similar plot for Test 6 and although the general shape of the curves is not unlike those for Tests 1 and 4, the absolute magnitude of strains is considerably reduced.

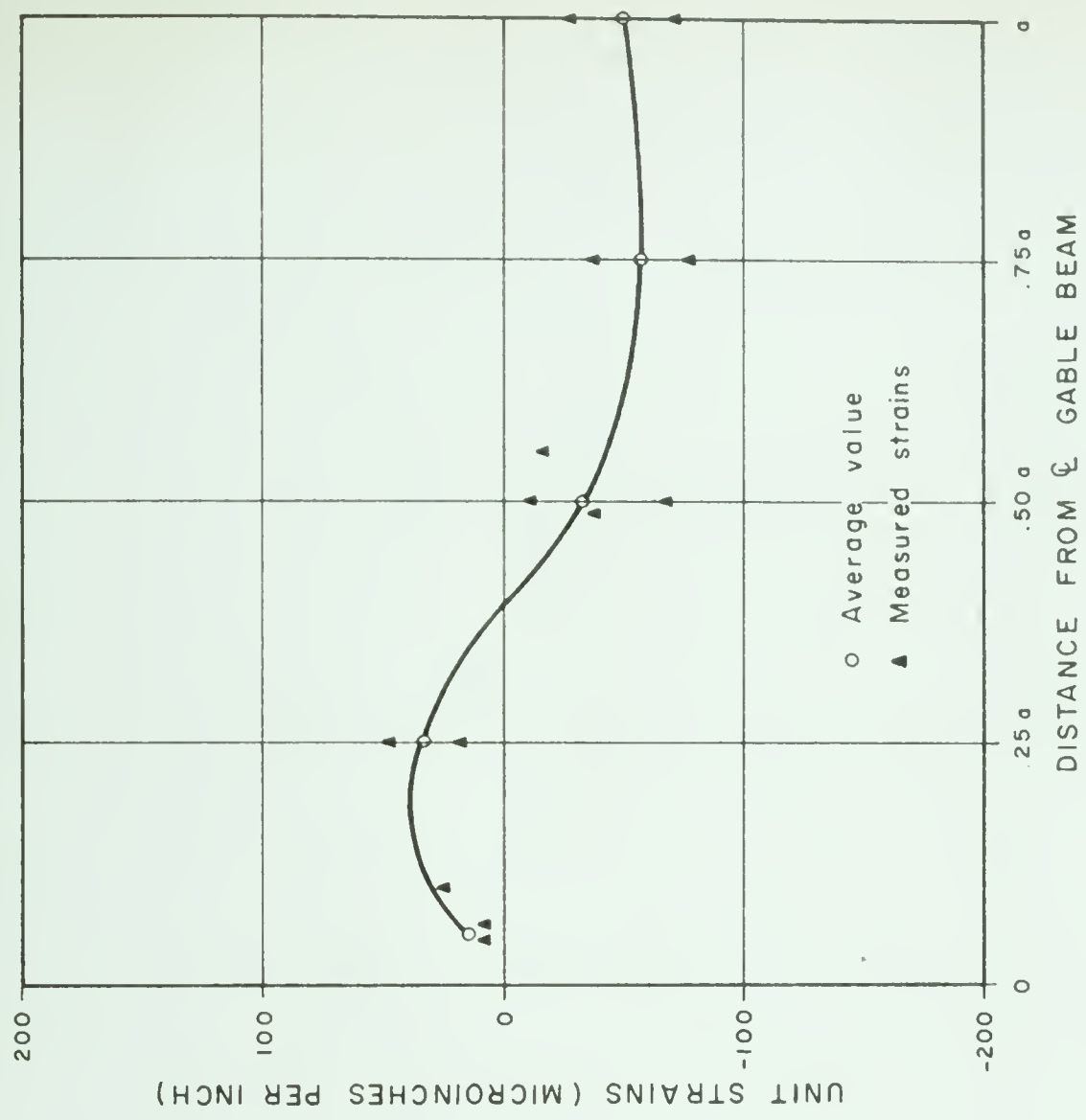
Ridge beam deflections for all symmetrical loading tests are plotted in FIGURE 6.13 (a) and (b). While the heavier tie rods appear to have slightly reduced deflections in the ridge beams, the effect is not so pronounced as it was in the case of the gables. This, of course, could be expected, since the tie rods are directly connected to the gable beams.

Ridge beam bending moments, calculated from deflections and strain readings are plotted in FIGURE 6.14. The heavier tie rods used in Tests 6 and 7 reduced the magnitude of the positive bending moment at midspan, although not so markedly as for the gable beams. The moments computed from deflections again provide a rough check on the strain measurements but suggest a shift in the point of inflection from the position found on the basis of strains.

Both curves are decidedly "S" shaped, the values of bending moment dropping off rapidly near the support and the ridge beam junction. The problem of computing bending moments from strain measurements at the junction of two ridge beams is a complex problem in the theory of elasticity. In the length of the junction, the effective width of each ridge beam is materially increased by the presence of the other beam. Assuming the ridge beams to be

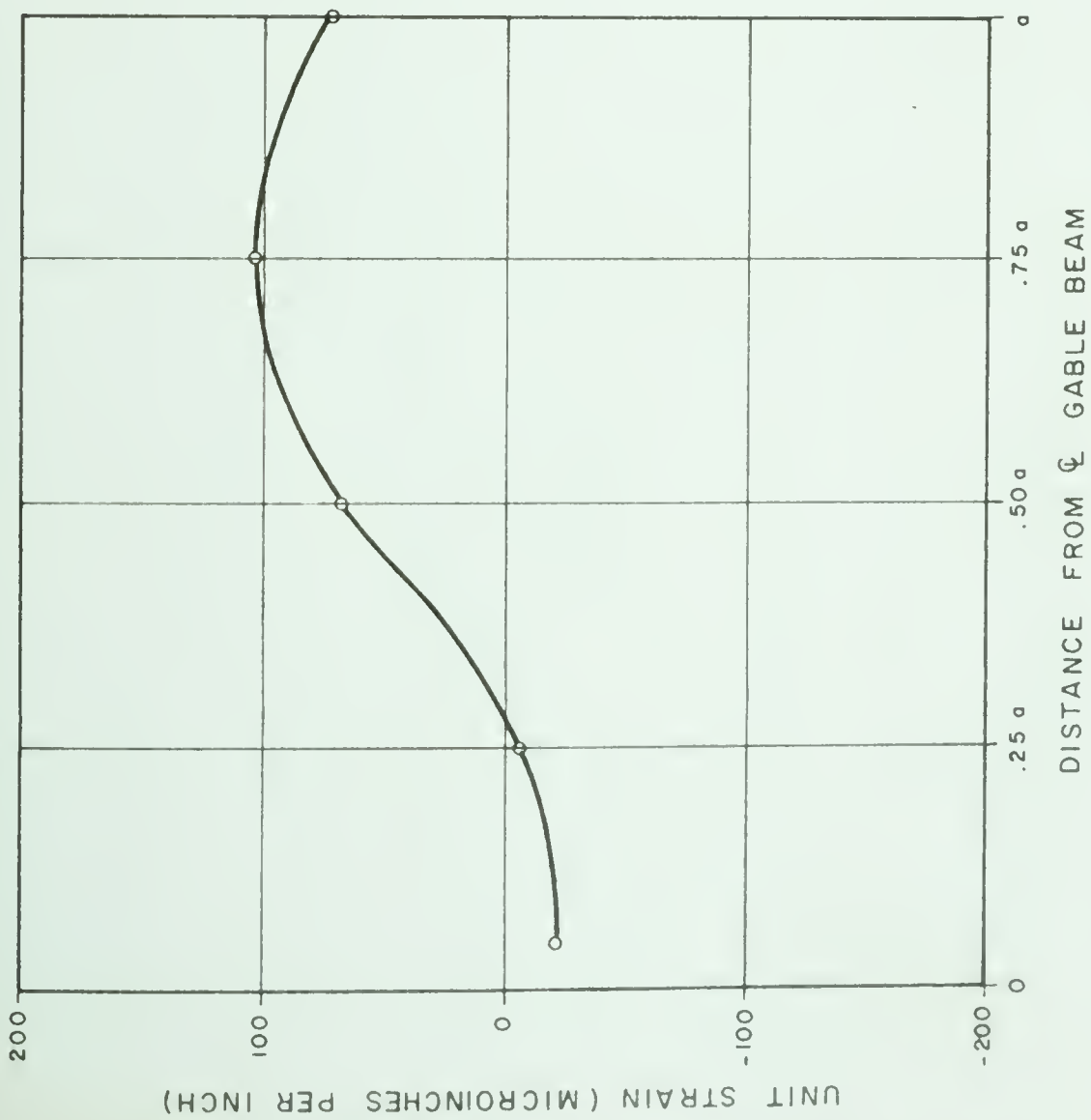


(a) STRAIN IN TOP FIBRE

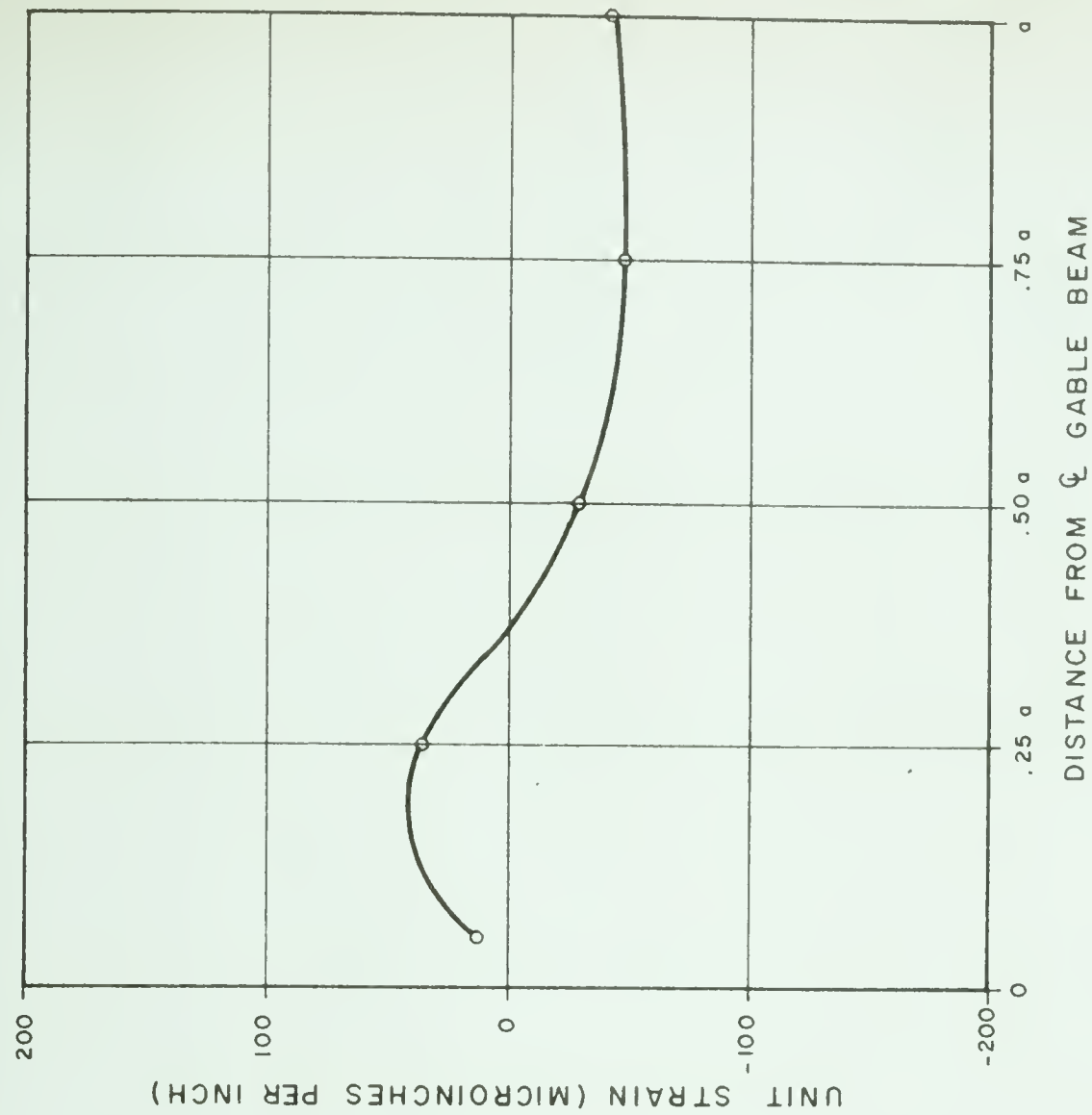


(b) STRAIN IN BOTTOM FIBRE

FIGURE 6.10 MEASURED STRAINS IN RIDGE BEAMS - TEST #1 - 6000 # LOAD

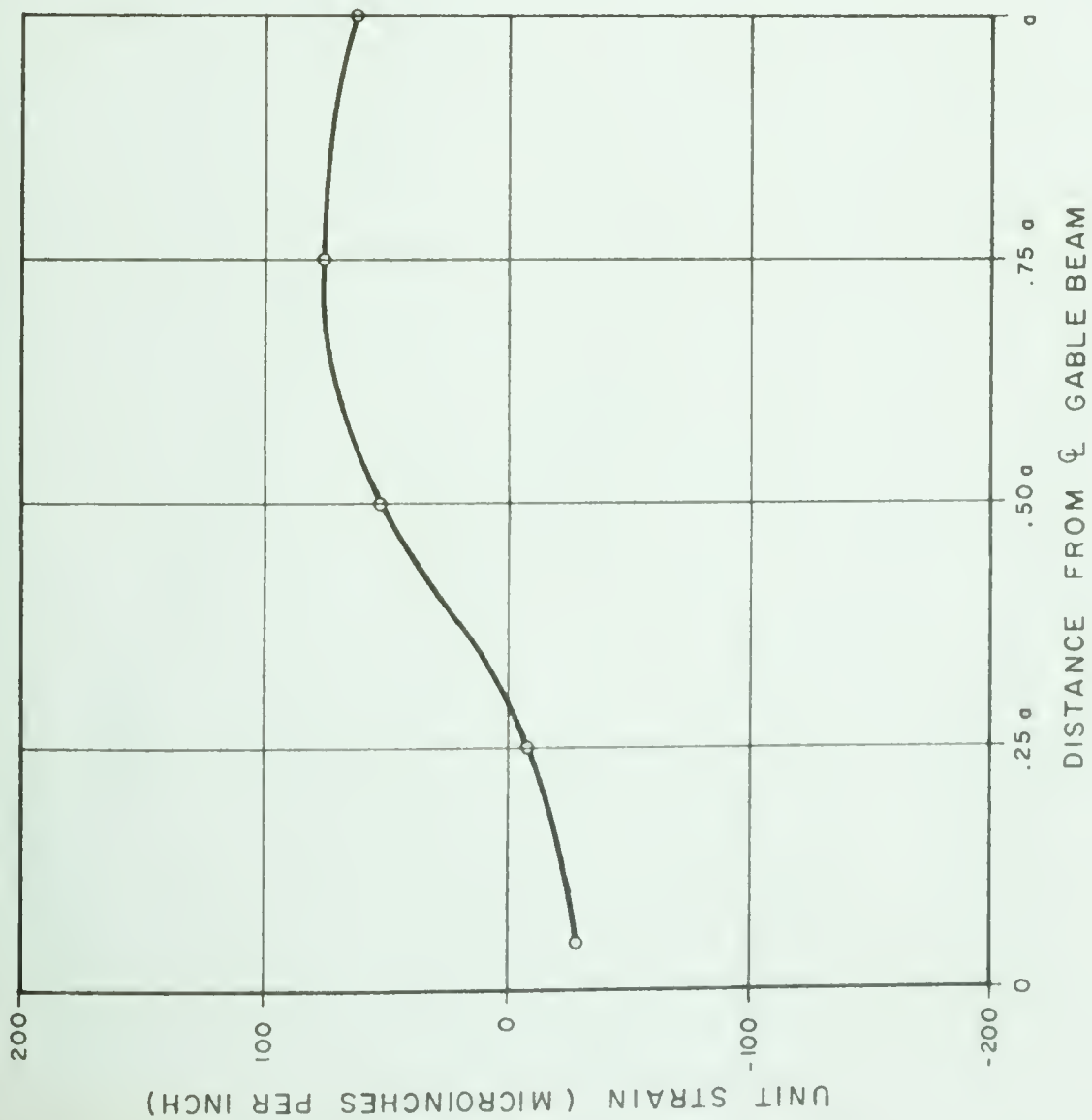


(a) STRAIN IN TOP FIBRE

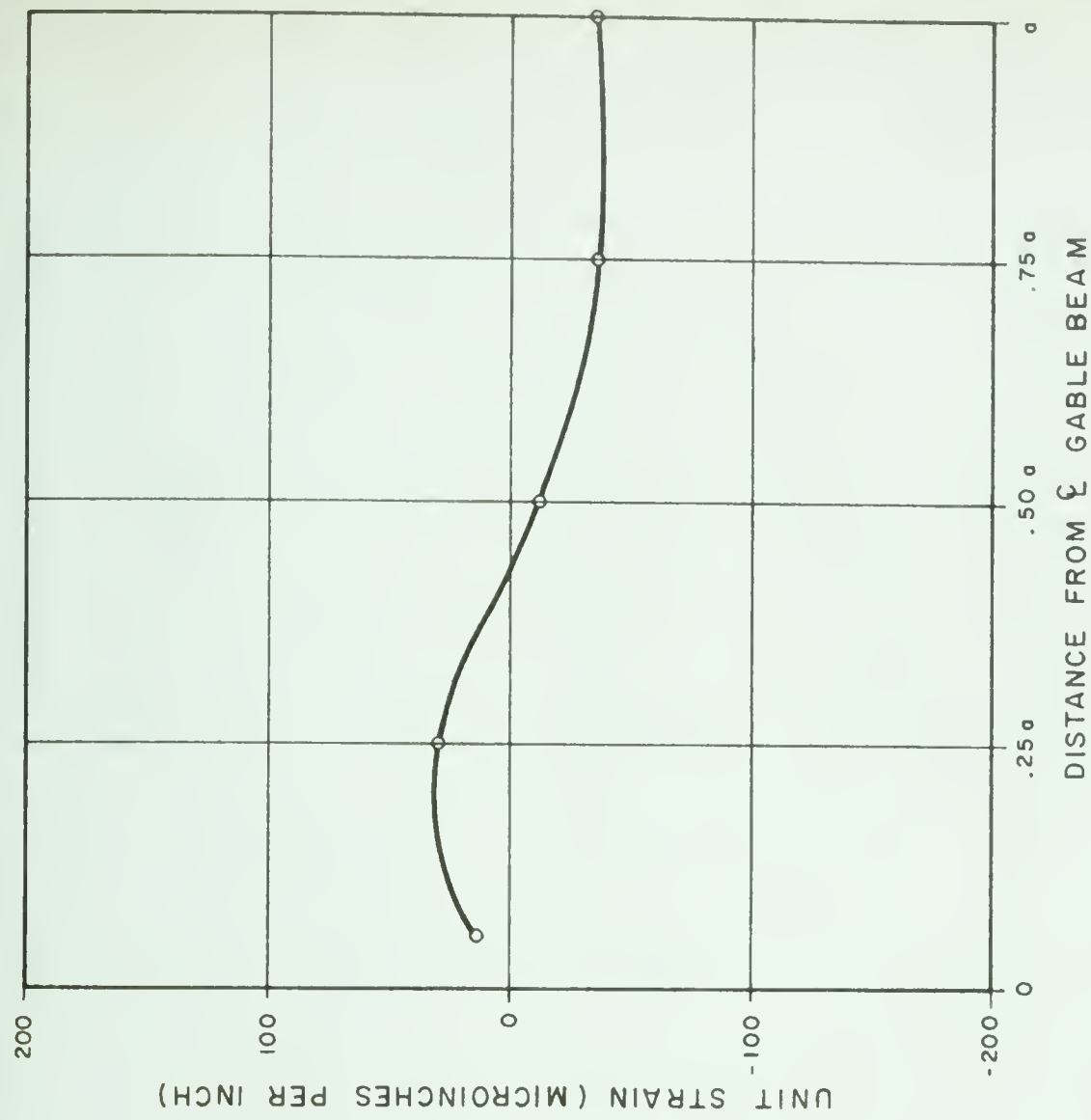


(b) STRAIN IN BOTTOM FIBRE

FIGURE 6.11 MEASURED STRAINS IN RIDGE BEAMS - TEST #4 - 6000# LOAD

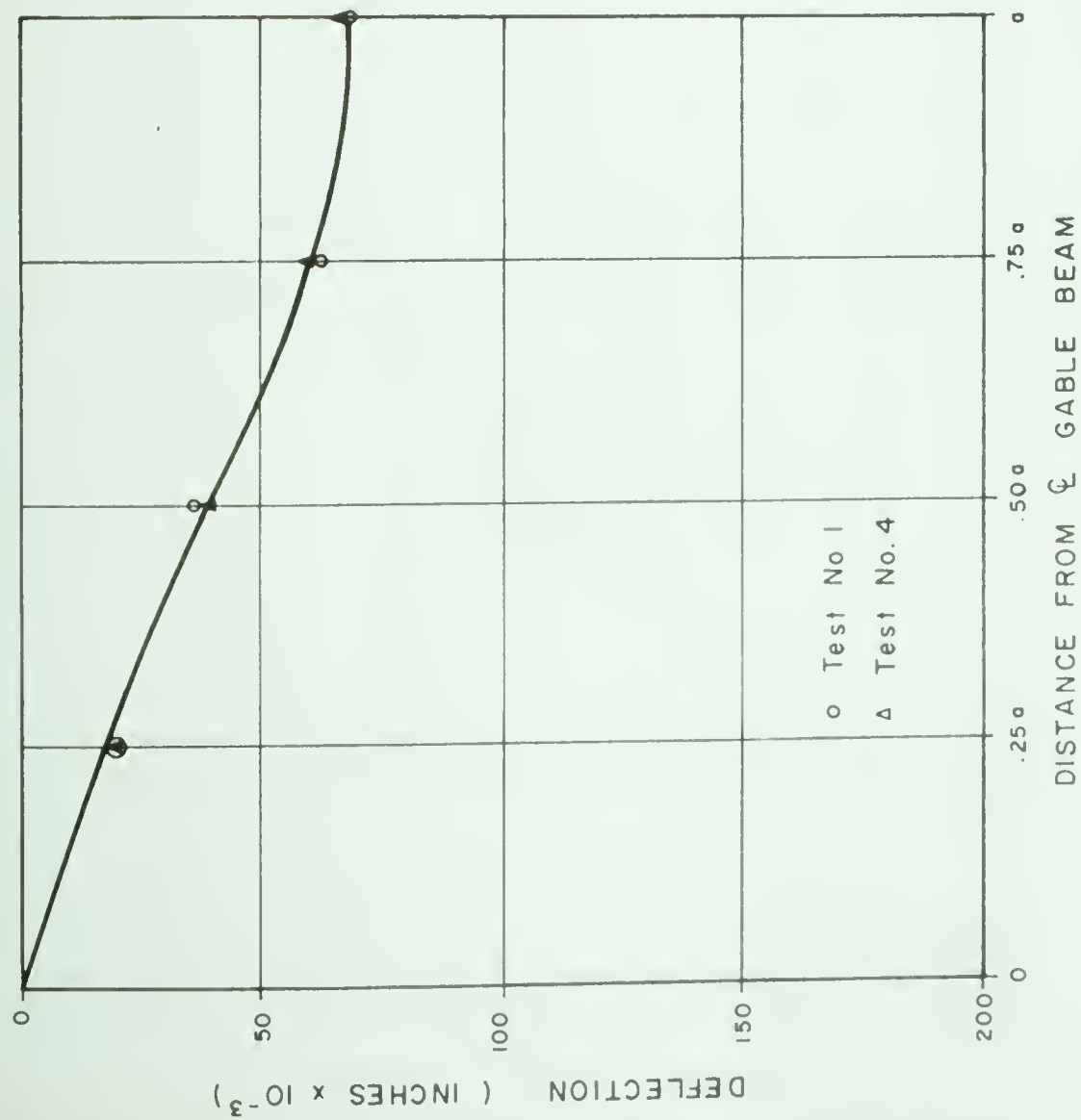


(a) STRAIN IN TOP FIBRE

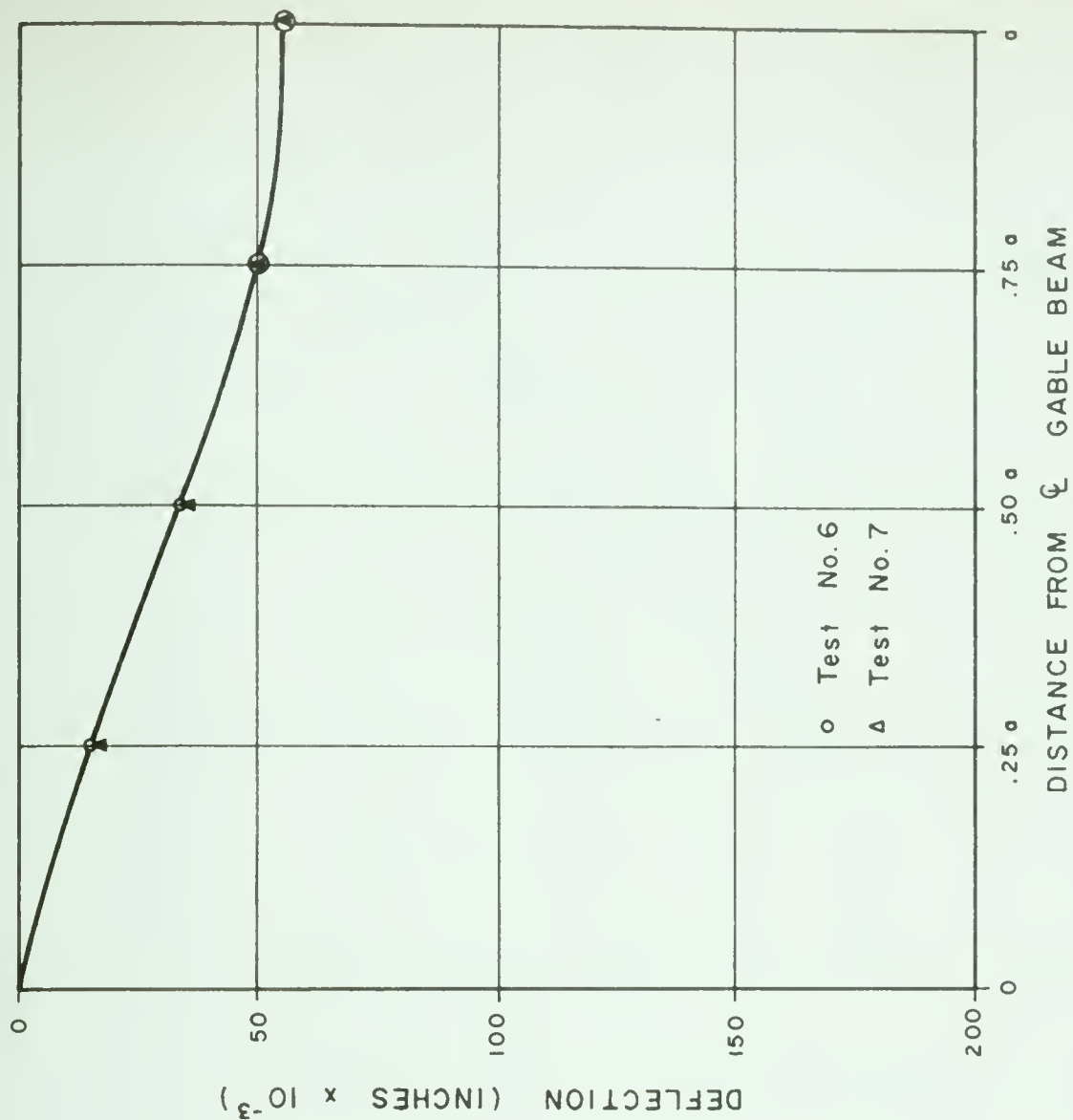


(b) STRAIN IN BOTTOM FIBRE

FIGURE 6.12 MEASURED STRAINS IN RIDGE BEAMS - TEST #6 - 6000 # LOAD

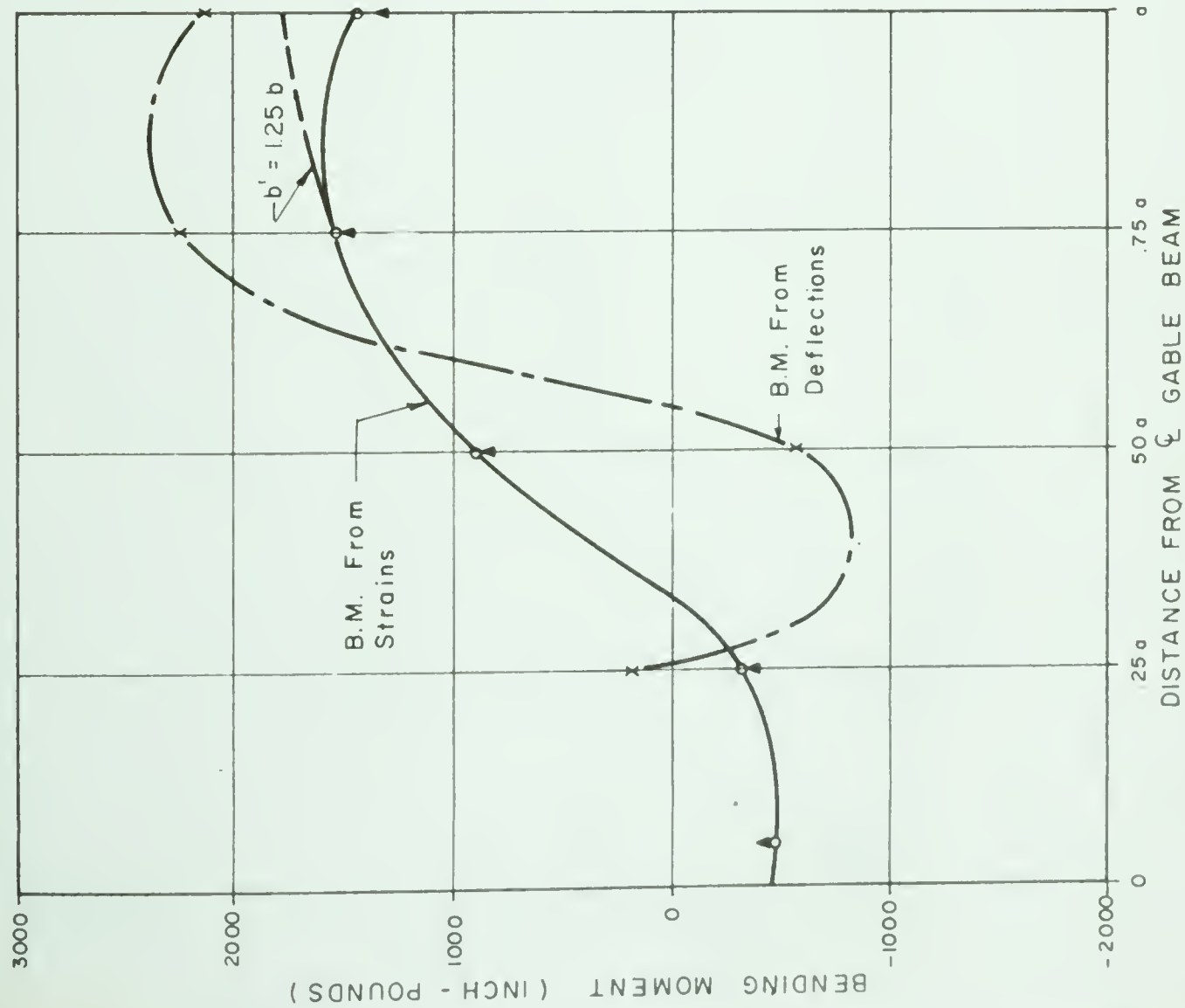


(a) TESTS No. 1 & 4 - 6000 # LOAD

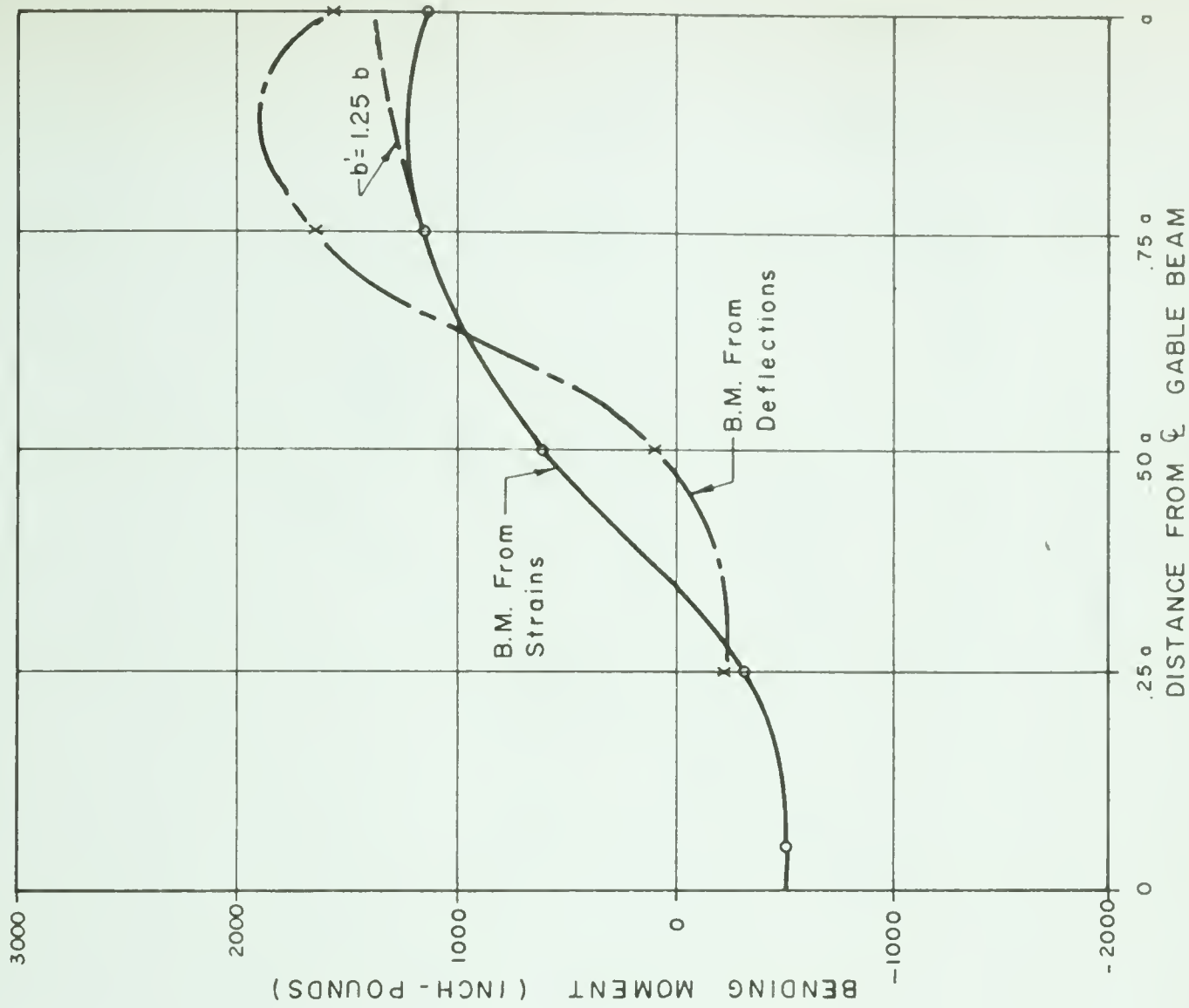


(b) TESTS No. 6 & 7 - 6000 # LOAD

FIGURE 6.13 RIDGE BEAM DEFLECTIONS (RELATIVE TO GABLE BEAM JUNCTION)



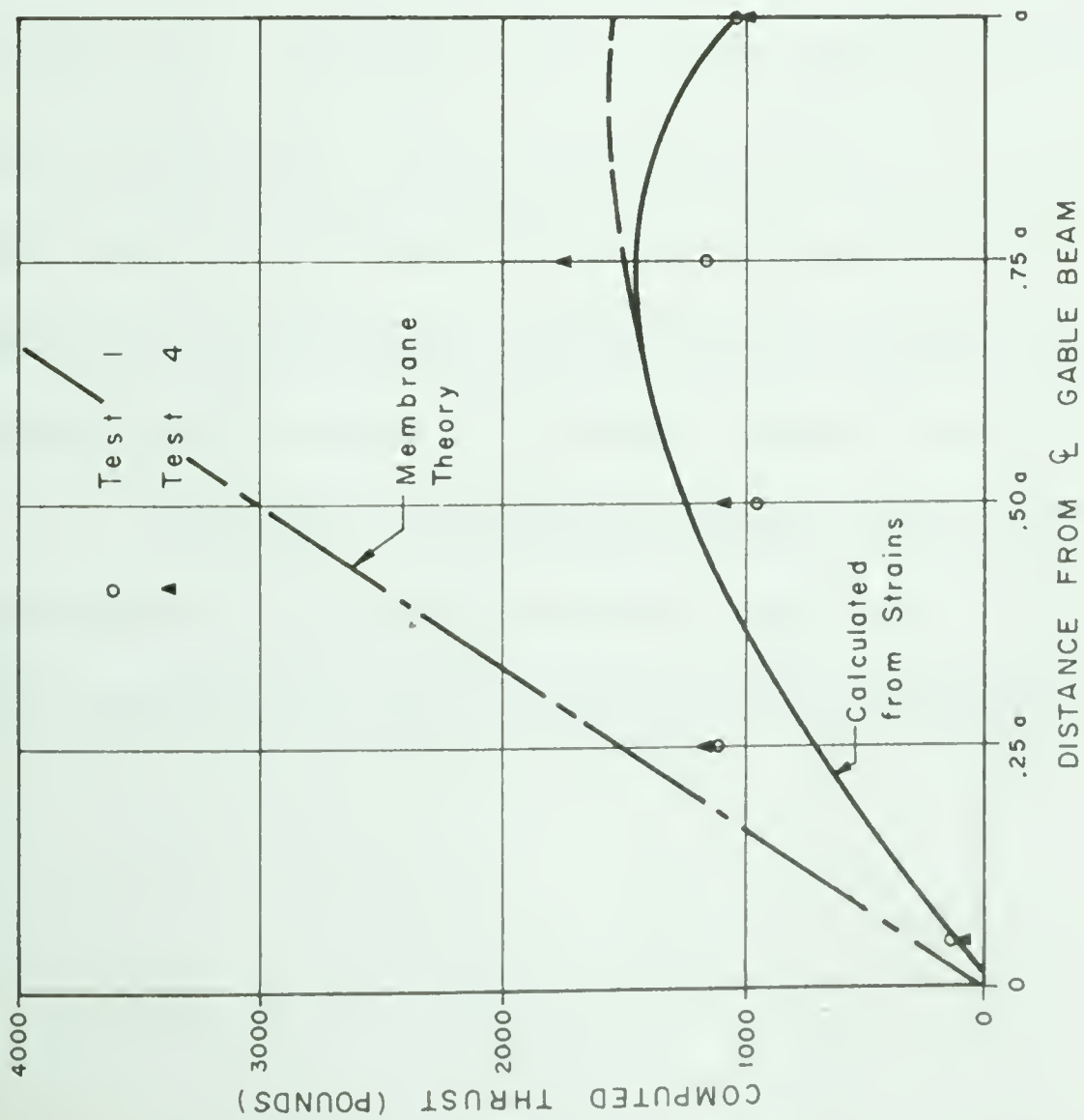
(a) TESTS 1 & 4 - (1/2" TIE ROD ONLY)



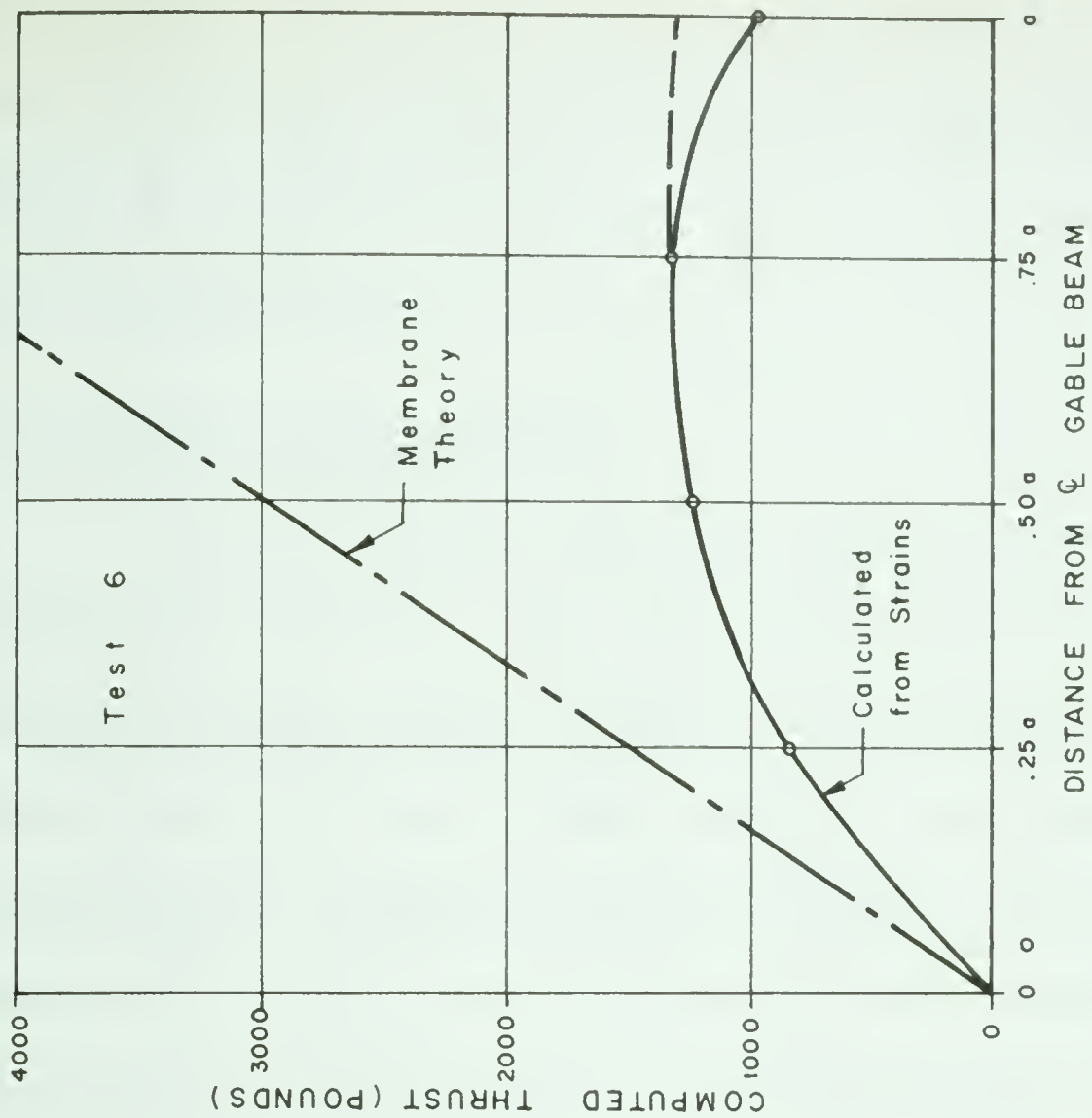
(b) TESTS 6 & 7 - (3/4" TIE RODS ADDED)

FIGURE 6.14 RIDGE BEAM BENDING MOMENTS DERIVED FROM STRAIN READINGS

6000# UNIFORM LOAD



(a) SINGLE 1/2" TIE ROD ONLY



(b) 3/4" TIE RODS ADDED

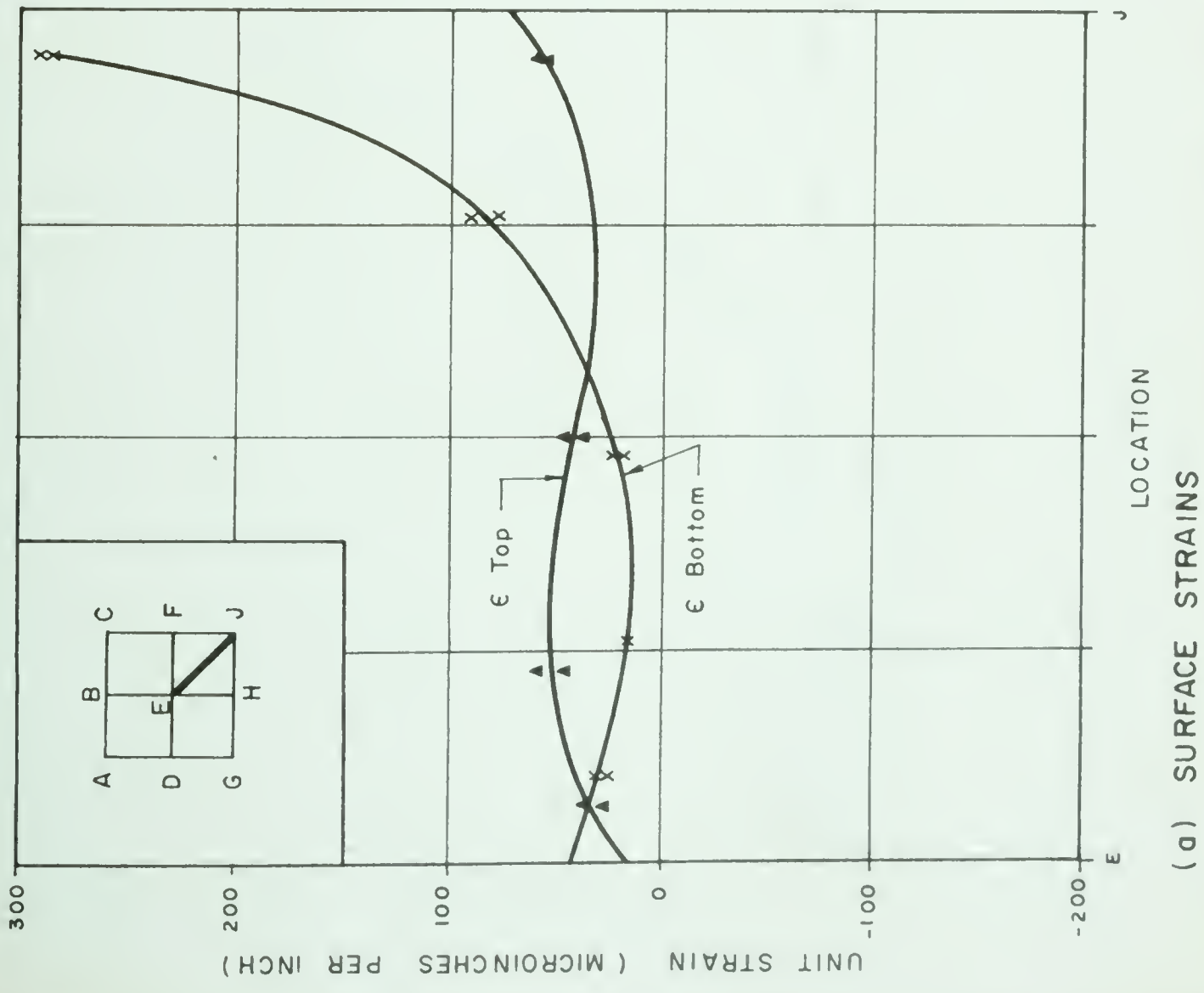
FIGURE 6.15 RIDGE THRUSTS DERIVED FROM STRAIN READINGS
6000# UNIFORM LOAD

fective width of flange increases toward the centre. This has the effect of increasing the area of the beam and raising the neutral axis, both producing a higher calculated thrust.

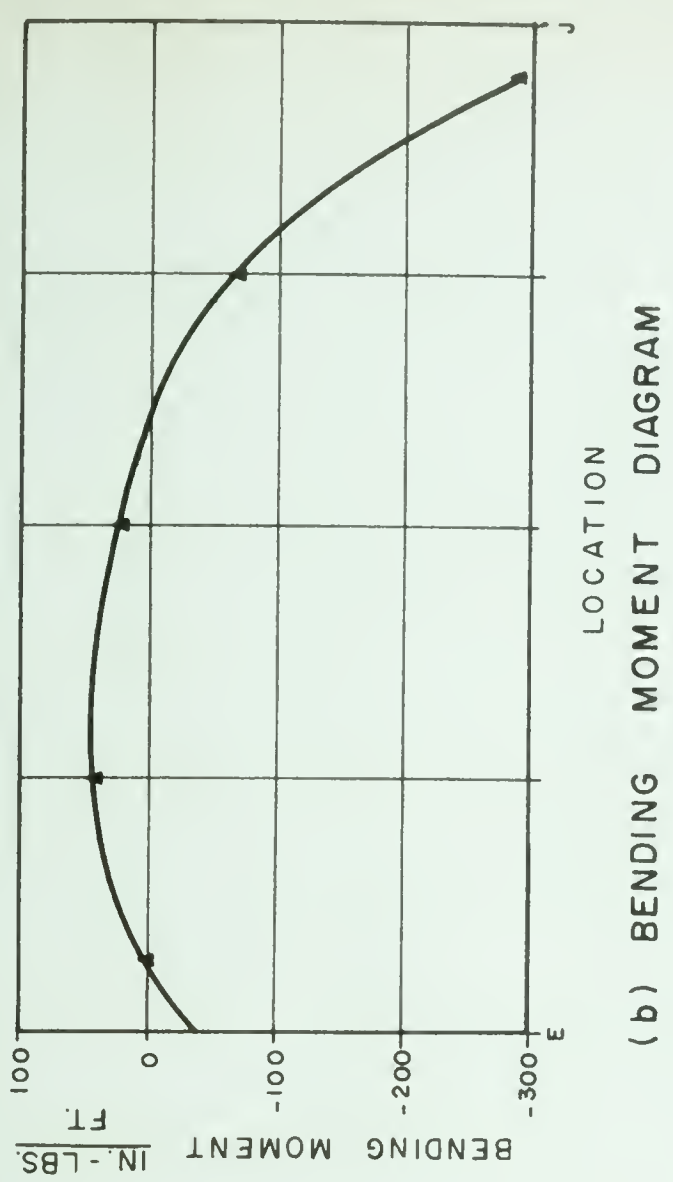
6.5 Compression diagonal of Shell

Measured strains in compression diagonal E J are plotted in FIGURE 6.16 (a) for Tests 1 and 4. The computed bending moments in the compression diagonal, plotted in FIGURE 6.16 (b) show that a small positive moment occurs in the central portion, changing to a large negative moment near the support. Axial stresses plotted in FIGURE 6.16 (c) remain nearly constant over most of the shell, rising sharply toward the support. The constant value in the central portion agrees well with membrane theory, being somewhat higher. The sudden increase in axial thrust toward the support is thought to be a contributing factor toward the negative moments in the gable beams in that region. The shell acted eccentrically to the neutral axis of the gable beam and was resisted by the tie rod force which was located at the neutral axis. These eccentric forces produced a couple acting at the end of the gable, which accounts for the bending moment at the end of the gable beams.

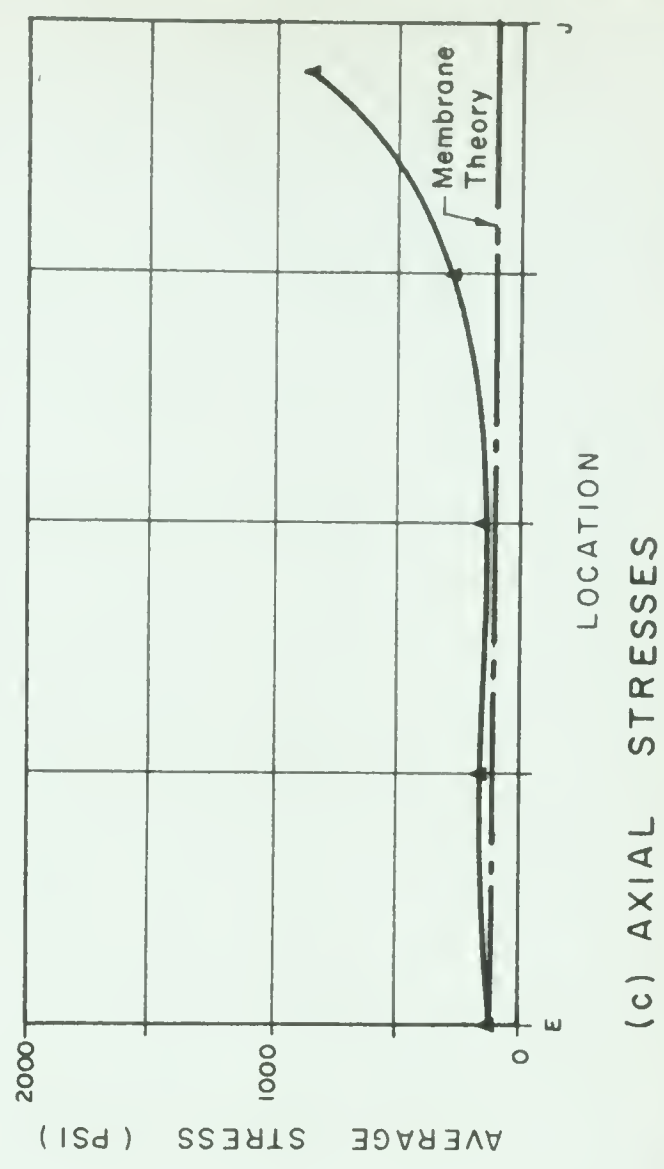
FIGURE 6.17 is a series of similar plots for Tests 6 and 7. The results are very similar to those found in Tests 1 and 4, so that the additional tie rods had little effect on the stresses in the compression diagonal.



(a) SURFACE STRAINS

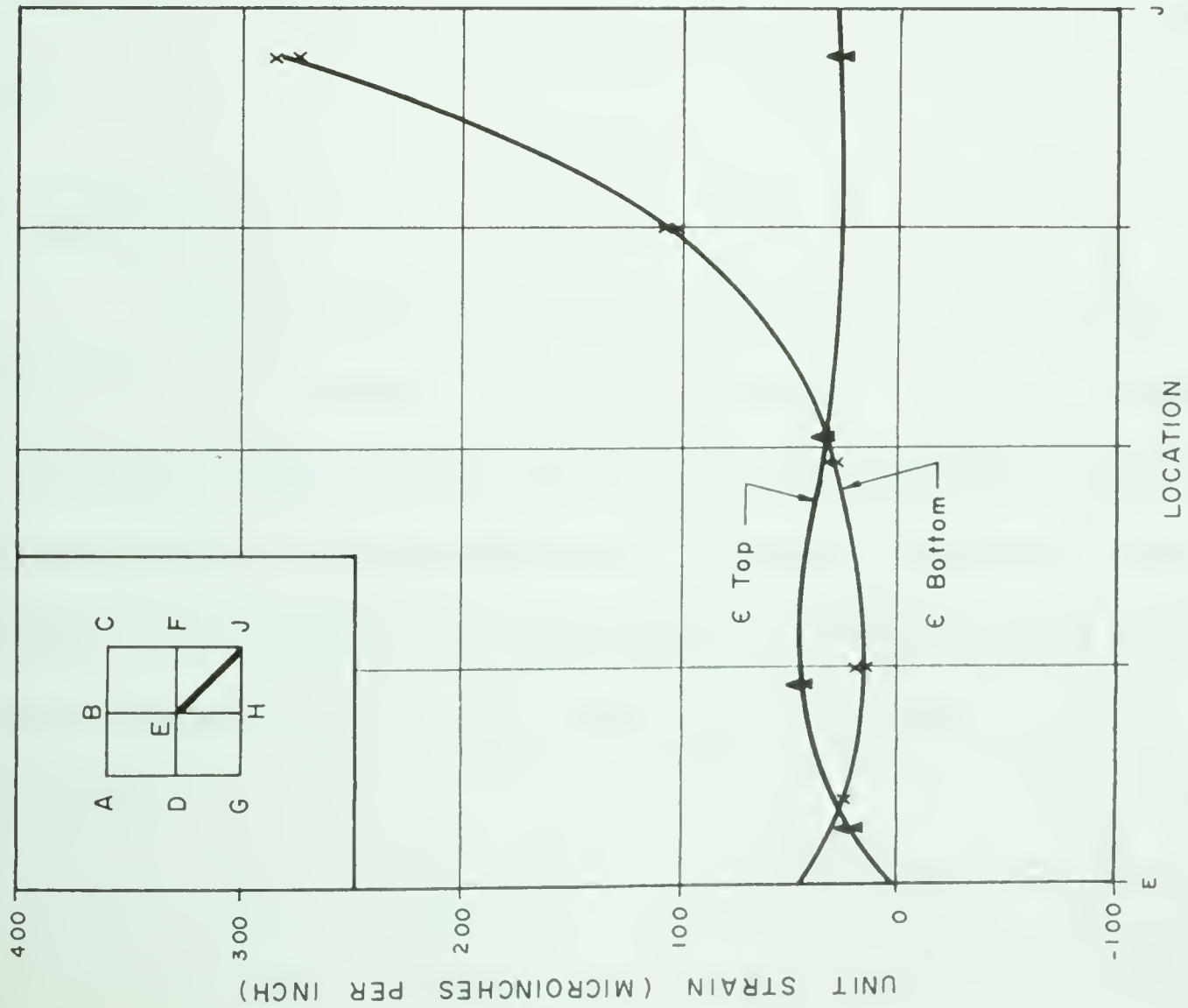


(b) BENDING MOMENT DIAGRAM

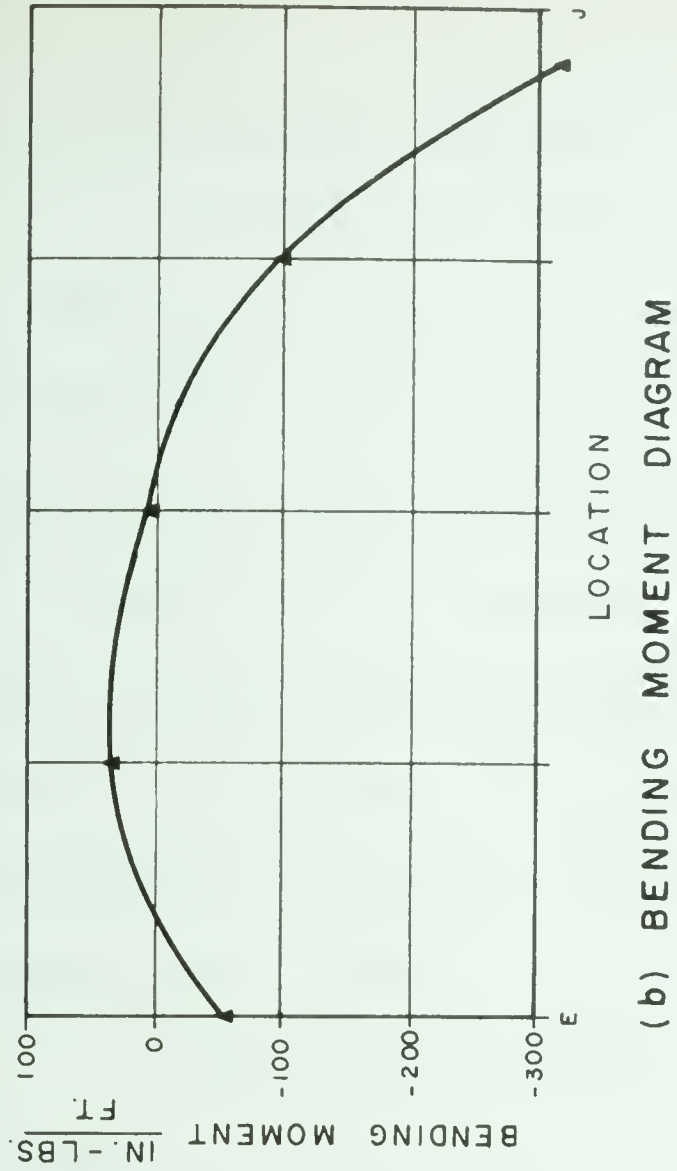


(c) AXIAL STRESSES

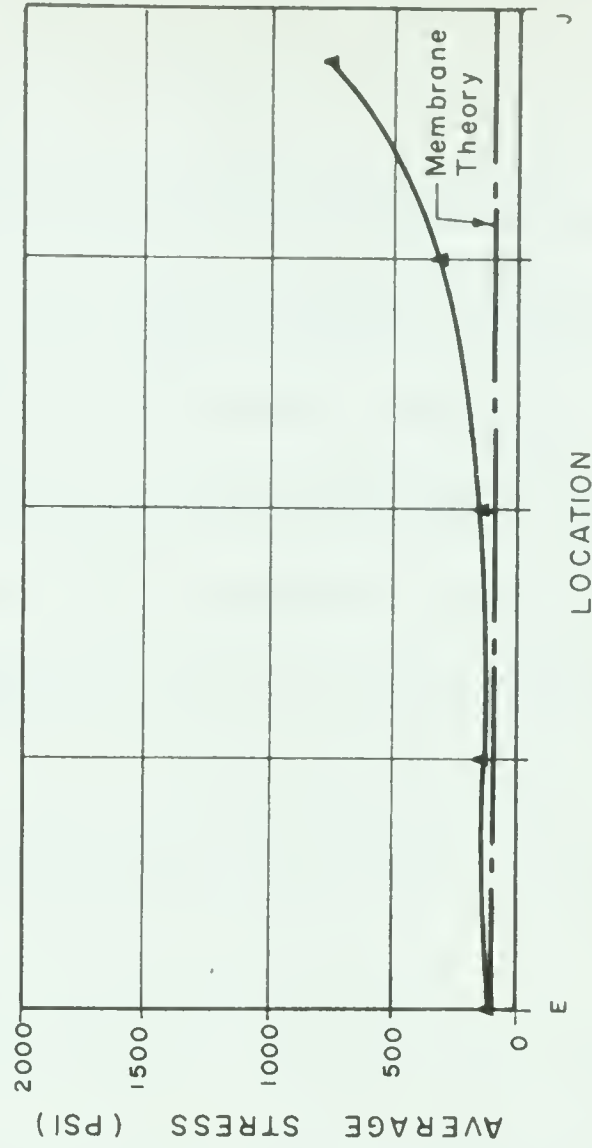
FIGURE 6.16 SURFACE STRAINS, BENDING MOMENTS & AXIAL STRESSES FOR DIAGONAL E-J TESTS #1 & #4 - 6 000 # UNIFORM LOAD



(a) SURFACE STRAINS



(b) BENDING MOMENT DIAGRAM



(c) AXIAL STRESSES

FIGURE 6.17 SURFACE STRAINS, BENDING MOMENTS & AXIAL STRESSES FOR DIAGONAL E-J TESTS #6 & #7 - 6000# UNIFORM LOAD

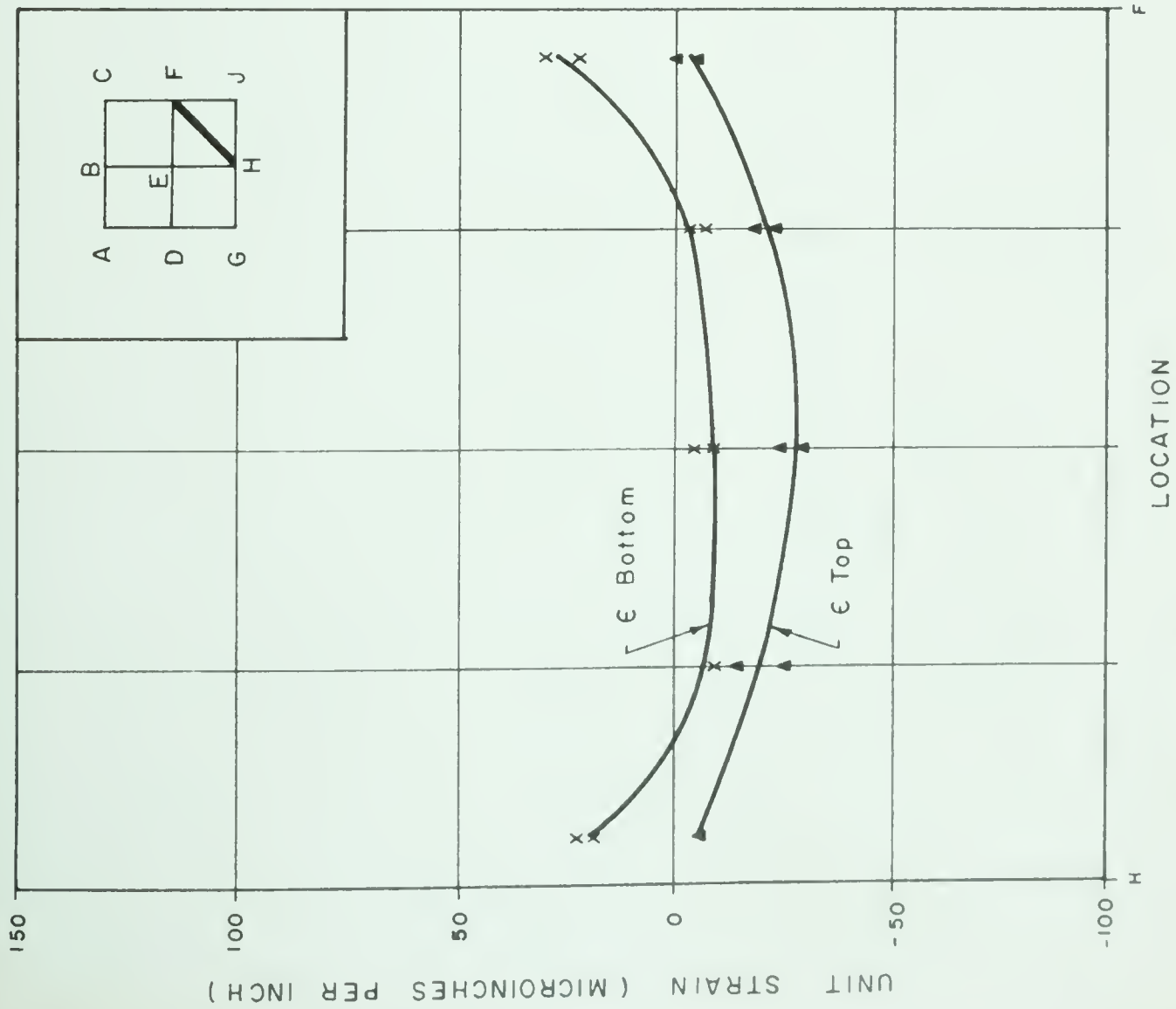
6.6 Tension Diagonal of the Shell

FIGURE 6.18 (a) shows fair agreement between surface strains at the various gauge points in Tests 1 and 4. The surface strains in the upper and lower fibres appear to be displaced by a constant amount, indicating a nearly constant negative bending moment which is plotted in FIGURE 6.18 (b). The magnitude of the bending moment is very low as expected by membrane theory. The axial stresses, plotted in FIGURE 6.18 (c) are nearly constant in the central portion and are slightly lower than membrane theory predicts. At the boundaries, the tension changes to a small compression which is not expected by membrane theory and is attributed to edge disturbances.

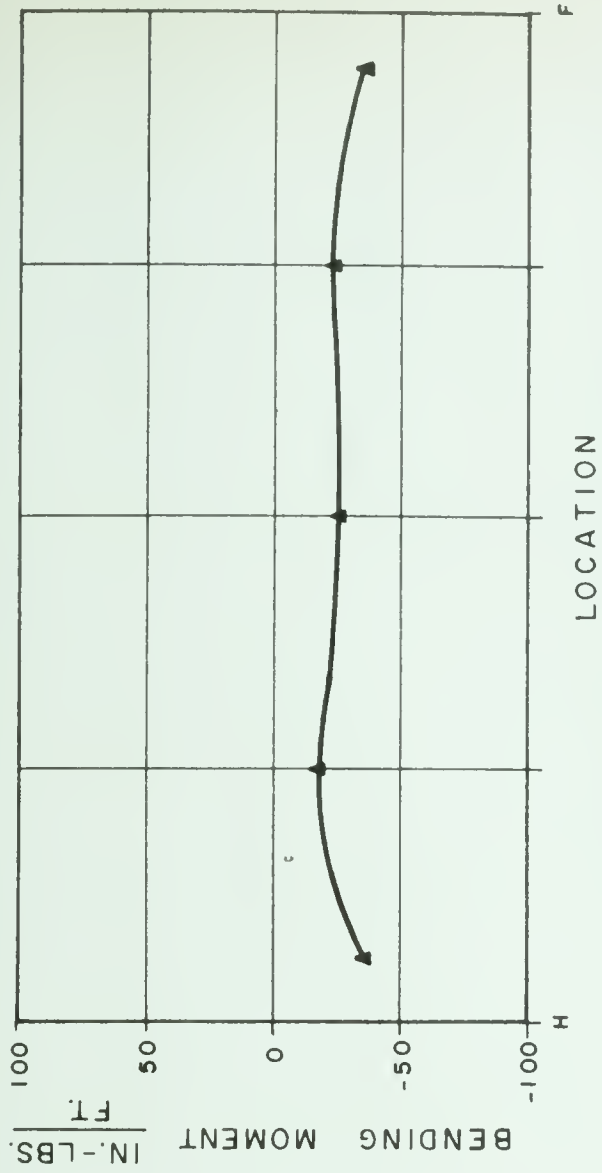
Similar plots are made for Tests 6 and 7 in FIGURE 6.19. The results are virtually identical to those found in Tests 1 and 4, indicating that the additional tie rods had no pronounced effect on the tension stresses in the shell.

6.7 Generator K L

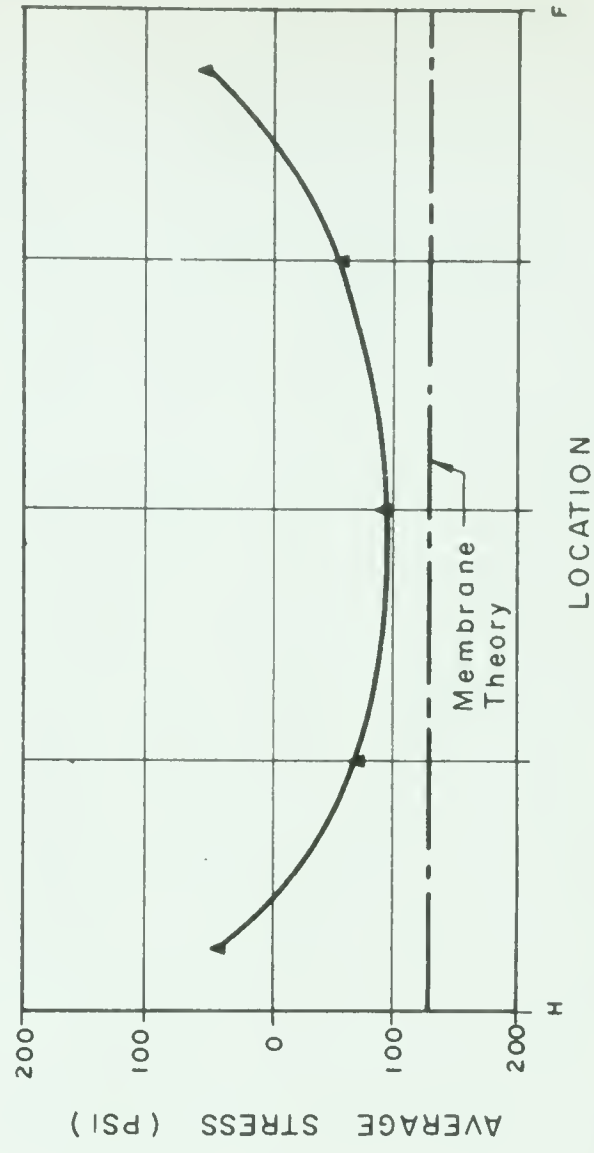
FIGURE 6.20 (a) traces the surface strains in the straight line generator K L. The results of Test 1 are not included as they did not appear to coincide with results in Tests 4, 6 or 7. The suggested reason for this disagreement has been explained earlier and is associated with the test procedure. FIGURE 6.20 (c) indicates that a nearly constant compression occurs in generator K L whereas membrane theory predicts that all generators have zero axial stress.



(a) SURFACE STRAINS

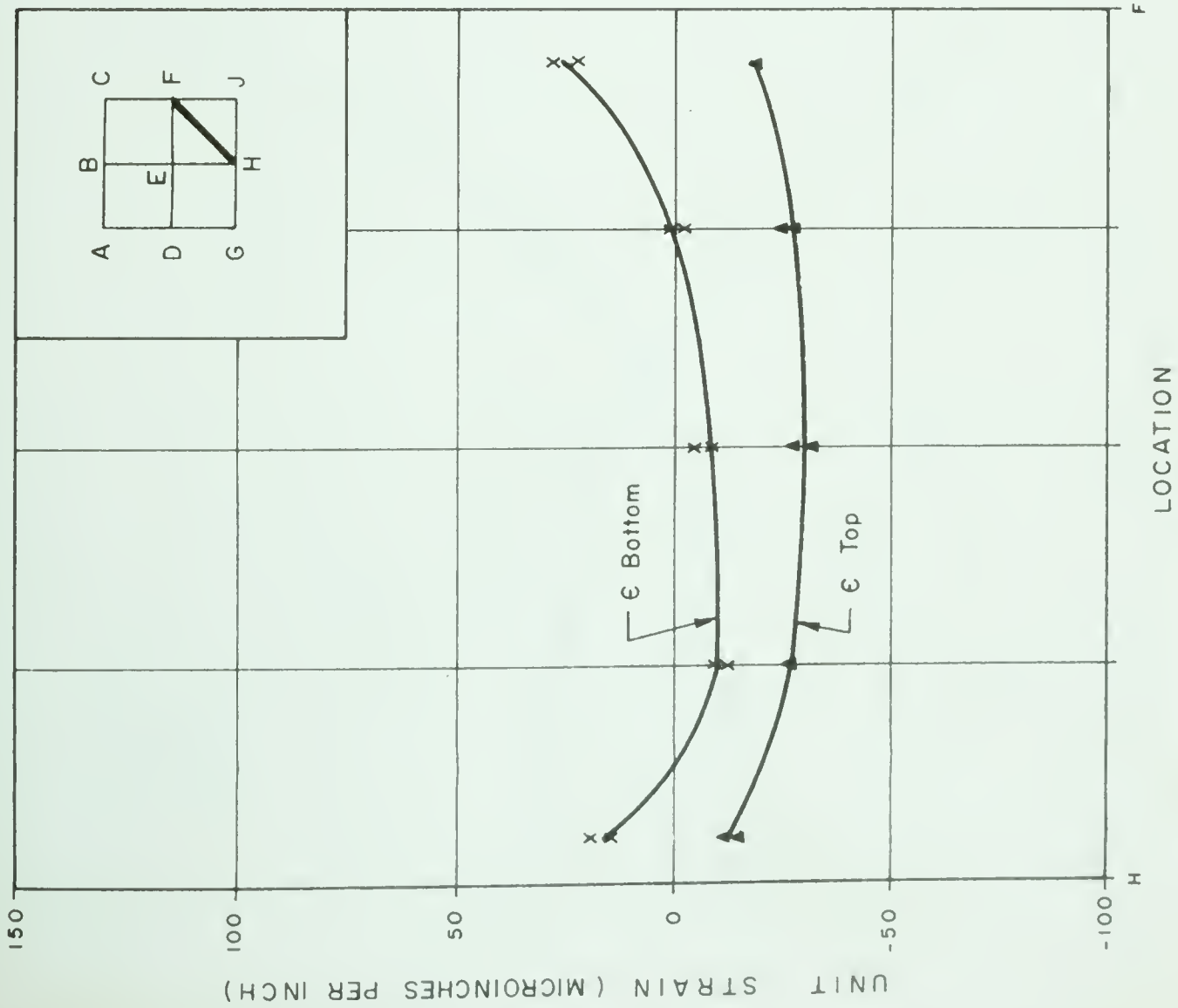


(b) BENDING MOMENT DIAGRAM

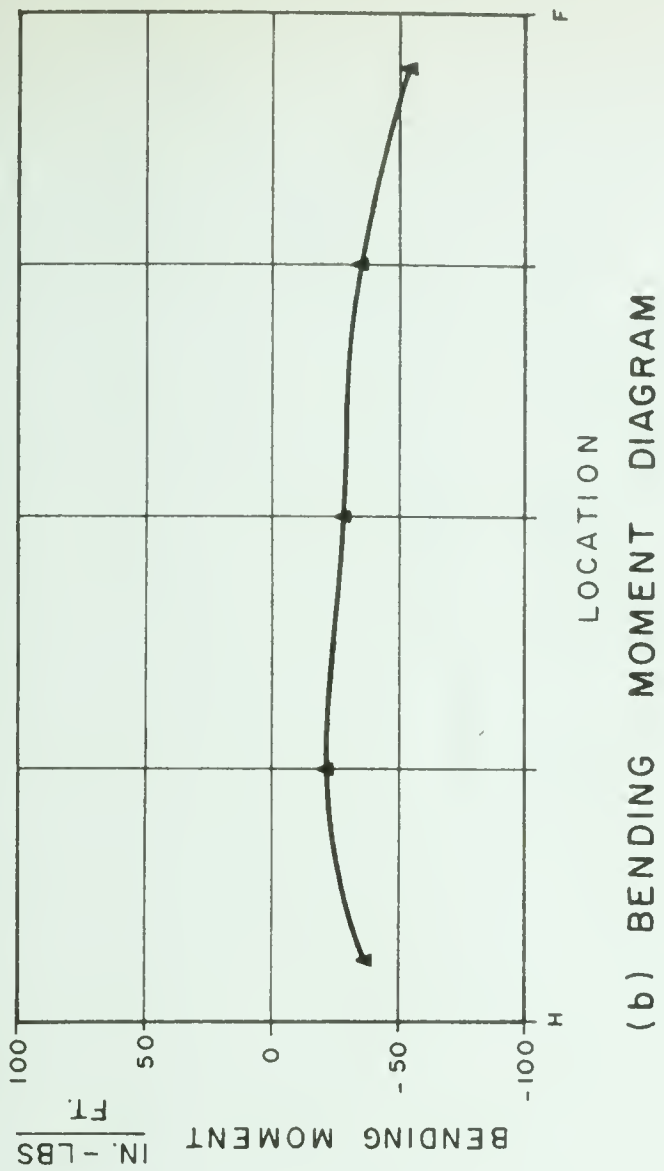


(c) AXIAL STRESSES

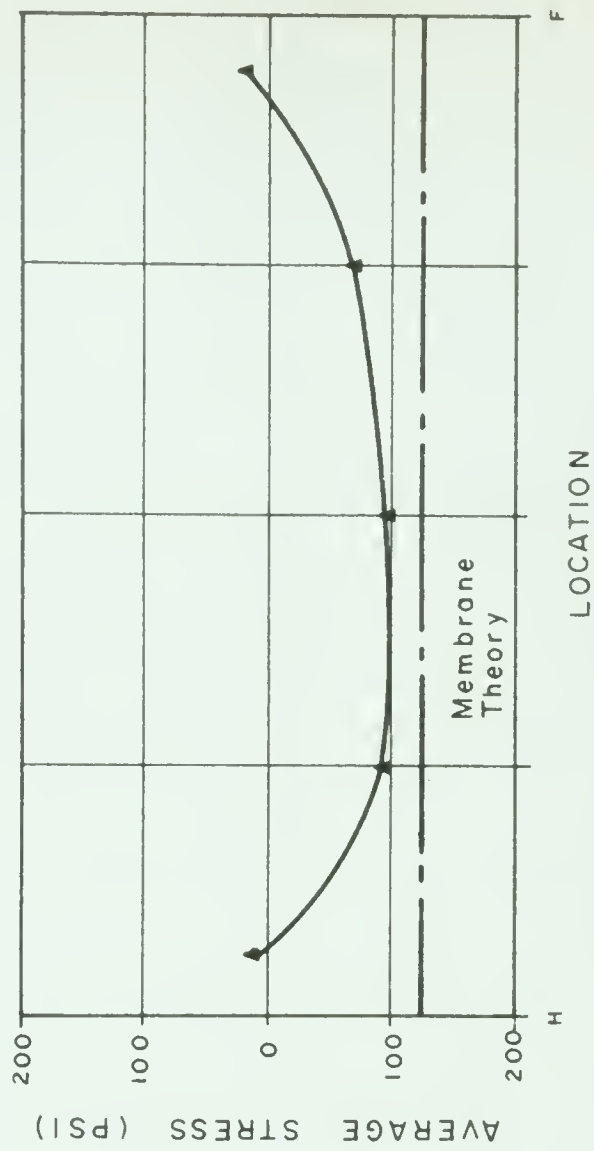
FIGURE 6.18 SURFACE STRAINS, BENDING MOMENTS & AXIAL STRESSES FOR DIAGONAL H-F TESTS # 1 & # 4 - 6000 # SYMMETRICAL LOAD



(a) SURFACE STRAINS

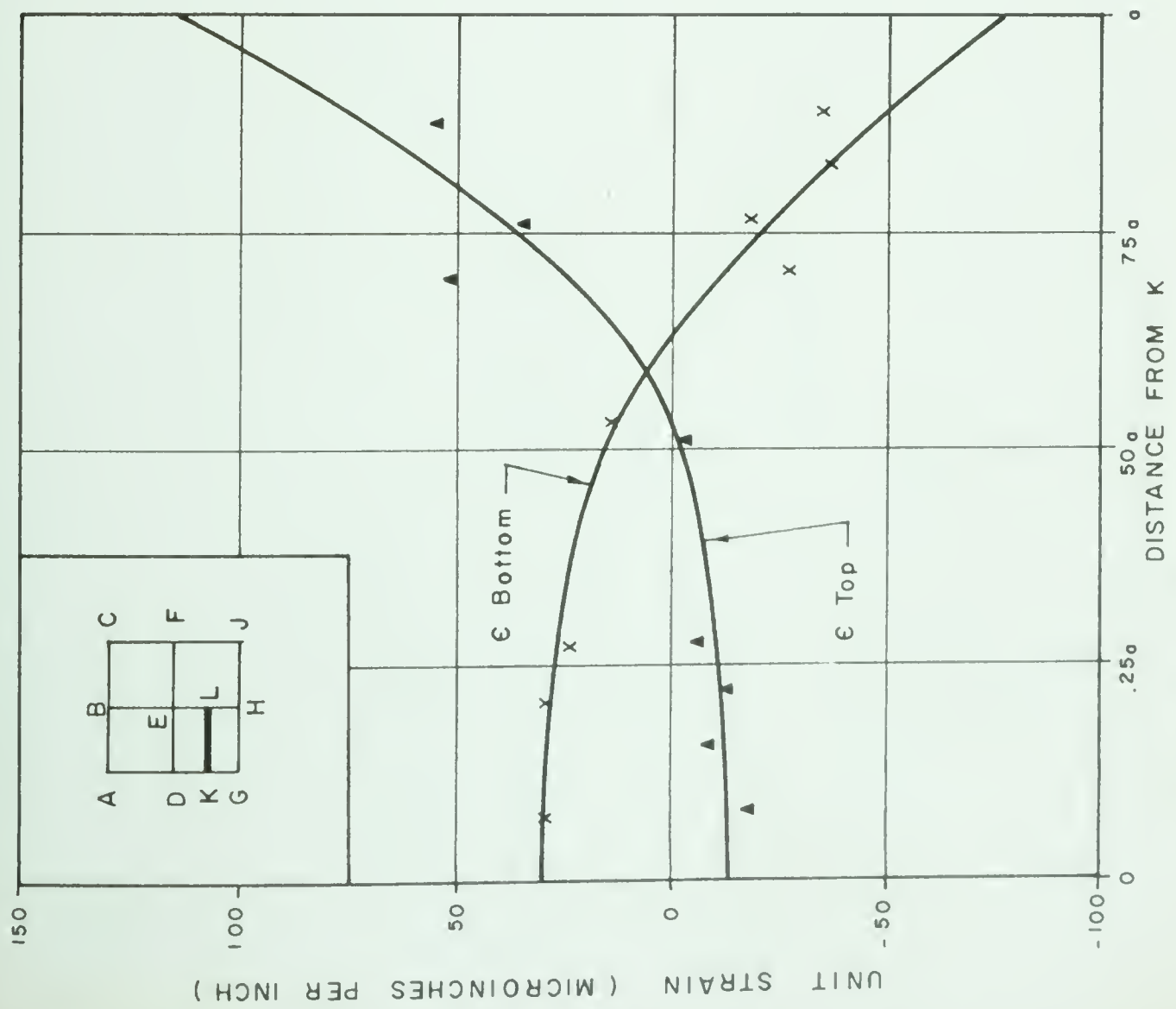


(b) BENDING MOMENT DIAGRAM

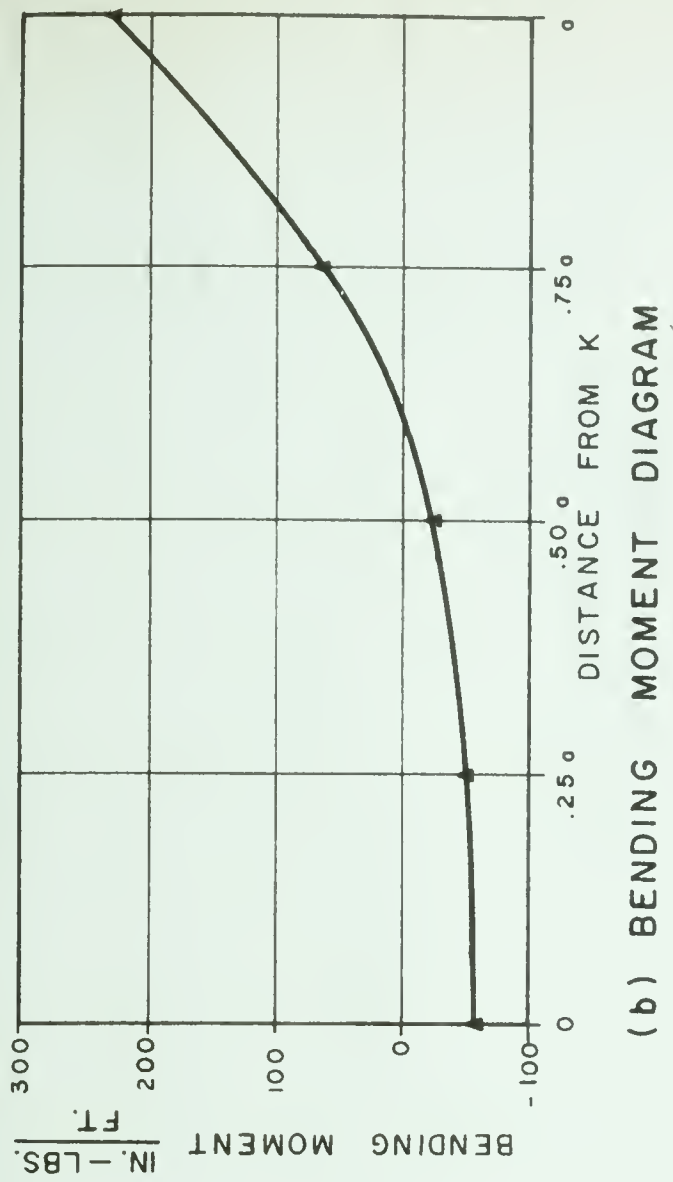


(c) AXIAL STRESSES

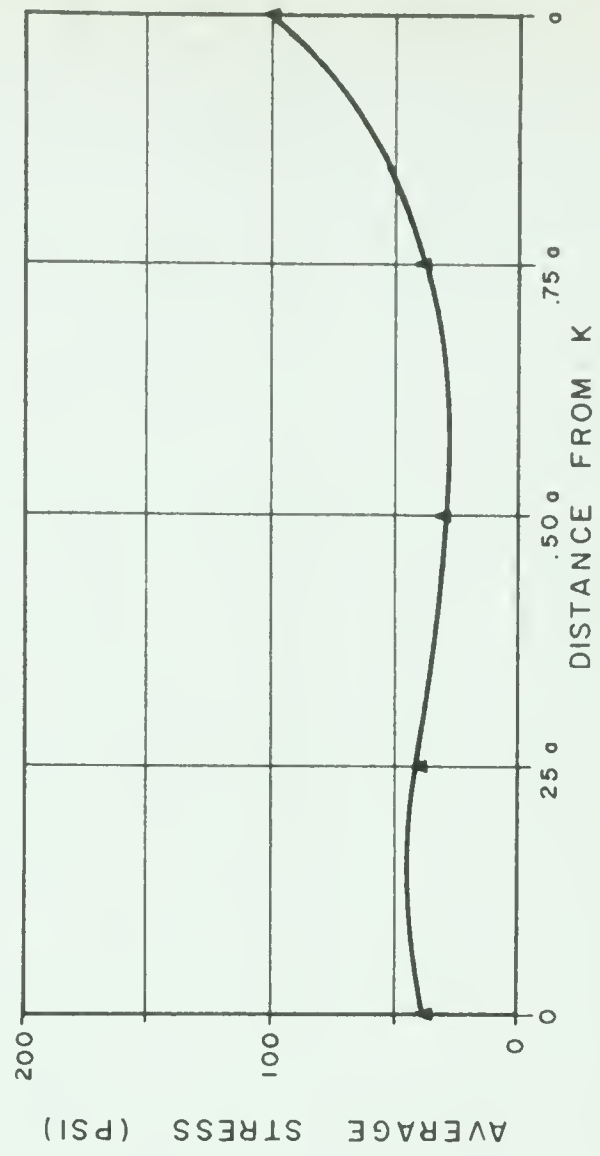
FIGURE 6.19 SURFACE STRAINS, BENDING MOMENTS & AXIAL STRESSES FOR DIAGONAL H-F TESTS #6 & #7 - 6000# SYMMETRICAL LOAD



(a) SURFACE STRAINS



(b) BENDING MOMENT DIAGRAM



(c) AXIAL STRESSES

FIGURE 6.20 SURFACE STRAINS, BENDING MOMENTS & AXIAL STRESSES FOR SECTION K-L
TEST #4 - 6000# SYMMETRICAL LOAD

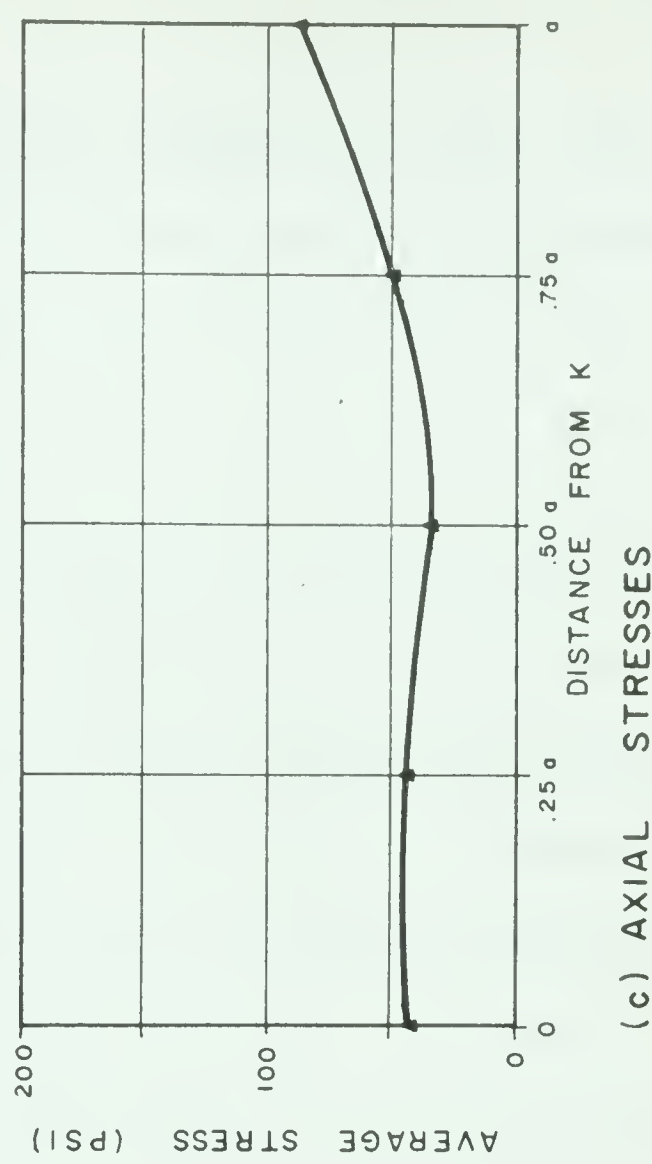
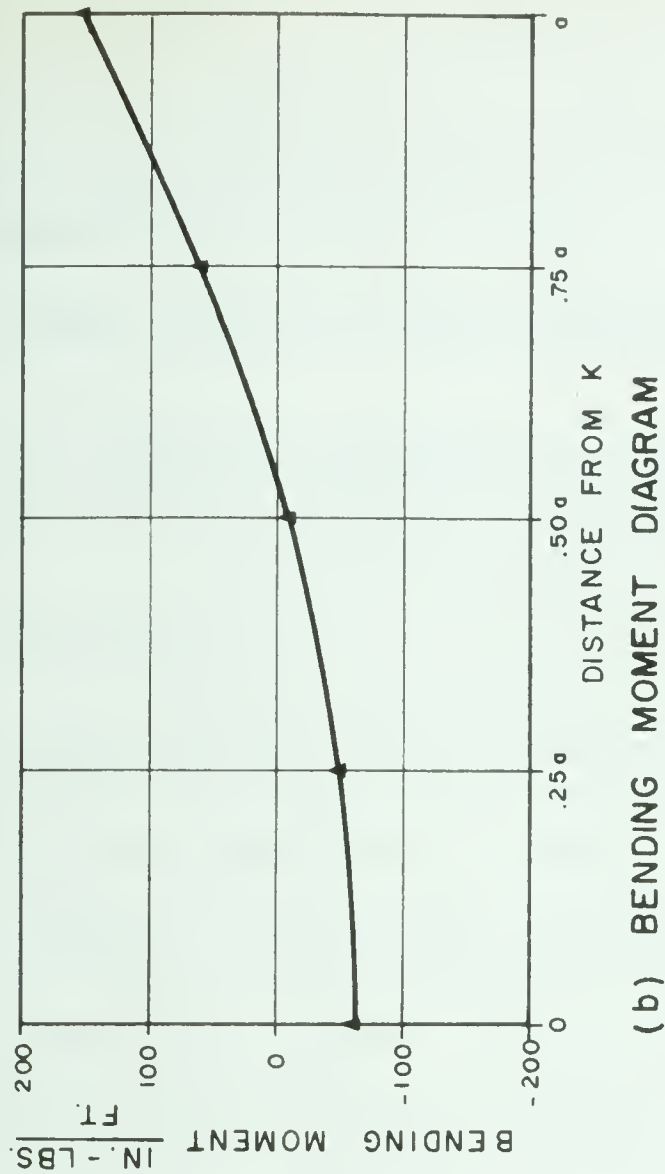
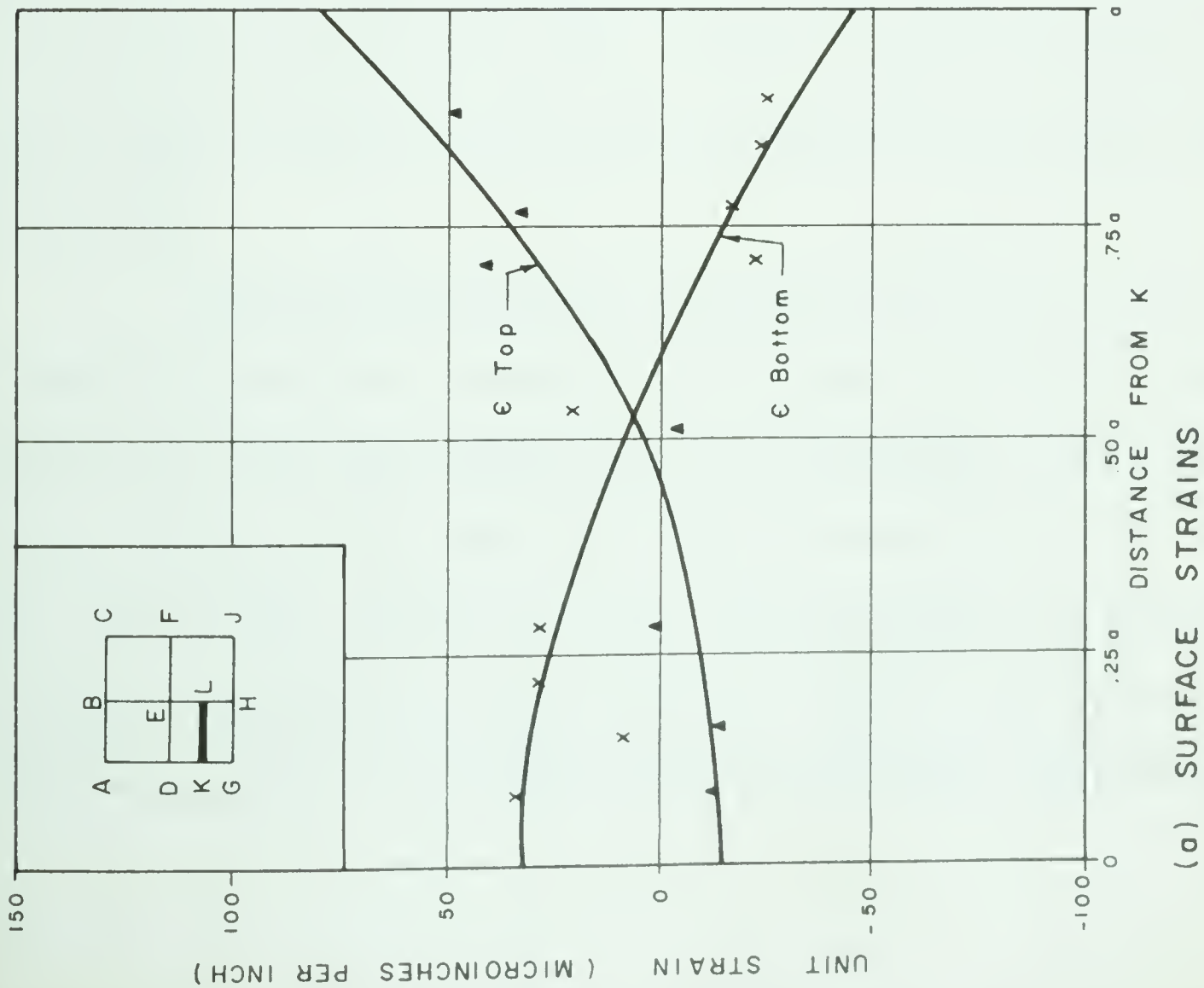


FIGURE 6.21 SURFACE STRAINS, BENDING MOMENTS & AXIAL STRESSES FOR SECTION K-L
TEST #6 - 6000 # SYMMETRICAL LOAD

Similar curves for Tests 6 and 7, in FIGURE 6.21, show very close agreement with Test 4 and again, the effect of augmenting the tie rods appears to have little effect on the shell stresses.

6.8 Discussion of Uniform Load Series

It must be remembered that all tests were conducted on one model and that the results are not sufficiently numerous to form any general conclusions which may be arbitrarily extended to shells of larger size, of different rise to span ratio or of different material. Scale effects in the aggregate would be a consideration in predicting the results on a prototype composed of conventional concrete. Variation in thickness to span ratio, eccentricity of beams to shell, variation in breadth to depth of beams, variations in spacing of reinforcing rods, degree of restraint provided at the support are but a few of the parameters which may be varied, and before any general conclusions can be drawn, it will be necessary to carry out exhaustive tests on many more paraboloids.

The strain measurements in the uniform load series showed generally good agreement for the construction materials used. The magnitude of the axial thrusts in the ridge and gable beams could be reasonably predicted from simple membrane theory, taking into account some flange action from the shell. The rate of transfer of load from the shell to the beam appears to be somewhat lower than membrane theory predicts, but this is expected since membrane theory does not take into account deformation of the members. End moments

are found in gable beams which are thought to be caused by the eccentricity of the shell which has a high compressive stress in the vicinity of the support and which produces a couple on the gable end. Also, the gable beam is not able to rotate freely at the support due to the restraint provided by the other gable beam intersecting at right angles, which has some torsional stiffness preventing free rotation.

The shell stresses appear to have higher compressions than would be predicted by membrane theory. This is evident from the higher compressive stresses in the compression diagonal, the lower tensions in the tension diagonal and the fact that the generator K L is in compression whereas membrane theory predicts no axial stress. This may be explained qualitatively as a result of deflections of the ridge beam. The ridge beams are connected by a series of straight line generators to the gable beams. In order for the ridge beam to deflect, the generator must either bend to allow this deflection or remain straight and force the gable beam to move downward and outward. A study of the bending moment diagram for generator K L indicates that some bending takes place, but not sufficient to essentially change its geometry, so that each generator must act as a compression strut, pushing against the gable beam. Unfortunately, no horizontal deflections were measured on the gable beams, but in the test to destruction, an outward movement could be visually detected, as will be mentioned in a later section. In the vicinity of the ridge beams, the slope of the shell was very nearly zero, so that a deflection could take place without

causing the above mentioned effect. At the generator K L, the slope was 1:8 but the gable beam was able to deflect both horizontally and vertically at its midspan. In the vicinity of the support, the slope of the shell was 1:4 and the gable beams were not able to deflect easily due to constraint at the corners. It is suggested that this confinement resulted in high compressive stresses in the edge generators which, in turn prevented free rotation of the ridge beams.

Positive bending moments in the gable beams appear to be due, almost entirely to the fact that the tie rods permitted the corner supports to spread apart. Considering the gable beam as a free body and spreading the supports by a distance equal to the measured extension of the tie rods produces a positive bending moment about ten percent lower than the measured value. Superimposing a negative couple at the ends, equal to the measured negative moment and correcting for displacement, the positive moment agrees almost identically with that measured. When the heavier tie rods were added, the gable beam positive moment was drastically reduced, as would be expected.

The ridge beams used in the model were eccentric to the neutral surface of the shell by a calculated distance of three quarters of an inch. The maximum thrust by membrane theory is 6,000 pounds at the centre. Applying this as an eccentric load ($e = 3/4''$) one might predict a positive bending moment of $3/4 \times 6,000 = 4,500$ inch pounds, considerably more than the measured value. Applying an end moment to the ridge beam of nearly 1,000 inch pounds, the predicted positive moment would be reduced to 3,500 inch pounds, whereas

the value found in the test was in the order of 2,000 inch pounds for the single tie rods and about 1,500 inch pounds for the double tie rods. It would appear that for this model, such a design technique would have erred on the side of safety. It would also appear that such a superficial analysis is not correct since the ridge beam bending moment is affected by the magnitude of the tie rod strain which was not considered in the above analysis.

In reviewing the test procedure in the light of results, it should be emphasized that in further tests of this type, two additional measurements should be made. The first is horizontal as well as vertical deflections of the gable beams. The second is that end rotations of the gable beams should be measured so that the end value of the bending moment could be determined from deflection measurements.

CHAPTER VII

PRESENTATION AND DISCUSSION OF ASYMMETRICAL LOAD TESTS

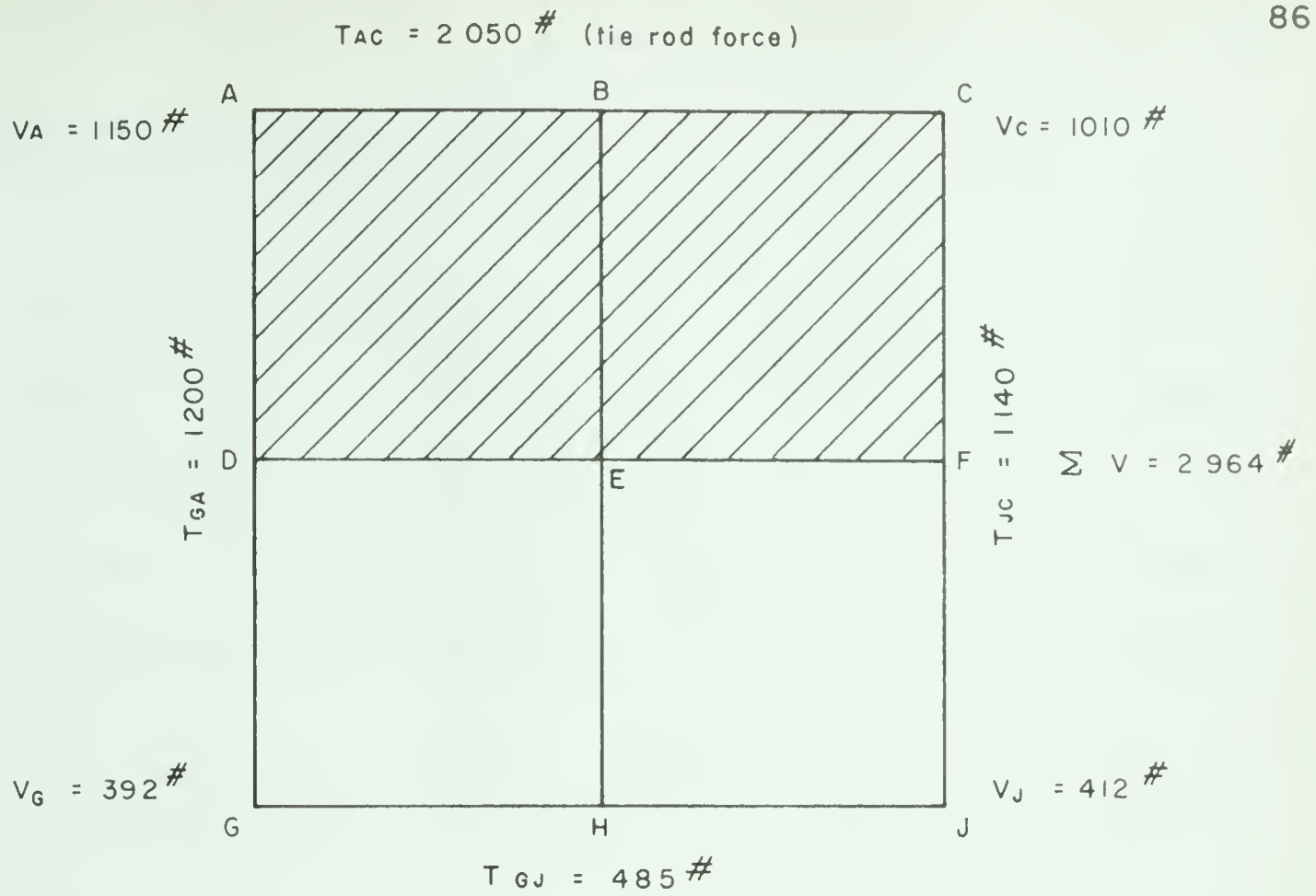
7.1 Introduction

Included in this chapter are the results of Tests 2 and 3 where load was placed uniformly over one half of the model only. This condition may occur in a prototype shell under an unbalanced snow load. While it is not likely to occur with a slope as flat as that of the model, the National Building Code of Canada (1960) requires that curved roofs be designed for an unbalance of snow.

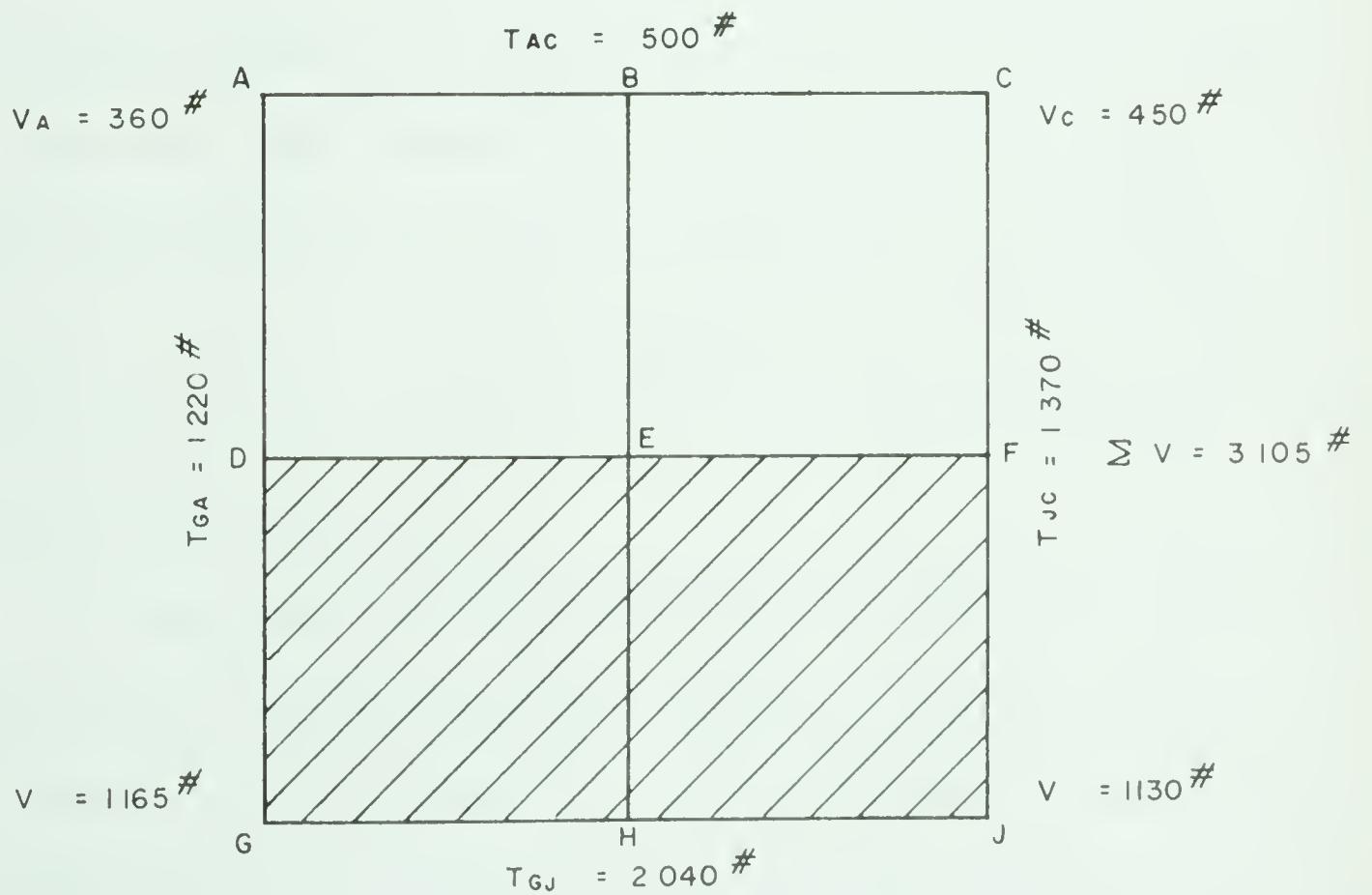
7.2 External Reactions

The horizontal and vertical reactions were found from strain readings in the tie rods and load cells respectively. The values are shown in FIGURE 7.1. In Test 2, the sum of the vertical reactions amounted to 2,964 pounds, only 36 pounds below the applied load. In Test 3, the vertical reactions total 3,105 pounds, slightly higher than the total applied load.

In both tests, some lack of symmetry is apparent, but Test 2 is more symmetrical than Test 3 which suggests that the load distributing apparatus was not functioning perfectly or that the model itself was not built in a symmetrical fashion.



TEST # 2



TEST # 3

FIGURE 7.1 HORIZONTAL AND VERTICAL REACTIONS AT THE CORNERS - TESTS # 2 & # 3

7.3 Gables Parallel to Axis of Symmetry

Surface strains for the top and bottom fibres respectively of gable beams parallel to the axis of symmetry are plotted in FIGURES 7.2 and 7.3. The inset figure on the upper right hand corner of each figure shows the beams under consideration in heavy outline. The loaded area is cross hatched.

Due to one less degree of symmetry, fewer points are plotted than was the case for the symmetrical loading series, so that, in general, less confidence may be placed on these results. A study of the strain values shows that considerable scatter is found, especially in the strains on the bottom surface of the beams.

Measured deflections, corrected for the lateral movement of the shell are plotted in FIGURE 7.4. It is interesting to note that in Test 3, Gable CFJ had a decidedly higher maximum deflection than Gable ADG and higher than either of the gables in Test 2. Reviewing FIGURE 7.1, it may be seen that Tie Rod CJ in Test 3 showed a correspondingly higher force than Tie Rod AG. This tends to confirm the theory that the loading was not symmetrical about the ridge beam in Test 3.

Bending moments for the unsymmetrically loaded gables are found in two ways, from the strain measurements and from the deflection measurements. These are plotted in FIGURE 7.5. As before, the deflection measurements yielded higher absolute values than the strain measurements, and it is felt that the true values lie somewhere between the two curves.

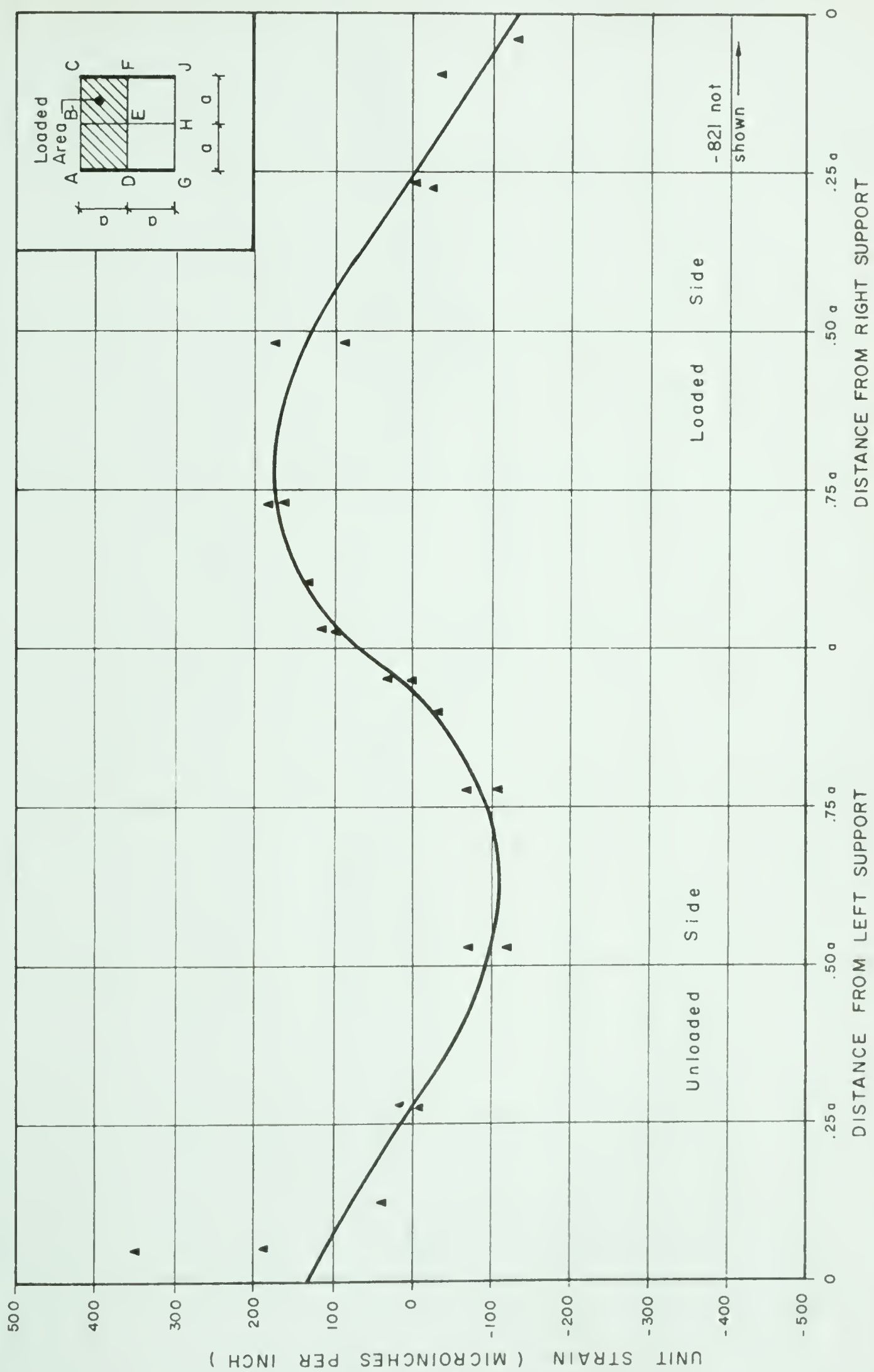


FIGURE 7.2 MEASURED STRAINS IN GABLE BEAMS WITHOUT LOADING SYMMETRY
TOP FIBRES - TESTS # 2 & #3 - 3000# ASYMMETRIC LOAD



FIGURE 7.3 MEASURED STRAINS IN GABLE BEAMS WITHOUT LOADING SYMMETRY
 BOTTOM FIBRES - TESTS #2 & #3 - 3000# ASYMMETRIC LOAD

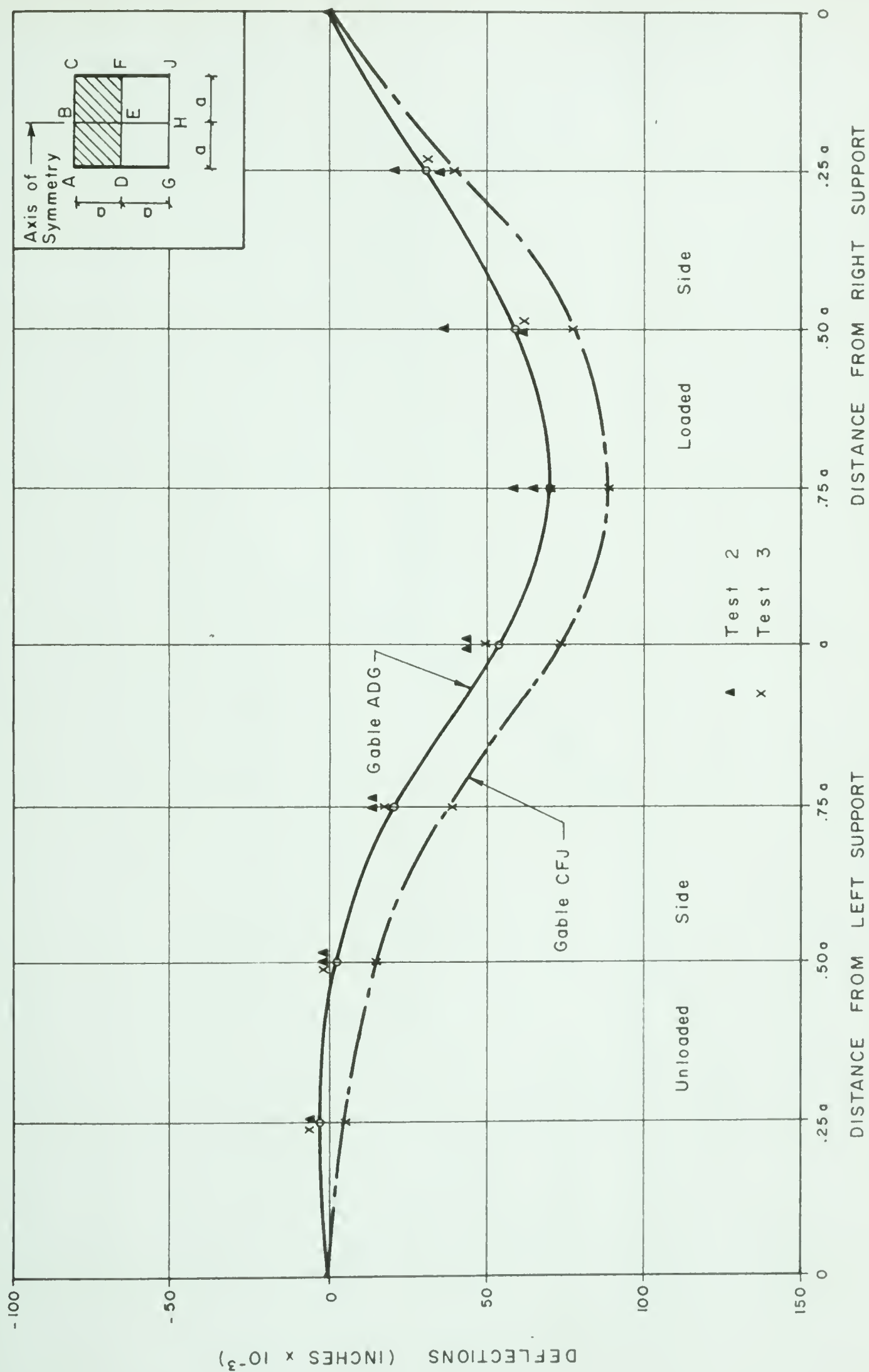


FIGURE 7.4 DEFLECTION OF GABLE BEAMS WITHOUT LOADING SYMMETRY
TESTS #2 & #3 - 3000# ASYMMETRIC LOAD

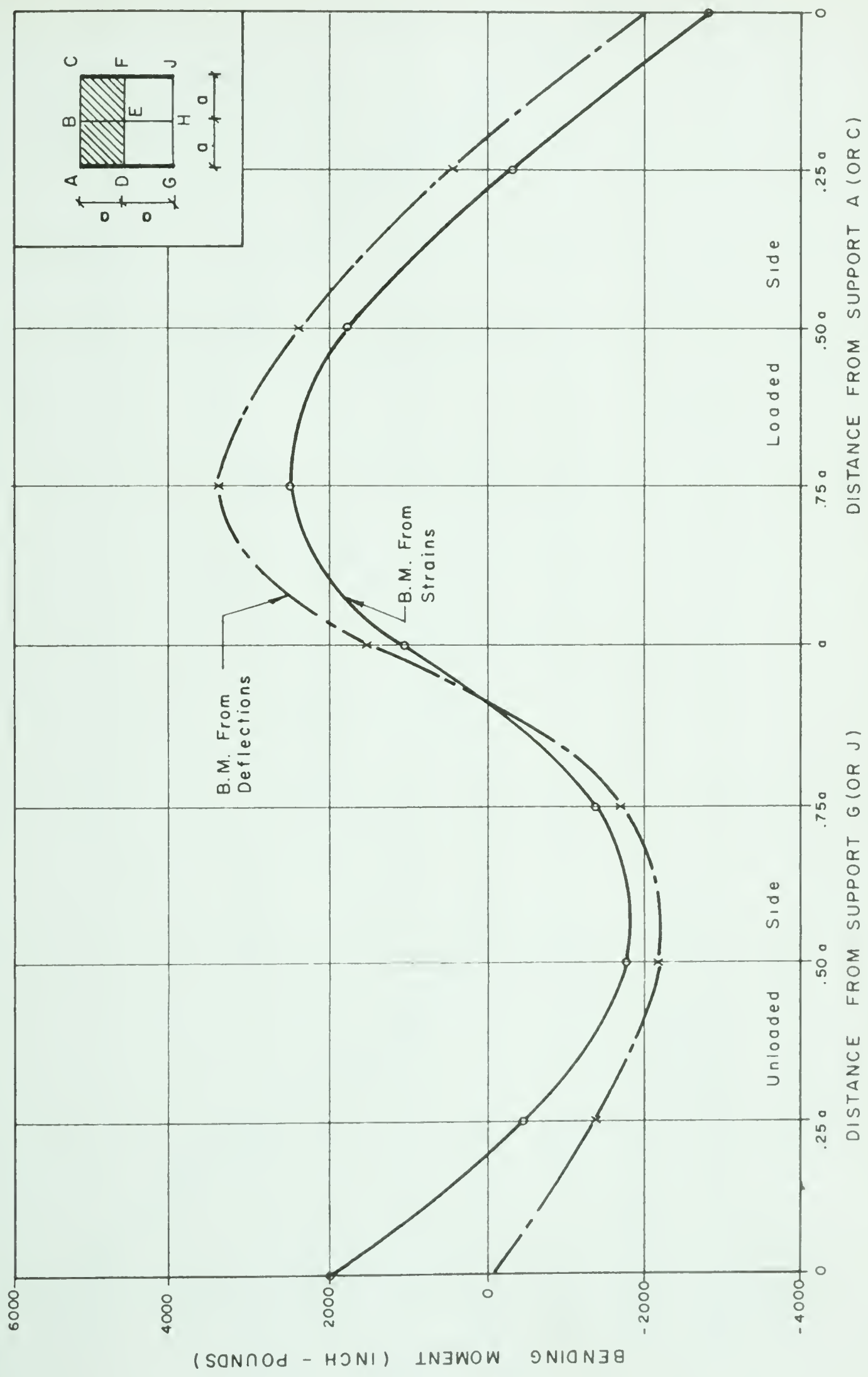


FIGURE 7.5 BENDING MOMENTS IN GABLE BEAMS WITHOUT LOADING SYMMETRY
TESTS #2 & #3 - 3000# ASYMMETRIC LOAD

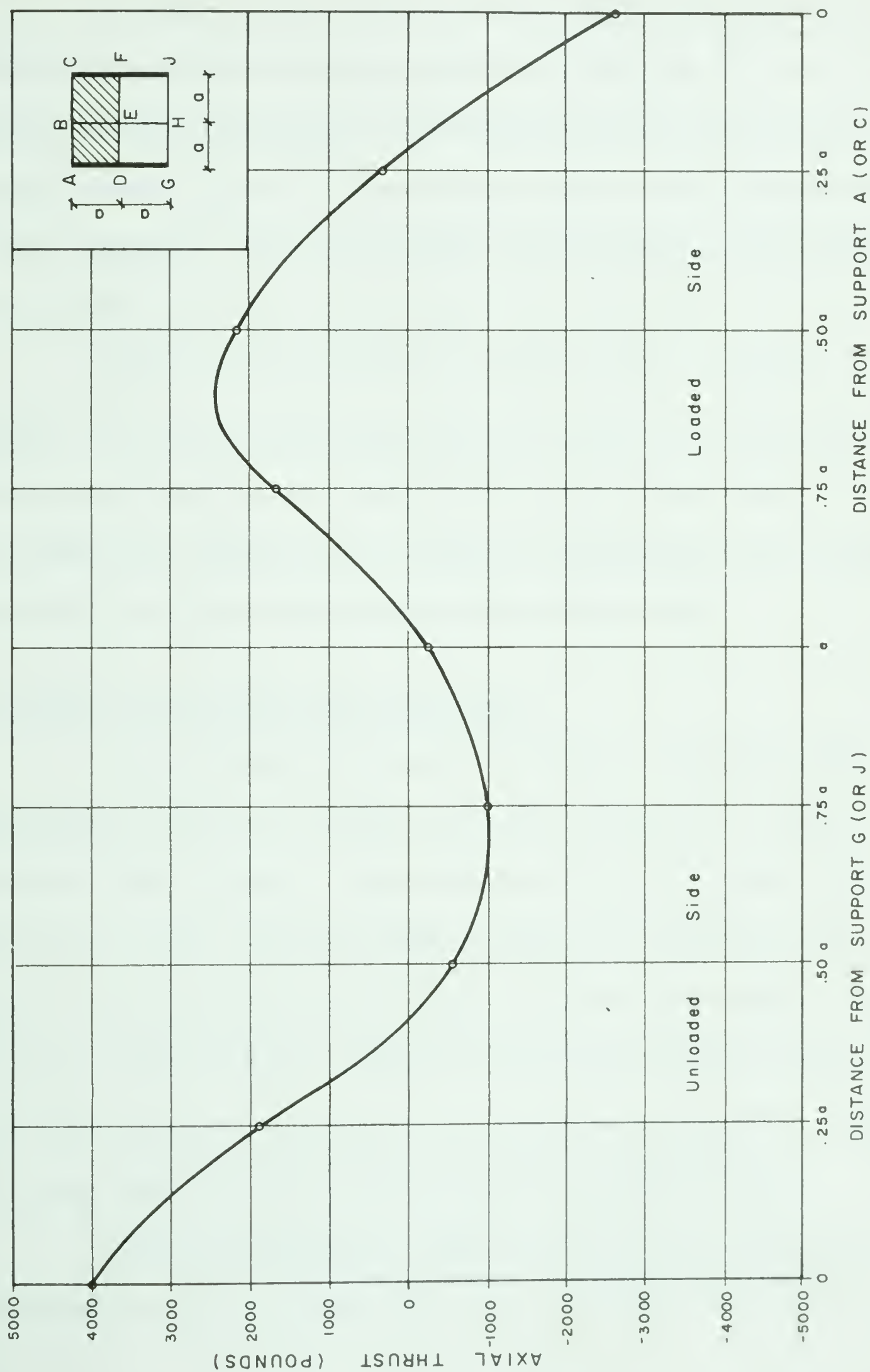


FIGURE 7.6 AXIAL THRUSTS IN GABLE BEAMS WITHOUT LOADING SYMMETRY
TESTS #2 & #3 - 3000# ASYMMETRIC LOAD

The shape of the bending moment curve corresponds very closely with a two span continuous beam having load on one span only, with some end restraint provided at the supports. The maximum positive value occurs at a distance of about $0.75a$ from the loaded support and has a value of approximately 3,000 inch pounds. The maximum negative moment occurs roughly midway in the unloaded span and has a value of about 2,000 inch pounds.

Axial thrust as computed from strain readings is plotted in FIGURE 7.6. A large compression is found in the middle of the loaded span, changing sign near the support, where the beam force becomes tension. On the unloaded side, a small tension is found near the ridge beam and this gradually builds up to a sizeable compression at the unloaded support.

7.4 Gables Perpendicular to Axis of Symmetry

Surface strains for the top and bottom fibres of the loaded gable perpendicular to the axis of symmetry are plotted in FIGURE 7.7. The top strains are widely scattered, so that it is not known with any certainty which way the curve slopes, but the best fitting straight line is drawn through the points. Most of these points are taken from Test 3 where the loading was suspect due to lack of symmetry. FIGURE 7.8 plots similar strains for the unloaded gable beam perpendicular to the axis of symmetry of the model. These values agree quite closely, the majority of values coming from Test 2.

Deflection measurements in the loaded and unloaded gables lying perpendicular to the axis of symmetry are found in FIGURE 7.9 (a) and (b).

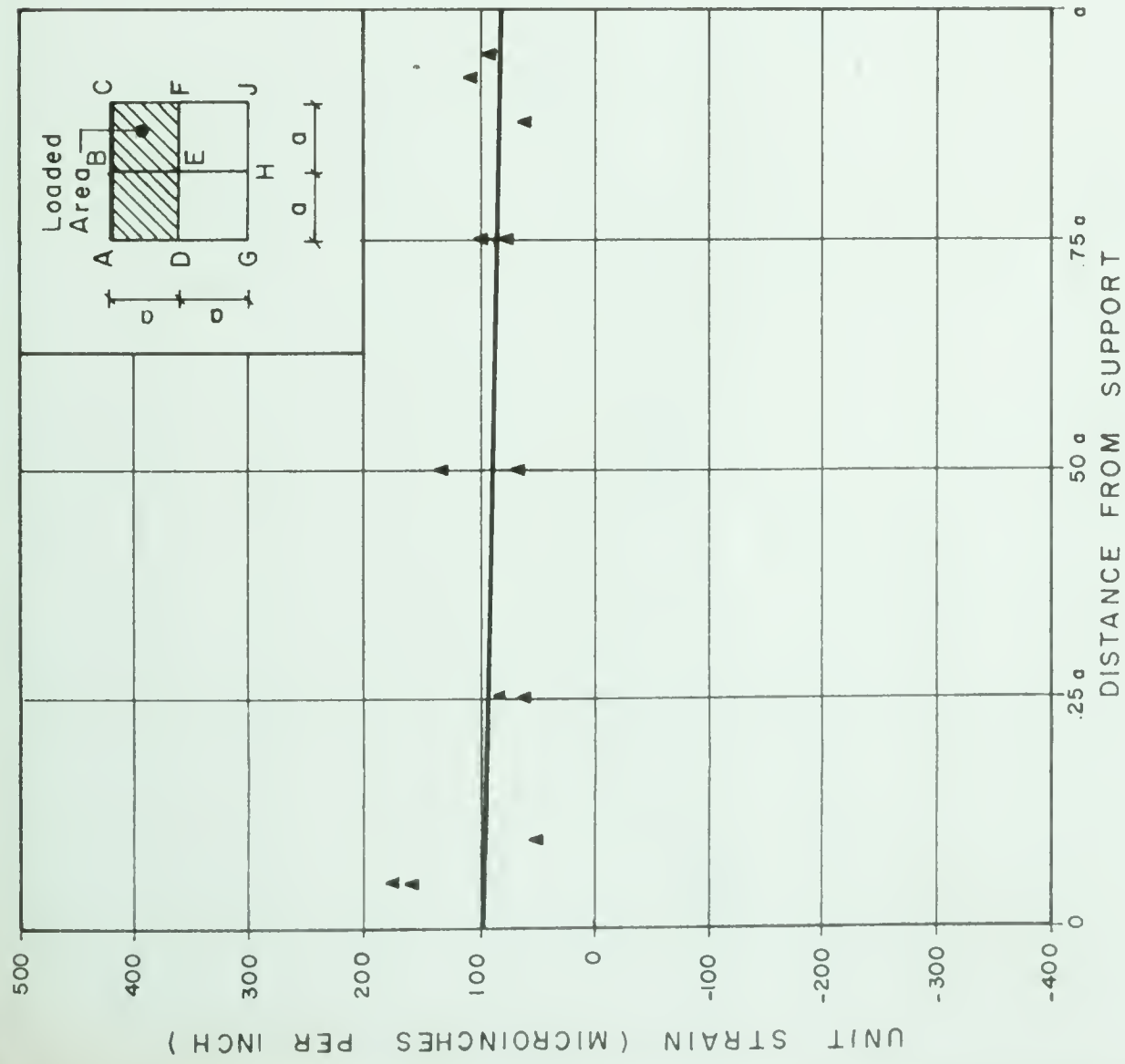
The unloaded gable has deflected significantly more in Test 2 than in Test 3 but the deflected shape of the beams are similar in each test.

The bending moment configuration of the loaded gable in FIGURE 7.10 (a) as determined from measured strains leaves serious doubts as to its validity. Probably the straight line approximation in the top fibre strains is responsible for the peculiar shape of curve. The dotted curve based on deflections suggests that a large positive moment exists over much of the span, probably dropping to zero at the support. A study of the deflected shape in FIGURE 7.9 (a) seems to bear this out.

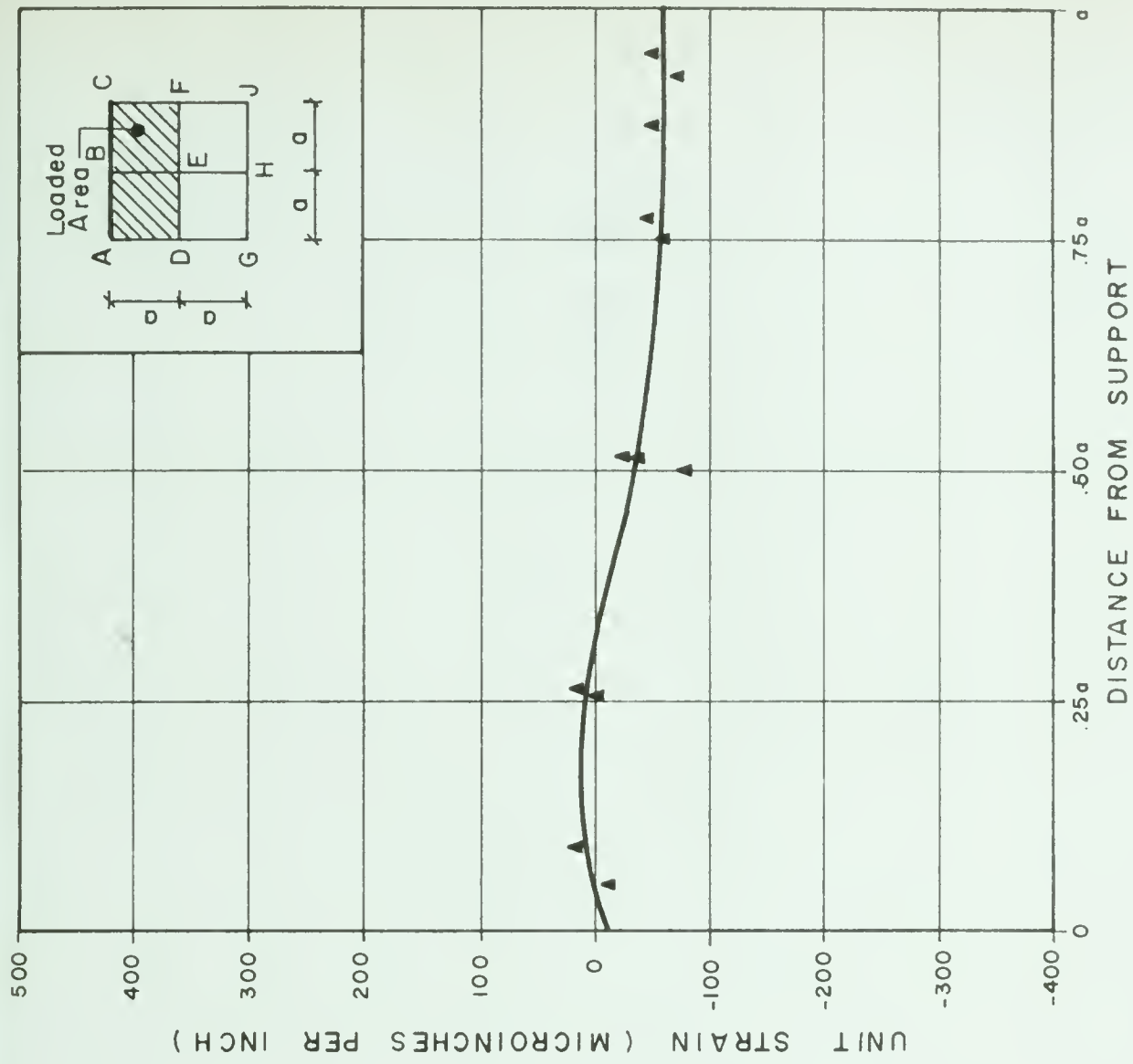
The solid and dotted curves for the unloaded gable in FIGURE 7.10 (b) show very nearly the same trend with the deflection values once again yielding higher values of moment than the strain readings. The value at the support is suspected to be incorrect based on the discontinuity of the curve and also deflected configuration in FIGURE 7.9. The true shape is thought to be as shown by the dashed line, so that the support moment is nearly zero.

The axial thrust for the loaded gable plotted in FIGURE 7.11 is similar to the thrust line for the symmetrically loaded gables in Chapter VI but the value of thrust appears to be somewhat higher at the support and lower at the ridge.

The unloaded gable has very nearly zero axial forces in the central portion, the values indicating in fact a tension. A sharp discontinuity at the support tends to confirm the suggested change to the bending moment diagram

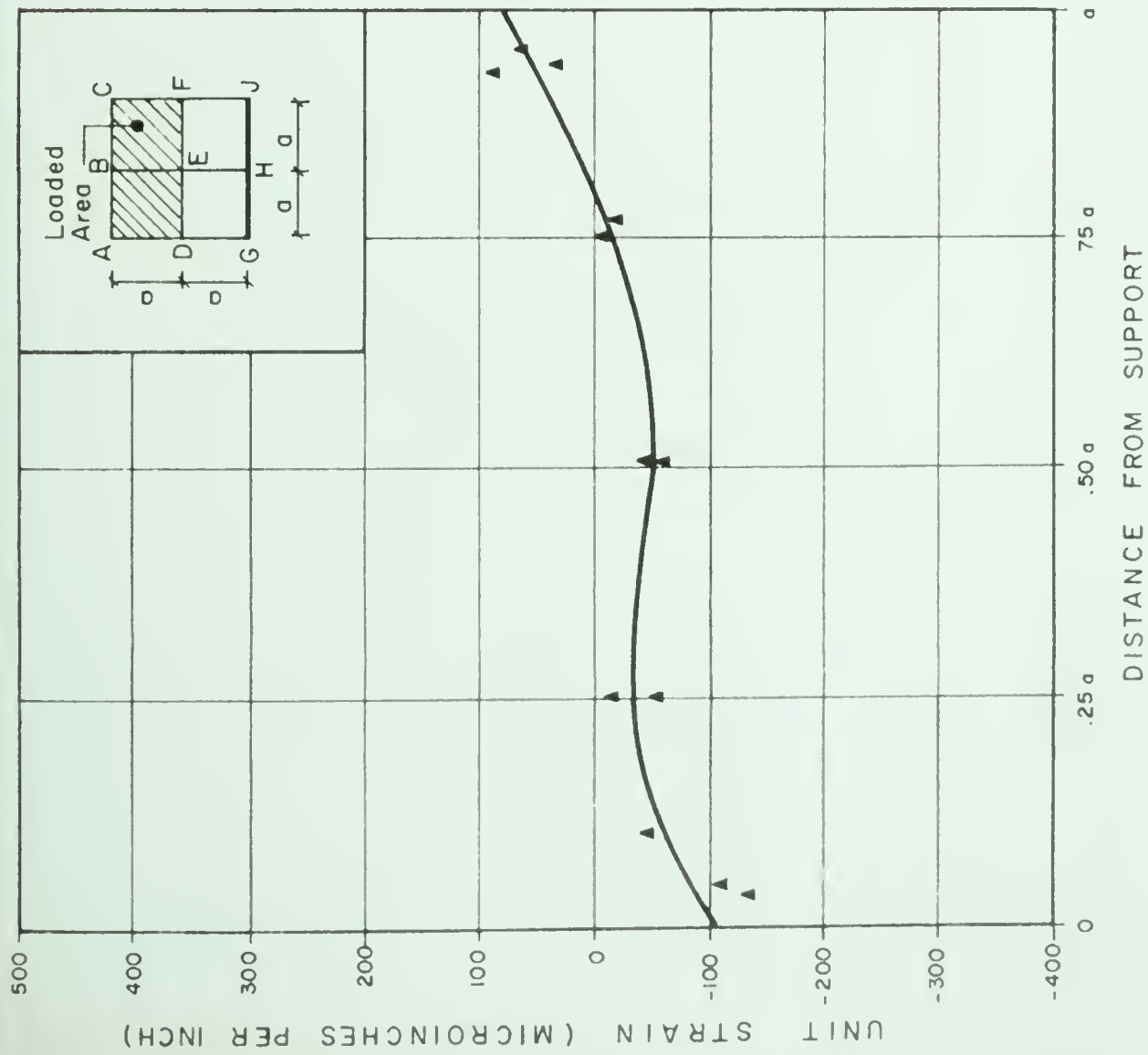


(a) STRAIN IN TOP FIBRES

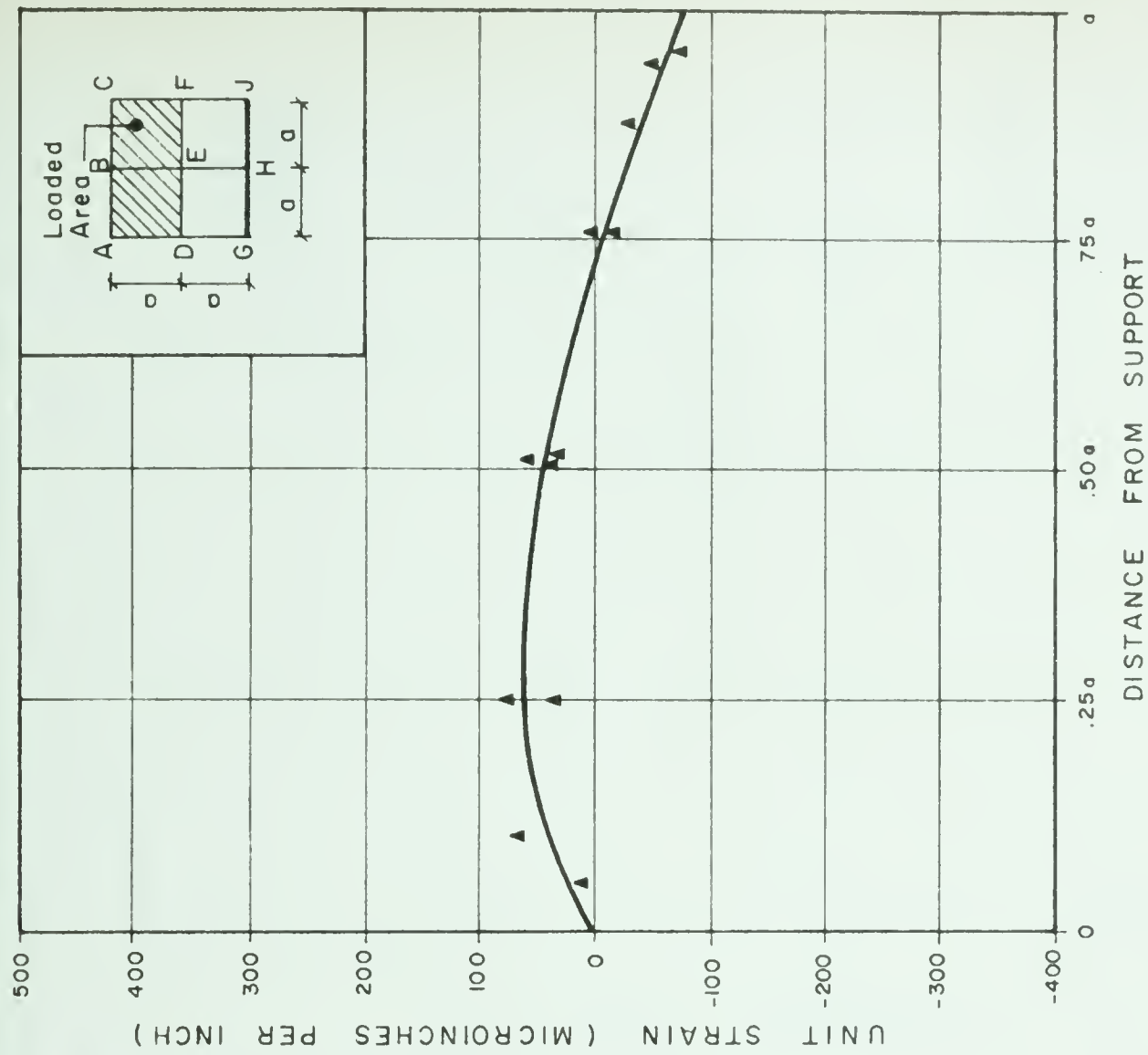


(b) STRAIN IN BOTTOM FIBRES

FIGURE 7.7 MEASURED STRAINS IN GABLE BEAMS HAVING LOADING SYMMETRY
(LOADED SIDE) - TEST #2 & #3 - 3000# ASYMMETRIC LOAD



(a) STRAIN IN TOP FIBRES



(b) STRAIN IN BOTTOM FIBRES

FIGURE 7.8 MEASURED STRAINS IN GABLE BEAMS HAVING LOADING SYMMETRY
(UNLOADED SIDE) - TEST # 28 # 3 - 3000# ASYMMETRIC LOAD

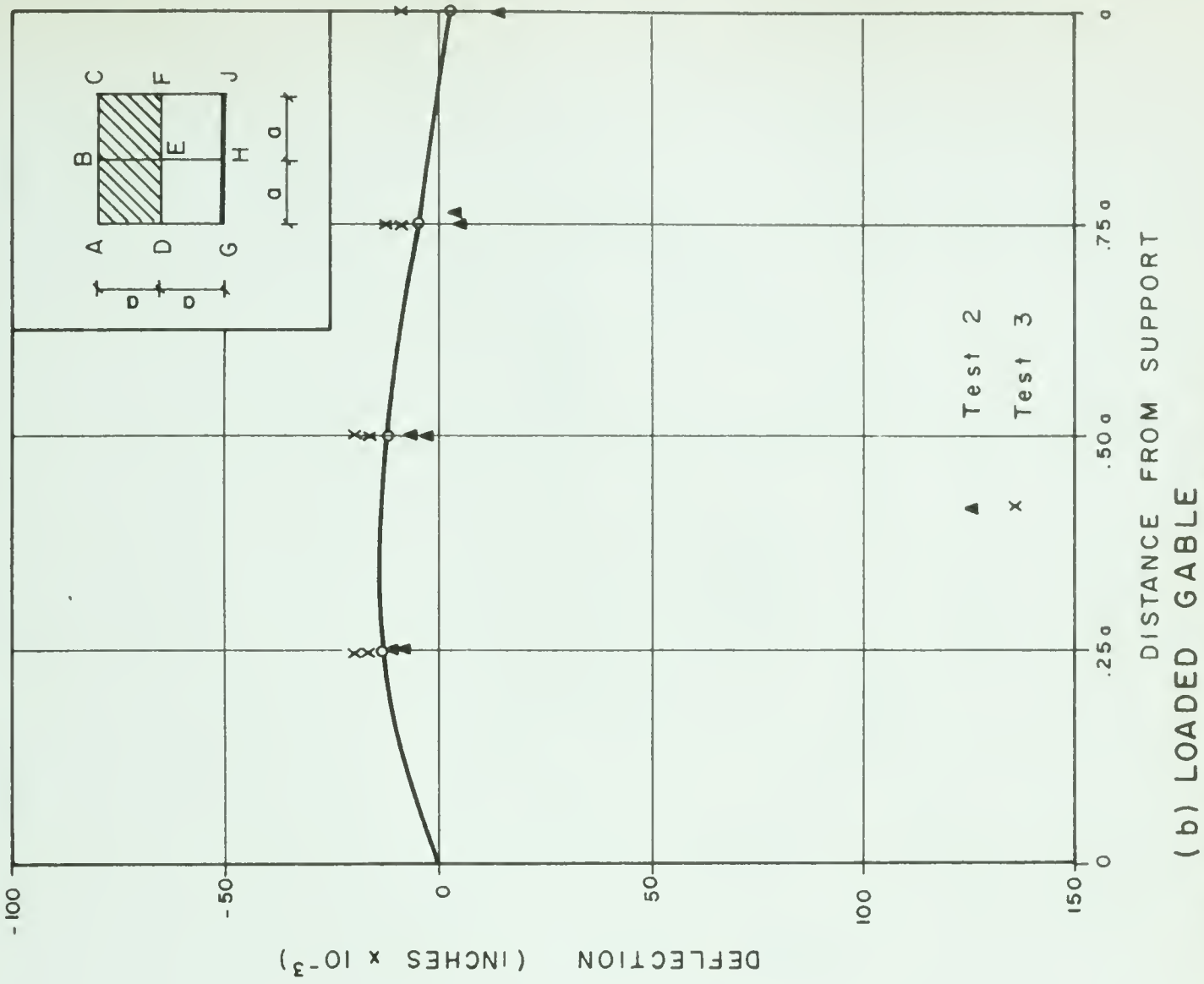
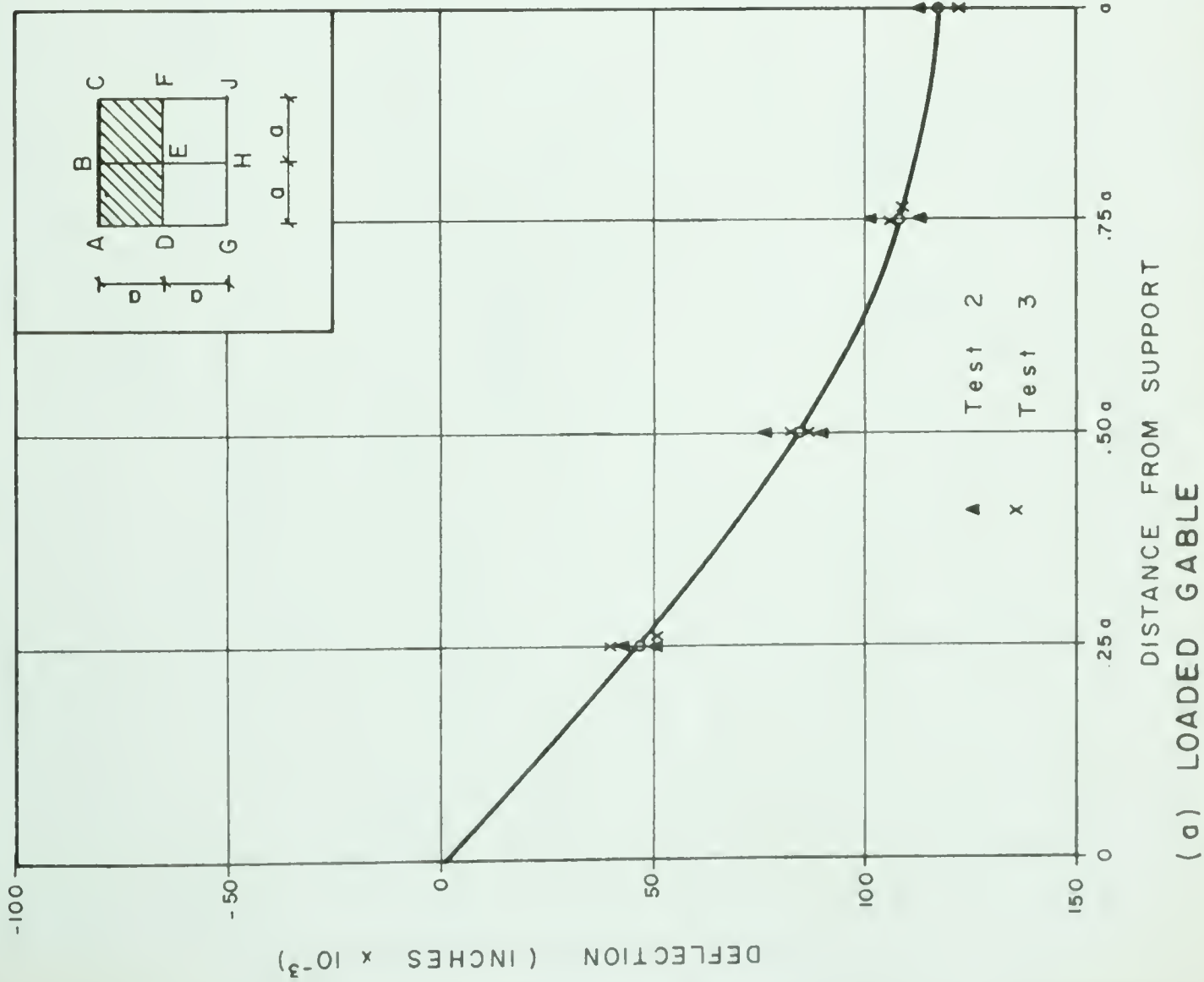
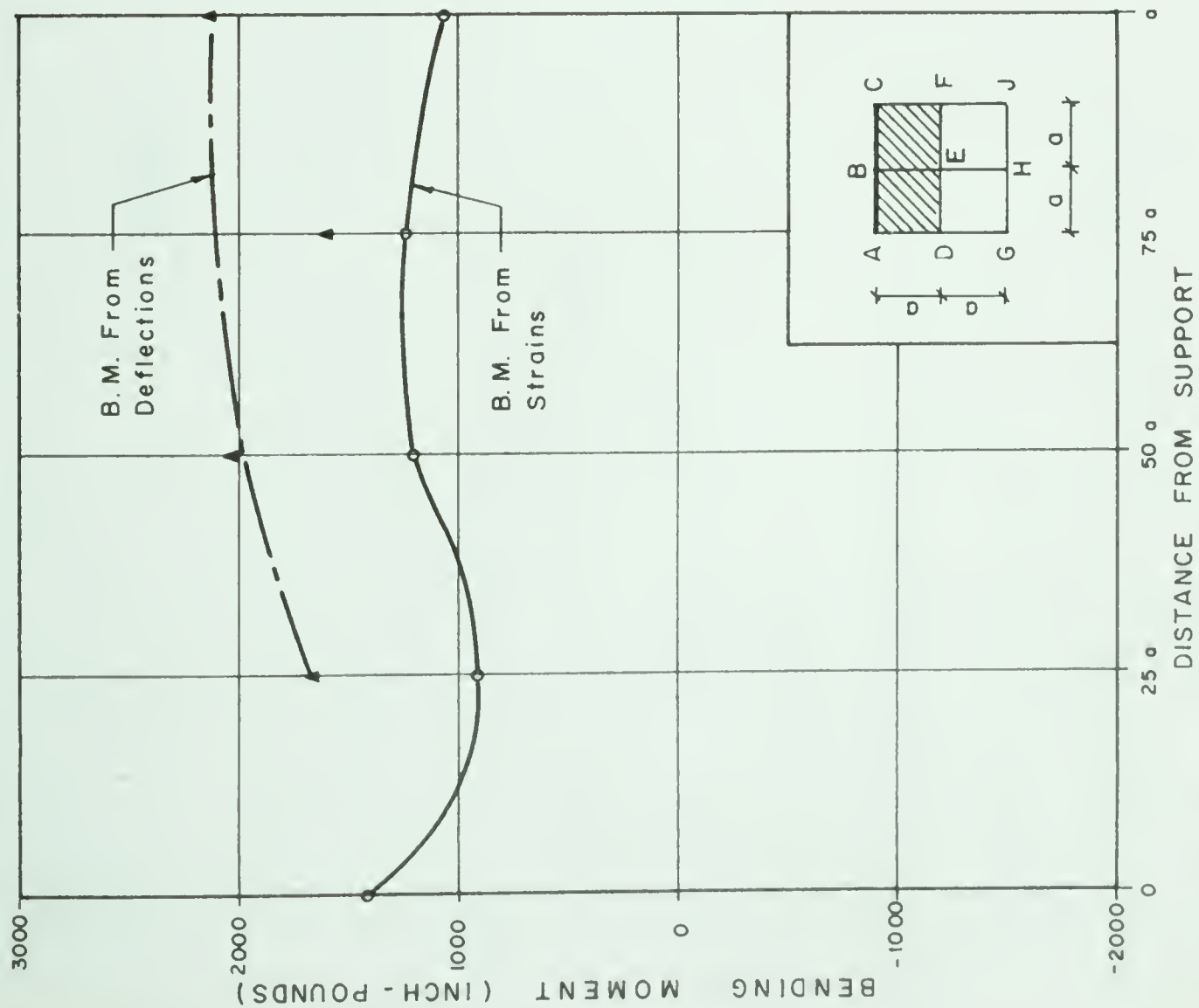
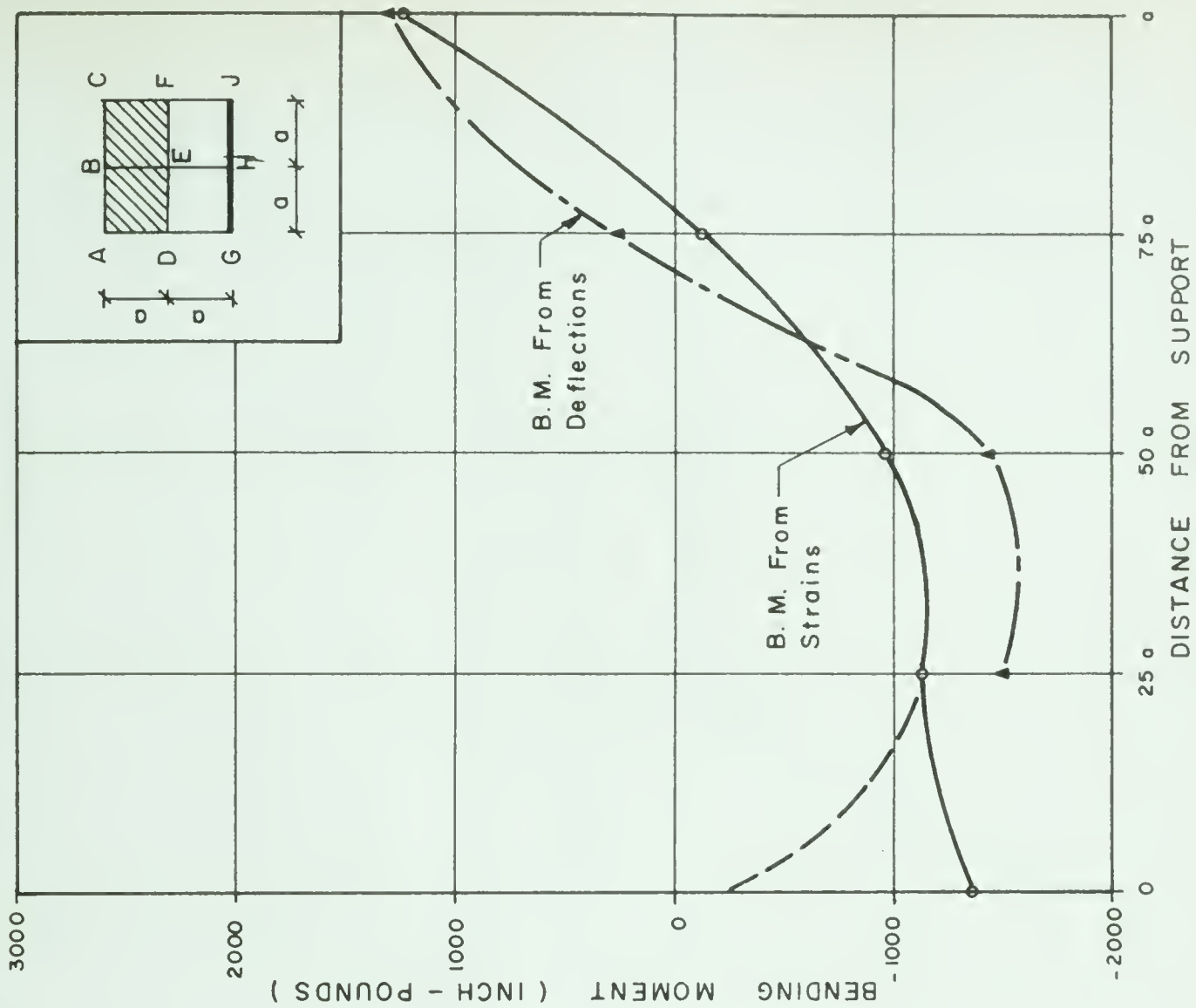


FIGURE 7.9 DEFLECTION OF GABLE BEAMS HAVING LOADING SYMMETRY
TESTS #2 & #3 - 3000# ASYMMETRIC LOAD



(a) LOADED GABLE



(b) UNLOADED GABLE

FIGURE 7.10 BENDING MOMENTS OF GABLE HAVING LOADING SYMMETRY TESTS # 2 & # 3 - 3000# ASYMMETRIC LOAD

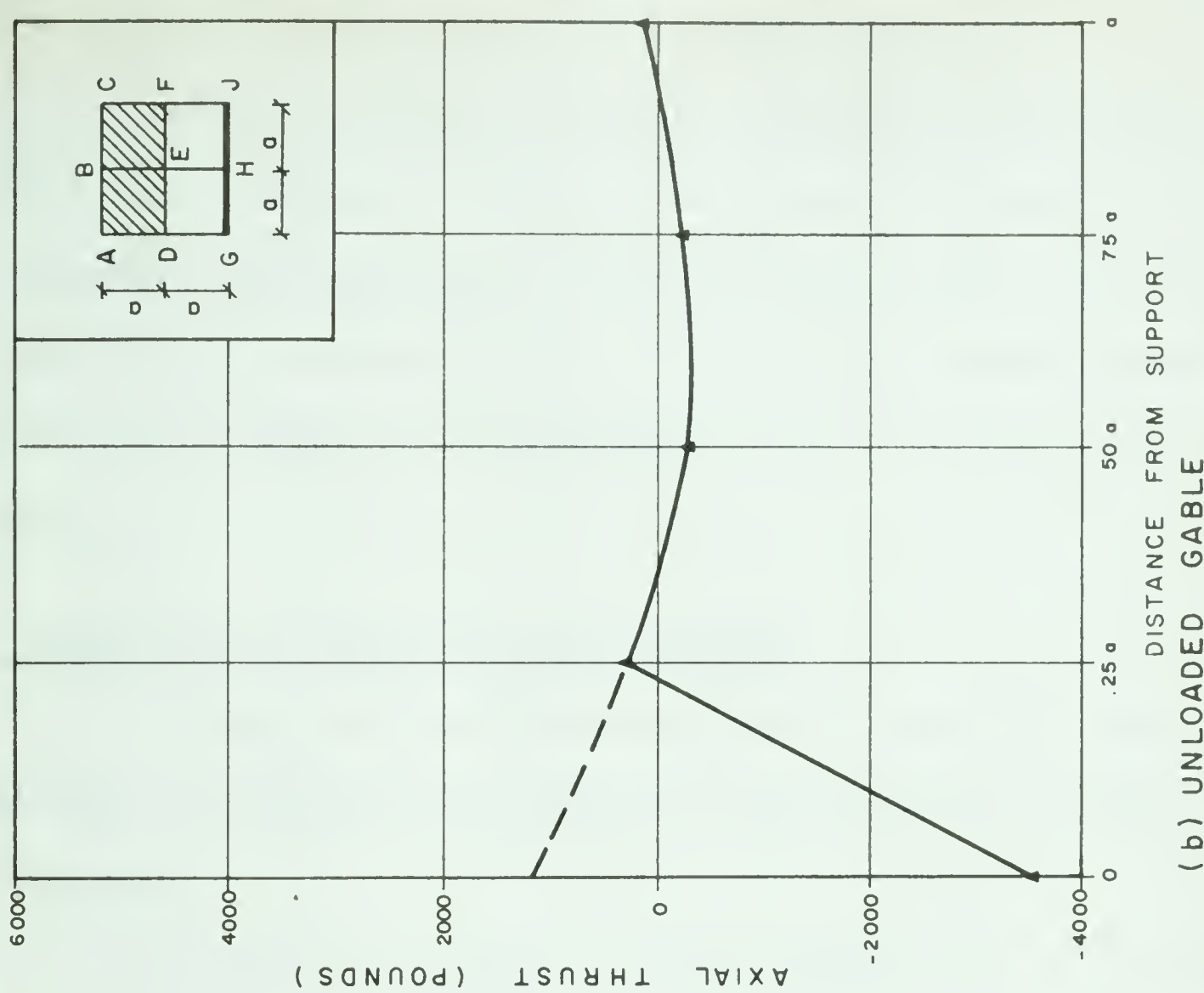
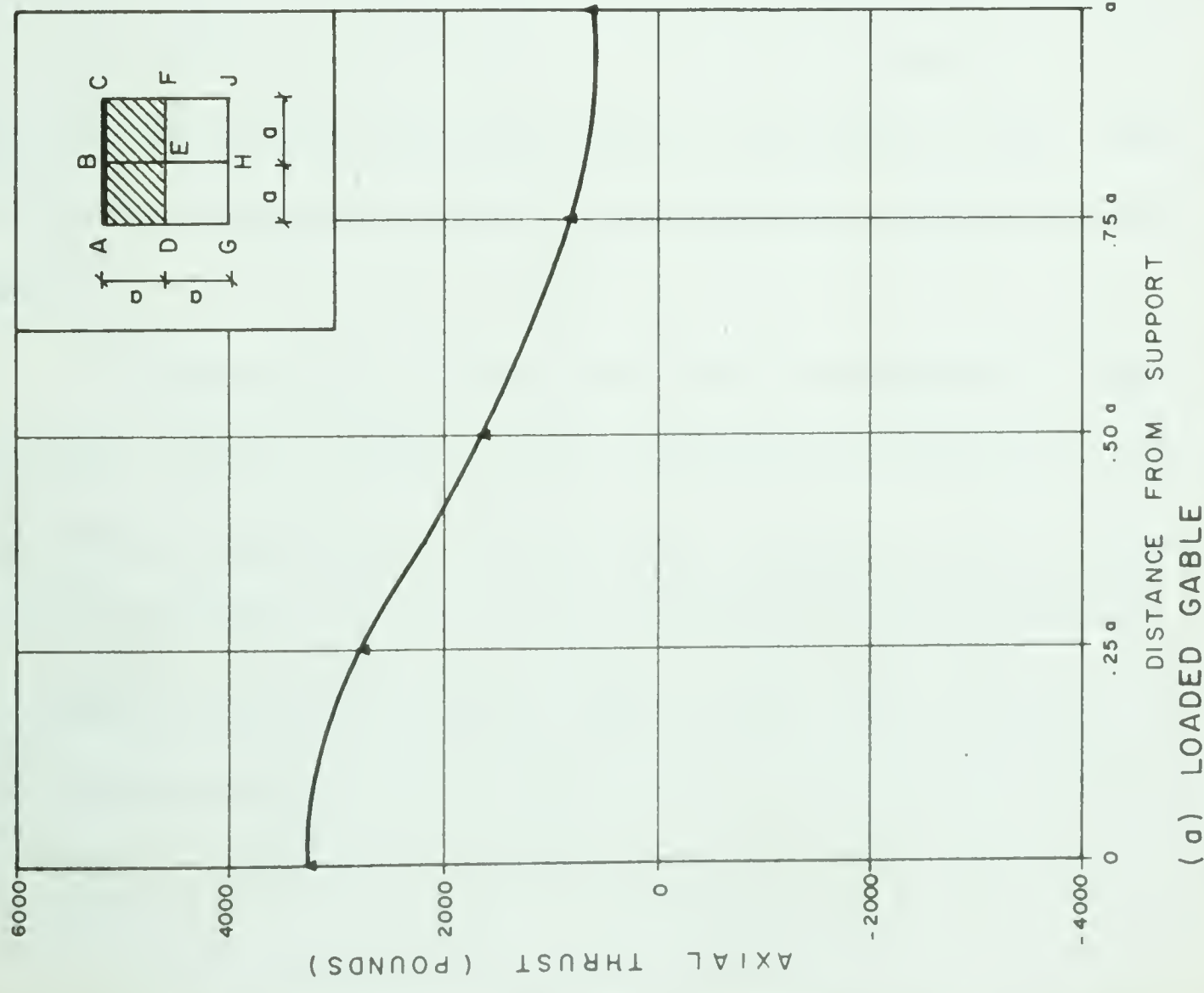


FIGURE 7.11 AXIAL THRUSTS IN GABLE BEAMS HAVING LOADING SYMMETRY TESTS #2 & #3 - 3000# ASYMMETRIC LOAD

mentioned previously and the dotted extension is consistent with the previous revision to the moment curve. Generally, throughout the testing program, it was found that strains near supports displayed the widest scatter. This is attributed to local disturbances due to the presence of torsion, bending about the vertical axis of the beam and the effect of the close proximity of the adjacent member.

7.5 Ridge Beam Perpendicular to Axis of Symmetry

Strains for the top and bottom fibres of the symmetrically loaded ridge beam are combined for each half beam in a composite plot in FIGURE 7.12 (a) and (b).

Deflection measurements are plotted in FIGURE 7.13. It may be seen that the results for Test 2 show a reasonably symmetrical deflection pattern for the ridge beam whereas the curve of Test 3 is displaced to the right, once more confirming the theory that symmetry was lacking in Test 3. Only the curve from Test 2 was used in determining bending moments from deflections.

Bending moments and axial thrusts for the symmetrically loaded ridge beam, plotted in FIGURE 7.14 show that the beam behaves almost identically with the ridge beams in the symmetrical loading series with the exception that the ordinates to the curves are almost identically half of the latter. The conclusion to be drawn from this is that a loaded quadrant of the shell exerts roughly the same shear forces on the ridge beam whether the load is

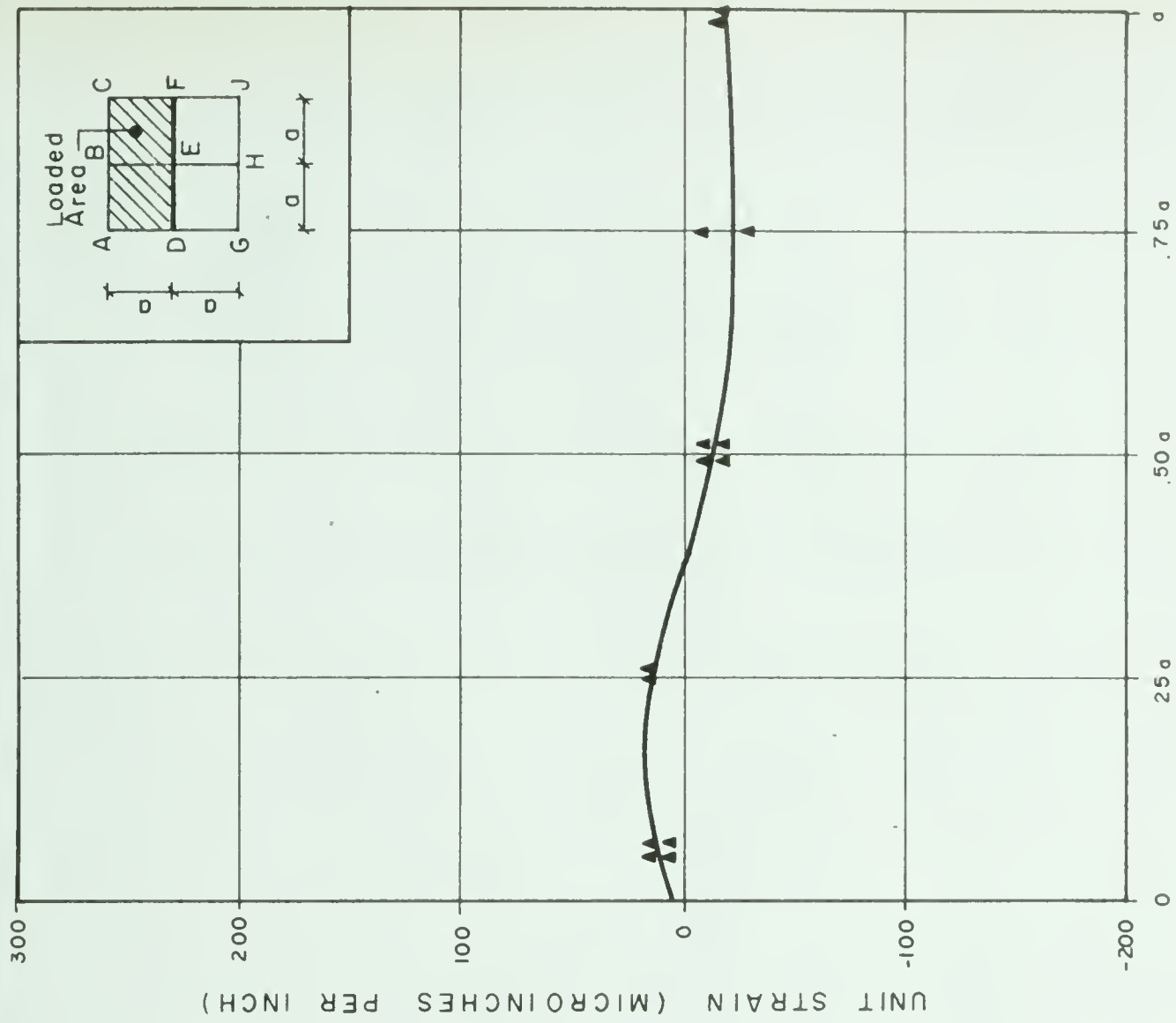
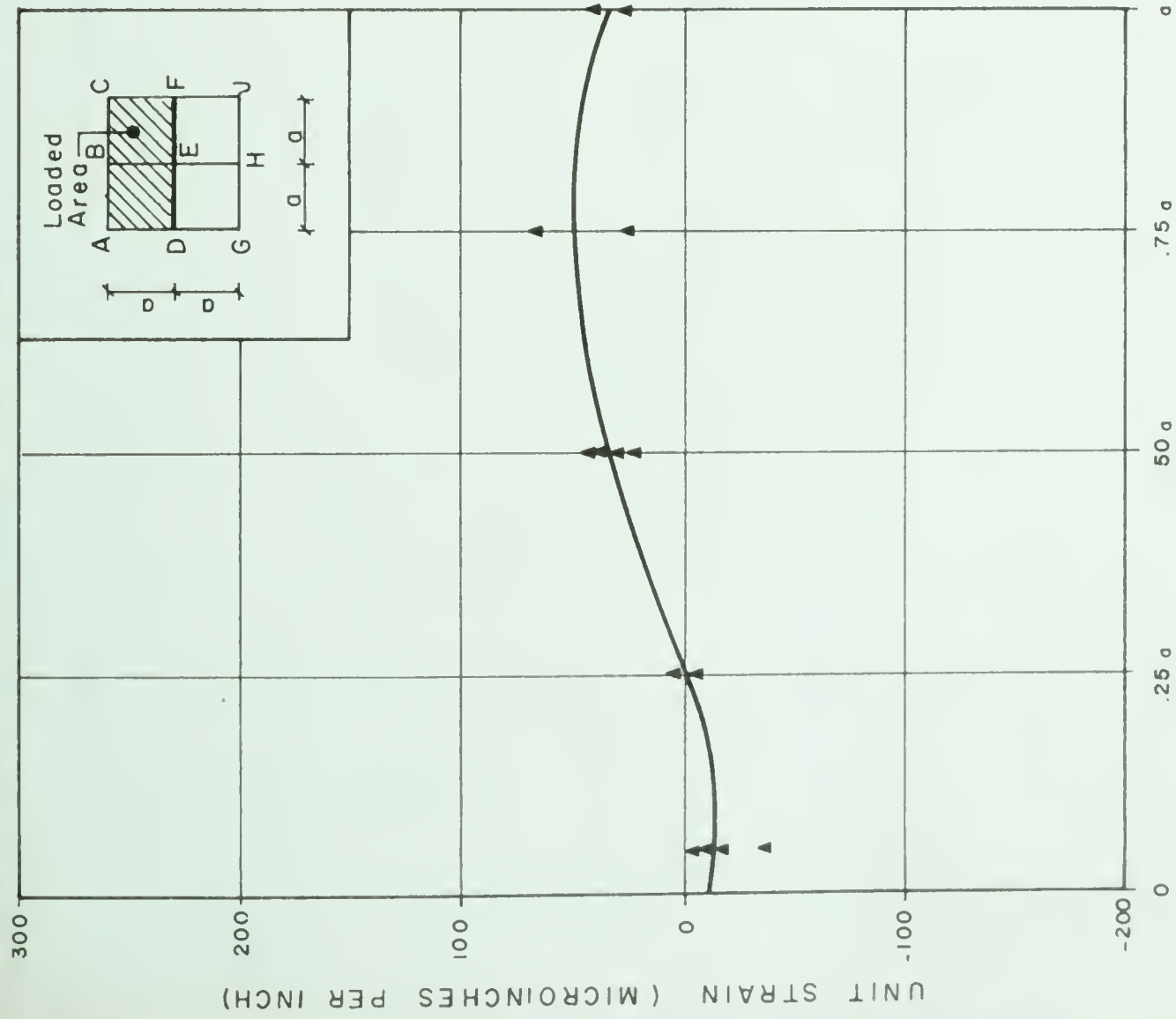


FIGURE 7.12 MEASURED STRAINS IN RIDGE BEAM HAVING LOADING SYMMETRY
TEST #2 & #3 - 3000# ASYMMETRIC LOAD

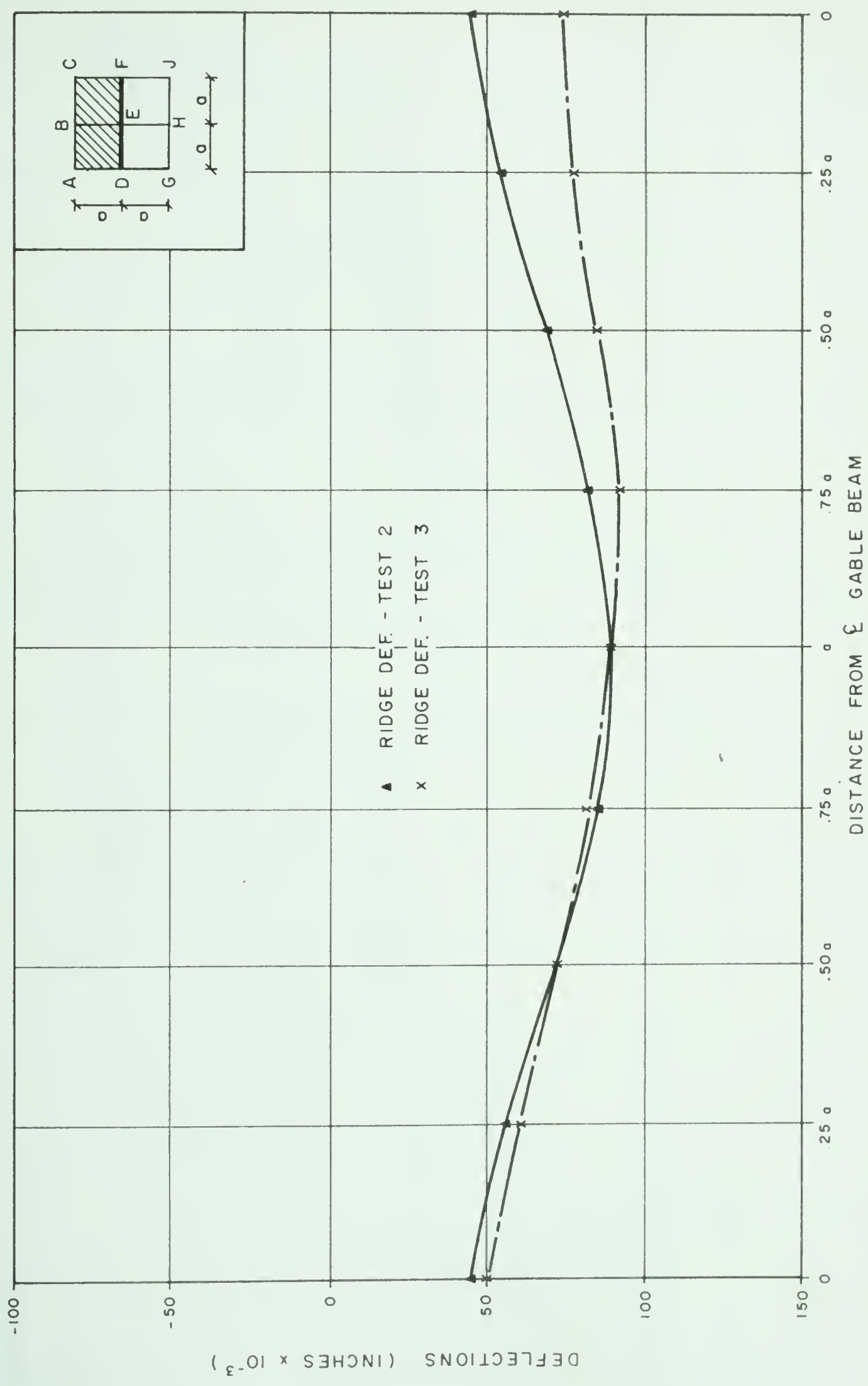
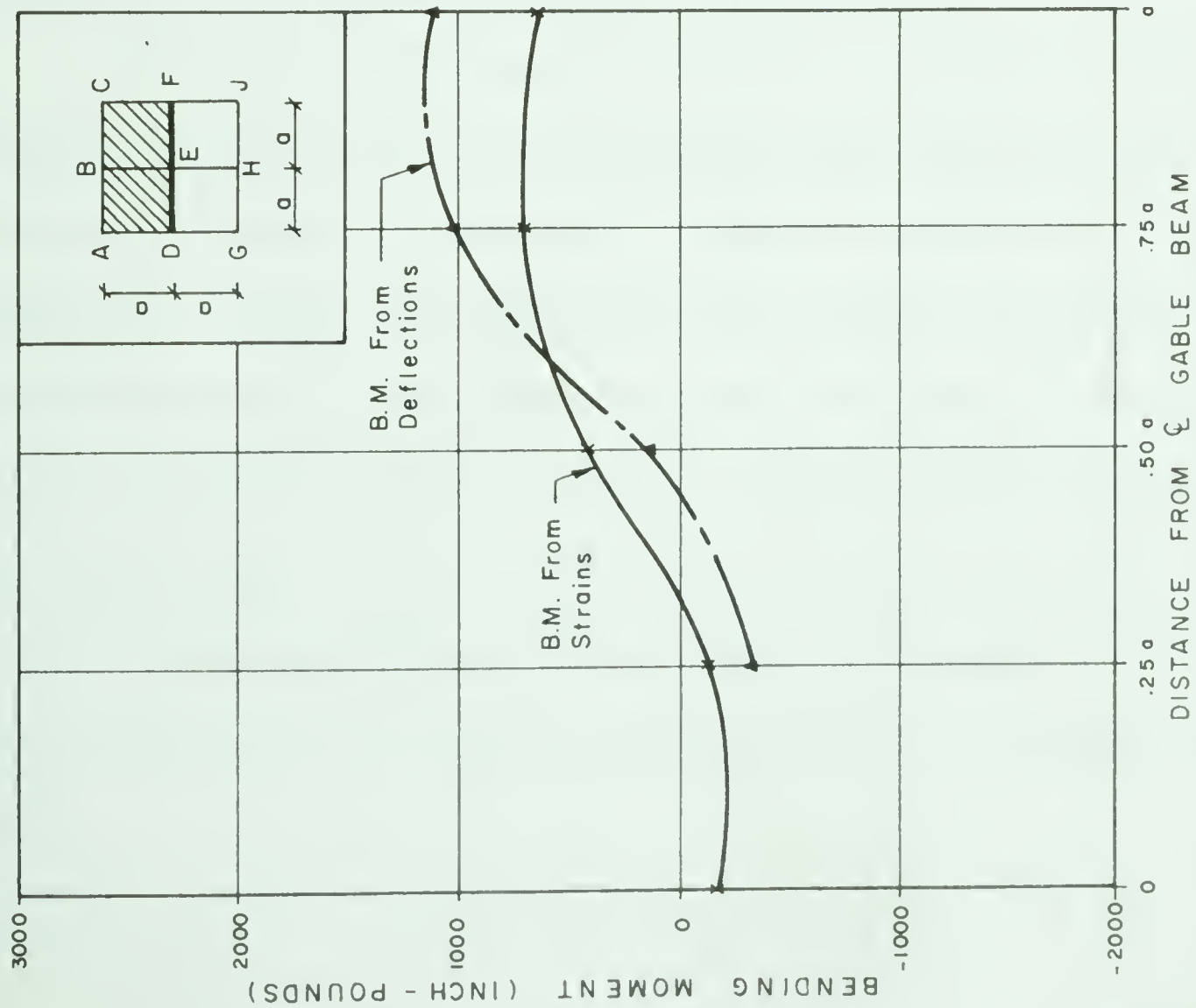
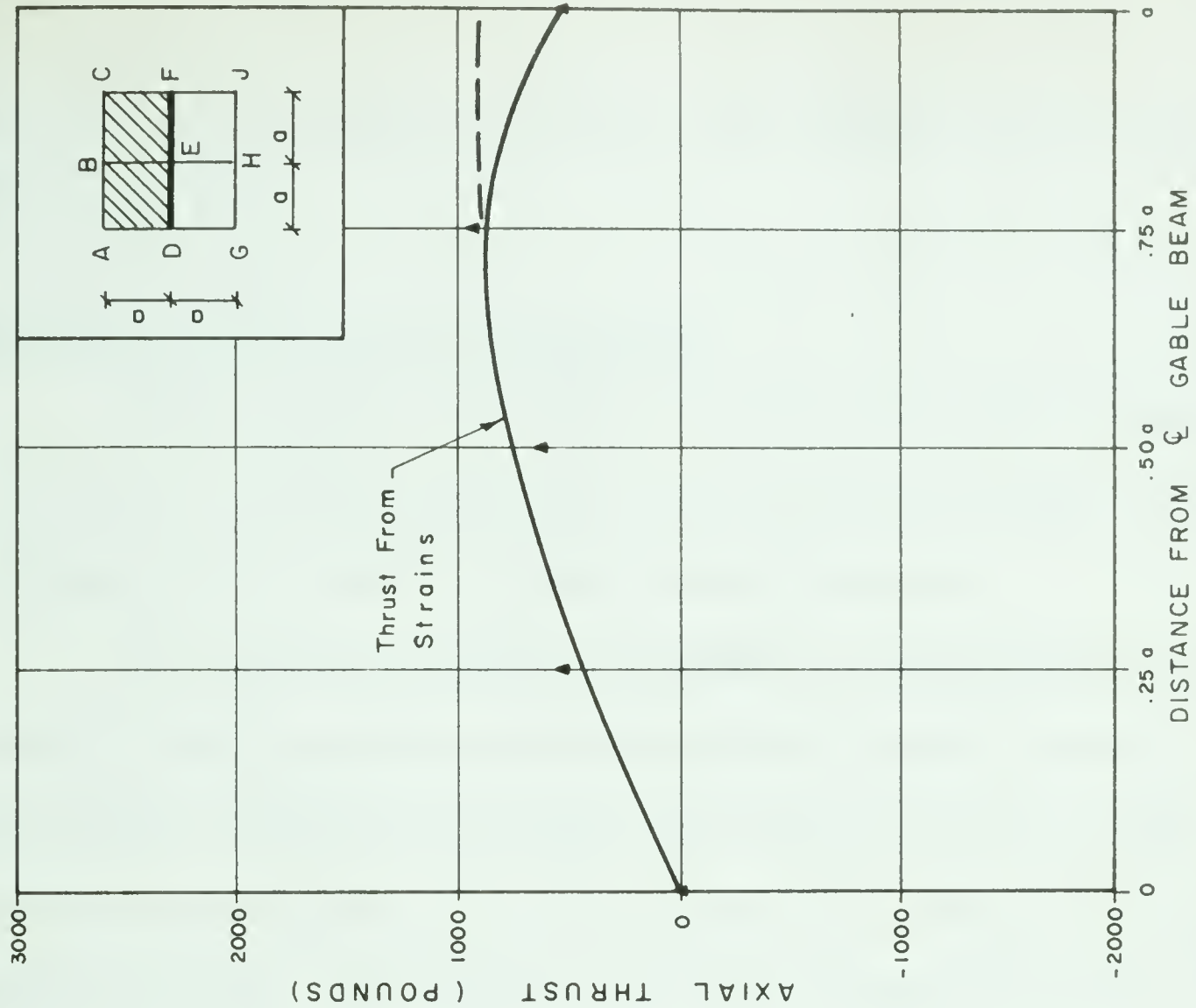


FIGURE 7.13 DEFLECTION OF RIDGE BEAM HAVING LOADING SYMMETRY
TESTS # 2 & # 3 - 3000# ASYMMETRIC LOAD



(a) CALCULATED BENDING MOMENTS



(b) CALCULATED AXIAL THRUSTS

FIGURE 7.14 MOMENTS & THRUSTS FOR RIDGE BEAM HAVING LOADING SYMMETRY
TESTS #2 & #3 - 3000# ASYMMETRIC LOAD

uniform over the entire model or not, but it must be uniform over the quadrant under consideration.

7.6 Ridge Beam Parallel to Axis of Symmetry

Strain measurements on the bottom fibres of the ridge beam parallel to the axis of symmetry display wide scatter and, due to the dearth of values, conclusions must be confined to a general pattern of behaviour.

The deflection configuration in FIGURE 7.17 demonstrates precisely the type of behaviour which would be expected from this type of loading. Under the load, the deflection is maximum and a positive bending is evident whereas the unloaded portion of the model appears to be exerting a restraining moment on the beam. The slope of the beam at the unloaded gable appears to be almost zero, corresponding to virtually a fully fixed end.

The bending moment diagram in FIGURE 7.18 indicates that the maximum positive moment has a value of approximately 2,000 inch pounds, just equal to the maximum value found for the uniformly loaded case, but the location of the maximum ordinate has shifted by one quarter of the panel length toward the loaded side. The negative moment achieves a value of 1,000 inch pounds at a point midway between the gable and ridge in the opposite direction. This value corresponds closely with the maximum negative moment found for the symmetrically loaded ridge reported in Chapter VI, but again, the location of the maximum moment has shifted toward the centre by about one half the panel length.

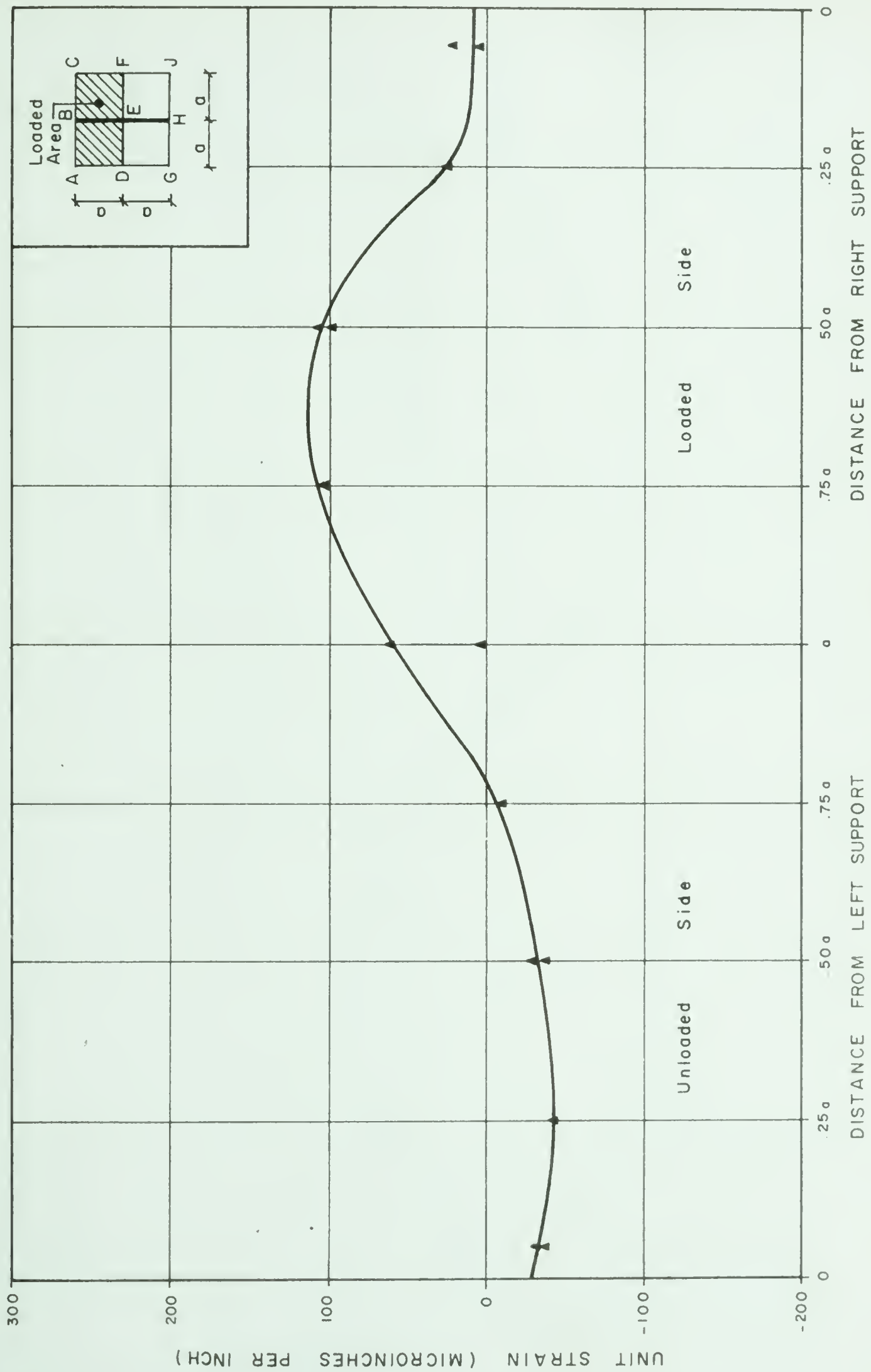


FIGURE 7.15 MEASURED STRAINS IN RIDGE BEAM WITHOUT LOADING SYMMETRY
TOP FIBRES - TEST #2 & #3 - 3000# ASYMMETRIC LOAD

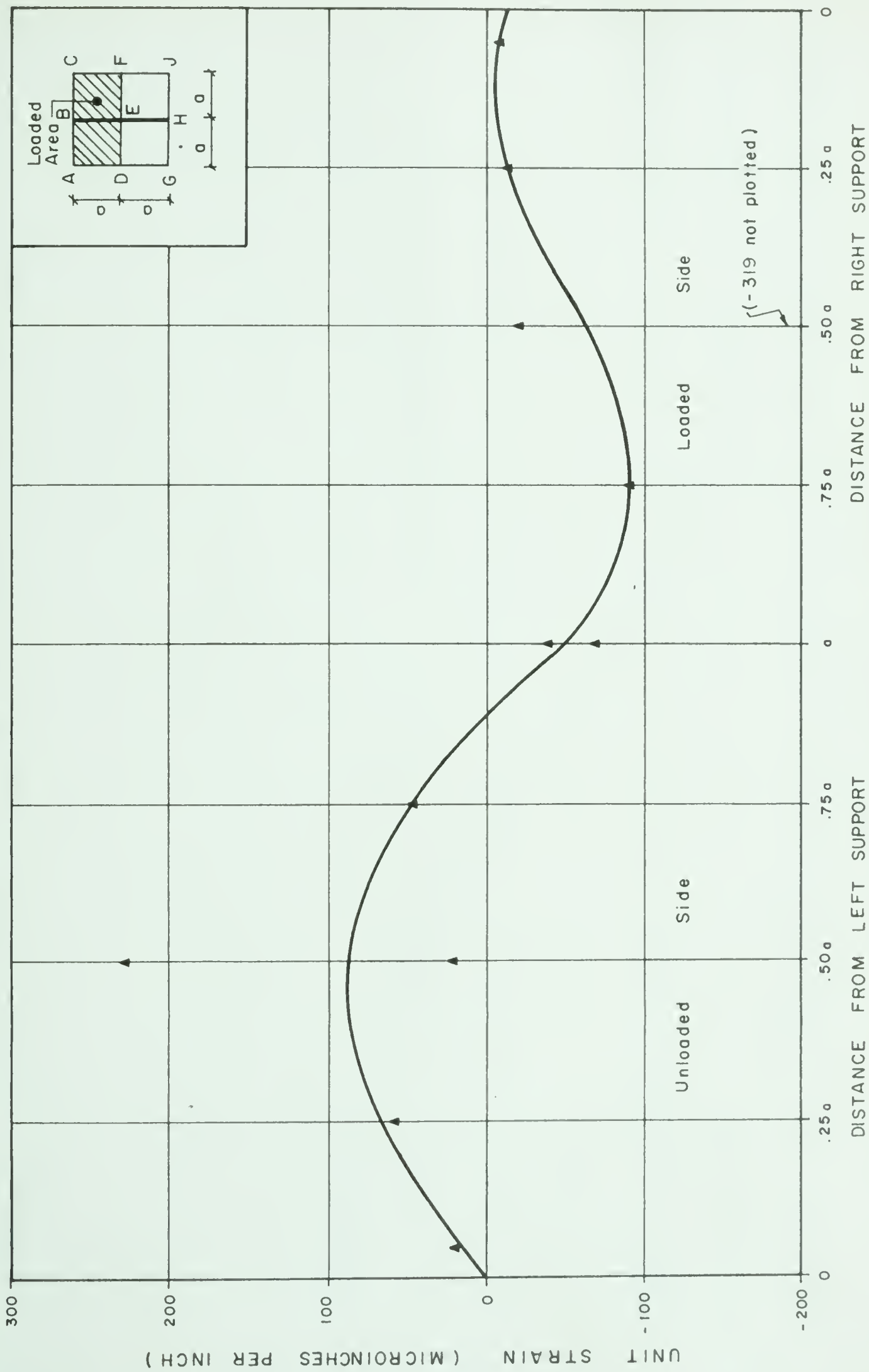


FIGURE 7.16 MEASURED STRAIN IN RIDGE BEAM WITHOUT LOADING SYMMETRY
BOTTOM FIBRES - TEST #28 & #3 - 3000# ASYMMETRIC LOAD

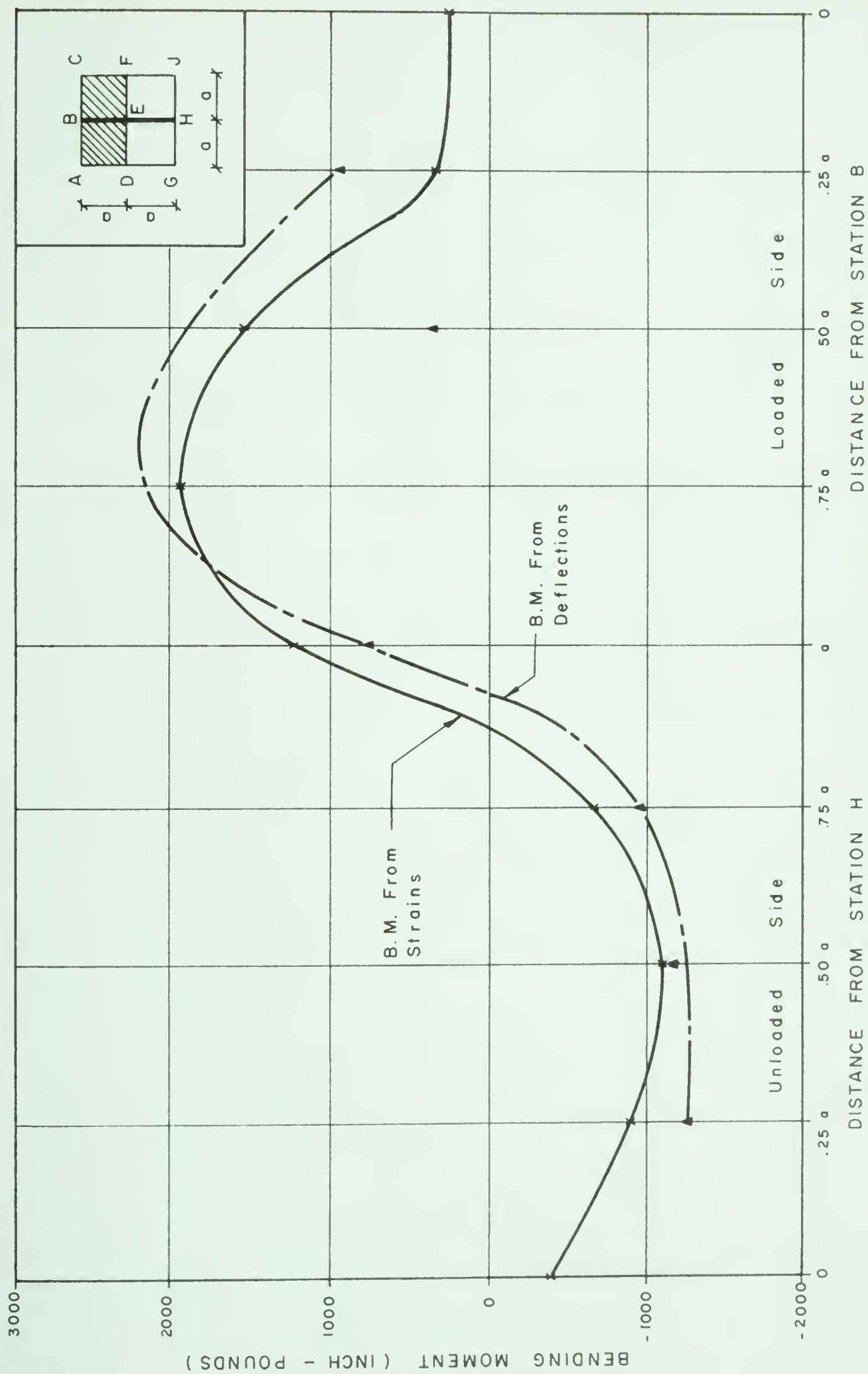


FIGURE 7.18 BENDING MOMENTS FOR RIDGE BEAM WITHOUT LOADING SYMMETRY
TESTS # 2 & # 3 - 3000# ASYMMETRIC LOAD

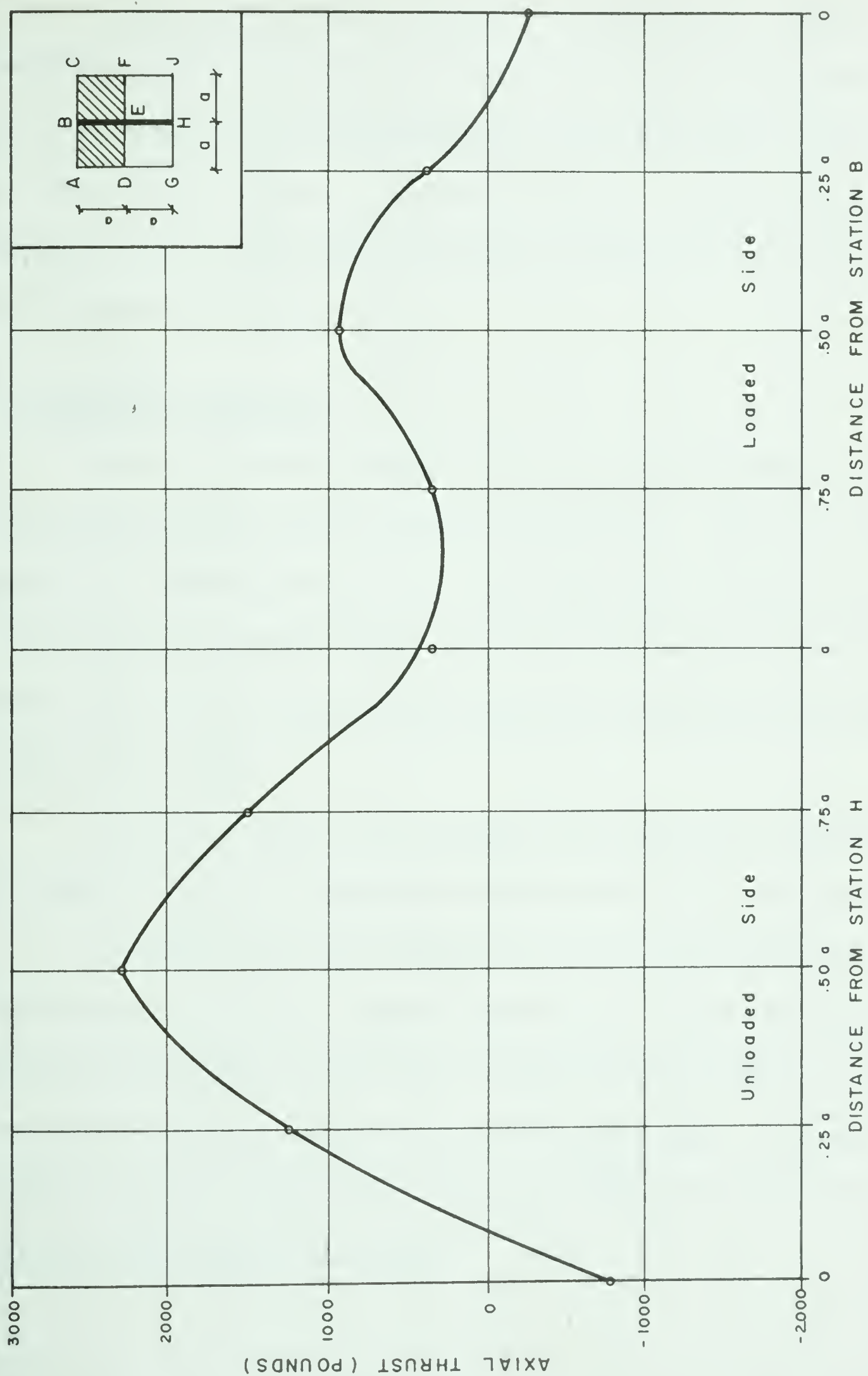


FIGURE 7.19 AXIAL THRUST FOR RIDGE BEAM WITHOUT LOADING SYMMETRY
TESTS #2 & #3 - 3000# ASYMMETRIC LOAD

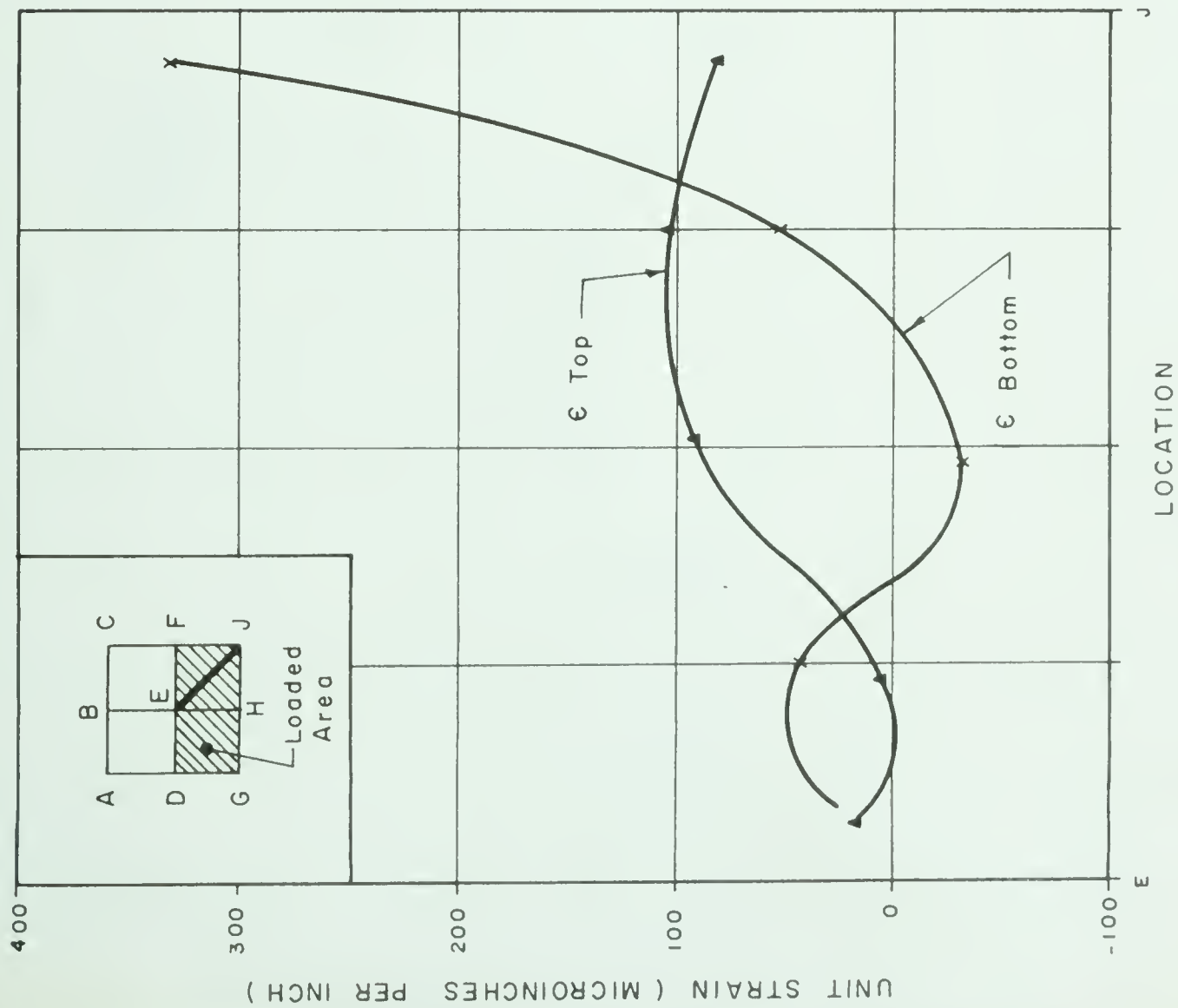
Ridge thrust variation in FIGURE 7.19 demonstrates a peculiar trend with two maximum ordinates, one in the loaded and one in the unloaded span. Surprisingly, the unloaded span appears to have the largest compression, although these results are by no means conclusive. A slight tension is indicated at each end of the ridge, and a definite reduction in thrust is found near the midspan of the beam.

7.7 Compression Diagonal EJ

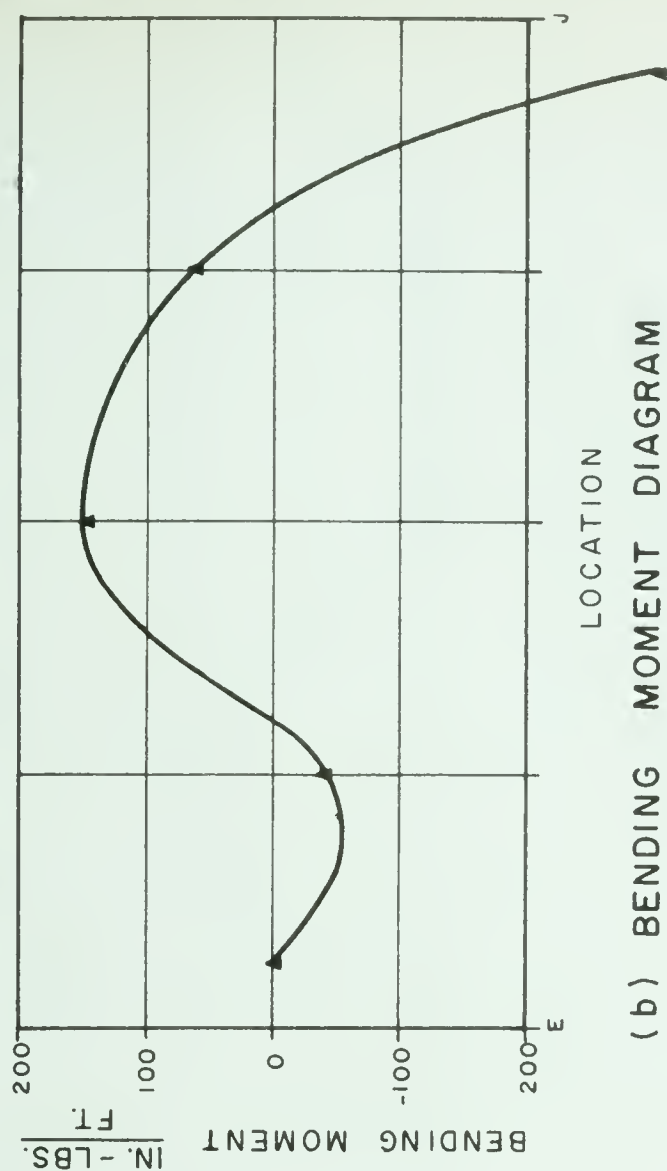
Strains, moments and axial stresses are found in FIGURE 7.20 for the compression diagonal loaded on the instrumented panel. The central region appears to have positive bending while a considerable negative moment builds up at the support and a smaller negative moment appears near the ridge beam junction. The moment is similar to the configuration found for the same diagonal under uniform loading.

The axial stresses in (c) correspond almost identically with those found earlier for the same diagonal under uniform load over the entire shell.

FIGURE 7.21 is a plot of the strains, moments and thrusts for compression diagonal EJ when load is placed on the far side. The bending moment diagram is almost a mirror image of the one just described in FIGURE 7.20 (c) indicating a predominantly negative bending in the central region. The axial stresses are very low, ranging from a small compression at the ridge beam junction to a small tension at the support.



(a) SURFACE STRAINS

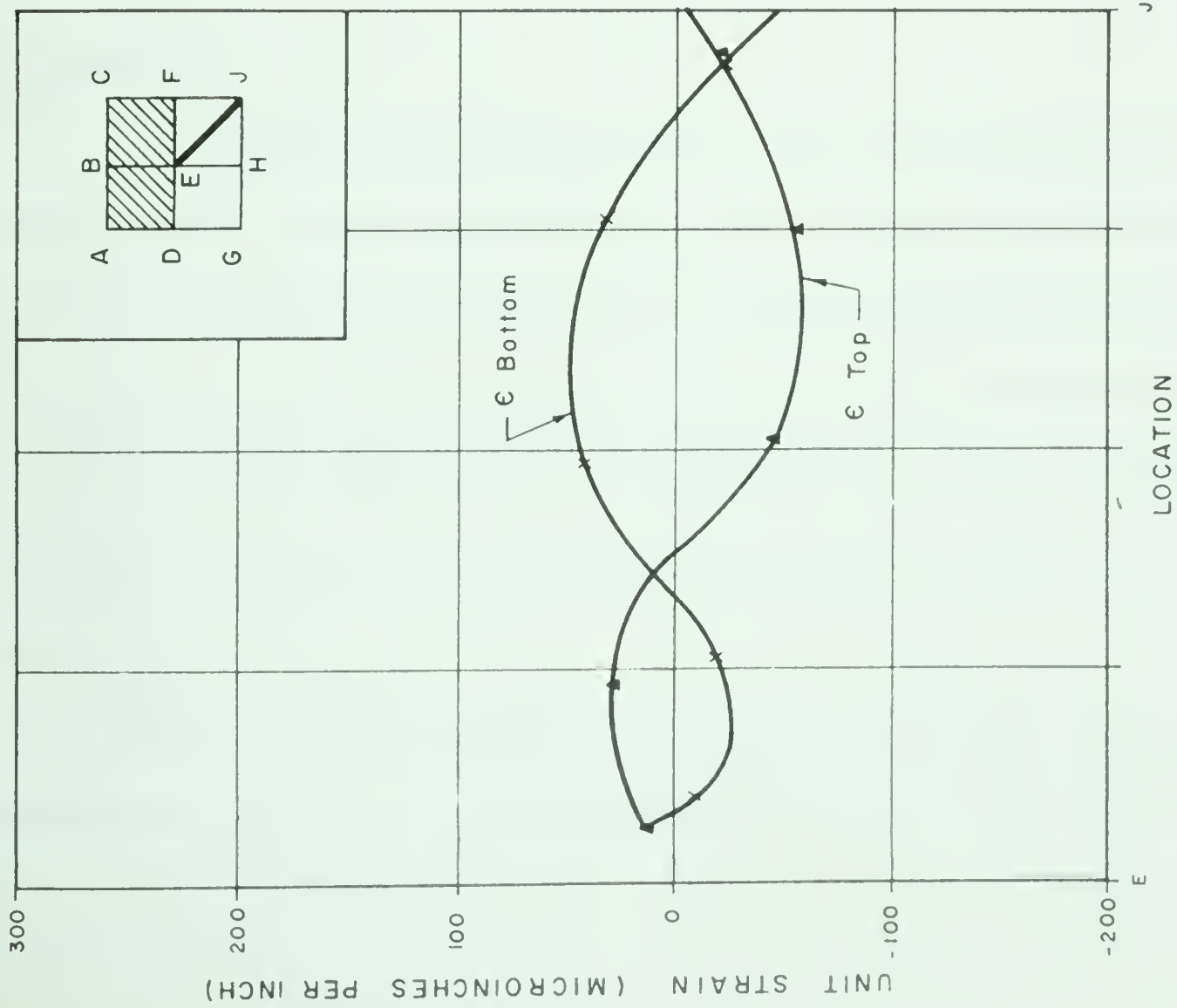


(b) BENDING MOMENT DIAGRAM



(c) AXIAL STRESSES

FIGURE 7.20 SURFACE STRAINS, BENDING MOMENTS & AXIAL STRESSES FOR DIAGONAL E-J
TEST #3 - 3000# ASYMMETRIC LOAD



(a) SURFACE STRAINS

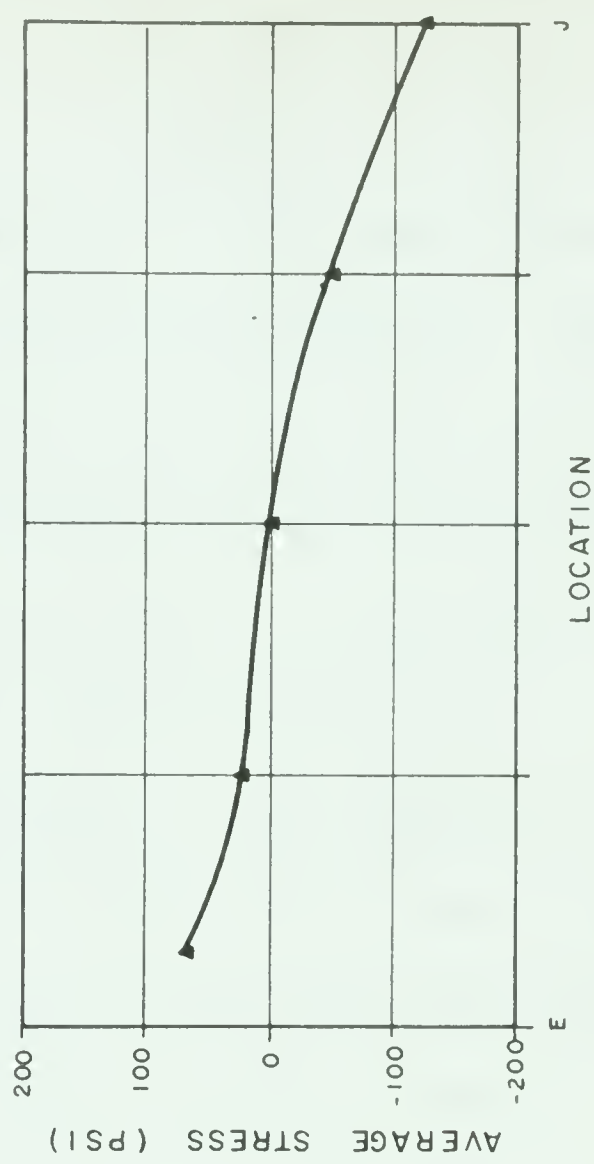
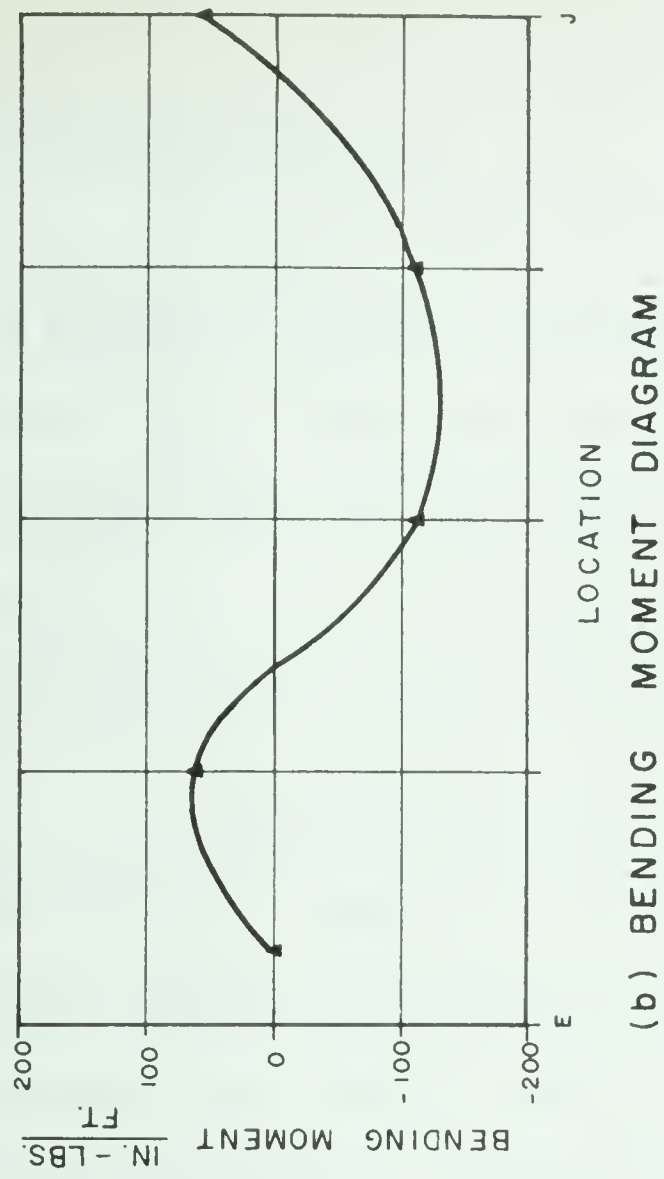


FIGURE 7.21 SURFACE STRAINS, BENDING MOMENTS & AXIAL STRESSES FOR DIAGONAL E-J
TEST #2 - 3000# ASYMMETRICAL LOAD

7.8 Tension Diagonal HF

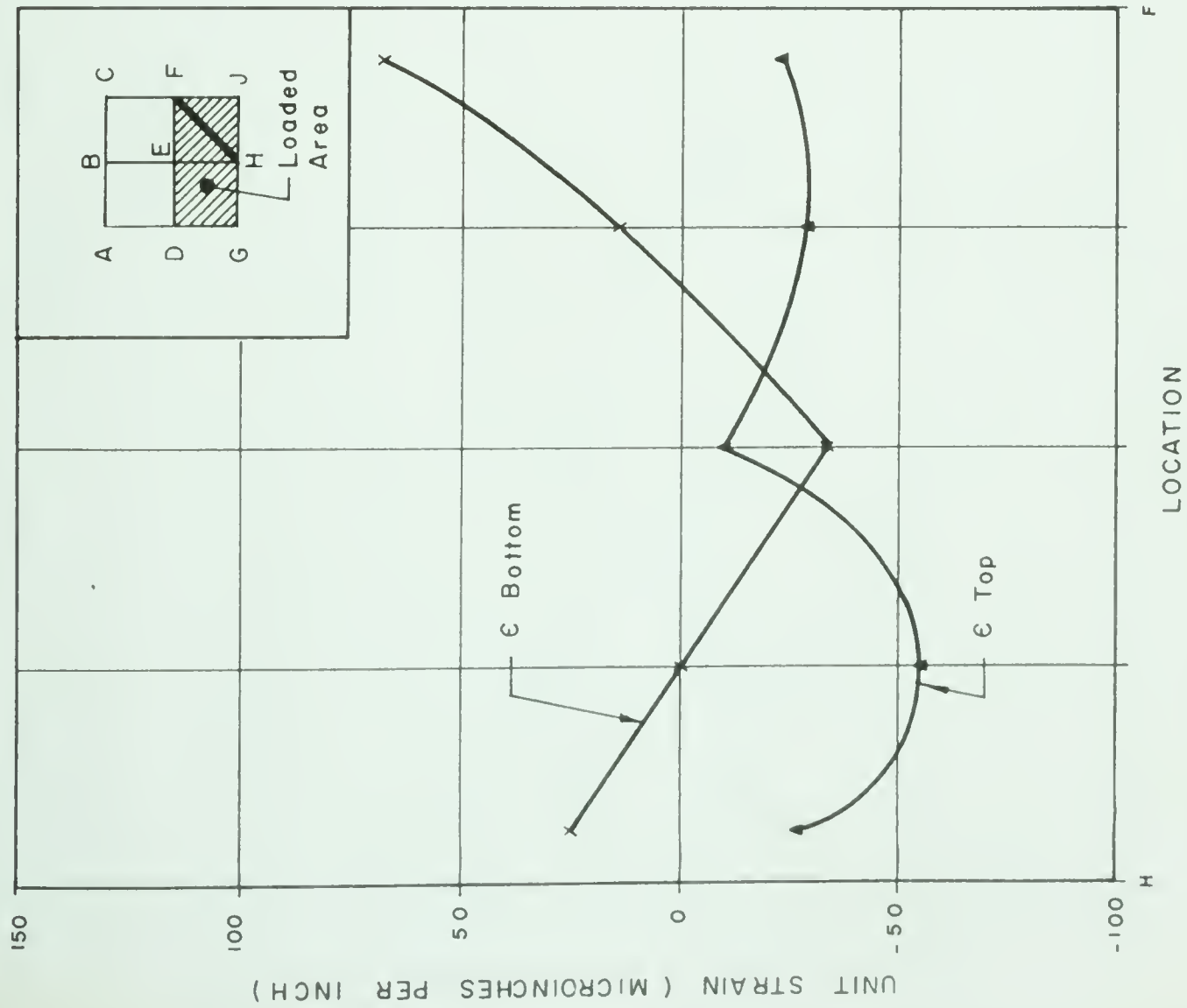
Sharp discontinuities are displayed in the strain diagram of FIGURE 7.22 (a) which may be due to local effects of the rubber bearing pads. These produce a similar discontinuity in the bending moment diagram which looks suspiciously like a concentrated load at the centre with negative end moments applied at the boundaries. The tensile stresses in (c) are not unlike those found under uniform, symmetrical loading, reported in Chapter VI.

The bending moments and axial thrusts in tension diagonal HF found in (b) and (c) respectively of FIGURE 7.23 when the load is placed in the opposite quadrants of the shell are very similar to those found for the compression diagonal under similar conditions (FIGURE 7.21) but the ordinates are roughly one half of those reported earlier.

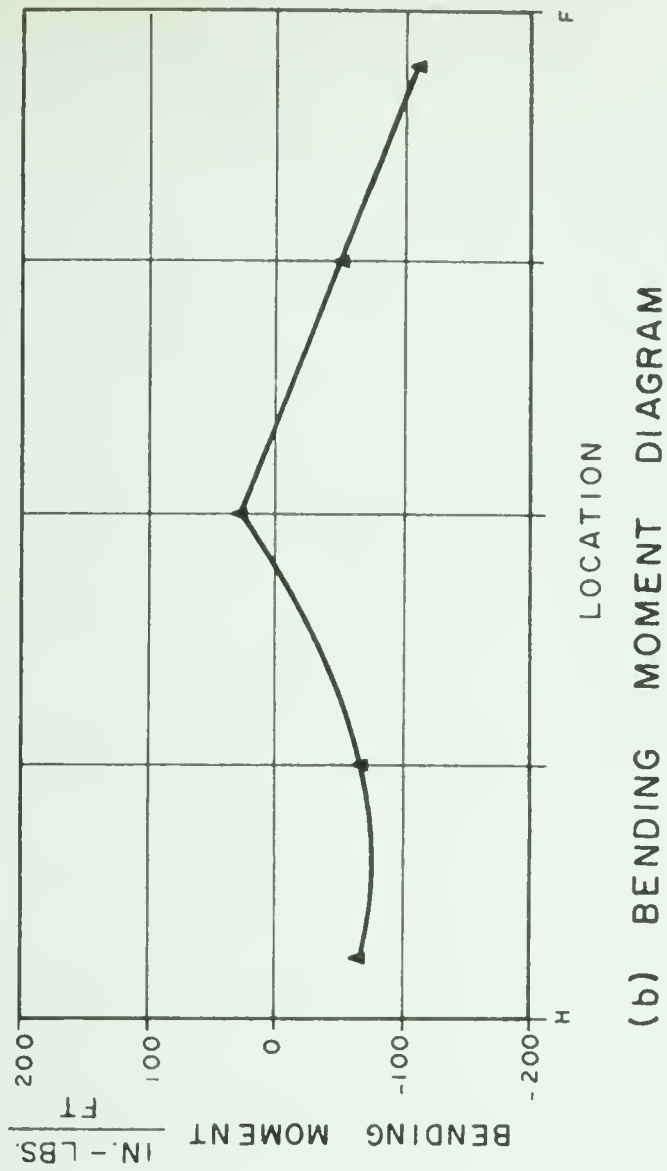
7.9 Generator KL

The moment found in Generator KL when the load was on the instrumented panel indicates a positive bending over the central portion (FIGURE 7.24). The discontinuity may be due to the local effect of the bearing pads. Axial stresses, however, closely resemble those found under uniform load for the same generator in Tests 1 and 4. The generator has a uniform compression of about 50 psi over most of its length, increasing at the ridge to about 200 psi.

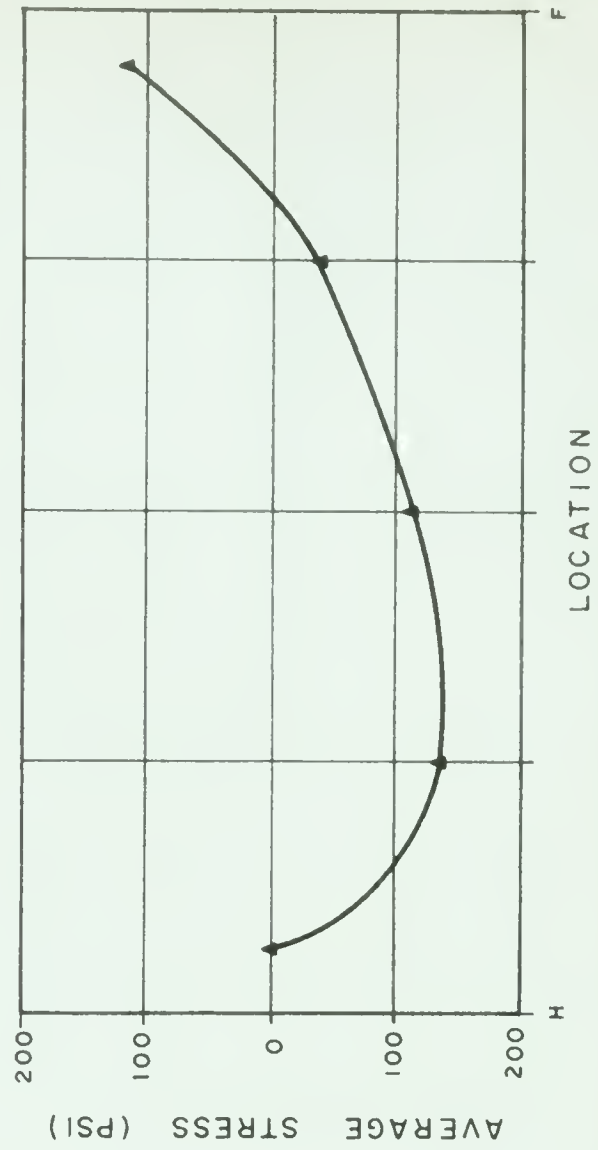
When the load is placed on the opposite side (FIGURE 7.25), the bending moment appears to be quite inconsequential and the thrust varies from



(a) SURFACE STRAINS

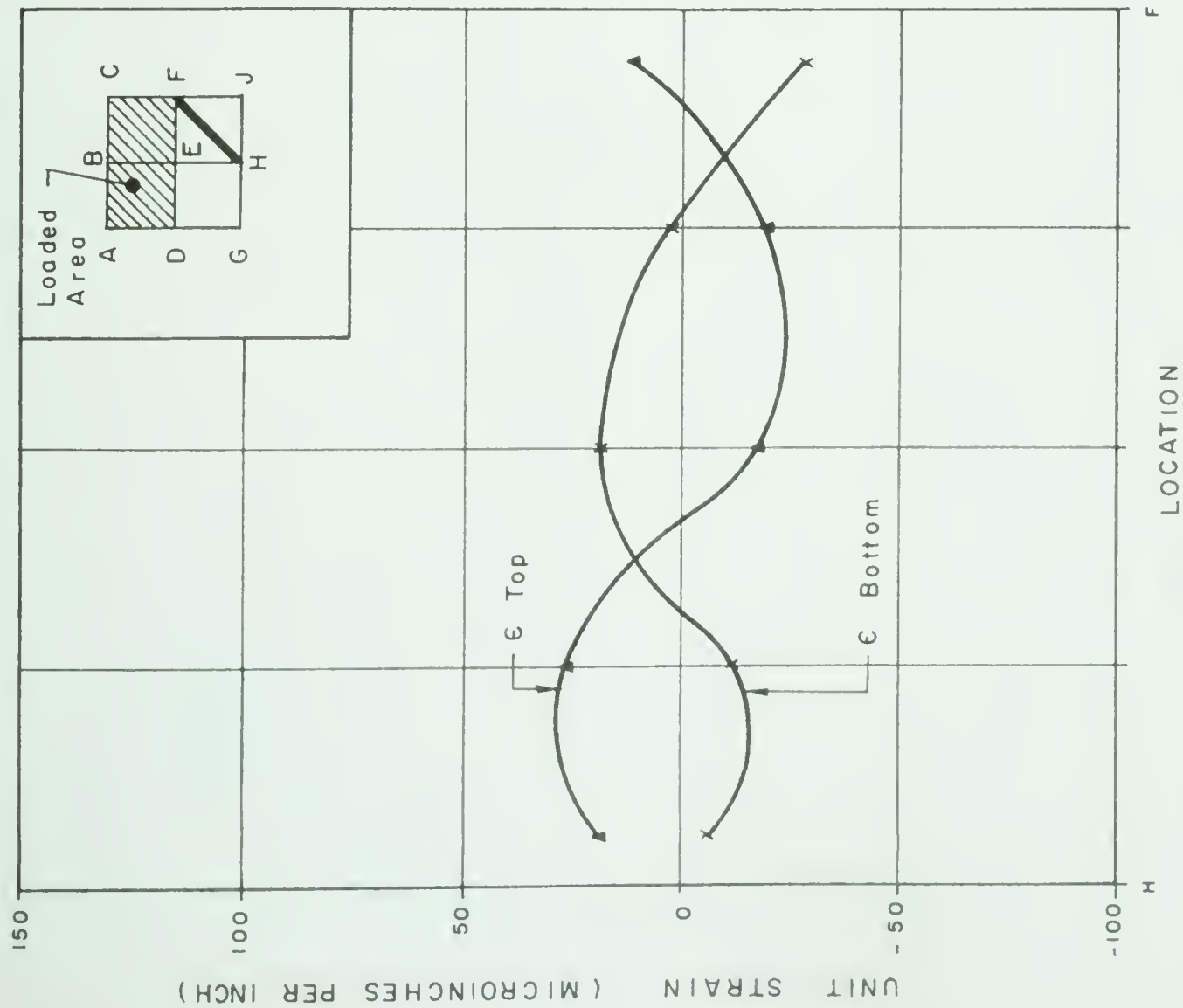


(b) BENDING MOMENT DIAGRAM

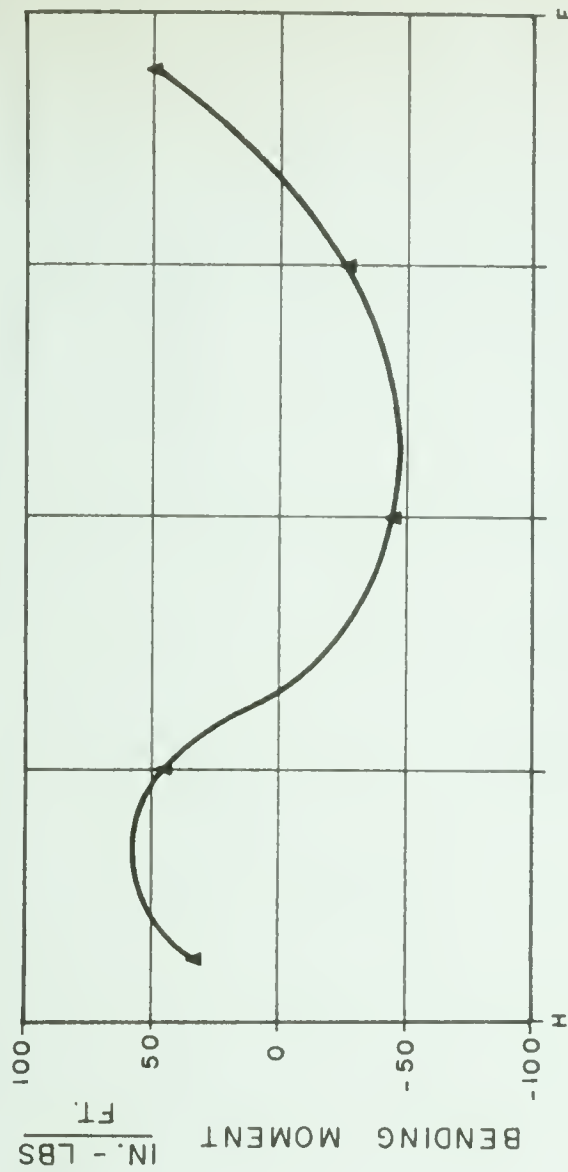


(c) AXIAL STRESSES

FIGURE 7.22 SURFACE STRAINS, BENDING MOMENTS & AXIAL STRESSES FOR DIAGONAL H-F TEST 3 - 3000 ASYMMETRICAL LOAD



(a) SURFACE STRAINS



(b) BENDING MOMENT DIAGRAM



(c) AXIAL STRESSES

FIGURE 7.23 SURFACE STRAINS, BENDING MOMENTS & AXIAL STRESSES FOR DIAGONAL H-F
TEST #2 - 3000 # ASYMMETRICAL LOAD

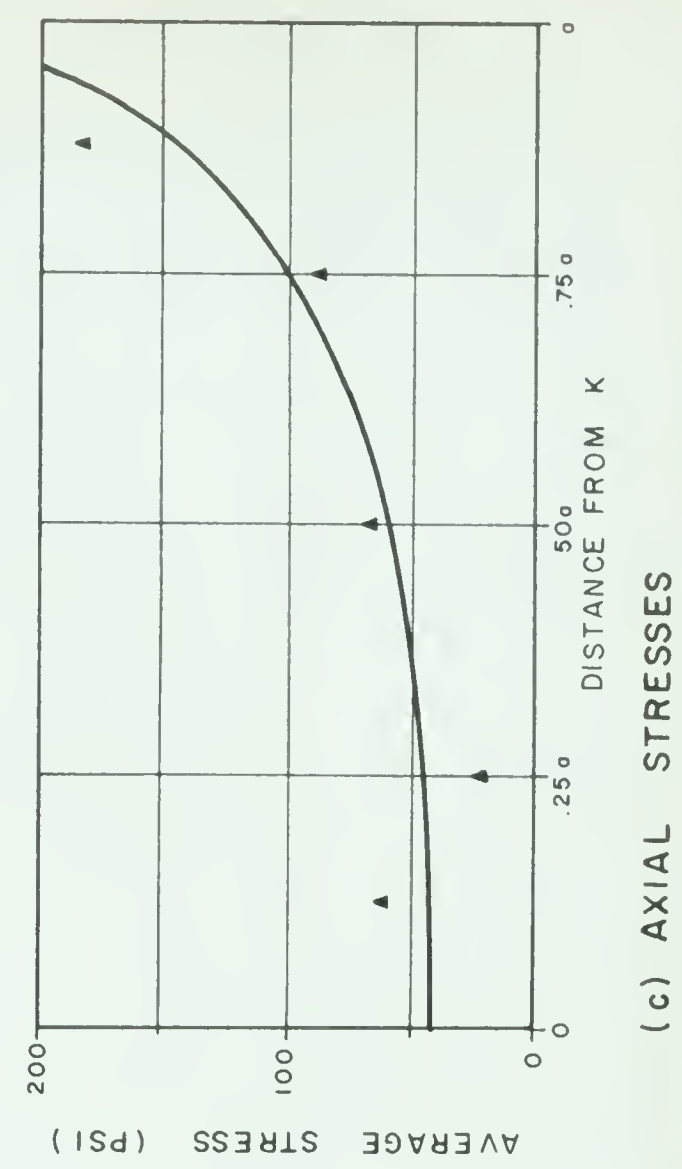
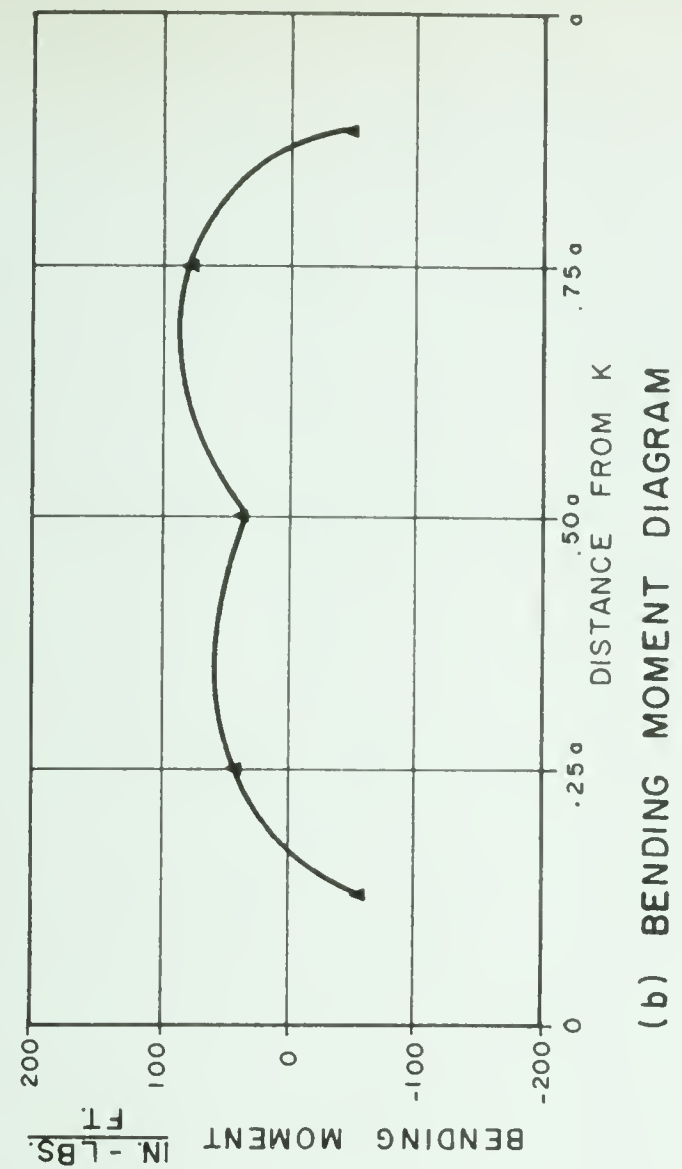
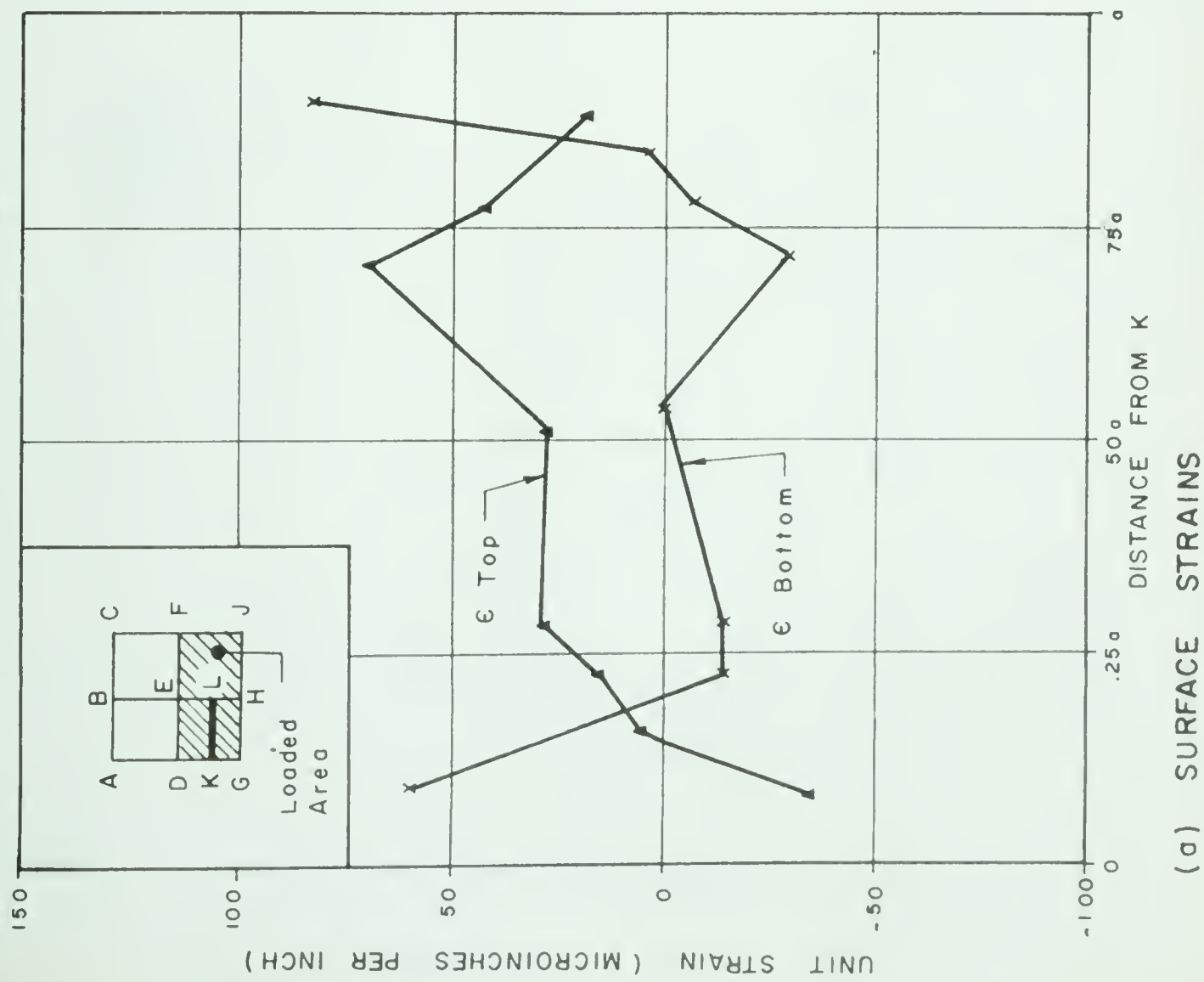
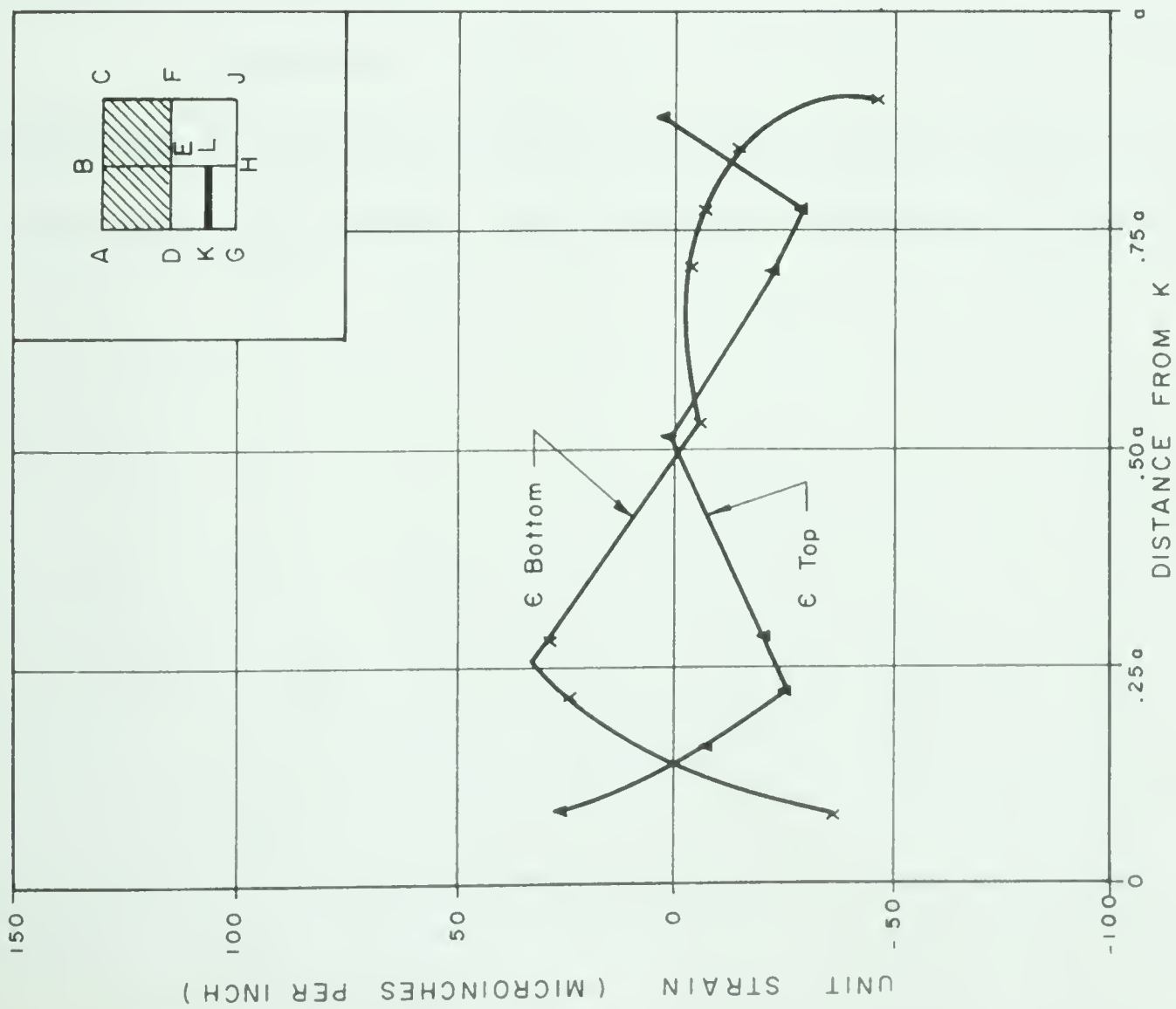
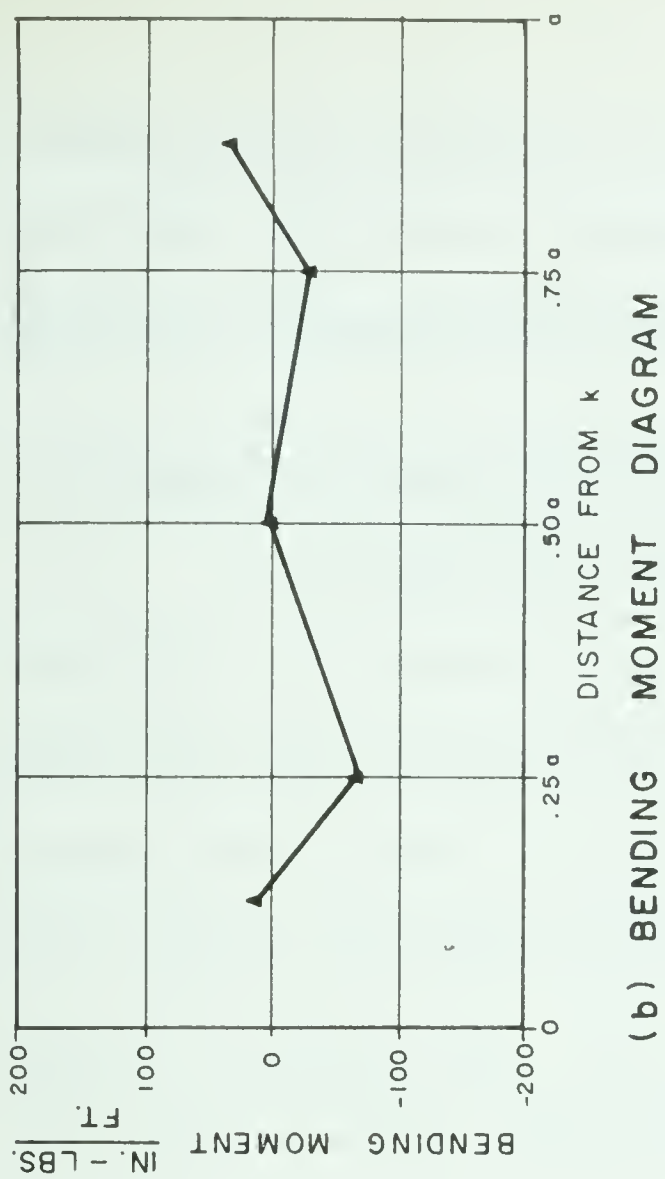


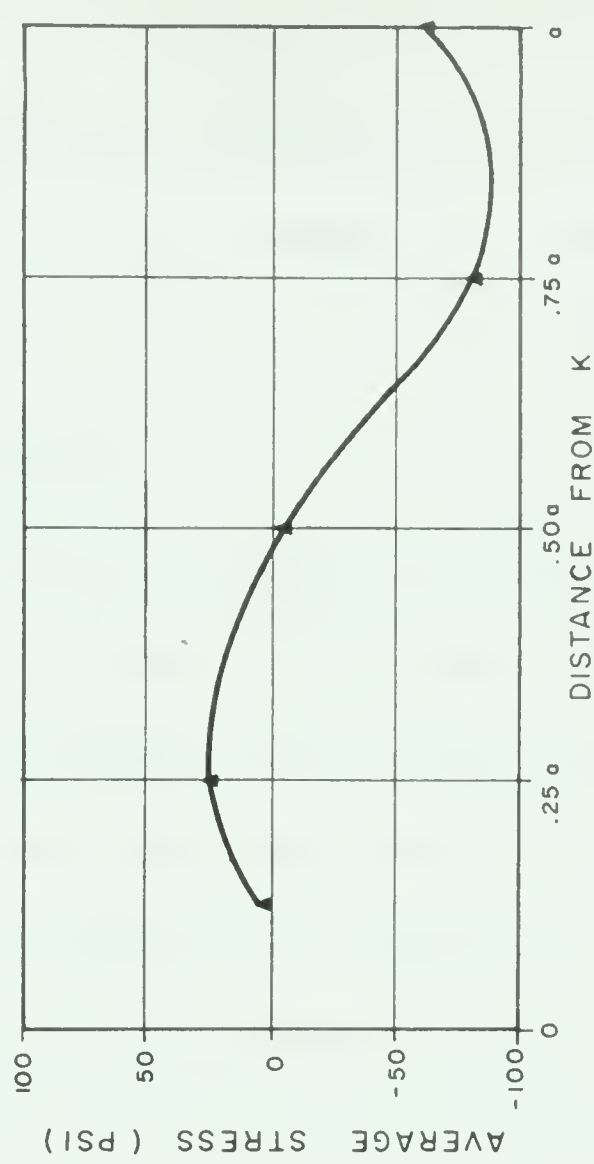
FIGURE 7.24 SURFACE STRAINS, BENDING MOMENTS & AXIAL STRESSES FOR SECTION K - L
TEST #3 - 3000# ASYMMETRIC LOAD



(a) SURFACE STRAINS



(b) BENDING MOMENT DIAGRAM



(c) AXIAL STRESSES

FIGURE 7.25 SURFACE STRAINS, BENDING MOMENTS & AXIAL STRESSES FOR SECTION K-L = 7
TEST # 2 - 3000# ASYMMETRICAL LOAD

a slight tension near the gable to a slightly larger compression in the vicinity of the ridge. All stresses are extremely low and do not appear to be very significant in designing similar shells.

7.10 Discussion of Asymmetrical Load Tests

From simple statics and symmetry, the vertical reactions may be found for a 3,000 pound load applied over one half of the model only. From statics, one quarter of the load goes to the supports G and J while three quarters of the load goes to supports A and C. Thus supports G and J should have a reaction of 375 pounds each while supports A and C should have a reaction of 1,125 pounds each. The load cell readings checked with these values with a maximum deviation of ten percent, which is not as close as expected but constitutes fair agreement.

Neglecting the bending moment in the shell elements, a check on statics may be made by summing the moments about the longitudinal axis of the ridge beams DEF and BEH. These results are tabulated in TABLES I & II.

TABLE I
CHECK ON EQUILIBRIUM ABOUT AXIS DEF

Item	Force (lbs.)	Arm (inches)	Moment (in.lbs.)
Tie Rod CJ	1,140	12.4	14,200
Tie Rod AG	1,200	12.4	14,900
Gable CFJ	(Moment measured directly)		1,200
Gable ADG	(Moment measured directly)		1,200
Ridge BEH	(Moment measured directly)		1,200
	Summation		<u>32,700</u>

TABLE II
CHECK ON EQUILIBRIUM ABOUT AXIS BEH

Item	Force (lbs.)	Arm (inches)	Moment (in.lbs.)
Tie Rod AC	2,050	12.4	25,400
Tie Rod GJ	485	12.4	6,000
Gable ABC	(Moment measured directly)		1,500
Gable GHJ	(Moment measured directly)		1,300
Ridge DEF	(Moment measured directly)		900
	Summation		35,100

From statics, a moment of 36,000 inch pounds may be calculated for the model in each principal direction, the maximum value occurring at centerline. A moment of 32,700 inch pounds (91% of statics) may be found by summing the moments of the beams and tie rods about the centerline when considering the span from supports G, J to A, C. A moment of 35,100 inch pounds is accounted for in summing the contributing members about Ridge BEH, which is 97.5% of statics. It may be concluded that the moment is largely carried by the tie rods, with the beams contributing a small portion due to the spreading of corner supports.

It would be unwise to attribute to shell action the 9% of statics which is unaccounted for in Table I due to other redundancies such as tie rod restraints and frictional resistance of the pin supports. In addition, the readings are not sufficiently numerous to preclude error, but it appears the shell elements spanning parallel to the axis of symmetry carried more moment than those spanning perpendicular to the axis of symmetry in Tests 2 and 3. Unfortunately, no generator in this direction was instrumented so that such a theory cannot be verified. This oversight should be rectified in subsequent tests on similar types of shells.

Since it has been established that in Test 3 the loading was lacking symmetry about axis BEH, the asymmetrical tests are of questionable value except in pointing up general trends as to the behaviour of the model. In addition, the reduction of symmetry in Tests 2 and 3 result in fewer values with

which to produce composite plots of bending moments and axial thrusts than was the case in the symmetrical loading series reported in Chapter VI.

Notwithstanding the foregoing, it would appear that the ridge and gable beams spanning parallel to the axis of symmetry develop bending moments similar to a two span continuous beam having load on one side only. The maximum values of the moments appear to be not more than those of the symmetrical loading series but the point of maximum moment occurs in a different location. If this be the case, the designer need not consider unbalanced loading in the analysis of beams, but should extend the reinforcing steel required at the point of maximum moment throughout the length of the beams to take care of the eventuality of unbalanced loading.

A comparison of FIGURE 7.6 and 7.19 show a unique shape to the axial thrust configurations for the gable beams and ridge beam respectively which span parallel to the line of symmetry. The absolute values of the curves are not claimed to be correct as it seems unlikely that a 2,000 pound tension should be developed at the right support of the gable beam, but it is interesting to note the similarity of the two curves, the curve for the gable beam closely resembling the right hand portion of the ridge beam curve, displaced a distance of about $0.5a$. It is suggested that the gable beam is "lagging" behind the ridge beam in picking up axial load.

Consider the loaded half of the model as a free body. For equilibrium, a "holding force" of 6,000 pounds is placed at point E in Ridge BEH,

pointing towards point B as shown in FIGURE 7.26. Horizontal reactions are required at A and C, each having a value of 3,000 pounds. With these fictitious forces, the loaded portion of the shell has all the conditions of membrane theory satisfied for a uniformly loaded shell. The unloaded half as a free body, has membrane conditions satisfied without any fictitious forces, since it carries no load. Joining the two halves together, and releasing the fictitious holding forces, a 6,000 pound force must be applied in the opposite direction to the original holding force.

This force is transmitted to the shell by planar shears which diminish the ridge thrust from E to B and gradually build up thrust from E to H. The maximum value is reached approximately midway between E and H and then gradually falls off to zero at the boundary which is a necessary condition of equilibrium.

The shears which were transferred from the ridge to the shell are transferred across the shell to the gable beams parallel to the ridge under consideration. A "shear lag", similar to that described by Timoshenko (1951) is experienced with the resulting lag in the axial thrust configuration as noted earlier.

FIGURE 7.11 shows that the behaviour of the loaded gable ABC is essentially the same as for the typical gables in the symmetrical loading series. FIGURE 7.14 confirms that Ridge DEF behaves as it did under symmetrical loading, except that all values of moment and axial thrust are halved, as could

be expected from membrane theory, since shear loading from the shell is introduced on one side only. The tension and compression diagonals and Generator KL behave almost identically when loaded in Tests 2 and 3 to the way they behaved in symmetrical Tests 1 and 4. It appears that, in general, the presence of unbalanced loading does not appreciably change the behaviour of the loaded portion of shell from its behaviour when the load is symmetrical.

CHAPTER VIII

PRESENTATION AND DISCUSSION OF TEST RESULTS

FOUNDATION SETTLEMENT

8.1 Introduction

Support A was lowered in increments of 0.1" to a maximum of one inch. Examination of the model during this test revealed no evidence of undue cracking although the settlement (1/96th of the span) would be cause for more than a little alarm should it occur in a prototype.

In permitting one support to subside, two lines of symmetry through the two diagonals are retained. To be strictly correct, supports A and J should each have been lowered one half inch, but the slight change in geometry resulting from this discrepancy was thought to have little significance.

8.2 Measured Reactions

Supports A and J showed a net decrease of 236 pounds and 147 pounds respectively, whereas supports C and G showed a gain of 234 pounds and 220 pounds respectively.

Since no load was applied to the model during this test, it is apparent that, to satisfy statics, the sum of the four vertical reactions must be zero. It may be safely concluded that the deviation was due to inaccuracy in the

load cell readings. It would appear from symmetry that the value of 147 pounds at support J was most in error.

8.3 Gable Beams

FIGURES 8.1 and 8.2 indicate large scatter in the measured strains in the top and bottom fibres of the gable beams. Few values are available on the left hand side of the curve, but a general trend is plainly in evidence.

The resulting bending moment diagram in FIGURE 8.3 is not verified by deflection readings as was the case in previous tests, but it would appear that the maximum ordinates appear at the mid point of each span, one side negative moment and the other, positive.

A study of FIGURE 8.4 reveals a similar trend in axial thrusts with the settled span displaying tension values of axial force and the stationary end showing a resultant compression at the centre. The maximum values in each case appear to change sign near the supports.

8.4 Ridge Beams

Few strain readings are available for the ridge beams since only one hundred gauges were read in this series. From the values in FIGURE 8.5, it appears that the ridge beam strains were very nearly zero throughout the length of the beam.

Bending moment and axial thrusts are not plotted for the ridge beams due to the absence of sufficient readings, but it would appear that very

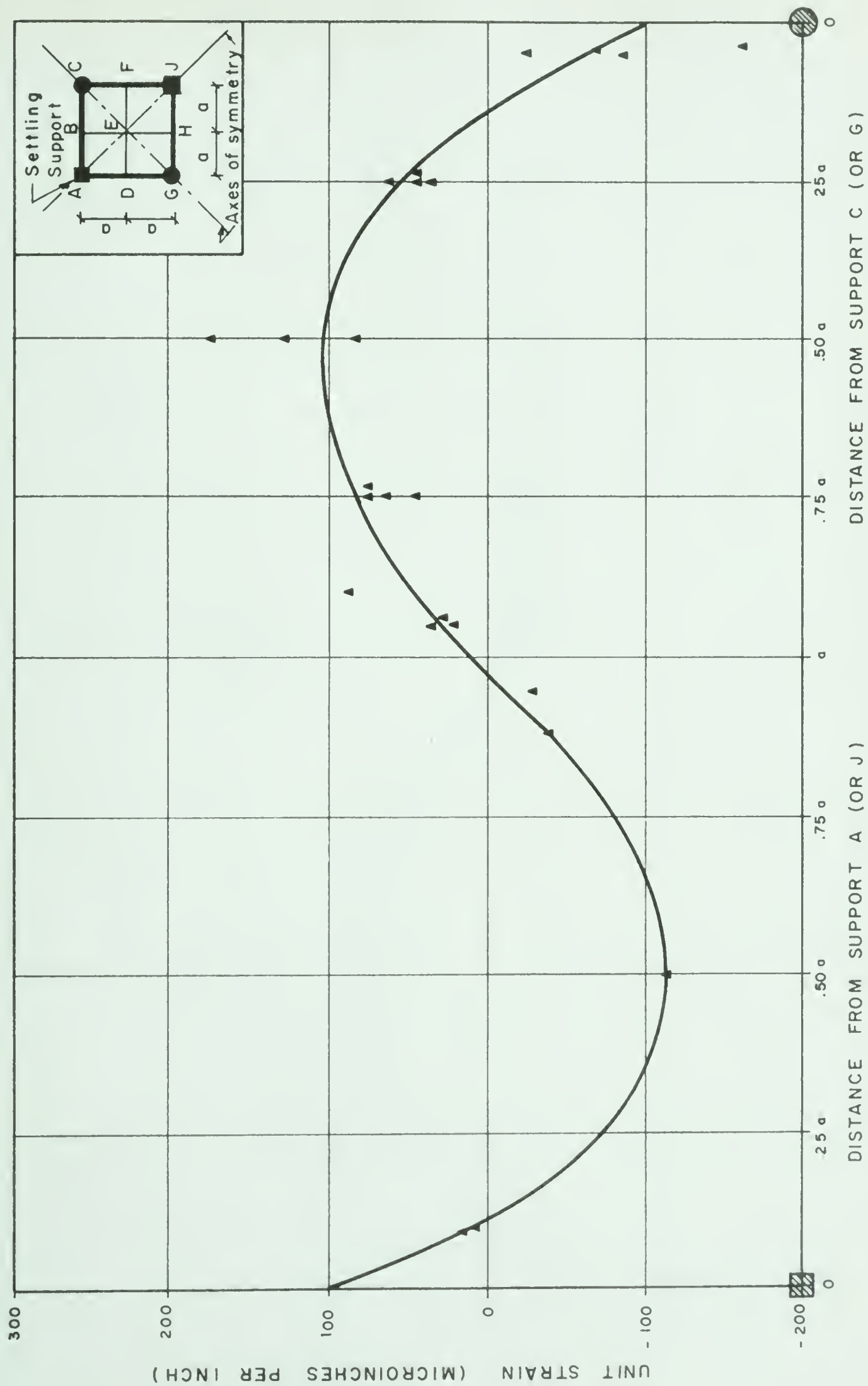


FIGURE 8.1 MEASURED STRAINS IN GABLE BEAMS - TOP FIBRES
TEST # 5 - FOUNDATION SETTLEMENT

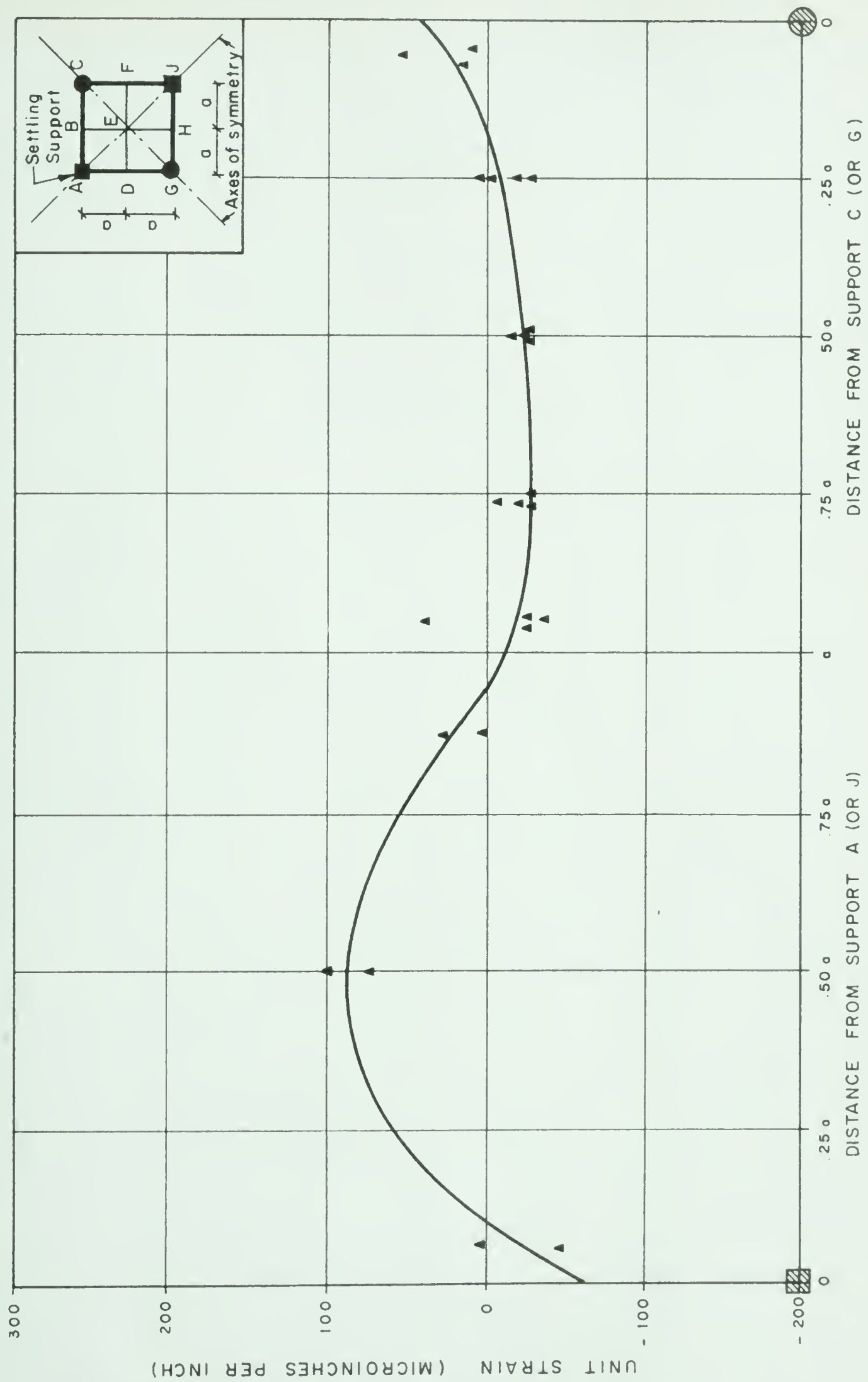


FIGURE 8.2 MEASURED STRAINS IN GABLE BEAMS - BOTTOM FIBRES
TEST #5 - FOUNDATION SETTLEMENT



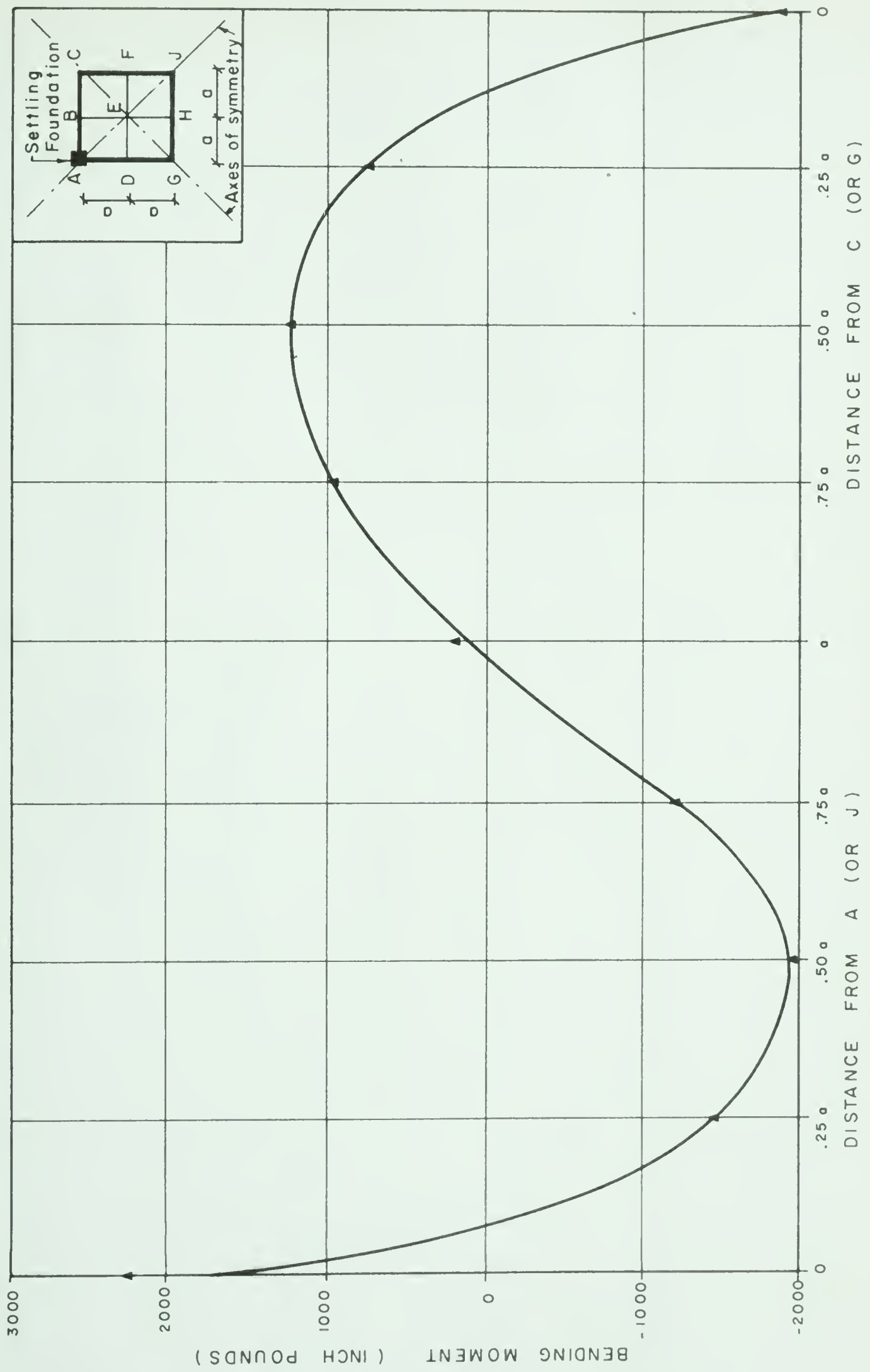


FIGURE 8.3 BENDING MOMENTS FOR GABLE BEAMS
TEST #5 - FOUNDATION SETTLEMENT

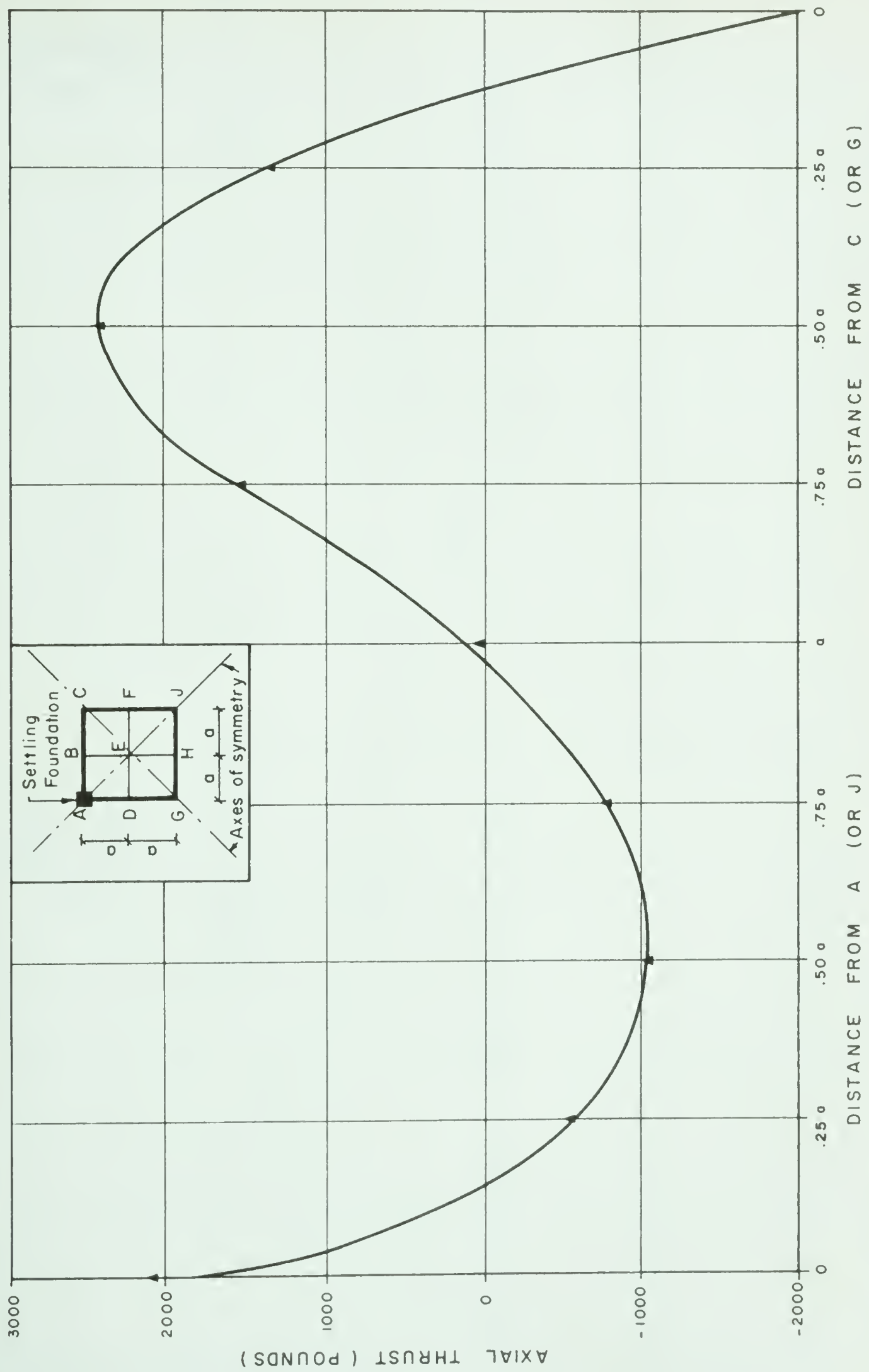
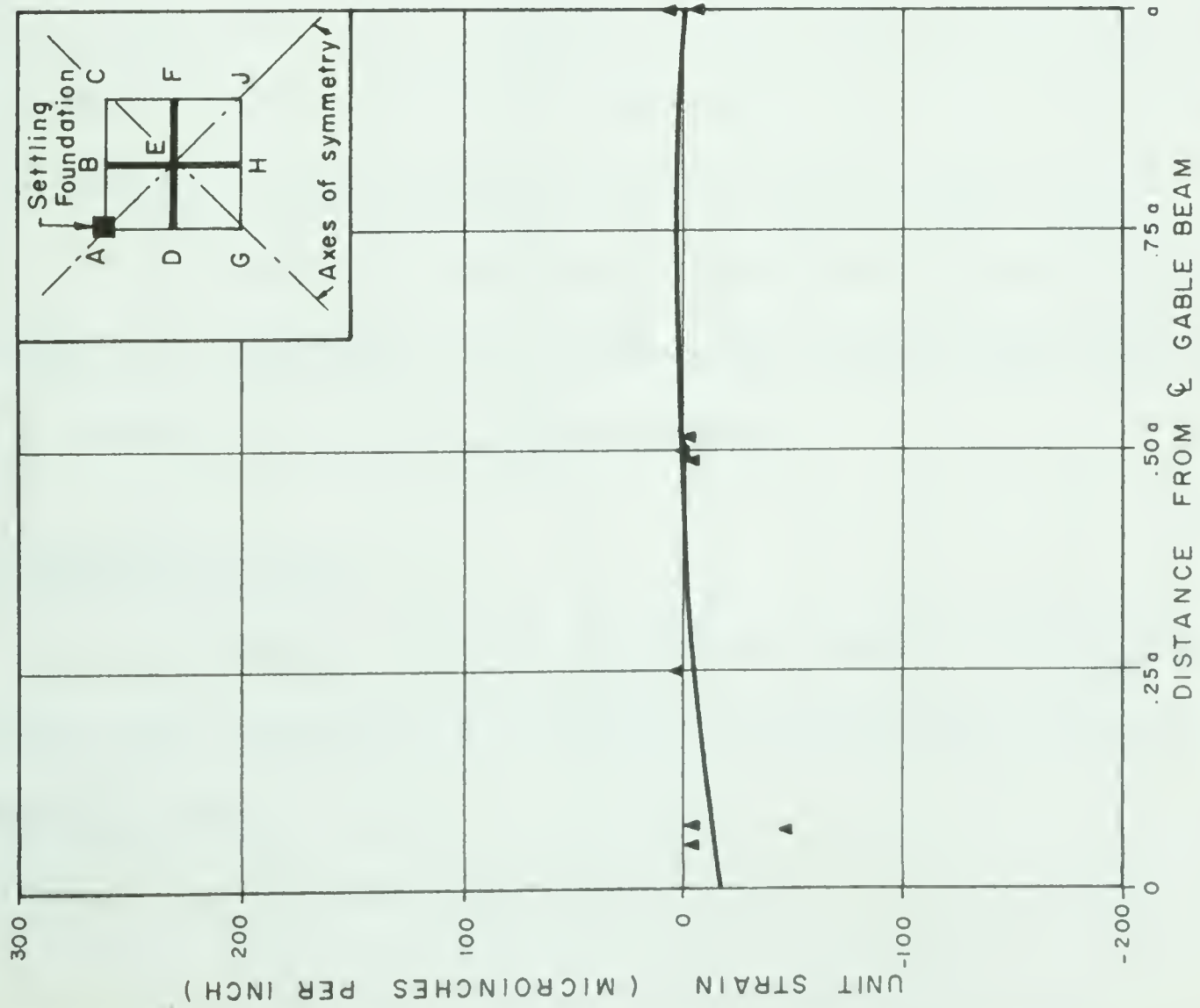
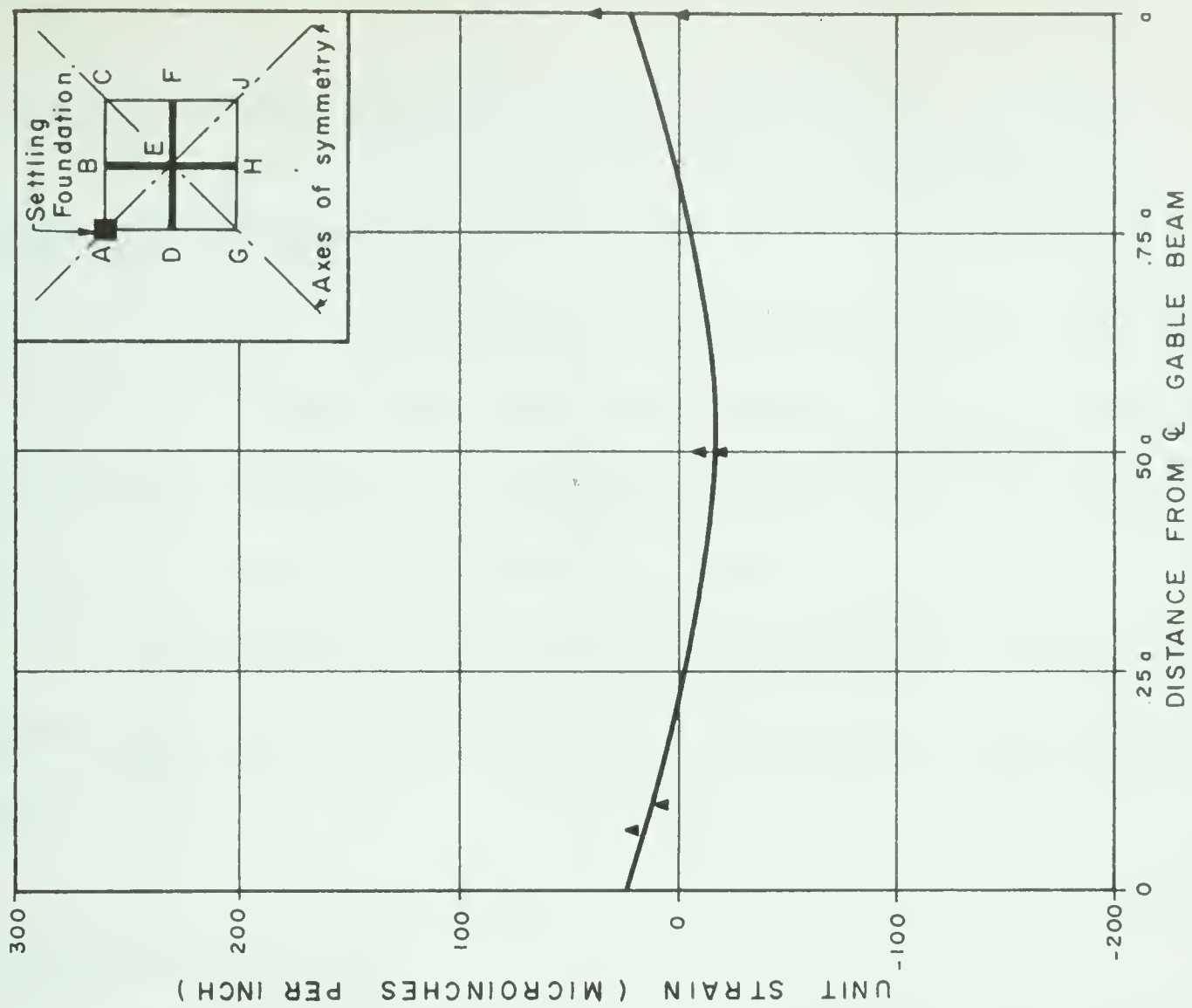


FIGURE 8.4 AXIAL THRUSTS FOR GABLE BEAMS
TEST #5 - FOUNDATION SETTLEMENT



(a) STRAINS IN TOP FIBRES



(b) STRAINS IN BOTTOM FIBRES

FIGURE 8.5 MEASURED STRAINS IN RIDGE BEAMS
TEST #5 - FOUNDATION SETTLEMENT

little moment or thrust exists in the ridge beams.

8.5 Compression Diagonal EJ

Strains, moments and axial stresses for the compression diagonal EJ are plotted in FIGURE 8.6. The value of the bending moment is quite low and the sharp discontinuity near the support may be an error in the measured values or it may be due to local disturbances near the boundary.

A compression in this diagonal, increasing from the ridge beam junction to the support defies intuition and no explanation for this behaviour is offered.

8.6 Tension Diagonal HF

The distribution of surface strains along diagonal HF reveals sharp discontinuities which cannot be explained. Strain versus settlement curves are superimposed in the lower part of the figure and it may be seen that the individual strain gauge readings remained essentially linear throughout the test.

Axial stresses in this diagonal remained compressive throughout its length. The magnitude of the compression was relatively small and would not be considered particularly significant in design.

8.7 Discussion of Test 5

An elaborate discussion of the effect of foundation settlement is beyond the scope of this study and the shortage of information does not permit extensive conclusions.

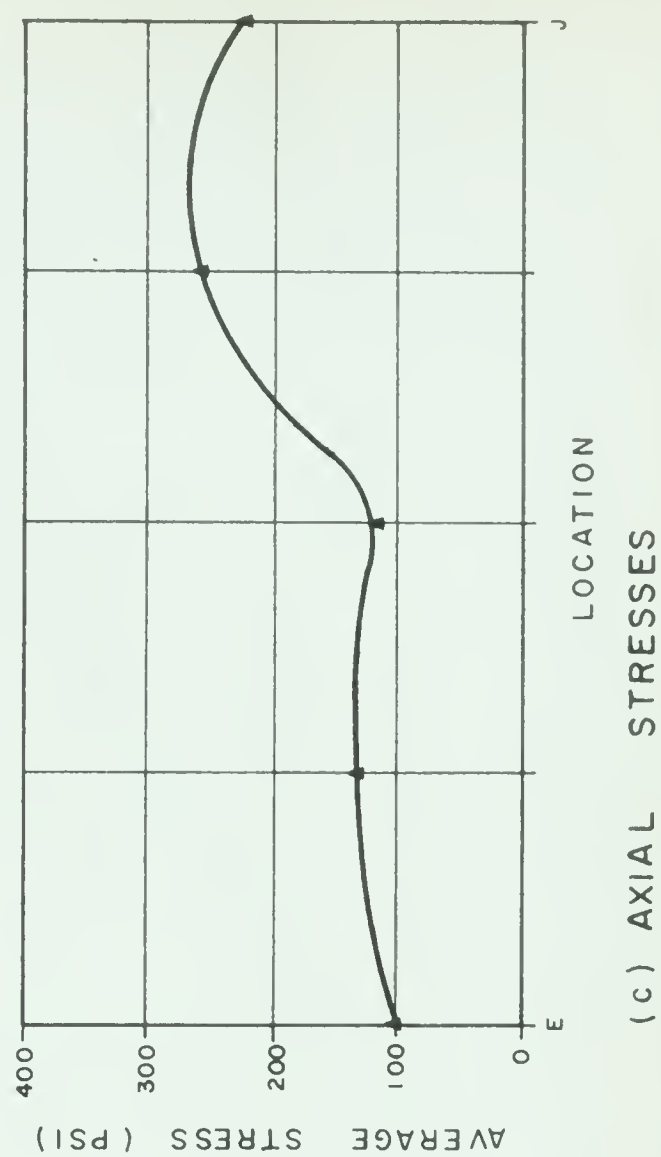
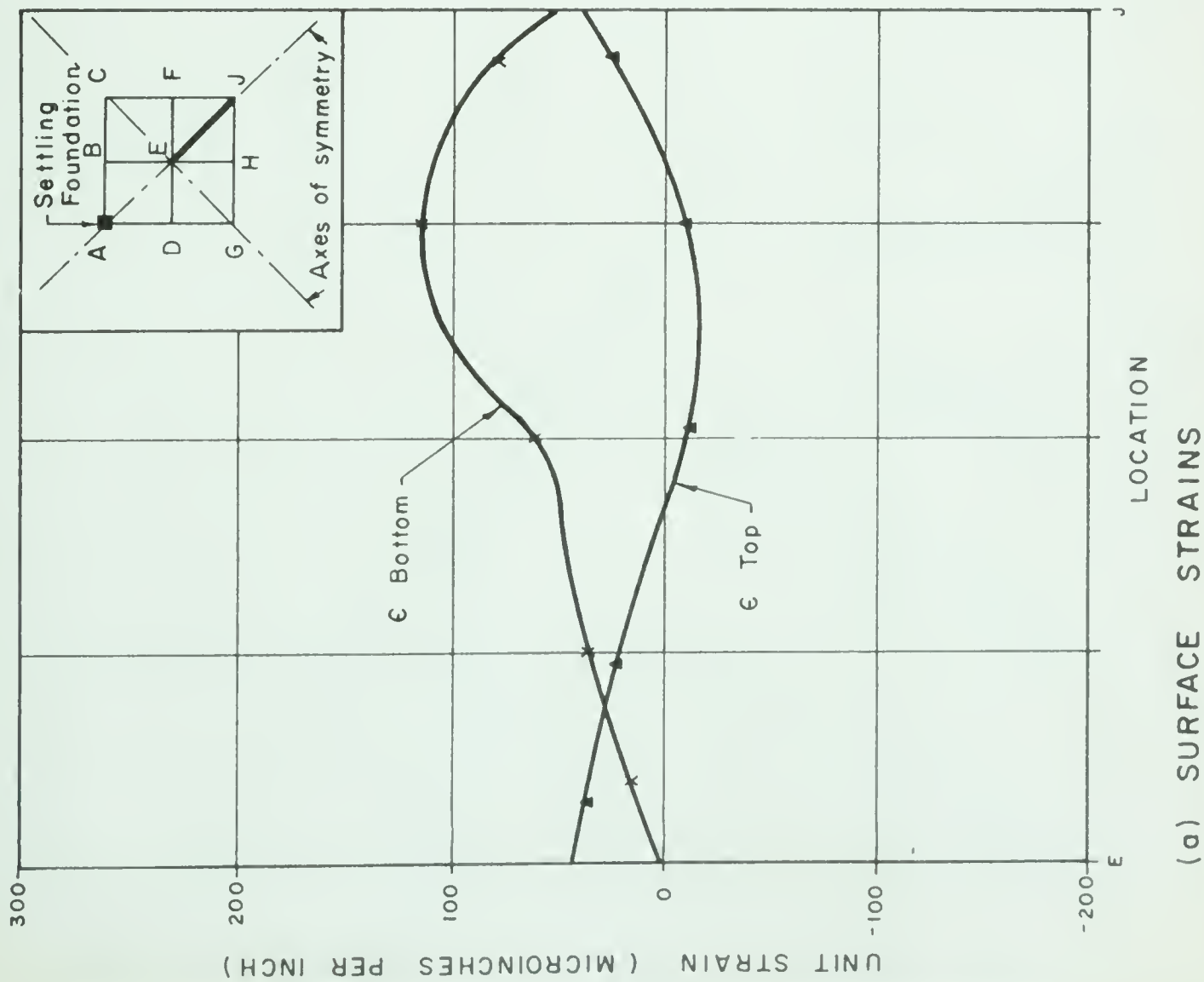
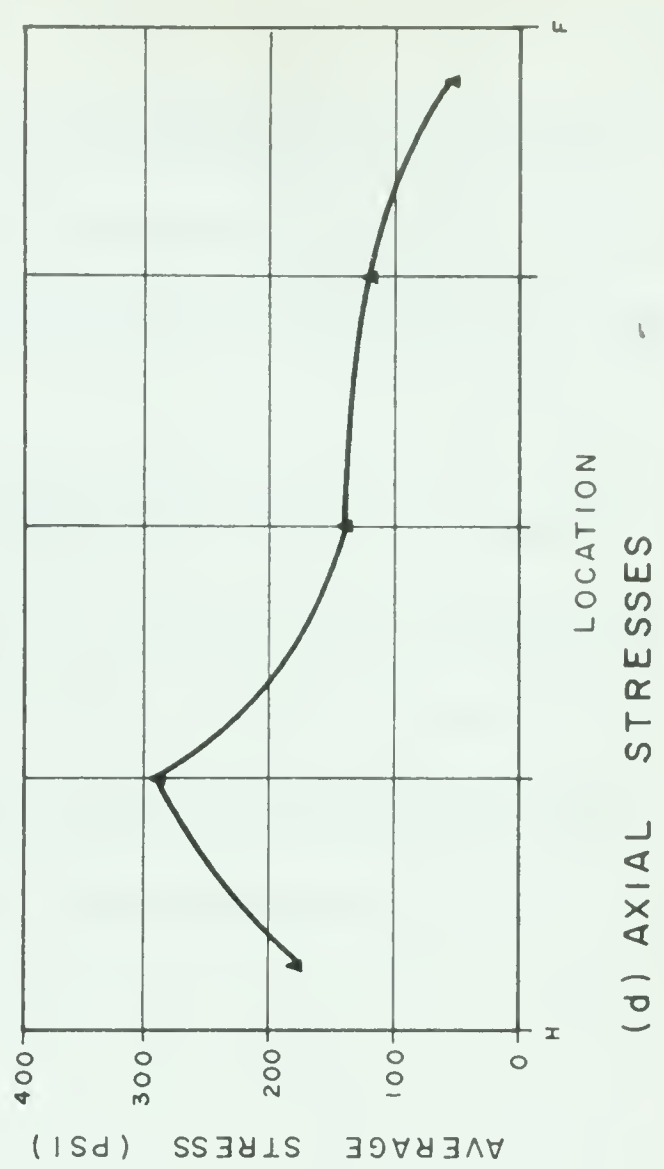
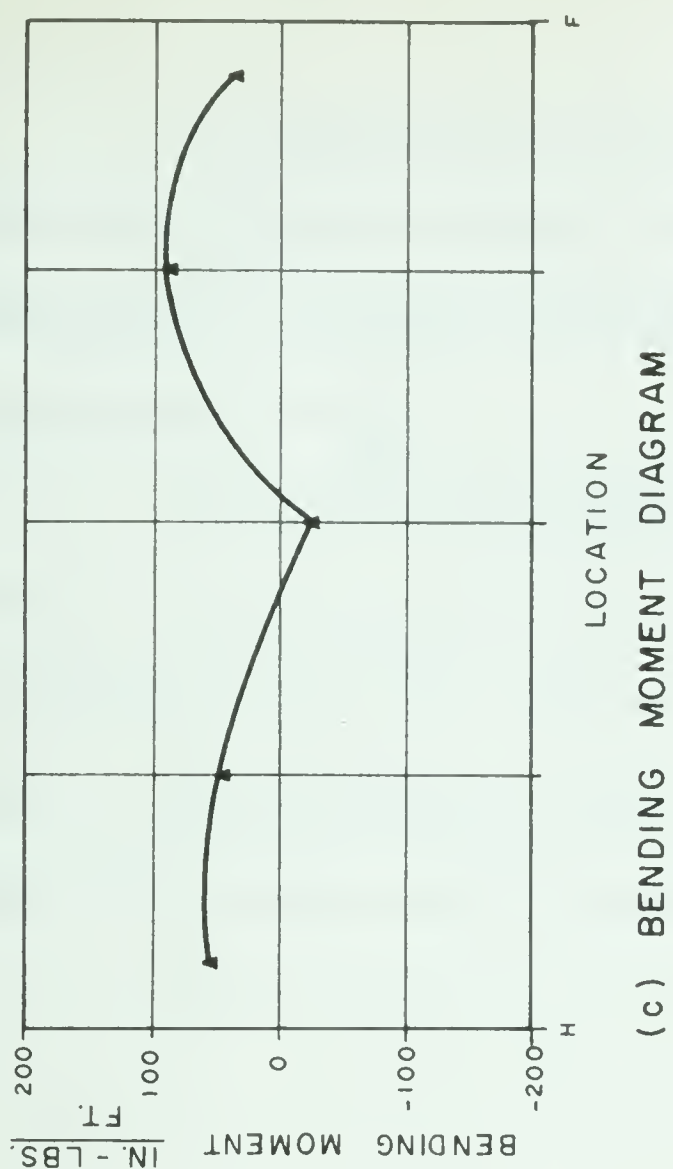
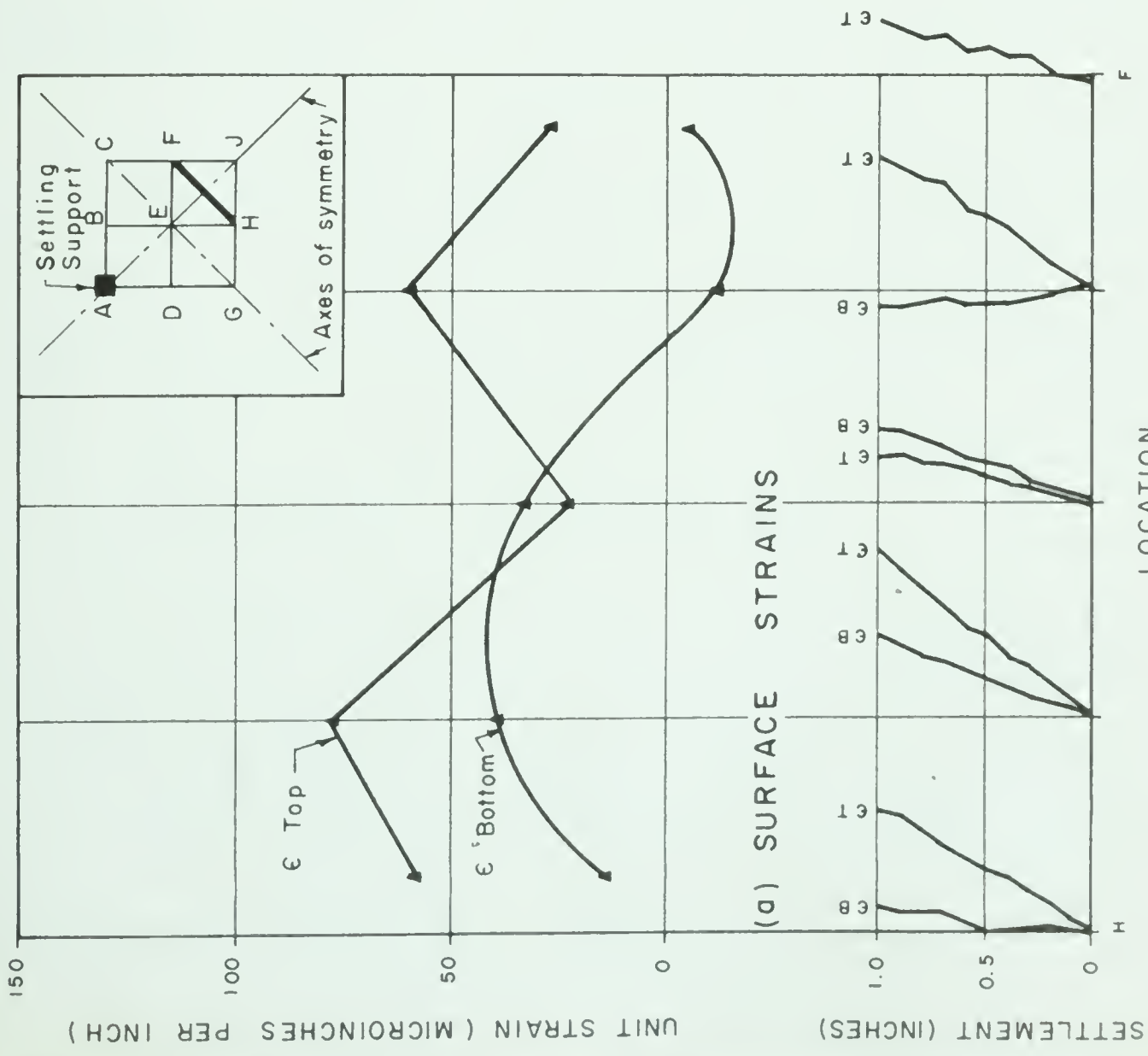


FIGURE 8.6 SURFACE STRAINS, BENDING MOMENTS & AXIAL STRESSES FOR DIAGONAL E-J
TEST #5 - SETTLING FOUNDATION



(b) LINEARITY OF READINGS

FIGURE 8.7 SURFACE STRAINS, BENDING MOMENTS & AXIAL STRESSES FOR DIAGONAL H-F TEST # 5 - FOUNDATION SETTLEMENT (ONE INCH)

It would appear that the hyperbolic paraboloid is able to deform under large differential foundation movements without serious effects on any of the members. The change in the vertical reactions at the corners due to settling one support is slight.

The members most affected by settlement appear to be the gable beams. The maximum moment in these gables is approximately equivalent to the cantilever moment of the support reaction over a cantilever span of $0.5 a$. However, since the magnitude of the vertical reaction is indeterminate, this approximation does not afford much help in designing the gables.

CHAPTER IX

PRESENTATION AND DISCUSSION OF TEST TO DESTRUCTION

9.1 Introduction

Test 7 was discussed earlier in connection with the uniform, symmetrical loading series of tests. In that discussion, only the elastic behaviour of the shell was considered. In the latter part of Test 7, however, the load was increased in two thousand pound increments until the shell failed.

9.2 Mode of Failure

Under an applied load of 26.75 kips, the model suddenly collapsed in the central portion, leaving the gable beams virtually intact. The load catching device, two pairs of rods suspended from the loading frame immediately engaged and continued to carry the load, although it fell off to a value of about 15 kips. Upon release of the load, the shell, with the weight of the load distributing system sprang back to almost its original shape.

FIGURE 9.1 is a photograph of the model after removal of the load distribution system. It may be seen that the model failed on the outside along a very nearly circular path, shown on the diagram as the "failure circle". This circle had a diameter of approximately eight feet with a large crack width

CHAPTER II

THEORY OF THE DISCRETE

THE DISCRETE

§ 1. THE DISCRETE

The first question which arises in connection with the discrete is the question of its definition. The discrete is defined as a function of a discrete variable. The discrete is a function of a discrete variable, and the discrete is a function of a discrete variable. The discrete is a function of a discrete variable, and the discrete is a function of a discrete variable. The discrete is a function of a discrete variable, and the discrete is a function of a discrete variable.

§ 2. THE DISCRETE

The second question which arises in connection with the discrete is the question of its properties. The discrete is a function of a discrete variable, and the discrete is a function of a discrete variable. The discrete is a function of a discrete variable, and the discrete is a function of a discrete variable. The discrete is a function of a discrete variable, and the discrete is a function of a discrete variable. The discrete is a function of a discrete variable, and the discrete is a function of a discrete variable.

The third question which arises in connection with the discrete is the question of its applications. The discrete is a function of a discrete variable, and the discrete is a function of a discrete variable. The discrete is a function of a discrete variable, and the discrete is a function of a discrete variable. The discrete is a function of a discrete variable, and the discrete is a function of a discrete variable. The discrete is a function of a discrete variable, and the discrete is a function of a discrete variable.

at the junction of the ridge and gable beams. The shell failed generally in compression along the failure circle near the corner supports, and in tension in the vicinity of the ends of the ridge beams. A compression failure in the top of Ridge DEF near point E was found which resulted from a premature tension failure in the bottom beam steel at the weld. This compression failure is marked in FIGURE 9.1.

FIGURE 9.2 shows a view of the underside of the ridge beam junction after failure. Transverse cracks occurred at approximately one and one half inches on centre, the same spacing used for the stirrups. A large split opened up adjacent to Ridge BEH which is shown in the picture as a cross hatched area. The cause of this large crack was the failure of the butt weld of the lower layer of reinforcing steel in Ridge DEF. For clarity in the picture, the edge of ridge beams are shown in dotted outline.

A view of the inside face of a typical gable beam may be seen in FIGURE 9.3. Again, the edges of beams have been outlined by a dotted line for clarity. The lower face of the ridge beams show no signs of cracking in this view, since the portion included in the picture was under negative bending moment and hence in compression. Diagonal cracking in the gable beam is typical of torsional cracking and it may be seen that the direction of applied torsion was the same from ridge to support, caused by a negative bending moment applied by the ridge beam.

FIGURE 9.4 is a view of the underside of one quadrant of the shell



FIGURE 9.1 TOP VIEW OF MODEL AFTER FAILURE



FIGURE 9.2 RIDGE BEAM JUNCTION VIEWED FROM UNDERSIDE AFTER FAILURE



FIGURE 9.3 CRACK PATTERN ON UNDERSIDE OF MODEL (SUPPORT "C")

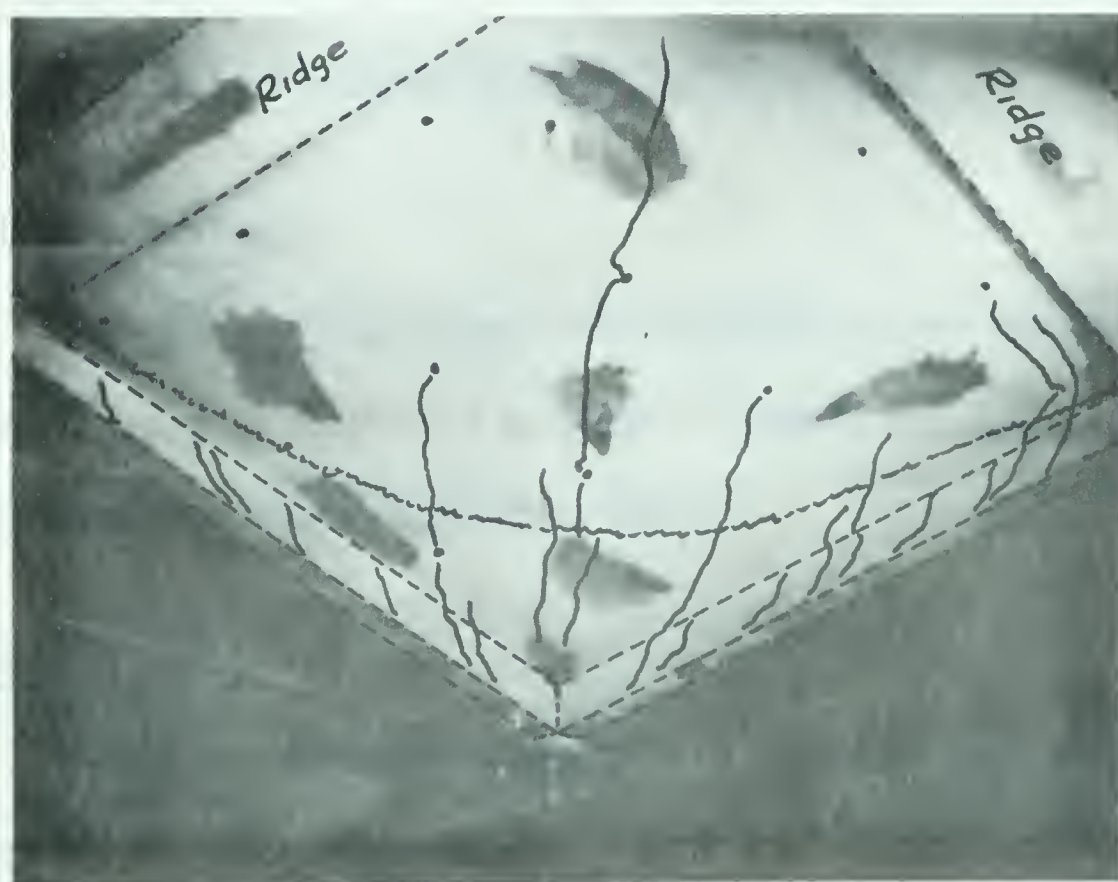


FIGURE 9.4 CRACK PATTERN ON UNDERSIDE OF MODEL (SUPPORT "A")

looking towards the support. Again, the diagonal cracks in the adjacent gable beams are plainly evident. The failure circle, not clearly seen in the picture, was accentuated by a zigzag line. Typical tension cracks which occurred in all quadrants of the model, normal to the tension diagonal are clearly visible, more closely spaced near the support.

9.3 Linearity of Strains

In an earlier section, it was found that the strain readings in virtually all the gauges increased linearly with respect to load. In Test 7, this was true up to a load of approximately 12,000 pounds. The deviation found in similarly located gauges beyond that load were not always consistent, so that interpretation of these results was not possible. FIGURE 9.5 and 9.6 show the strain versus load relationship for the strain gauges on the top and bottom fibres of Gable GH. From these, it may be seen that the model was no longer behaving elastically for loads in excess of 12,000 pounds.

9.4 Deflection Readings

Deflection measurements were continued up to a load of 24 kips at which time many of the dials were no longer in contact with the surface of the model, so no further readings could be taken.

9.5 Bending Moments

Bending moments for Ridge DEF as computed from deflection measurements are plotted in FIGURE 9.7 from a load of 4,000 pounds to

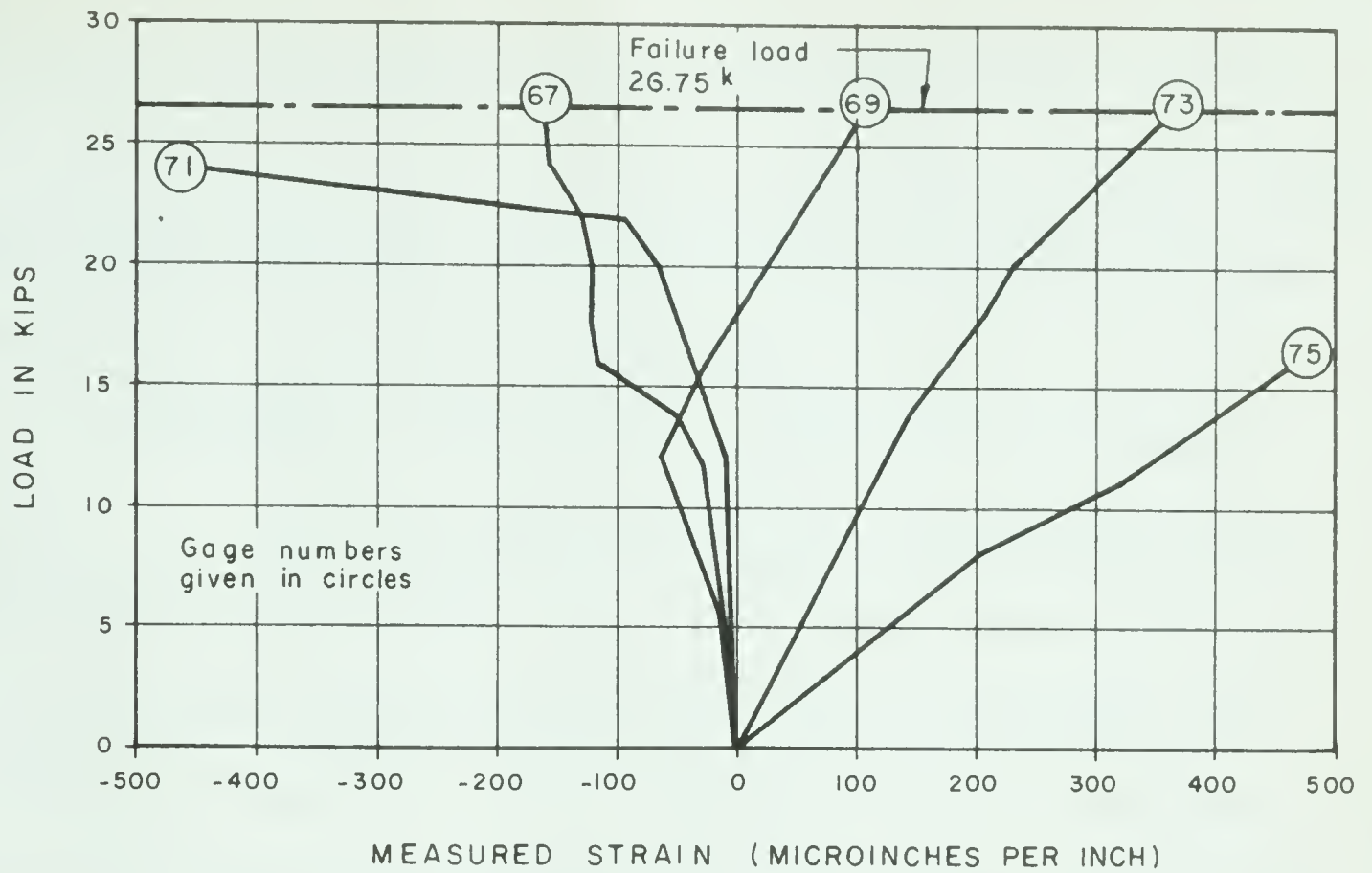


FIGURE 9.5 STRAIN VS. LOAD FOR GAUGES ON TOP OF GABLE G-H, TEST #7 - LOAD TO DESTRUCTION

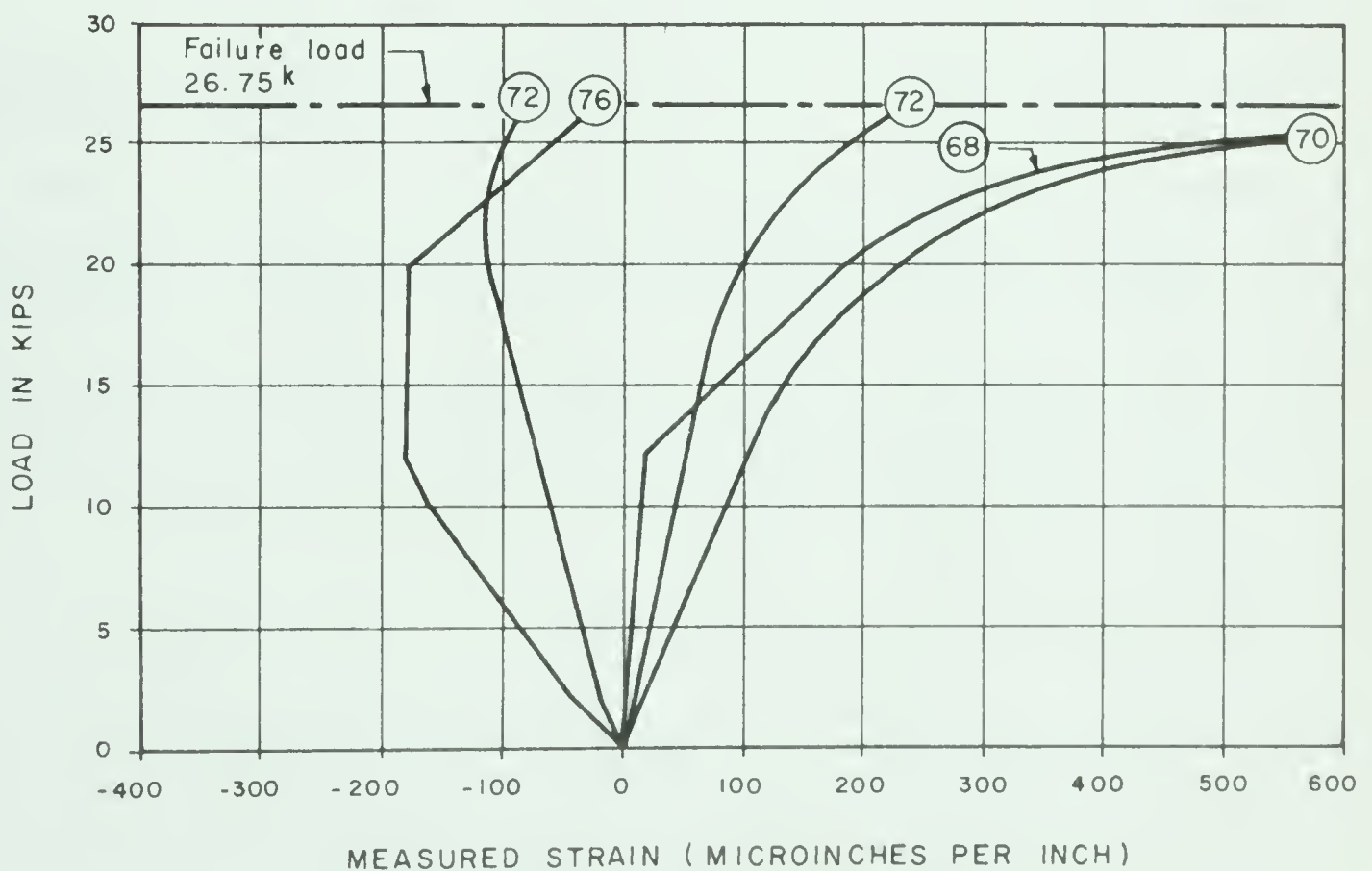


FIGURE 9.6 STRAIN VS. LOAD FOR GAUGES ON BOTTOM OF GABLE G-H, TEST #7 - LOAD TO DESTRUCTION

24,000 pounds in 4,000 pound increments. The inelastic behaviour of the material is again evident from the rate of increase of the maximum positive bending moment ordinate at the centre. All moment curves are calculated on the basis of the uncracked moment of inertia of the section.

In FIGURE 9.8, similar bending moment curves are plotted for Gable CFJ. To a lesser extent than was noted in the case of the ridge beams, the inelastic behaviour is apparent. Due to the presence of the tie rods, the gable beams could be expected to act in a more nearly elastic manner, since the effective span is only half of the overall span of the model. The positive moment at the peak is caused largely by the extension of the tie rods which remained in the elastic range up to failure load.

9.6 Primary Cause of Failure

The ultimate failure was caused by a failure in the welding of the bottom layer of reinforcing bars in the ridge beam. To determine the approximate ultimate capacity of the welds, three samples of reinforcing steel from the same supply as used in the model were welded by the same mechanic, using the same welding machine as used earlier. Samples of unwelded bar were compared. The ultimate failure load for these samples is tabulated in TABLE III.

The first of these is the fact that the
government has been unable to
bring about a general agreement
among the various departments
concerning the proposed
amendment to the constitution.

It is true that the
government has been unable to
bring about a general agreement
among the various departments
concerning the proposed
amendment to the constitution.
The second of these is the fact that
the government has been unable to
bring about a general agreement
among the various departments
concerning the proposed
amendment to the constitution.

2.1. The second of these is the fact that

The second of these is the fact that
the government has been unable to
bring about a general agreement
among the various departments
concerning the proposed
amendment to the constitution.
The third of these is the fact that
the government has been unable to
bring about a general agreement
among the various departments
concerning the proposed
amendment to the constitution.

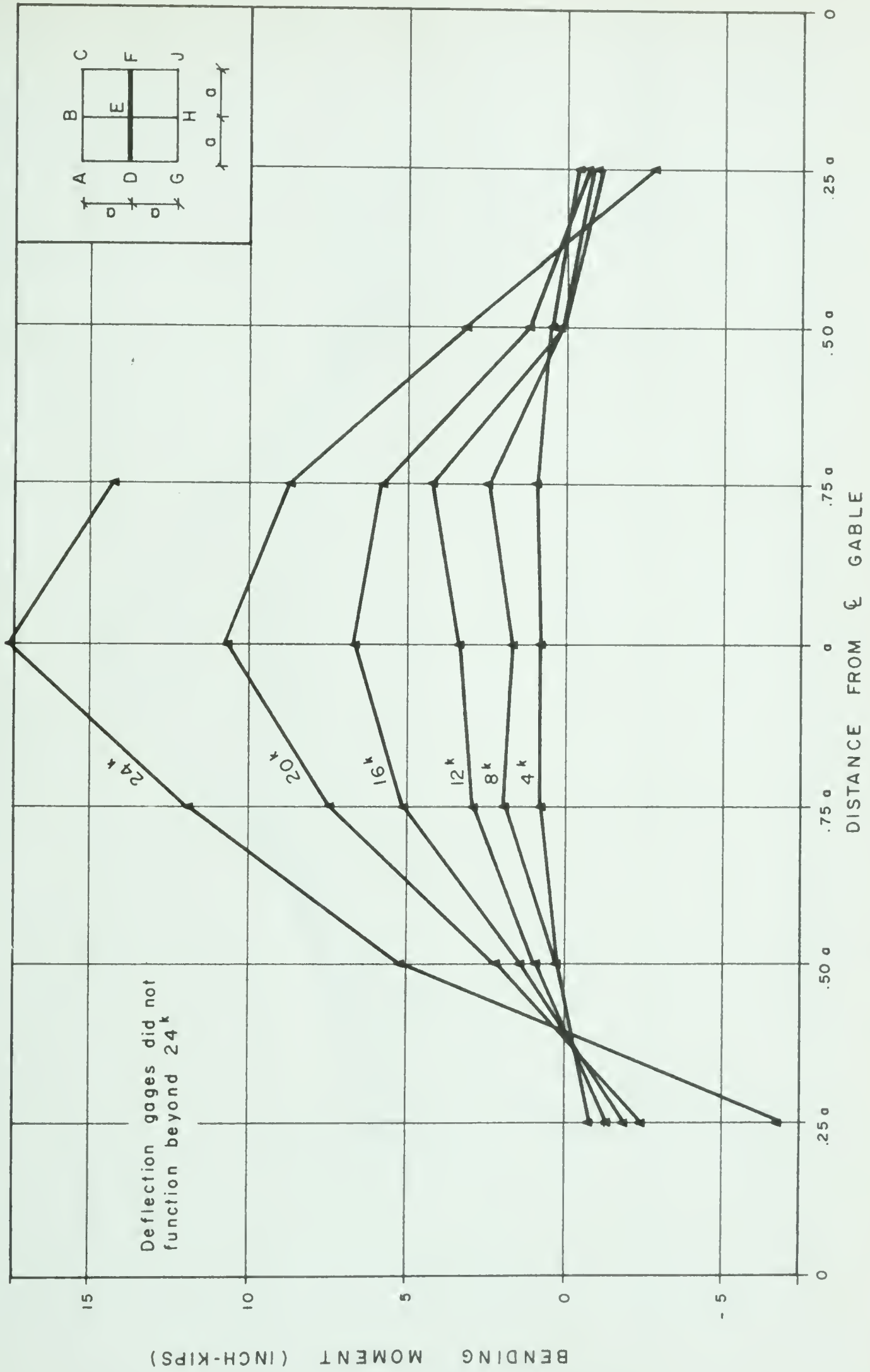


FIGURE 9.7 BENDING MOMENTS FOR RIDGE BEAM DEF AT VARIOUS LOAD INCREMENTS
TEST #7 - LOAD TO DESTRUCTION

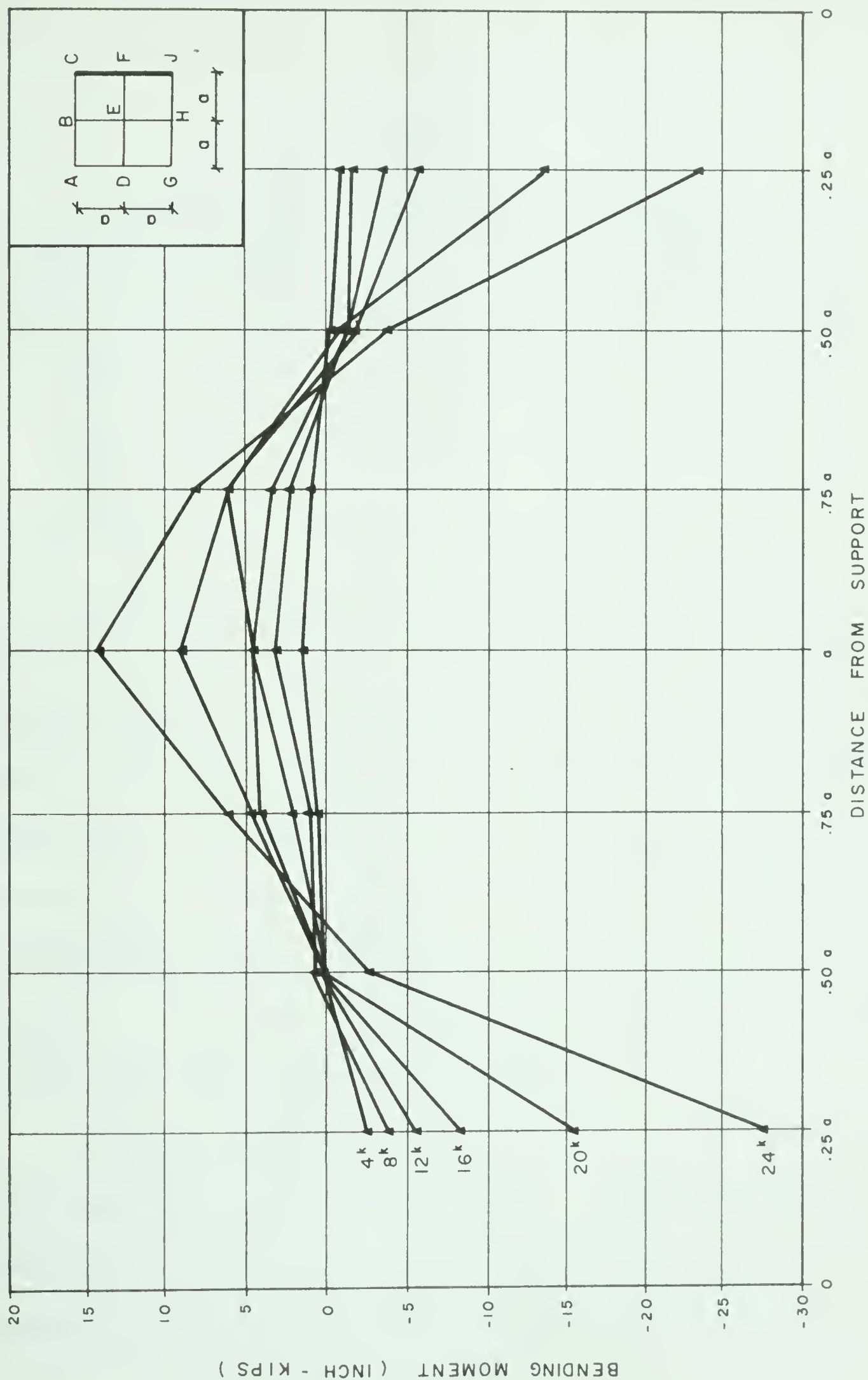


FIGURE 9.8 BENDING MOMENTS FOR GABLE JFC AT VARIOUS LOAD INCREMENTS
TEST #7 - LOAD TO DESTRUCTION

TABLE III
ULTIMATE FAILURE OF REINFORCING SPECIMENS

UNWELDED SPECIMENS			WELDED SPECIMENS		
Ultimate Load		Ultimate Stress	Ultimate Load		Ultimate Stress
A	9,125	83,000	D	3,310	30,000
B	9,090	82,800	E	4,190	38,000
C	9,090	82,800	F	5,200	47,200

The average breaking strength for the unwelded bar samples was found to be slightly less than 83,000 psi with very little deviation from the mean. On the other hand, the welded specimens displayed a wide range of values which presented a considerable obstacle in evaluating the ultimate capacity of the actual member. For the purposes of determining the ultimate capacity of the ridge beam, it was assumed that the ultimate strength of the reinforcing in tension was 40,000 psi which is approximately the average value found in the welded samples. Based on this assumption, an interaction curve was developed for the ridge beam, which is illustrated in FIGURE 9.9.

The actual eccentricity of the middle surface of the shell to the centroid of the ridge beam was three quarters of an inch. A study of FIGURE 9.9 reveals that the $e = 3/4"$ line crosses the interaction curve at a load of approximately 28.0 kips. The actual failure load was found to be 28.1 kips, composed

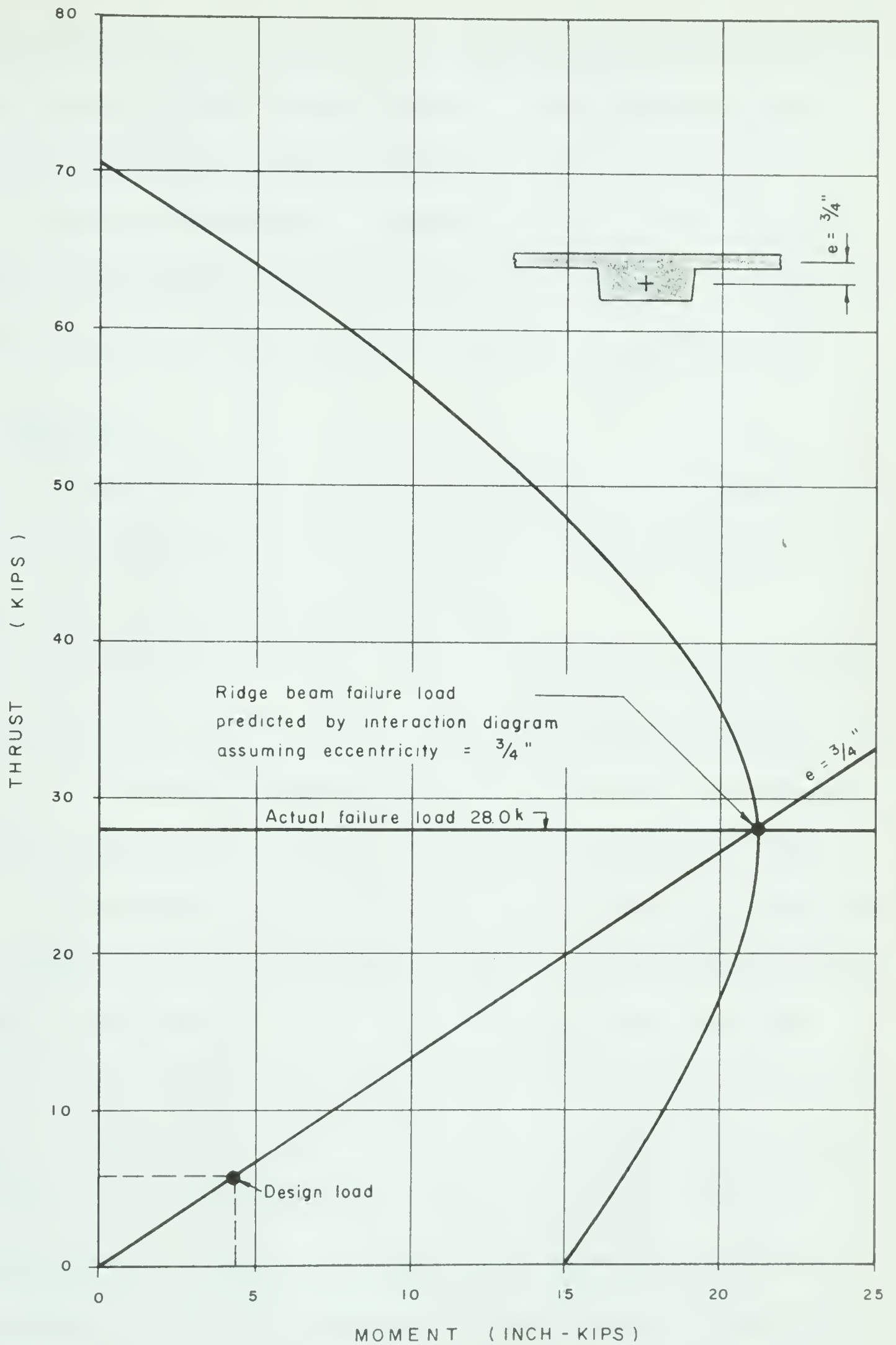


FIGURE 9.9 INTERACTION DIAGRAM FOR RIDGE BEAM AT \mathcal{C}

of 26.75 applied loading, 0.615 kips for the load distribution system, and 0.735 kips for the dead weight of the model, which, by membrane theory, produces a maximum compression in each ridge beam of 28.1 kips.

The design load of 90 psf, or a total load of 5.76 kips over the entire surface, corresponding to a maximum ridge beam compression of 5.76 kips, is shown in the lower part of the figure. The load factor is found to be 4.9.

9.7 Discussion

The model behaved reasonably elastically until the load reached approximately twice design load. Beyond that point, the inelastic behaviour was apparent in both the strain and deflection readings.

Assuming that failure of the model takes place by a ridge beam failure, the ultimate load of the shell could be predicted by using simple membrane theory and the interaction diagram of the beam, and assuming an eccentricity equivalent to the actual eccentricity of the shell to the centroid of the beam.

The agreement between predicted and measured results was much closer than expected. It should be remembered, however, that the actual value of the strength of the butt weld in the lower layer of ridge beam reinforcing, which formed the basis of the calculation of ultimate load, was rather nebulous. Actually, the strength of weld in the model was likely lower than assumed in computing the interaction diagram, which would result in a somewhat lower predicted failure load. This theory is suggested since some end restraint must have existed in the ends of the ridge beams just prior to failure, although they

were not specifically reinforced for this condition and the failure of the model was accompanied by the formation of almost a complete hinge at the junction of the ridge beam to the gable. It was not possible to observe whether the ridge beams failed first at the ends or at the centre, but it is thought that, logically, the ends must have first yielded, giving rise to a redistribution of moments to the centre of the beam, which caused ultimate collapse. Had the ends been reinforced for negative moment, the ultimate load might have been substantially greater or ultimate failure may have been by another cause such as torsional failure of the gable beams or shear failure in the shell.

CHAPTER X

SUMMARY, RECOMMENDATIONS AND CONCLUSIONS

10.1 Summary

A pneumatically placed mortar model of a gable type hyperbolic paraboloid shell was tested (a) with a uniform, symmetrical load applied over the entire surface of the model, (b) with a uniform load over two adjacent quadrants of the model and (c) under the settlement of one of the four corner supports.

Mortar cubes had a 28 day compressive strength of 5,200 psi. The shell was reinforced with sixteen gauge cold drawn steel wire. The beams were reinforced with #3 deformed steel bars having a yield point of 55,000 psi and an ultimate strength of 83,000 psi.

The model spanned eight feet from corner to corner, having a shell thickness of one half inch and a rise of one foot. The ridge and gable beams were "downturned" so that the middle surface of the shell was eccentric to the centroid of the beams. One support was hinged by a ball bearing and translation at that corner was prevented. The three remaining supports were on roller bearings which permitted the corners to move freely in a direction away from the pinned support.

The only variable, apart from the loading patterns, was the size of the

tie rod used. The tie rod used for the initial tests was one half inch in diameter. To preclude tie rod failure in the test to destruction, a three quarter inch diameter rod was added.

With uniform load over the entire shell surface, the indicated axial thrusts in the ridge and gable beams were lower than membrane theory predicts, due to the flange action of the shell on either side of the beam. The stresses in the shell agreed well with membrane theory, except that it appeared that a small biaxial compression was superimposed. The compression diagonal had higher compressions and the tension diagonal had lower tensions than indicated by membrane theory, each deviating by approximately 30 to 40 psi. In addition, Generator KL was a uniform compression of about 30 to 40 psi over its length, whereas membrane theory predicts it to be in pure shear. Positive bending occurred in the peak of the gable beams, caused by the extension of the tie rods, which permitted a spreading of the supports. Bending occurred in the ridge beams, which was thought to be largely due to the eccentricity of the shell with respect to the centroid of the beam.

Under asymmetrical loading over only two quadrants, the loaded panels displayed virtually the same magnitude of thrust and moment as found under the uniform, symmetrical loading. The ridge beam, having loading symmetry, carried axial thrusts and bending moments with a similar configuration to those curves found in the symmetrical loading series, but the ordinates to the curves were just one half of the latter. The gable beams without loading symmetry be-

haved similarly to a two span continuous beam having load on one span only. A similarity in the shape of the axial thrust diagrams for the gable and ridge beams without loading symmetry indicates the possibility of a transfer of thrust from the ridge to the gable, through planar shears in the shell. The fact that the two thrust curves are out of phase by about one half the panel width indicates a "shear lag" taking place over the width of the panel.

When one of the corner supports was permitted to settle one inch, or $1/96$ th of the span, no visible evidence of distress in the shell could be found. Strain measurements indicated that the gable beams were most affected by differential settlement. The gable beams spanning to the settled support behaved as cantilever beams with the maximum bending moment occurring approximately two feet (or one half panel width) from the support.

The model was loaded to failure by the application of a uniform load. Final failure took place at an applied load of 26.75 kips and a total load of 28.1 kips. The cause was the failure of the welds in the bottom reinforcing in one of the ridge beams. Subsequent tests on samples of reinforcing steel showed that the welded specimens failed at less than half the load carried by the unwelded specimens.

Up to a load of 12,000 pounds, strain and deflection readings were linear with respect to load. Beyond 12,000 pounds, however, many of the gauges strayed considerably, indicating that portions of the shell were stressed beyond the elastic limit. Analysis of ridge beams, using membrane theory to

assess the magnitude of axial thrust, coupled with an interaction diagram for the beam predicted a failure load of 28 kips. The agreement between predicted and measured results was extremely close and indicated the membrane theory was valid far beyond the elastic limit.

Diagonal cracking on the inside face of gable beams indicated the presence of large torsional stresses, thought to be caused by the end rotation of the ridge beams. The shell panels failed on a nearly circular path having a diameter of slightly less than the span of the model. After failure, a slight outward bowing of the gable beams could be visually detected.

10.2 Recommendations for Future Work

As a result of difficulties encountered in building the model and in processing the data, the following recommendations are made:

- (a) After coating the forms with form oil, and before weaving the shell reinforcing, spread a layer of polyethylene over the forms. When the wire is finally in position, this layer may be removed through gaps between the wires. In this way, the reinforcing wire will be free of bond destroying oil.
- (b) Use a more ductile wire for shell reinforcing which may be repeatedly bent and straightened without breaking.
- (c) Devise a splice for reinforcing steel at the ridge beam junction which can develop the full strength of the bars.
- (d) Under the deflection gauges, mount the bearing platens on a

horizontal surface using a fisheye bubble.

In this way, no correction will be found necessary for the lateral movement of the shell.

- (e) Measure horizontal deflections of the gable beams.
- (f) To get a value of bending moment at the ends of beams, measure end rotations of all beams.
- (g) Instrument an additional generator perpendicular to Generator KL.

Many parameters could be varied. One interesting variation would be to choose "upturned" beams rather than "downturned" as used in this study. If the conclusions drawn from this experiment have been correct, the use of upturned beams should result in a reversal of sign in the bending moments. For a prototype structure, the bending moments in an upturned ridge beam could be proportioned to balance the dead load moment of the beam itself, which cannot be carried by shell action (Flugge, 1962).

To avoid shrinkage cracking, it may be desirable to prestress the beams and perhaps the shell reinforcing, or to use a different material which remains elastic throughout the testing program.

To test the limitations of membrane theory, models of low height to span ratio should be tested. Variation of aggregate size, concrete strength and methods of reinforcing should be investigated.

10.3 Conclusions

The conclusions outlined below are made on the basis of this study only.

They should not be regarded as generally applicable to H.P. shells.

(a) Uniform Load Series

- (i) Measured axial stresses in the gable beams were lower than predicted by membrane theory due to flange action of the shell.
- (ii) Measured axial stresses in the ridge beams were much lower than predicted by membrane theory due to tee beam action.
- (iii) Actual stresses in the shell are very nearly as predicted by membrane theory, but tend to be somewhat more compressive.
- (iv) Bending moments in ridge beams were largely caused by the eccentricity of the shell.
- (v) Bending moments in the gable beams were attributed to a spreading of the supports as the tie rods were stressed.
- (vi) Bending moments in the shell are very small and of little consequence in the design.
- (vii) Membrane theory corrected for shell eccentricity, appears to remain essentially valid well beyond the elastic range of the material, and forms a reliable basis for predicting the ultimate behaviour of the shell under uniform load.

(b) Asymmetrical Load Tests

- (i) Under uniform load over two adjacent panels, the loaded

THE JOURNAL OF THE AMERICAN MEDICAL ASSOCIATION
PUBLISHED WEEKLY

CHICAGO, ILL., U.S.A.

Subscription price, Five Dollars Per Annum in Advance

Single Copies, Fifteen Cents

Entered as Second-Class Matter, June 26, 1902

Postage paid at Chicago, Ill., and at additional mailing offices

Acceptance for mailing at special rate of postage provided for in Act of October 3, 1917

Authorizes the mailing of this publication at the special rate of postage provided for in Act of October 3, 1917

Copyright, 1938, by American Medical Association

Printed at the American Medical Association, 535 North Dearborn Street, Chicago, Ill.

Second-Class

Postmaster: Please send address changes to JOURNAL OF THE AMERICAN MEDICAL ASSOCIATION, 535 North Dearborn Street, Chicago, Ill.

Subscription orders, notices, and other correspondence should be sent to the Editor

and notices to the publisher should be sent to the Business Manager

Advertisements should be sent to the Advertising Manager

Claims for missing issues will only be considered if made immediately on receipt of following issue

Entered as Second-Class Matter, June 26, 1902

Postage paid at Chicago, Ill., and at additional mailing offices

Acceptance for mailing at special rate of postage provided for in Act of October 3, 1917

Authorizes the mailing of this publication at the special rate of postage provided for in Act of October 3, 1917

Copyright, 1938, by American Medical Association

Printed at the American Medical Association, 535 North Dearborn Street, Chicago, Ill.

Subscription price, Five Dollars Per Annum in Advance

panels behave essentially as they did under symmetrical loading.

- (ii) Moments and thrusts in the beams under unbalanced loading were not more critical than under balanced loading, but the maximum ordinate was in a different location.
- (iii) An approximate method of design for shells having unbalanced loading is suggested, introducing a hypothetical "holding" force and later, removing it.

(c) Foundation Settlement

- (i) The shell could withstand large differential settlements without visible signs of distress.
- (ii) Gable beams are most affected by foundation settlement.

BIBLIOGRAPHY

G. D. Base - "Tests on a Perspex Model Anticlastic Roof of Lattice Construction - Technical Report TRA/358 - Cement and Concrete Association, London, England.

D. G. Bellow and J. S. Kennedy (1963) - "Multi-Channel Strain Analysis",
E. I. C. Transactions.

Building Research Station, Garston, Watford, Herts, England - Note No. A 31
"Concrete Shell Roofing".

F. Candella (1960) - "General Formulas for Membrane Stresses in Hyperbolic Paraboloidal Shells" - A. C. I. Proceedings Vol. 57, October, 1960.

W. Flugge (1962) - "Stresses in Shells" - Springer - Verlag Publication.

F. A. Gerard (1959) - "The Analysis of Hyperbolic Paraboloidal Shell Roofs"
E. I. C. Transactions - Vol. 3 No. 1 April, 1959.

E. Hognestad, N. W. Hanson, L. B. Kriz and O. A. Kurvits - "Facilities and Test Methods of P. C. A. Structural Laboratory" - P. C. A. Bull. D 33.

L. L. Jones (1960) - "Tests on a one-tenth Scale Model of a Hyperbolic Para-

boloid Shell Roof" - Technical Report TRA/334 - Cement and Concrete Association, London, England.

L. L. Jones (1961) - "Tests on a one-sixth Scale Model of a Hyperbolic Paraboloid Umbrella Shell Roof" - Technical Report TRA/347 - Cement and Concrete Association, London, England.

G. R. Mitchell (1957) - "Shell Roof Research at the Building Research Station" - Second Symposium on Concrete Shell Roof Construction, Oslo.

G. R. Mitchell (1959) - "Notes on the Testing of Reinforced Concrete Model Shells" - Indian Concrete Journal - December, 1959.

A. H. Nilson (1962) - "Testing a Light Gage Steel Hyperbolic Paraboloid Shell" - A. S. C. E. Proceedings, October, 1962.

A. L. Parme (1958) - "Shells of Double Curvature" - A. S. C. E. Trans. Vol. 123, 1958.

C. C. Perry (1957) - "How to Measure Principal Stresses" - Product Engineering October, 1957.

Pfluger - "Elementary Statics of Shells".

Portland Cement Association - "Elementary Analysis of Hyperbolic Paraboloid Shells" - Structural and Railways Bureau - Bull. ST - 85.

J. Schwaighofer (1963) - "The Analysis of Structures by Aid of Models" - Engineering Journal - July, 1963.

F. G. Thomas (1958) - "Structural Engineering Research" - Jubilee Issue of the Structural Engineer, 1958.

S. Timoshenko and J. N. Goodier (1951) - "Theory of Elasticity" - McGraw-Hill Publication.

S. Timoshenko and S. Woinowsky-Krieger (1959) - "Theory of Plates and Shells" - McGraw-Hill Publication.

APPENDIX A

CEMENTS FOR THE APPLICATION OF STRAIN GAUGES TO A CONCRETE SURFACE

A number of cements were tried on a sample of concrete with a view to choosing the most successful cement on the model. The concrete sample chosen was a two foot square slab about two inches thick which had an exceedingly rough surface. The surface had to be sized first and strain gauges applied to the sizing.

Armstrong A-2 epoxy cement was first mixed with the catalyst and spread over an area of approximately four square inches. It was easily worked into the voids of the concrete and its filling qualities were found to be excellent, but the drying time is roughly two weeks and it forms a skin on the outer surface before it is thoroughly dried, thus slowing the drying time for the glue below the skin. It was considered wholly unsatisfactory as a sizing, although it may be adequate after complete drying.

Armstrong C-2 used at room temperature with type "A" activator formed an extremely gelatinous mixture which was difficult to spread evenly over the concrete surface. In working the spatula back and forth over the cement, the entire patch of cement would adhere to the spatula, leaving no

visual trace of cement on the concrete sample. It appeared to have more of a tendency to adhere to a smooth surface than the rough concrete surface. When allowed to dry, however, the cement formed an extremely hard and waterproof bond to the concrete, but dispersed throughout the cement matrix were very minute air pockets.

Budd B-12 cement is available in a small plastic container, with the cement separated from the activator by a plastic clamp. When the clamp is removed, the cement and activator are thoroughly mixed by kneading the container. As a sizing material, this was excellent. The surface voids are thoroughly filled and no air pockets are found in the cement. For the application of strain gauges, however, considerable difficulty was experienced. Due to the inherent spring in a paperback gauge, the gauge has to be held down firmly until the cement has set. The setting time is twelve hours and the pot life is only one half hour. The pot life may be considerably extended by spreading the cement in a thin layer on a flat glass plate at room temperature. By keeping the cement in the freezing compartment of the refrigerator it could be kept indefinitely. This cement is intended for adhering metal film gauges and for that purpose it is likely excellent, but for paperback gauges a faster setting time is required.

Budd GA-5 cement was found to be an excellent sizing material. Somewhat less gelatinous than Armstrong C-2, it had a tendency to form minute air pockets, but these could be removed by careful working. When the surface was

ground, the cement was found to penetrate deep into the voids of the concrete, forming an intimate bond with the surface of the specimen. After grinding the sizing, the same cement was used to fasten the gauges and while it appeared to be satisfactory at the time of application, it was later found that the gauges could be easily removed by hand.

CIL household cement was found to be a very easy material to use in applying the strain gauges. Each gauge is firmly held in position for about one minute at which time the cement has hardened sufficiently to hold the gauge in position. The main objection to household cement is the fact that it is not a waterproof glue and is subject to changes in atmospheric conditions. Also, it has been found that this glue has a tendency to creep when it is subjected to stress over an extended period of time. For this test series, neither of these objections were important since each test was completed in a matter of a few hours.

Kriz (1959) recommends the use of an epoxy resin known as "Cycleweld" as produced by the Chrysler Corporation for the application of strain gauges to concrete. Unfortunately, this was not known in time for this test series, but it is recommended that for further tests of this type, this material be tried.

APPENDIX B

CONCRETE PROPERTIES

B-1 Cube Tests

Six mortar cubes were cast at the time the mortar was placed on the model. The 28 day strengths are tabulated in TABLE IV.

TABLE IV

CUBE STRENGTHS

Sample	28 Day Strength (ksi)
A	5.32
B	5.38
C	5.63
D	4.57
E	5.01
F	5.19
	31.10
Average	5.20

B-2 Tension Tests

Three tension tests were taken. The ultimate tensile strength at 28 days was found to be 435, 493 and 450 psi respectively, or an average of 459 psi.

B-3 Flexural Rigidity

At the time of casting the model, a flat plate 1'- 6" x 3'- 0" x 1/2" thick was cast using the same material with the same reinforcing as the model. The purpose of this plate was to measure the flexural rigidity (D) of the shell, where

$$D = \frac{Eh^3}{12(1-\mu^2)}$$

Unfortunately, the plate was accidentally broken before it could be used for this purpose so that no measurements were taken.

Throughout the thesis, it has been assumed that $E = 5,000,000$ psi and that $\mu = 0$.

B29827